BEILSTEIN JOURNAL OF ORGANIC CHEMISTRY

Organic synthesis using photoredox catalysis

Edited by Axel G. Griesbeck

Imprint

Beilstein Journal of Organic Chemistry
www.bjoc.org
ISSN 1860-5397
Email: journals-support@beilstein-institut.de

The *Beilstein Journal of Organic Chemistry* is published by the Beilstein-Institut zur Förderung der Chemischen Wissenschaften.

Beilstein-Institut zur Förderung der Chemischen Wissenschaften
Trakehner Straße 7–9
60487 Frankfurt am Main
Germany
www.beilstein-institut.de

Beilstein Journal of Organic Chemistry

Organic synthesis using photoredox catalysis

Axel G. Griesbeck

Editorial

Open Access

Address:
University of Cologne, Department of Chemistry, Organic Chemistry, Greinstr. 4, D-50939 Köln, Germany; Fax: +49 (221) 470 5057

Email:
Axel G. Griesbeck - griesbeck@uni-koeln.de

Keywords:
photoredox catalysis

Beilstein J. Org. Chem. **2014,** *10,* 1097–1098.
doi:10.3762/bjoc.10.107

Received: 17 April 2014
Accepted: 30 April 2014
Published: 12 May 2014

This article is part of the Thematic Series "Organic synthesis using photoredox catalysis".

Guest Editor: A. G. Griesbeck

Natural photosynthesis is a remarkable chemical machinery that enables our life on earth and delivers a constant stream of oxygen and organic biomass. We should acknowledge this fact with humbleness, especially because we have not been able yet to mimic this process in a reliable way even after decades of intense research. The basic mechanistic principle behind photosynthesis is photoredox catalysis or light-driven charge separation, which leads to an energy harvesting process by taking advantage of the reduction products and filling the holes by a sacrificial electron donor, water. Fortunately, we can use the waste product from this process, oxygen, for breathing.

For applications in organic synthesis, the principles of photoredox chemistry serve as guidelines, i.e., photoinduced electron transfer (PET) kinetics and thermodynamics as expressed in the Rehm–Weller and Marcus equations. For catalytic versions, the photoinduced redox processes require efficient and robust photocatalysts, and in many cases appropriate sacrificial components. In recent years, three major groups of light-absorbing molecules/materials have been (re)investigated, which facilitate a wide range of redox activation from their excited states: transition metal complexes (e.g., the thoroughly investigated $Ru(bipy)_3$ and other Ru or Ir complexes) with strong MLCT transitions, organic dyes such as xanthene, porphyrine or phthalocyanine dyes (e.g., eosin Y), and colloidal semiconductor particles (e.g., TiO_2) [1-9]. In addition, combinations of light-absorbing materials have been studied such as dye-coated semiconductor nanoparticles. On the substrate side, the focus is on redox-active donor/acceptor molecules, which range from all kind of aromatic, olefinic and carbonyl-type electron acceptor compounds to heteroatom-linked electron donors. The relevance of carbon–carbon bond formation for organic synthesis is also depicted in these processes, and in recent years, enantioselective versions of these processes as well as unusual activation and coupling modes have been developed. In contrast to the “traditional” catalysis areas such as metal-, organo- and biocatalysis, photoredox catalysis (and photocatalysis in general) is a young research field with regard to synthetic applications. The collection of papers in this Thematic Series on organic synthesis using photoredox catalysis shows this convincingly.

It was a great pleasure to act as the editor of this Thematic Series on photochemical reactions, and I would like to thank all

authors for their excellent contributions and the staff of the Beilstein-Institut for their professional support.

Axel G. Griesbeck

Cologne, April 2014

References

1. Narayanam, J. M. R.; Stephenson, C. R. J. *Chem. Soc. Rev.* **2011,** *40,* 102–113. doi:10.1039/b913880n
2. Xuan, J.; Xiao, W.-J. *Angew. Chem., Int. Ed.* **2012,** *51,* 6828–6838. doi:10.1002/anie.201200223
3. Tucker, J. W.; Stephenson, C. R. J. *J. Org. Chem.* **2012,** *77,* 1617–1622. doi:10.1021/jo202538x
4. König, B., Ed. *Photoredox Catalysis;* De Gruyter: Berlin/Boston, 2013.
5. Prier, C. K.; Rankic, D. A.; MacMillan, D. W. C. *Chem. Rev.* **2013,** *113,* 5322–5363. doi:10.1021/cr300503r
6. Xi, Y.; Yi, H.; Lei, A. *Org. Biomol. Chem.* **2013,** *11,* 2387–2403. doi:10.1039/c3ob40137e
7. Reckenthäler, M.; Griesbeck, A. G. *Adv. Synth. Catal.* **2013,** *355,* 2727–2744. doi:10.1002/adsc.201300751
8. Zou, Y.-Q.; Chen, J.-R.; Xiao, W.-J. *Angew. Chem., Int. Ed.* **2013,** *52,* 11701–11703. doi:10.1002/anie.201307206
9. Garlets, Z. J.; Nguyen, J. D.; Stephenson, C. R. J. *Isr. J. Chem.* **2014,** *54,* 351–360. doi:10.1002/ijch.201300136

License and Terms

Beilstein Journal of Organic Chemistry

Visible-light photoredox catalysis enabled bromination of phenols and alkenes

Yating Zhao, Zhe Li, Chao Yang, Run Lin and Wujiong Xia*

Full Research Paper

Open Access

Address:
State Key Lab of Urban Water Resource and Environment, The Academy of Fundamental and Interdisciplinary Sciences, Harbin Institute of Technology, Harbin 150080, China

Email:
Wujiong Xia* - xiawj@hit.edu.cn

* Corresponding author

Keywords:
alkenes; bromination; phenols; photoredox catalyst; visible light

Beilstein J. Org. Chem. **2014,** *10,* 622–627.
doi:10.3762/bjoc.10.53

Received: 21 November 2013
Accepted: 03 February 2014
Published: 07 March 2014

This article is part of the Thematic Series "Organic synthesis using photoredox catalysis".

Guest Editor: A. G. Griesbeck

Abstract

A mild and efficient methodology for the bromination of phenols and alkenes has been developed utilizing visible light-induced photoredox catalysis. The bromine was generated in situ from the oxidation of Br^- by $Ru(bpy)_3^{3+}$, both of which resulted from the oxidative quenching process.

Introduction

Bromophenols serve as important synthetic intermediates for a variety of naturally occurring biologically active compounds and are also important constituents of industrial chemicals [1-5]. Thus, numerous methods were developed for the electrophilic bromination of phenols. The typical approaches include direct electrophilic halogenation by using molecular bromine or *N*-bromosuccinimide (NBS) [6-8], organometallic catalyst-promoted bromination [9-12], and the oxidative bromination of phenols [13-15]. Nevertheless, most of the methods suffer from several drawbacks such as toxic reagents, harsh conditions, low yields, and low chemo- and regioselectivity. Hence, the development of an environmentally friendly methodology for the bromination of phenols with high chemoselectivity under mild and operationally simple conditions is still appealing.

Recently, an intriguing and promising strategy for the application of photoredox catalysts to initiate single electron transfer processes have been developed [16-22]. Since the pioneering work from the groups of MacMillan [23-25], Stephenson [26-28], Yoon [29-31] and others [32-44] demonstrated the usefulness of $Ru(bpy)_3Cl_2$ and its application to various visible-light-induced synthetic transformations, visible-light-photoredox catalysis has emerged as a growing field in organic chemistry and has been successfully applied in a variety of reactions. In the oxidative quenching process [45-47], $Ru(bpy)_3^{2+}$ excited by visible light generates $Ru(bpy)_3^{2+*}$, which was oxidized to $Ru(bpy)_3^{3+}$ in the presence of oxidative quenchers. CBr_4 is an example of a suitable oxidative quencher and leads to the formation of Br^- and $\bullet CBr_3$. We envision that $Ru(bpy)_3^{3+}$ is a

strong oxidant (1.29 V vs SCE, in CH_3CN) that could sequentially oxidize the resulting Br^- (1.087 V vs SCE, in CH_3CN) to generate the bromine for the bromination of phenols and other substrates in situ (Scheme 1), thus avoiding the use of highly toxic and volatile liquid bromine.

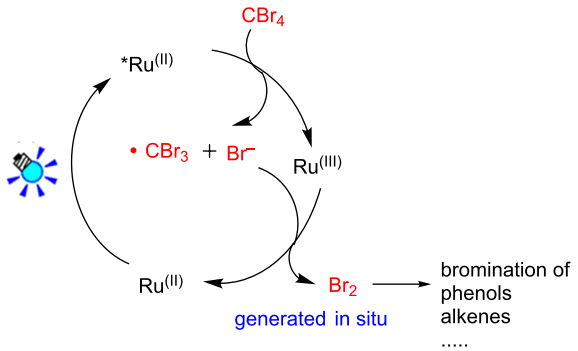

Scheme 1: Strategy for in situ generation of bromine.

Results and Discussion

Our initial investigation was carried out on protected 4-methoxyphenol **1a** and CBr_4 in dried CH_3CN in the presence of $Ru(bpy)_3Cl_2$ (5.0 mol %) with visible light irradiation (blue LEDs, λ_{max} = 435 nm) for 6 hours. The corresponding 2-bromo-4-methoxyphenol (**2a**) was obtained in 78% yield (Table 1, entry 1), whereas 3-bromo-4-methoxyphenol was not observed. The optimization of the reaction conditions were conducted by screening selected solvents and the amount of the photoredox catalyst using **1a** as the representative substrate. As can be seen in Table 1, the solvent had a significant effect on the reaction efficiency. The reaction did not work well in DMF, MeOH, THF, CH_2Cl_2, EtOAc, CH_3CN with 10 equivalents of H_2O or 1,4-dioxane (Table 1, entries 5–11). The reaction in CH_3CN and open to air led to the highest yield, 94% (Table 1, entry 4), whereas the reaction conducted under N_2 or O_2, or in DMSO and open to air gave lower yields (Table 1, entries 2, 3, 12). Our final optimization showed that the reaction also provided comparable results when the catalyst loading was reduced to 3% or 1% (Table 1, entry 13). It should be pointed out that an exclusion of either the photocatalyst or the light source did not afford the desired product **2a**. Therefore, the reaction conditions of CBr_4 (1 equiv) in dried CH_3CN in the presence of $Ru(bpy)_3Cl_2$ (5.0 mol %) with visible light irradiation (blue LEDs, λ_{max} = 435 nm) and open to air were utilized to test the scope of the reaction.

With the optimized conditions in hand, we prepared a variety of phenols which were subjected to the photocatalytic reaction. In general, both electron-withdrawing and electron–donating

Table 1: Survey of the photocatalytic bromination reaction conditions.

1a **2a**

entry	conditions[a]	yield (%)[b]
1	CH_3CN, tube closed	78
2	CH_3CN, N_2	89
3	CH_3CN, O_2	46
4	**CH_3CN, open to air**	**94**
5	CH_3OH, open to air	23
6	CH_2Cl_2, open to air	0
7	DMF, open to air	63
8	THF, open to air	0
9	EtOAc, open to air	0
10	1,4-dioxane, open to air	0
11	CH_3CN + 10 equiv H_2O, open to air	0
12	DMSO, open to air	82
13	CH_3CN, $Ru(bpy)_3Cl_2$ (3%), open to air	86

[a]Reaction conditions: substrate **1a** (0.1 mmol), CBr_4 (0.1 mmol), $Ru(bpy)_3Cl_2$ (5 mol %), solvent (0.1 M), blue LEDs (1W). [b]Yields were determined by GC analysis.

groups were tolerated as substituents R^2 in this process. Interestingly, the substrates protected with TMS (trimethylsilyl), TBS (*tert*-butyldimethylsilyl), MOM (methoxymethyl) and THP (tetrahydropyranyl) groups led to the corresponding bromophenols via a Tandem bromination/deprotection reaction (Table 2, entries 1–8, 12, 13, and 15), among which the cases with substituents at *para*- and *ortho*-position afforded 2- and 4-bromophenol, respectively, in good to excellent yields (Table 2, entries 1–5 and 12). The compound substituted with a methoxy group at the *meta*-position (**1b**) led to both 2- and 4-bromophenols **2b** and **2b'** with a ratio of 2:1 (Table 2, entry 8). Without any substituent at the phenol moiety mono- and dibromophenols were obtained with a ratio of 3:2 (Table 2, entries 6 and 7). Notably, 1-bromonaphthalen-2-ol and 1-bromo-2-methoxynaphthalene could be prepared in good yields with high regioselectivity from TMS and methyl protected naphthalen-2-ol (Table 2, entries 13 and 14). The direct treatment of 3-methoxyphenol under the same reaction conditions afforded 2- and 4-bromo-3-methoxyphenol with a ratio of 3:2 in a synthetically acceptable yield (Table 2, entry 11). Phenols protected with Bn or Ms groups led to 2- and 4-bromophenol derivatives in excellent yields without the loss of Bn or Ms groups (Table 2, entries 9 and 10).

Table 2: Scope of the photocatalytic bromination of phenols.

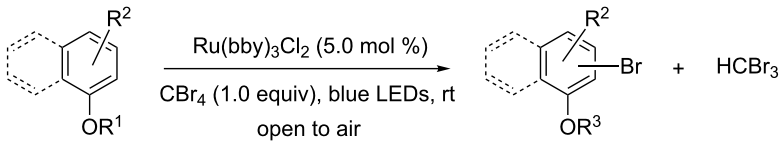

1 **2**

Entry	Substrate	Product	Yield (%)[a]
	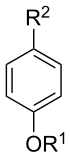	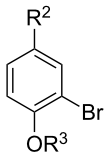	Conditions[b]
1	R^1 = TMS; R^2 = OMe; R^3 = H		88
2	R^1 = TMS; R^2 = Me; R^3 = H		69
3	R^1 = TMS; R^2 = Cl; R^3 = H		58
4	R^1 = TBS; R^2 = OMe; R^3 = H		85
5	R^1 = MOM; R^2 = Me; R^3 = H		97
	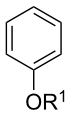	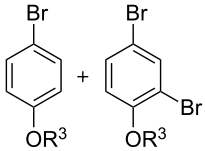	
6	R^1 = TMS; R^3 = H (3:2)[c]		79
7	R^1 = THP; R^3 = H (3:2)[c]		79
	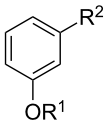	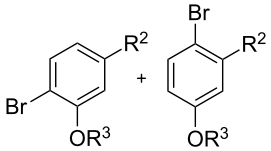	
8	R^1 = TMS; R^2 = OMe; R^3 = H (2:1)[c]		73
9	R^1 = Ms; R^2 = OMe; R^3 = Ms (5:1)[c]		95
10	R^1 = Bn; R^2 = OMe; R^3 = Bn (5:3)[c]		98
11	R^1 = H; R^2 = OMe; R^3 = H (3:2)[c]		40
12	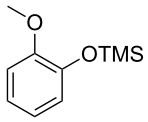	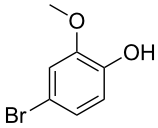	84
	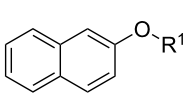	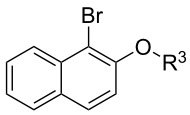	
13	R^1 = TMS; R^3 = H		76
14	R^1 = Me; R^3 = Me		98
15	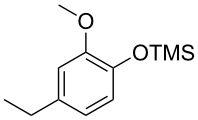	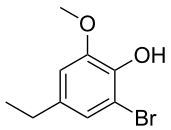	46

[a]Isolated yield based on complete consume of the starting material. [b]Reaction conditions: substrate **1** (0.1 mmol), CBr_4 (0.1 mmol), $Ru(bpy)_3Cl_2$ (5 mol %), dried CH_3CN, blue LEDs (1 W), open to air. [c]Ratio of the isomers in parentheses.

The bromination of phenols could be controlled by the amount of CBr_4. For example, when TMS protected 3-methoxyphenol was treated with 2 equivalents of CBr_4 under similar conditions (Table 2), a dibromophenol product was directly obtained in a high yield (95%) (Scheme 2), which also could be prepared from the same starting materials in two steps (Table 2).

We also conducted a control experiment by reacting stilbene with CBr_4 (1 equiv) in dry CH_3CN in the presence of $Ru(bpy)_3Cl_2$ (5.0 mol %) with visible-light irradiation (blue LEDs, λ_{max} = 435 nm) for 72 hours, which led to the *anti*-1,2-dibromo-1,2-diphenylethane in 92% yield. This result is in accordance with the direct bromination of stilbene from liquid bromine [47]. Based on this result, our protocol provides an easily manageable and environment-friendly pathway to the bromination of alkenes. We further examined the scope of the reaction, and the results are summarized in Scheme 3. The 1,2-dibromo products were obtained in moderate to high yields.

With the success of the bromination of phenols and alkenes, we further focused on the complementary bromination of diketones and cyclization reactions. The treatment of cyclohexane-1,3-dione (**5**) and (*E*)-4-(4-methoxyphenyl)but-3-en-1-ol (**7**) under the same reaction conditions led to 2,2-dibromocyclohexane-1,3-dione (**6**) and bromofuran compound **8** in 22% and 52% yield, respectively (Scheme 4). This outcome demonstrates the efficiency of the $Ru(bpy)_3Cl_2/CBr_4$ photocatalytic system. The stereochemistry of the bromofuran compound was determined by 2D NMR spectra.

Conclusion

In summary, we have developed a mild and operationally simple method for the in situ preparation of bromine utilizing a visible-light photoredox catalyst. The reaction proceeds with high chemical yield and regioselectivity for the bromination of phenols and alkenes. Further development of photoredox catalysis in the context of radical chemistry and its application in other reactions are currently underway in our laboratory.

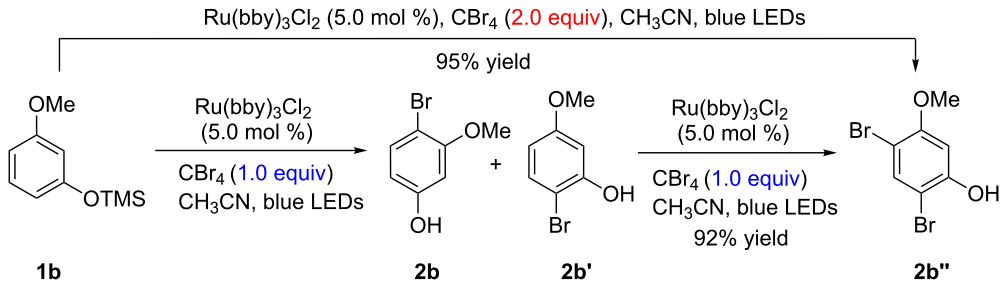

Scheme 2: Synthesis of dibromophenol product **2b"**.

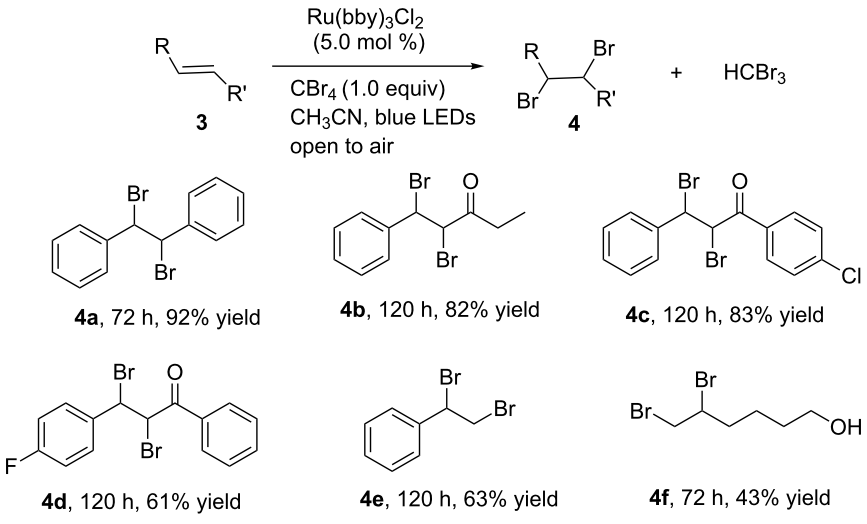

Scheme 3: Scope of the photocatalytic bromination of alkenes.

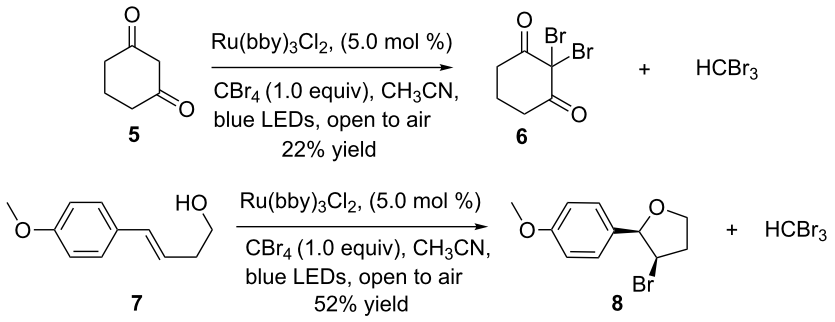

Scheme 4: Bromination of diketones and cyclization reactions.

Experimental

General procedure for the bromination of phenols and alkenes

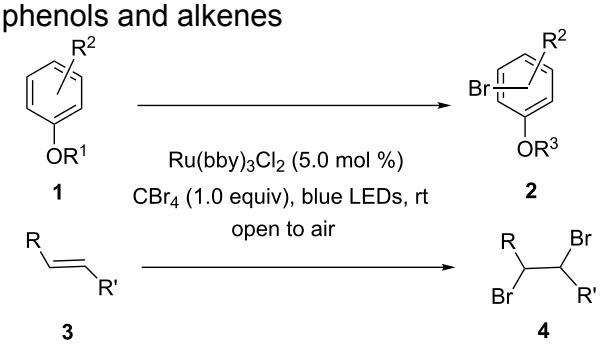

To a 10 mL round bottom flask equipped with a magnetic stir bar were added phenols or alkenes (0.1 mmol), CBr_4 (33 mg, 0.1 mmol), dry CH_3CN (1 mL) and $Ru(bpy)_3Cl_2$ (3.8 mg, 0.005 mmol). The mixture was irradiated with blue LEDs (1 W) at room temperature open to air until the starting material disappeared completely (monitored by TLC). After the reaction was completed, the solvent was concentrated in vacuo. The residue was purified by flash column chromatography to give the final product.

Bromination of diketones

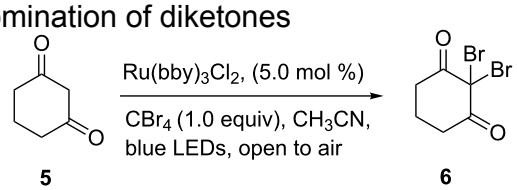

To a 10 mL round bottom flask equipped with a magnetic stir bar were added **5** (0.4 mmol), CBr_4 (133 mg, 0.4 mmol), dry CH_3CN (2 mL) and $Ru(bpy)_3Cl_2$ (15 mg, 0.02 mmol). The mixture was irradiated with blue LEDs (1 W) at room temperature open to air until the starting material was largely consumed (monitored by TLC). After the reaction was completed the solvent was concentrated in vacuo. The residue was purified by flash column chromatography to give the final product **6**.

Synthesis of bromofuran

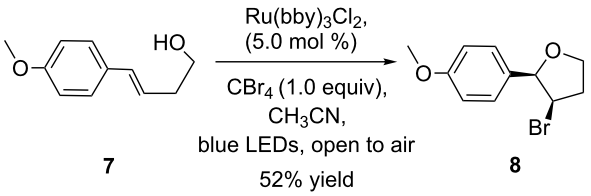

To a 10 mL round bottom flask equipped with a magnetic stir bar were added **7** (0.13 mmol), CBr_4 (43 mg, 0.13 mmol), LiBr (11 mg, 0.13 mmol), dry CH_3CN (1 mL) and $Ru(bpy)_3Cl_2$ (4.5 mg, 0.006 mmol). The mixture was irradiated with blue LEDs (1 W) at room temperature open to air until the starting material disappeared completely (monitored by TLC). After the reaction was completed the solvent was concentrated in vacuo. The residue was purified by flash column chromatography to give the final product **8**.

Supporting Information

Supporting Information File 1

^1H and ^{13}C NMR spectra for products.
[http://www.beilstein-journals.org/bjoc/content/supplementary/1860-5397-10-53-S1.pdf]

Acknowledgements

We are grateful for the financial supports from China NSFC (Nos. 21272047 and 21372055), SKLUWRE (No. 2012DX10), the Fundamental Research Funds for the Central Universities (Grant No. HIT.BRETIV.201310), and ZJNSF (No. LY12B02009).

References

1. Butler, A.; Walker, J. V. *Chem. Rev.* **1993,** *93,* 1937–1944. doi:10.1021/cr00021a014
2. Heck, R. F. *Org. React.* **1982,** *27,* 345–390.

3. Stille, J. K. *Angew. Chem., Int. Ed. Engl.* **1986,** *25,* 508–524. doi:10.1002/anie.198605081
4. Miyaura, N.; Suzuki, A. *Chem. Rev.* **1995,** *95,* 2457–2483. doi:10.1021/cr00039a007
5. Ma, D.; Cai, Q. *Acc. Chem. Res.* **2008,** *41,* 1450–1460. doi:10.1021/ar8000298
6. Mitchell, R. H.; Lai, Y.-H.; Williams, R. V. *J. Org. Chem.* **1979,** *44,* 4733–4735. doi:10.1021/jo00393a066
7. Carreno, M. C.; Garcia Ruano, J. L.; Sanz, G.; Toledo, M. A.; Urbano, A. *J. Org. Chem.* **1995,** *60,* 5328–5331. doi:10.1021/jo00121a064
8. Park, M. Y.; Yang, S. G.; Jadhav, V.; Kim, Y. H. *Tetrahedron Lett.* **2004,** *45,* 4887–4890. doi:10.1016/j.tetlet.2004.04.112
9. Wan, X.; Ma, Z.; Li, B.; Zhang, K.; Cao, S.; Zhang, S.; Shi, Z. *J. Am. Chem. Soc.* **2006,** *128,* 7416–7417. doi:10.1021/ja060232j
10. Song, B.; Zheng, X.; Mo, J.; Xu, B. *Adv. Synth. Catal.* **2010,** *352,* 329–335. doi:10.1002/adsc.200900778
11. Mei, T.-S.; Giri, R.; Maugel, N.; Yu, J.-Q. *Angew. Chem., Int. Ed.* **2008,** *47,* 5215–5219. doi:10.1002/anie.200705613
12. Castro, C. E.; Gaughan, E. J.; Owsley, D. C. *J. Org. Chem.* **1965,** *30,* 587–592. doi:10.1021/jo01013a069
13. Bora, U.; Bose, G.; Chaudhuri, M. K.; Dhar, S. S.; Gopinath, R.; Khan, A. T.; Patel, B. K. *Org. Lett.* **2000,** *2,* 247–249. doi:10.1021/ol9902935
14. Narender, N.; Mohan, K. V. V. K.; Reddy, R. V.; Srinivasu, P.; Kulkarni, S. J.; Raghavan, K. V. *J. Mol. Catal. A: Chem.* **2003,** *192,* 73–77. doi:10.1016/S1381-1169(02)00131-0
15. Adibi, H.; Hajipour, A. R.; Hashemi, M. *Tetrahedron Lett.* **2007,** *48,* 1255–1259. doi:10.1016/j.tetlet.2006.12.033
16. Yoon, T. P.; Ischay, M. A.; Du, J. *Nat. Chem.* **2010,** *2,* 527–532. doi:10.1038/nchem.687
17. Inagaki, A.; Akita, M. *Coord. Chem. Rev.* **2010,** *254,* 1220–1239. doi:10.1016/j.ccr.2009.11.003
18. Narayanam, J. M. R.; Stephenson, C. R. J. *Chem. Soc. Rev.* **2011,** *40,* 102–113. doi:10.1039/b913880n
19. Xuan, J.; Xiao, W.-J. *Angew. Chem., Int. Ed.* **2012,** *51,* 6828–6838. doi:10.1002/anie.201200223
20. Shi, L.; Xia, W. *Chem. Soc. Rev.* **2012,** *41,* 7687–7697. doi:10.1039/c2cs35203f
21. Prier, C. K.; Rankic, D. A.; MacMillan, D. W. C. *Chem. Rev.* **2013,** *113,* 5322–5363. doi:10.1021/cr300503r
22. Tucker, J. W.; Stephenson, C. R. J. *J. Org. Chem.* **2012,** *77,* 1617–1622. doi:10.1021/jo202538x
23. McNally, A.; Prier, C. K.; MacMillan, D. W. C. *Science* **2011,** *334,* 1114–1117. doi:10.1126/science.1213920
24. Nicewicz, D. A.; MacMillan, D. W. C. *Science* **2008,** *322,* 77–80. doi:10.1126/science.1161976
25. Nagib, D. A.; MacMillan, D. W. C. *Nature* **2011,** *480,* 224–228. doi:10.1038/nature10647
26. Condie, A. G.; González-Gómez, J. C.; Stephenson, C. R. J. *J. Am. Chem. Soc.* **2010,** *132,* 1464–1465. doi:10.1021/ja909145y
27. Narayanam, J. M. R.; Tucker, J. W.; Stephenson, C. R. J. *J. Am. Chem. Soc.* **2009,** *131,* 8756–8757. doi:10.1021/ja9033582
28. Dai, C.; Narayanam, J. M. R.; Stephenson, C. R. J. *Nat. Chem.* **2011,** *3,* 140–145. doi:10.1038/nchem.949
29. Ischay, M. A.; Lu, Z.; Yoon, T. P. *J. Am. Chem. Soc.* **2010,** *132,* 8572–8574. doi:10.1021/ja103934y
30. Ischay, M. A.; Anzovino, M. E.; Du, J.; Yoon, T. P. *J. Am. Chem. Soc.* **2008,** *130,* 12886–12887. doi:10.1021/ja805387f
31. Du, J.; Yoon, T. P. *J. Am. Chem. Soc.* **2009,** *131,* 14604–14605. doi:10.1021/ja903732v
32. Tucker, J. W.; Narayanam, J. M. R.; Krabbe, S. W.; Stephenson, C. R. J. *Org. Lett.* **2010,** *12,* 368–371. doi:10.1021/ol902703k
33. Furst, L.; Matsuura, B. S.; Narayanam, J. M. R.; Tucker, J. W.; Stephenson, C. R. J. *Org. Lett.* **2010,** *12,* 3104–3107. doi:10.1021/ol101146f
34. Maji, T.; Karmakar, A.; Reiser, O. *J. Org. Chem.* **2011,** *76,* 736–739. doi:10.1021/jo102239x
35. Lu, Z.; Shen, M.; Yoon, T. P. *J. Am. Chem. Soc.* **2011,** *133,* 1162–1164. doi:10.1021/ja107849y
36. Zhao, G.; Yang, C.; Guo, L.; Sun, H.; Chen, C.; Xia, W. *Chem. Commun.* **2012,** *48,* 2337–2339. doi:10.1039/c2cc17130a
37. Sun, H.; Yang, C.; Gao, F.; Li, Z.; Xia, W. *Org. Lett.* **2013,** *15,* 624–627. doi:10.1021/ol303437m
38. Zhu, S.; Das, A.; Bui, L.; Zhou, H.; Curran, D. P.; Rueping, M. *J. Am. Chem. Soc.* **2013,** *135,* 1823–1829. doi:10.1021/ja309580a
39. Xie, J.; Xue, Q.; Jin, H.; Li, J.; Cheng, Y.; Zhu, C. *Chem. Sci.* **2013,** *4,* 1281–1286. doi:10.1039/c2sc22131d
40. Liu, Q.; Li, Y.-N.; Zhang, H.-H.; Chen, B.; Tung, C.-H.; Wu, L.-Z. *Chem.–Eur. J.* **2012,** *18,* 620–627. doi:10.1002/chem.201102299
41. Chen, M.; Huang, Z.-T.; Zheng, Q.-Y. *Chem. Commun.* **2012,** *48,* 11686–11688. doi:10.1039/c2cc36866h
42. Cai, S.; Zhao, X.; Wang, X.; Liu, Q.; Li, Z.; Wang, D. Z. *Angew. Chem., Int. Ed.* **2012,** *51,* 8050–8053. doi:10.1002/anie.201202880
43. Zou, Y.-Q.; Lu, L.-Q.; Fu, L.; Chang, N.-J.; Rong, J.; Chen, J.-R.; Xiao, W.-J. *Angew. Chem., Int. Ed.* **2011,** *50,* 7171–7175. doi:10.1002/anie.201102306
44. Shih, H.-W.; Vander Wal, M. N.; Grange, R. L.; MacMillan, D. W. C. *J. Am. Chem. Soc.* **2010,** *132,* 13600–13603. doi:10.1021/ja106593m
45. Nguyen, J. D.; Tucker, J. W.; Konieczynska, M. D.; Stephenson, C. R. J. *J. Am. Chem. Soc.* **2011,** *133,* 4160–4163. doi:10.1021/ja108560e
46. Wallentin, C.-J.; Nguyen, J. D.; Finkbeiner, P.; Stephenson, C. R. J. *J. Am. Chem. Soc.* **2012,** *134,* 8875–8884. doi:10.1021/ja300798k
47. Ma, K.; Li, S.; Weiss, R. G. *Org. Lett.* **2008,** *10,* 4155–4158. doi:10.1021/ol801327n

License and Terms

Beilstein Journal of Organic Chemistry

Metal and metal-free photocatalysts: mechanistic approach and application as photoinitiators of photopolymerization

Jacques Lalevée[*1], Sofia Telitel[1], Pu Xiao[1], Marc Lepeltier[2], Frédéric Dumur[3,4,5], Fabrice Morlet-Savary[1], Didier Gigmes[3] and Jean-Pierre Fouassier[6]

Full Research Paper

Open Access

Address:
[1]Institut de Science des Matériaux de Mulhouse IS2M – UMR CNRS 7361 –UHA; 15 rue Jean Starcky, 68057 Mulhouse Cedex, France, [2]Institut Lavoisier de Versailles, UMR 8180 CNRS, Université de Versailles Saint-Quentin en Yvelines, 45 avenue des Etats-Unis, 78035 Versailles Cedex, France, [3]Aix-Marseille Université, CNRS, Institut de Chimie Radicalaire, UMR 7273, F-13397 Marseille, France, [4]Univ. Bordeaux, IMS, UMR 5218, F-33400 Talence, France, [5]CNRS, IMS, UMR 5218, F-33400 Talence, France and [6]formerly: University of Haute Alsace/ENSCMu, 3 rue Alfred Werner, 68093 Mulhouse Cedex, France

Email:
Jacques Lalevée* - jacques.lalevee@uha.fr

* Corresponding author

Keywords:
LEDs; photoinitiators; photopolymerization; photoredox catalysis

Beilstein J. Org. Chem. **2014,** *10,* 863–876.
doi:10.3762/bjoc.10.83

Received: 17 January 2014
Accepted: 21 March 2014
Published: 15 April 2014

This article is part of the Thematic Series "Organic synthesis using photoredox catalysis".

Guest Editor: A. G. Griesbeck

Abstract

In the present paper, the photoredox catalysis is presented as a unique approach in the field of photoinitiators of polymerization. The principal photocatalysts already reported as well as the typical oxidation and reduction agents used in both reductive or oxidative cycles are gathered. The chemical mechanisms associated with various systems are also given. As compared to classical iridium-based photocatalysts which are mainly active upon blue light irradiation, a new photocatalyst Ir(piq)$_2$(tmd) (also known as bis(1-phenylisoquinolinato-*N*,*C*$^{2'}$)iridium(2,2,6,6-tetramethyl-3,5-heptanedionate) is also proposed as an example of green light photocatalyst (toward the long wavelength irradiation). The chemical mechanisms associated with Ir(piq)$_2$(tmd) are investigated by ESR spin-trapping, laser flash photolysis, steady state photolysis, cyclic voltammetry and luminescence experiments.

Introduction

Photoredox catalysis is now well-known and largely used in organic synthesis, especially in the development of sustainable radical-mediated chemical processes under very soft irradiation conditions (e.g., household fluorescence or LED bulbs, halogen lamps, sunlight, Xe lamp), e.g., enantioselective alkylation, cycloaddition, etc. [1-14]. Ruthenium- and iridium-based

organometallic complexes are mostly employed as radical sources: they exhibit an excellent visible-light absorption, long lived excited states and suitable redox potentials and they work through either an oxidation or a reduction cycle [1-12]. To avoid, however, the high cost, potential toxicity and limited availability of these structures, metal-free organic dye compounds (e.g., Eosin-Y, Nile Red, Alizarine Red S, perylene derivative or Rhodamine B etc.) were recently proposed for cooperative asymmetric organophotoredox catalysis [13,14].

Photoredox catalysis was then introduced into the polymer photochemistry field (area) in the very past years (see a review in [15-22]). Indeed, in this area, free-radical photopolymerization (FRP, Scheme 1, reactions 1 and 2), cationic photopolymerization (CP, Scheme 1, reactions 3 and 4), free-radical promoted cationic photopolymerization (FRPCP, Scheme 1, reactions 5–7) or acid and base-catalyzed photocrosslinking (reactions 8 and 9) are initiated using photoinitiators (PI) which generate reactive species (radicals, cations, anions, radical cations, acids, bases). These PIs are often incorporated into multicomponent photoinitiating systems (PIS) where they primarily react with the other concomitant reagents or additives.

PIs and PISs have been extensively developed both in industrial R&D and academic laboratories [15-40]. PIs are usually organic molecules that are consumed during the light exposure [15-40]. The use of organometallic compounds as PIs was reported many years ago (see a review in [41]) and reintroduced in some recent papers dealing with, e.g., Cr, Ti, Fe, Rh, W, Pt, Ru, Ir, Zn, Zr-based derivatives [42-44]. On this occasion, it appeared that a photoredox catalysis behavior (allowing a PI regeneration while keeping a high reactivity/efficiency) can be introduced through a suitable selection of the PIs and PISs [45-55].

This approach opened up [45-53] a new way for the design of a novel high performance class of PIs for FRP and FRPCP (where the photoinitiator is now referred as a photoinitiator catalyst PIC). It brings, among others, the following novel properties [45-55]:

- Almost no photoinitiator is consumed.
- Since the spectral photosensitivity extends now from the UV to the visible, laser excitation in the purple, blue, yellow, green or red is feasible.
- Low light intensities (as delivered, e.g., by household lamps and LED bulbs) can be used; this is a catalytic process without loss of efficiency with irradiation.
- Photopolymerization under sunlight becomes reachable.
- The production of the radical or cationic initiating species for the FRP of acrylates or the FRPCP of epoxides, respectively, is quite easy; polymerization of sustainable monomers can also be achieved (e.g., epoxidized soybean oil).
- A possible dual behavior (simultaneous generation of radicals and cations that ensure the formation of, e.g., an epoxy/acrylate interpenetrated network IPN) is achieved.

Examples of PICs proposed by us in the photopolymerization reactions are depicted in Figure 1 and Figure 2 (for metal based PICs and metal free PICs, respectively) [45-55]. Their reactivity parameters (redox potentials, excited state lifetimes) are given in the associated references. These PICs are typically used (see below) in combination with various additives (see Figure 3 below) in three-component photoinitiating systems, e.g., based PIC/iodonium salt (or sulfonium salt)/tris(trimethylsilyl)silane (or *N*-vinylcarbazole) or PIC/amine/alkyl halide. Also, relatively high intensity light sources (Hg, Xe or Hg–Xe lamps, laser diodes) can be obviously employed.

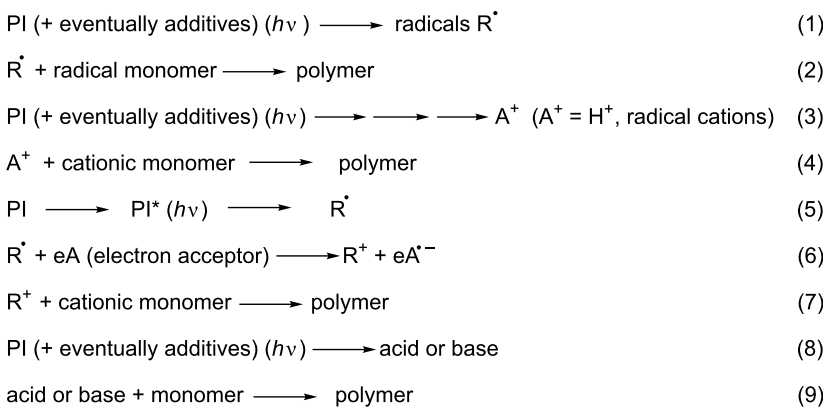

Scheme 1: Examples of photoinitiating systems.

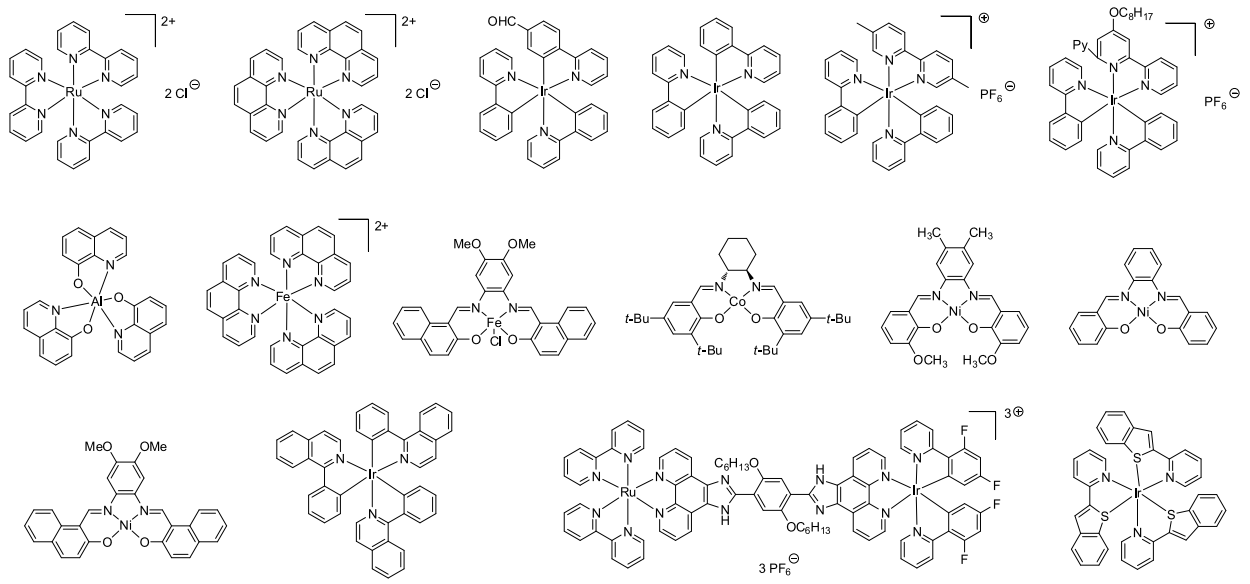

Figure 1: Previously reported PIC (based on metal complexes) [45-52].

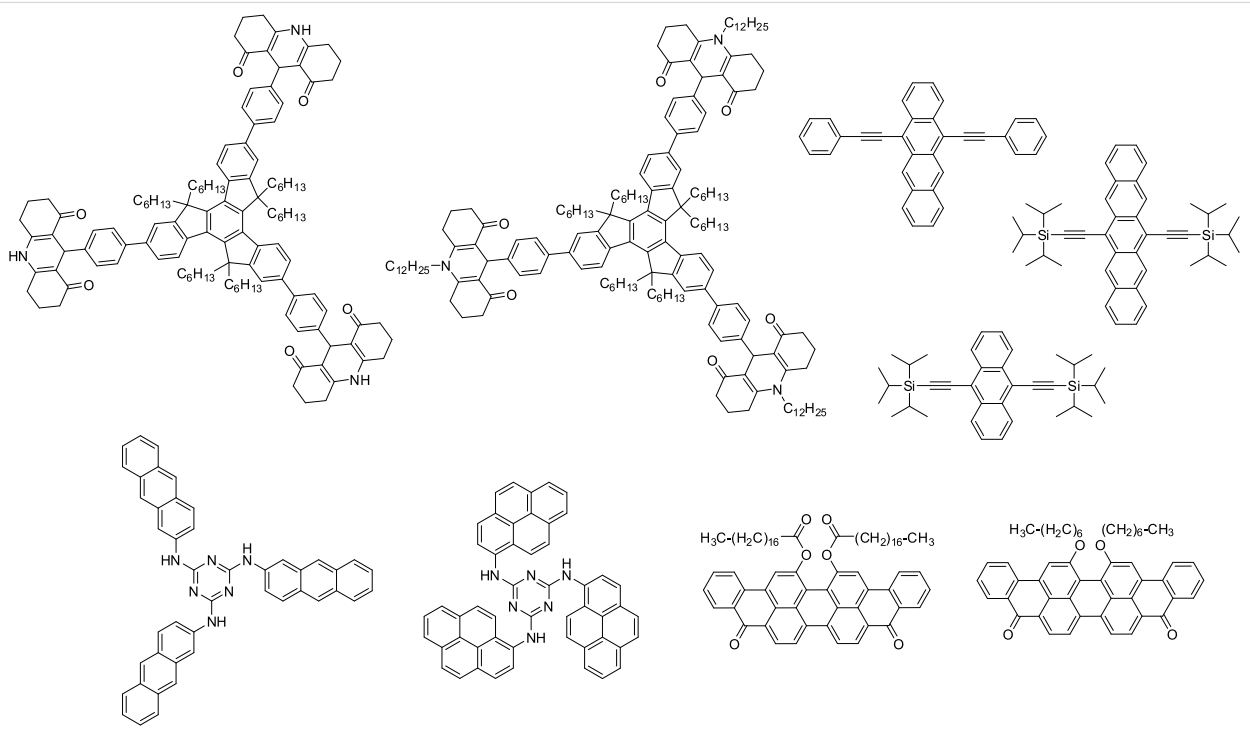

Figure 2: Previously reported PIC (metal free organic molecules) [54,55].

However, and with more interest, very soft irradiation conditions (using, e.g., household fluorescence or LED bulbs, halogen lamps or even sunlight) are also suitable to polymerize radical and cationic monomers (see Figure 4 below) under polychromatic or monochromatic lights in the 350–700 nm and to get tack free coatings.

The present paper will i) review the various possible mechanistic schemes using metal and metal free oxidizable or reducible PICs for FRP, CP and FRPCP, ii) show examples of reported PICs, iii) discuss the encountered mechanisms in various PIC based photoinitiating systems, iv) highlight some examples of high performance PISs and v) present the effi-

ciency of a novel PIC in photopolymerization reactions as well as the excited state processes involved in the photoinitiating systems used.

Experimental

i) Compounds: The synthesis of bis(1-phenylisoquinolinato-$N,C^{2'}$)iridium(2,2,6,6-tetramethyl-3,5-heptanedionate) is described below (following a published procedure). All reagents and solvents were purchased from Aldrich or Alfa Aesar and used as received without further purification.

ii) Irradiation sources: Several lights were used: 1) polychromatic light from a halogen lamp (Fiber-Lite, DC-950 – incident light intensity: $I_0 \approx 12$ mW/cm^2; in the 370–800 nm range); 2) monochromatic light delivered by a laser diode at 532 nm ($I_0 \approx 100$ mW/cm^2) and 3) LEDs at 514 nm.

iii) Free radical photopolymerization (FRP) of acrylates: The experiments were carried out in laminated conditions or under air. The prepared formulations deposited on a BaF_2 pellet (25 µm thick) were irradiated (see the irradiation devices). The evolution of the double bond content was continuously followed by real time FTIR spectroscopy (JASCO FTIR 4100) at about 1630 cm^{-1} as in [15].

iv) The ring opening polymerization of epoxides: The photosensitive formulations were deposited (25 µm thick) on a BaF_2 pellet under air. The evolution of the epoxy group content was continuously followed by real time FTIR spectroscopy (JASCO FTIR 4100) at about 790 cm^{-1}, respectively [15].

v) ESR spin trapping (ESR-ST) experiments: The ESR-ST experiments were carried out using an X-band spectrometer (MS 400 Magnettech). The radicals were produced at room temperature upon a light exposure (see the irradiation devices) under N_2 and trapped by phenyl-*N*-*tert*-butylnitrone (PBN) according to a procedure described in detail in [15]. The ESR spectra simulations were carried out with the PEST WINSIM program.

Results and Discussion

Possible usable strategies for the design of PICs in the photopolymerization area

Oxidizable photoinitiator catalysts

Using oxidizable photoinitiator catalysts, three possibilities can be briefly considered. The simplest first situation is depicted in Scheme 2. Through light excitation in the presence of an electron acceptor (eA), the oxidized form of the photoinitiator catalyst (PIC$^{\bullet+}$) is produced. A E-Z compound should be added to recover the PIC in its ground state and generate a radical and a cation. Suitable E-Z or E-Z$^-$ structures have to be designed.

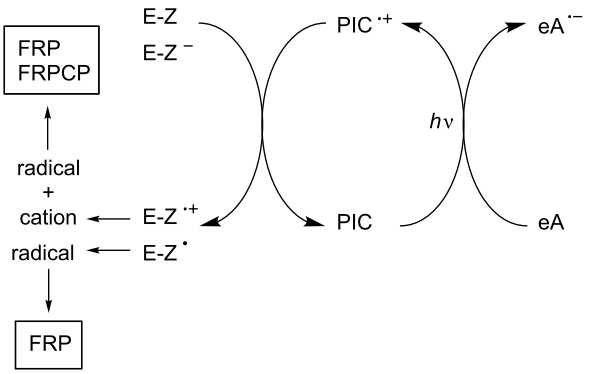

Scheme 2: Reaction mechanisms for the three-component system PIC/eA/E-Z.

A second situation is shown in Scheme 3. It consists in using the radical formed from the eA radical anion to recover the PIC. Both a radical and a cation are thus generated. The easiness of the radical → cation step as well as the nature of the cationic centers remains connected with the nature of eA. The key point is to find a radical directly formed through this way and that can be easily oxidized by PIC$^{\bullet+}$.

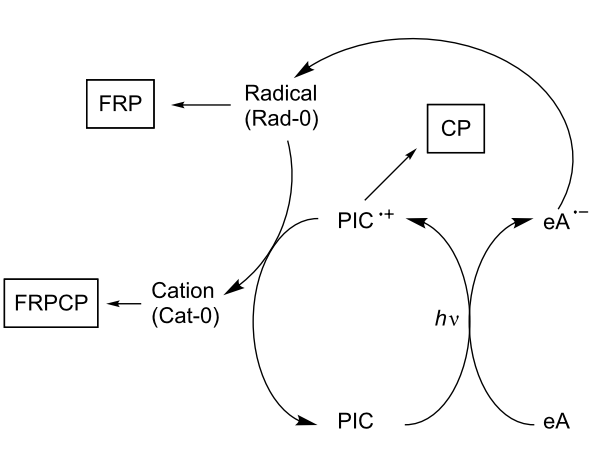

Scheme 3: Reaction mechanisms for the two-component system PIC/eA.

Another situation is encountered in Scheme 4 where the initially formed radical Rad-m (from the decomposition of a suitable electron donor as before) is converted into another radical Rad-1 (upon addition of a convenient radical source), this novel radical being able to favorably react with PIC$^{\bullet+}$. Such a process should be likely more feasible.

According to these different Schemes, both FRP, CP and FRPCP can be initiated from the free radicals and cations generated. In these three situations, as a function of its structure, the PIC radical cation PIC$^{\bullet+}$ can behave as an initiating species.

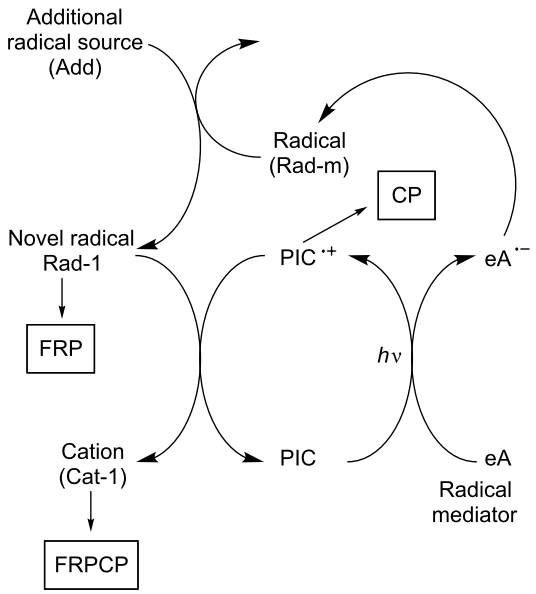

Scheme 4: Reaction mechanisms for the system PIC/eA/add.

Reductible photoinitiator catalysts

Scheme 5 shows a situation where the PIC is reduced through a photoinduced electron transfer with an electron donor eD. A suitable B-Y (or B-Y^+) compound leads to a regeneration of PIC and the formation of a radical and an anion (or a radical and a neutral product). Therefore, FRP can be achieved.

Examples of PICs in the photopolymerization area

Examples of PICs are shown above in Figure 1 and Figure 2. Typical oxidation and reduction agents used in catalytic (oxidation and reduction) cycles are gathered in Figure 3; the monomers that have been polymerized in previous works are given in Figure 4 [45-55].

Oxidizable photoinitiator catalysts

The oxidation of a PIC is quite easily realized. For example, the excitation of $Ru(bpy)_3^{2+}$ (with bpy = bipyridine) in the presence of an iodonium salt (e.g., Ph_2I^+) as eA leads to $Ru(bpy)_3^{3+}$. However, very few systems involving a E-Z structure or a E-Z anion (as suggested in Scheme 2) and allowing a regeneration of a ground state PIC together with efficient

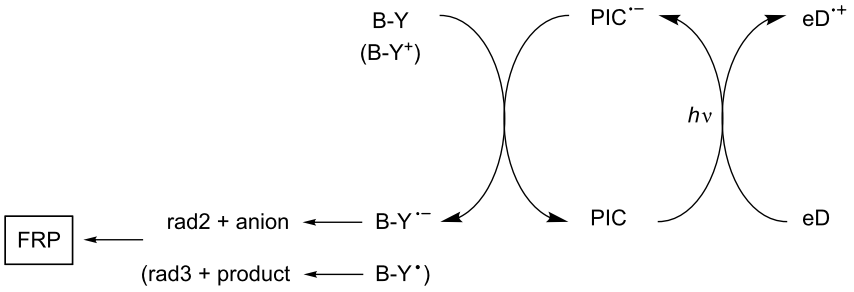

Scheme 5: Reaction mechanisms for the system PIC/eD/B-Y.

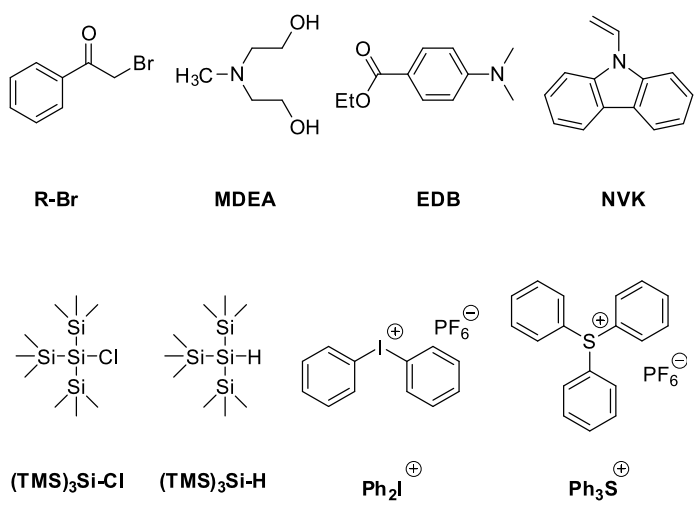

Figure 3: Typical oxidation and reduction agents used through the photoredox catalysis approach in polymerization photoinitiating systems.

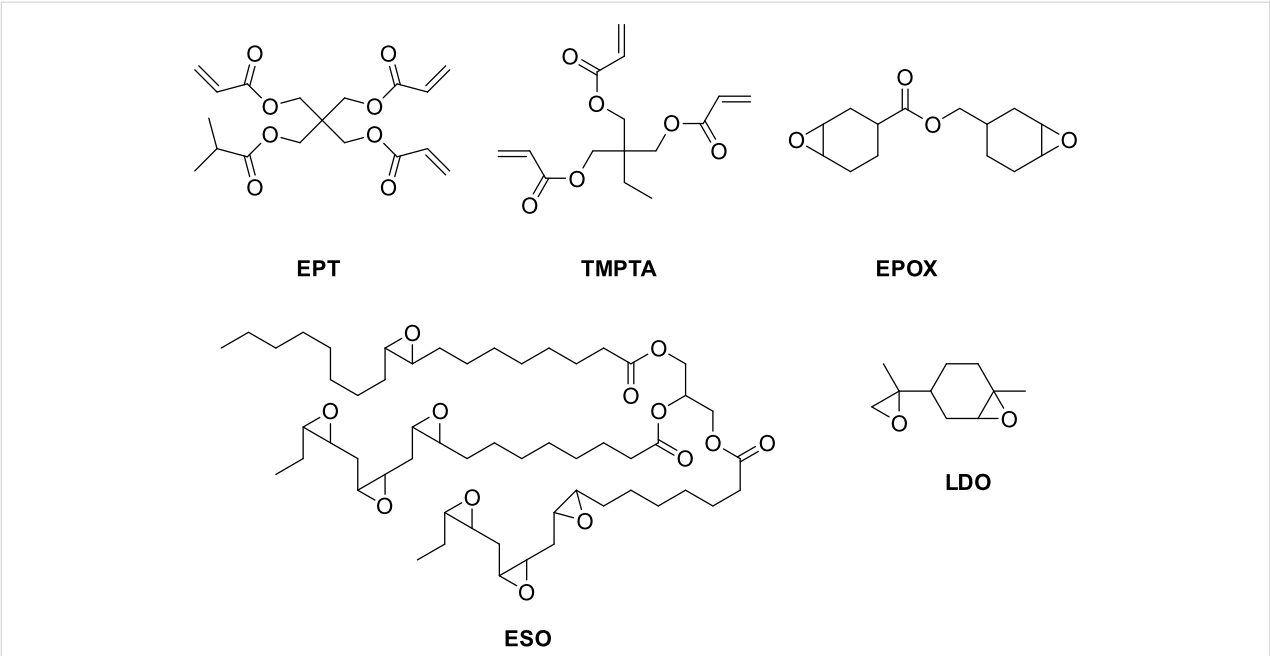

Figure 4: Typical monomers that can be polymerized through a photoredox catalysis approach.

radical and cationic initiating species for FRP/CP/FRPCP has been reported yet [45-55].

Interestingly, when using a Ru complex as PIC and Ph_2I^+ salt as eA as above, a phenyl radical $Ph^\bullet$ is formed (Scheme 3). Unfortunately, the oxidation reaction of $Ph^\bullet$ by $PIC^{\bullet+}$ is rather hard [45-52] and such a system does not work. Sulfonium salts were also used as eA but the reactivity is lower than that for iodonium salts (see below) [56].

A typical efficient system based on Scheme 4 involving $Ru(bpy)_3^{2+}$ as PIC, Ph_2I^+ as eA and a silane R_3SiH (e.g., tris(trimethylsilyl)silane TTMSS) as Add is detailed in Scheme 6. A phenyl radical is generated (previously noted Rad-m in Scheme 4). A silyl radical $R_3Si^\bullet$ (noted Rad-1 above) and a silylium R_3Si^+ are formed through a subsequent $Ph^\bullet$/R_3SiH hydrogen abstraction and $R_3Si^\bullet$/$PIC^{\bullet+}$ interaction, respectively (the eA serves both as an electron donor and a radical mediator source) [45-52]. The Ph_2I^+/$R_3Si^\bullet$ interaction increases

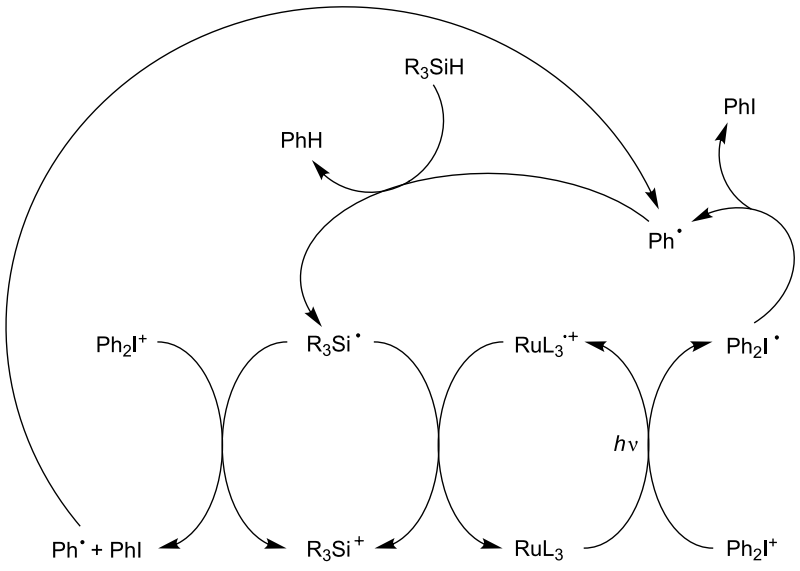

Scheme 6: Reaction mechanisms for the system $Ru(bpy)_3^{2+}$/Ph_2I^+/R_3SiH.

the yields in both phenyl radicals and silylium species [45-52]. The nature of the PIC is responsible for the absorption properties. Interestingly, whatever the PIC, the nature of the cation is only dependent of the choice of Add. The three-component system behaves here as an efficient dual radical/cation source. Moreover, as already known [57], the introduction of the silane also reduces the oxygen inhibition of the radical stages of the FRP and FRPCP reactions.

Many photoinitiating systems have been designed on the basis of Scheme 6 [45-52]. Ruthenium and iridium-containing PICs are relatively well known and a large variety of derivatives have been recently tested in the photopolymerization area. Thus, more or less successful attempts using Fe, Pt, Ni, Zn-based complexes have been also recently reported [56,58-60].

Other examples of eA and Add are also available. In some cases, a sulfonium salt (e.g., a triphenylsulfonium salt) can be introduced instead of the iodonium salt (Scheme 7) [56].

The silane has been also changed for *N*-vinylcarbazole NVK (Scheme 8). The phenyl radical adds to the NVK double bond and the resulting radical is electron rich and can be easily oxidized. NVK is a cheaper additive than silane (R_3SiH) and exhibits a relatively similar performance in photoinitiating systems of cationic polymerization [45-52,54,55].

Examples of metal-free pure organic PICs for FRP and FRPCP have also been very recently reported [54,55,61,62]. For example, they involve a violanthrone dye Vi [61,62] or an anthracene derivative (e.g. bis[(triisopropylsilyl)ethynyl]-anthracene) [54,55] as PIC, Ph_2I^+ as eA and TTMSS as Add (see the simplified Scheme 9 based on Scheme 6). Using violanthrone-79/Ph_2I^+/TTMSS allowed, for the first time, the formation of an initiating cationic species under a red laser line exposure at 635 nm. This result was very important as cationic polymerization in these irradiation conditions was not possible previously. Changing Vi or the anthracene derivative for a hydrocarbon (e.g. pyrene, naphthacene, pentacene) allows a tunable absorption of the system from 400 nm to 650 nm: exposure of the hydrocarbon/Ph_2I^+/TTMSS system to soft purple (405 nm), blue (457, 462 or 473 nm), green (514, 532 nm), yellow (591 nm) or red (630, 635 nm) LED bulbs or laser diodes becomes successful.

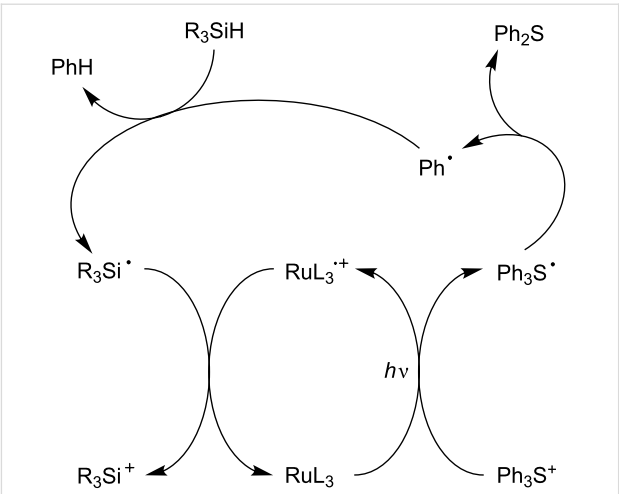

Scheme 7: Reaction mechanisms for the Ru(ligand)$_3^{2+}$/Ph_3S^+/R_3SiH system.

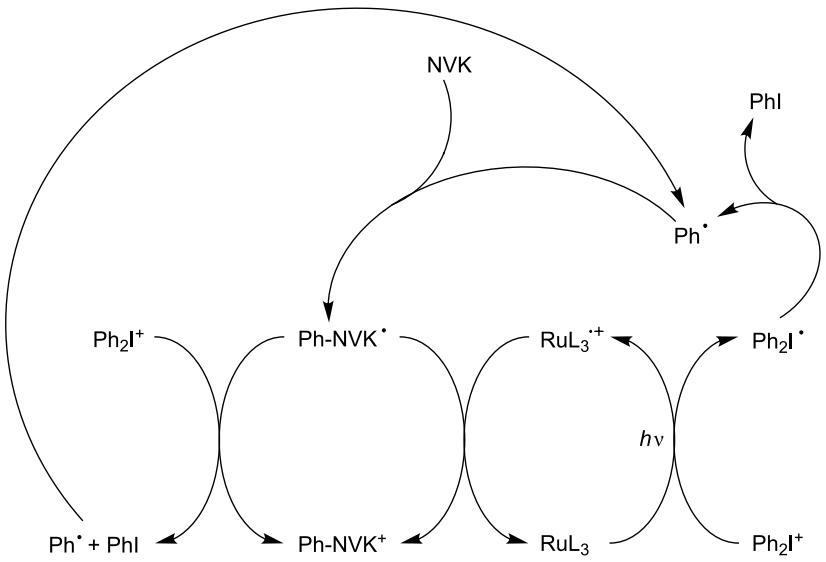

Scheme 8: Reaction mechanisms for the Ru(ligand)$_3^{2+}$/Ph_2I^+/NVK system upon visible lights.

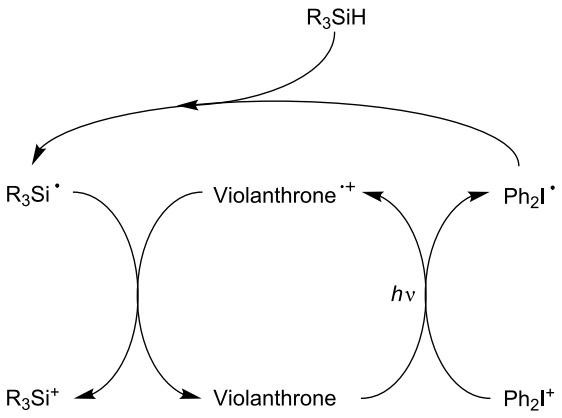

Scheme 9: Reaction mechanisms for the violanthrone/Ph_2I^+/TTMSS (R_3SiH) system upon red lights.

In rare examples, the PIC/methyldiethanolamine MDEA/phenacyl bromide R-Br (that usually operates through a reductive cycle; see below) works according to an oxidative cycle (Scheme 10). This is the case when the PIC stands for a truxene-acridinedione derivative Tr-AD (this is one of the possible examples for Scheme 2) [63]. For these PICs, the interaction of the excited states of Tr-AD with R-Br is much more favorable than the interaction with the amine.

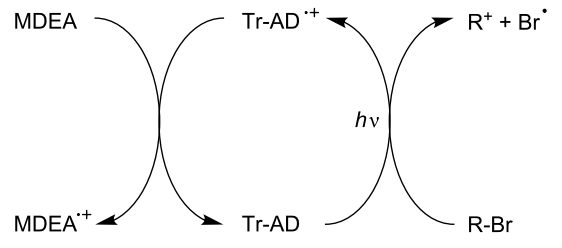

Scheme 10: Reaction mechanisms for the Tr-AD/R-Br/MDEA system upon visible lights.

Recently, an iridium complex ($Ir(ppy)_3$) (with ppy = 2-phenylpyridine) was proposed for the controlled photopolymerization reactions through a photoATRP process based on a photoredox catalysis approach (oxidative cycle; Scheme 11) [64].

All these described systems, producing radicals, cations or radical cations, allow efficient CP and FRPCP of cationic monomers, FRP of acrylates, simultaneous radical/cationic polymerization of epoxide/acrylate blend. The reactions can be carried out (see in [45-55]) in formulations containing multifunctional synthetic epoxides, acrylates, monomers/oligomers or epoxide/acrylate blends (renewable raw or modified materials are usable to some extent) with lights extending from the

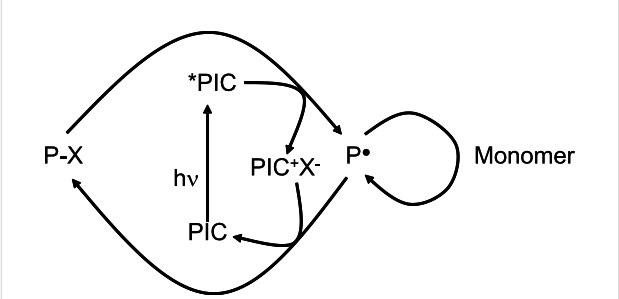

Scheme 11: The photoredox catalysis for controlled polymerization reactions.

UV to the red, using polychromatic or monochromatic light sources, even with low intensity of light emission (sun, household devices).

Reductible photoinitiator catalysts

Reported systems based on a reductive cycle are mainly based on Ru complexes [45-53]. Such a reductible PIC was first mentioned in FRP (Scheme 12) in a system composed of a Ru complex as PIC, an amine (methyldiethanolamine, MDEA) as an electron/proton donor and a phenacyl bromide R-Br [45]. In this mechanism, a reduced form of the Ru complex is formed (e.g., $Ru(bpy)_3^+$) and a phenacyl radical is produced upon the subsequent cleavage of the phenacyl halide radical anion. Later on, other amines (*N*,*N*-diisopropylethylamine, *N*,*N*-dimethylformamide) and bromides (ethyl 2-bromoisobutyrate, benzyl bromide) were proposed for the photocatalytic radical polymerization of various methacrylates [53]. Ir complexes can also be used.

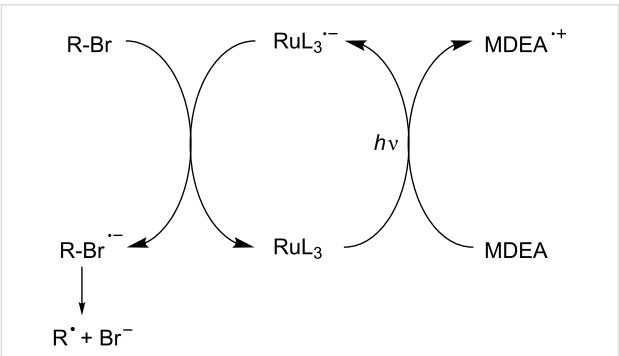

Scheme 12: Reaction mechanisms for the $Ru(ligand)_3^{2+}$/MDEA/R-Br system upon visible lights.

As only carbon centered radicals can be generated in Scheme 12, the change of the phenacyl bromide for a compound being able to generate more efficient radicals towards the addition to double bonds was tentatively achieved in the Ru complex/amine (ethyl diaminoethylbenzoate)/chlorosilane (e.g.,

$(TMS)_3SiCl$) system (see Scheme 12 and change R-Br and MDEA for $(TMS)_3SiCl$ and EDB, respectively); the performance in FRP remains unfortunately rather low [56]. Despite the presence of aminoalkyl and silyl initiating radicals (known as very reactive radicals towards the addition process onto acrylate double bond [65]), a lower reactivity of $(TMS)_3SiCl$ towards $PIC^{\bullet -}$ or/and a lower ability of the $(TMS)_3SiCl^{\bullet -}$ radical anion to decompose into a silyl radical and a chlorine anion likely play a detrimental role. Bromosilanes might be considered but they are not easily accessible.

Works using metal-free PIC proceeding through a reduction cycle have been recently achieved in FRP for the first time [54,55]: they involve hydrocarbon derivatives (e.g., pyrene, naphtacene, pentacene), an amine (e.g., ethyl dimethylaminobenzoate) and an alkyl halide (e.g., phenacyl bromide); the mechanism is similar to that shown in Scheme 12. As above, a tunable absorption of the system is achieved by carefully selecting the hydrocarbon (the system is sensitive to lights ranging from 300 to 670 nm) [54,55]. Other colored PICs might be dyes (as suggested in experiments for organic synthesis purposes [54-56]) but preliminary experiments using common dyes such as Eosin suggest that their behavior as PICs is not straightforward. The redox processes with organic dyes are not always fully reversible: this plays a detrimental role in the catalytic cycle with a lost of the efficiency through a PIC degradation.

A striking example concerns the use of a Ru complex ($Ru(bpy)_3^{2+}$) as PIC which is reduced here into $Ru(bpy)_3^{+}$ although as shown above, it usually works through an oxidation cycle [61,62]. A violanthrone derivative (violanthrone-79) is employed as eD and Ph_2I^+ as $B\text{-}Y^+$ (see Scheme 5); TTMSS is added. This multicomponent system works according to the detailed Scheme 12. A phenyl radical is produced from $B\text{-}Y^{\bullet}$ (= $Ph_2I^{\bullet}$). As shown before, the silane ensures the formation of $R_3Si^{\bullet}$ and R_3Si^+ (Scheme 13), respectively [45-52]. This is presumably the most famous example so far for the generation of an initiating cation under a green laser line at 532 nm; the photosensitivity is extremely high.

A more complicated situation has also been found in some PIC/amine/alkyl halide system where both a reduction and an oxidation cycle simultaneously operate, e.g., in Michler's ketone derivative MK/amine AH (e.g., MDEA)/chlorotriazine Tz-Cl (Scheme 14) [66].

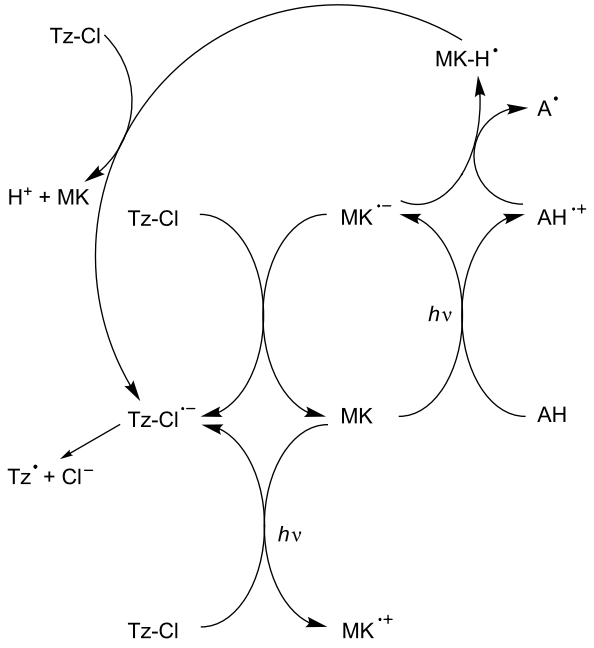

Scheme 14: Reaction mechanisms for the MK/amine/triazine system upon visible lights.

All these reactions allowed the radical photopolymerization of formulations containing multifunctional synthetic acrylates using UV to red lights delivered by low intensity sources.

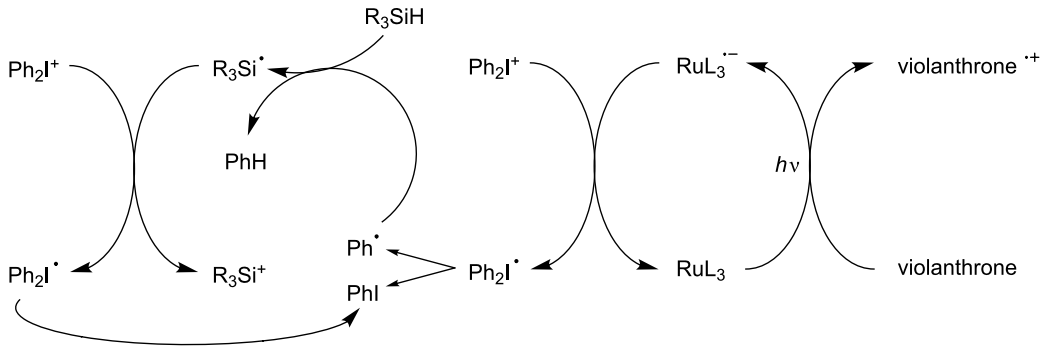

Scheme 13: Reaction mechanisms for the Violanthrone/$Ru(ligand)_3^{2+}$/Ph_2I^+/R_3SiH system upon visible lights.

A new PIC based on a panchromatic iridium complex and the associated performance in the photopolymerization area

There is still a need for the development of new PICs with i) improved light absorption properties and ii) high reactivity. These new PICs can be highly worthwhile for the use of very soft irradiation conditions. For example, the actual Ir and Ru-based PICs are mainly characterized by a blue light absorption and are operative in the 400–480 nm spectral range, i.e., the well-known and commercially available Ir derivative $Ir(ppy)_3$ (tris[2-phenylpyridinato-C^2,N]iridium(III)) is characterized by an intense absorption at 370 nm and exhibits an only moderate absorption at $\lambda > 400$ nm. Among others, the design of green light sensitive Ir complexes is an interesting challenge. This is the reason why the new Ir based PIC (bis(1-phenylisoquinolinato-N,$C^{2'}$)iridium(2,2,6,6-tetramethyl-3,5-heptanedionate) noted $Ir(piq)_2(tmd)$; Figure 5), already synthesized in [67] but never used as PIC in photoinitiating systems is presented here.

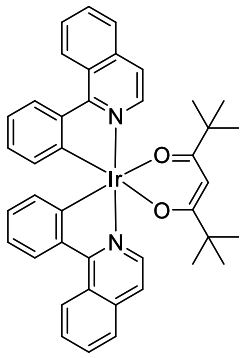

Figure 5: The new proposed PIC ($Ir(piq)_2(tmd)$).

Indeed, the visible light absorption properties of $Ir(piq)_2(tmd)$ are much better than those of $Ir(ppy)_3$ (Figure 6). Remarkably, $Ir(piq)_2(tmd)$ is perfectly adapted for applications under green light exposure (LED bulb at 514 nm or a laser diode at 532 nm) and exhibits an almost panchromatic behavior in the 400–650 nm range.

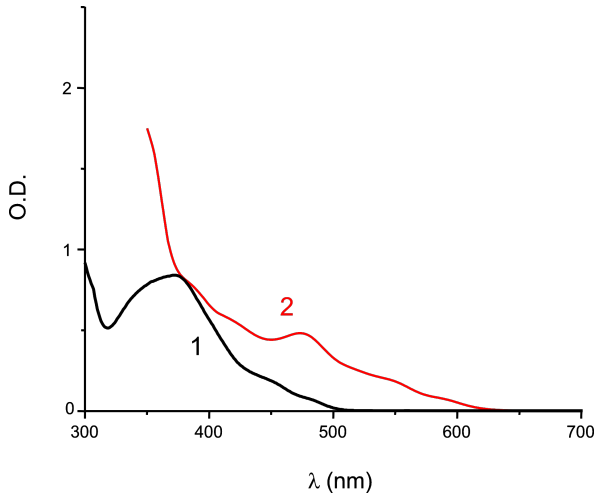

Figure 6: UV–visible light absorption spectra for $Ir(piq)_2(tmd)$ (2) and $Ir(ppy)_3$ (1); solvent: acetonitrile.

The PIC/Ph_2I^+/NVK system

The photochemical properties of $Ir(piq)_2(tmd)$

A triplet-state lifetime of 1.1 µs has been determined for $Ir(piq)_2(tmd)$ by laser flash photolysis experiments. A relatively similar lifetime (1.3 µs) was previously measured for $^3Ir(ppy)_3$ [68]. Such long lifetimes for triplet states are important in photoredox catalysis to ensure an efficient quenching by the oxidation agents.

$Ir(piq)_2(tmd)$ is characterized by an oxidation potential of 0.67 V vs SCE (Figure 7A); its triplet-state energy level ($E_T \sim 2.07$ eV) was determined from absorption/luminescence experiments (Figure 7B). From these data, a favorable $^3Ir(piq)_2(tmd)/Ph_2I^+$ oxidation process can be expected, i.e., the free energy change ΔG for the corresponding electron transfer is

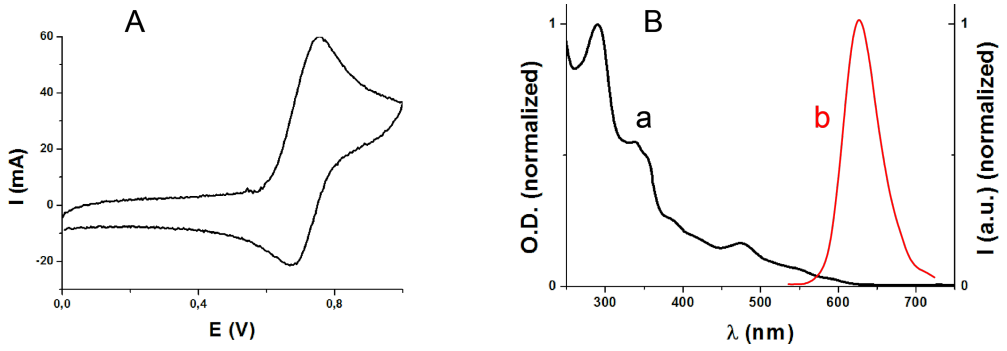

Figure 7: (A) cyclic voltamogramm for $Ir(piq)_2(tmd)$ in acetonitrile; (B) absorption (a) and luminescence (b) spectra for $Ir(piq)_2(tmd)$ (in acetonitrile).

negative (ΔG = −1.2 eV as calculated from the classical Rehm–Weller $\Delta G = E_{ox} - E_{red} - E_T + C$ where E_{ox}, E_{red}, E_T and C are the oxidation potential of $Ir(piq)_2(tmd)$, the reduction potential of Ph_2I^+, the excited triplet state energy of $Ir(piq)_2(tmd)$, and the electrostatic interaction energy for the initially formed ion pair, generally considered as negligible in polar solvents) [69].

This favorable $^3PIC/Ph_2I^+$ interaction is also in line with a fast photolysis of the PIC observed during the irradiation of $Ir(piq)_2(tmd)/Ph_2I^+$ (Figure 8). In ESR spin-trapping experiments on irradiated $Ir(piq)_2(tmd)/Ph_2I^+$ in the presence of phenyl-*N*-*tert*-butylnitrone (PBN), phenyl radicals are also detected (Figure 9). In the presence of NVK, the formation of Ph-NVK˙ is also observed (the PBN radical adducts are characterized by a_N = 14.4 G and a_H = 2.5 G, in agreement with previous data [45-52]). All these results are fully consistent with the Scheme 8 presented above. Therefore, $Ir(piq)_2(tmd)$ can be used in an oxidative cycle in combination with Ph_2I^+ and NVK.

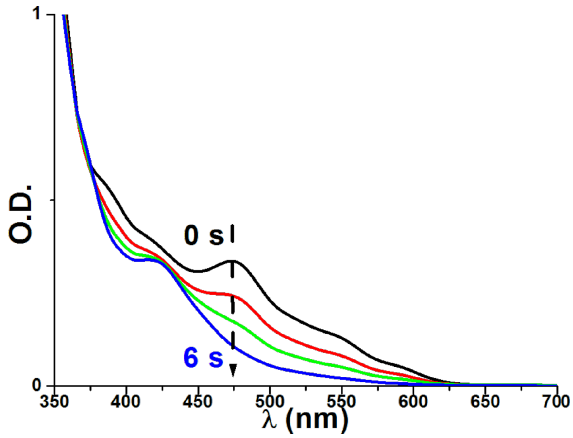

Figure 8: Photolysis of a $Ir(piq)_2(tmd)/Ph_2I^+$ solution ($[Ph_2I^+]$ = 0.023 M, in acetonitrile) upon a halogen lamp exposure.

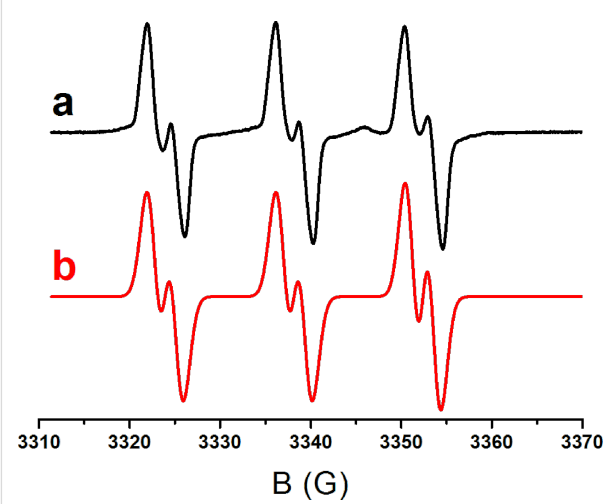

Figure 9: ESR spin-trapping spectra for the irradiation of a $Ir(piq)_2(tmd)/Ph_2I^+$ solution in the presence of PBN; green LED bulb at 514 nm irradiation (the phenyl radical adducts are characterized by a_N = 14.2 G, a_H = 2.2 G, in full agreement with previous data) [45-52].

The polymerization initiating ability of the $Ir(piq)_2(tmd)/Ph_2I^+$/NVK system

The polymerization profile for the ring-opening polymerization of EPOX using a $Ir(piq)_2(tmd)/Ph_2I^+$/NVK initiating system upon a laser diode at 532 nm is depicted in Figure 10A (it was obtained by a classical procedure already presented in [68]). An excellent polymerization is obtained (~60% of conversion for 700 s of irradiation; tack-free coating); on the opposite, in the same conditions, $Ir(ppy)_3/Ph_2I^+$/NVK leads to a low conversion (<20%) in full agreement with the low absorption of $Ir(ppy)_3$ under green lights (see Figure 6). Remarkably, the consumption of the NVK double bonds, followed in the course of the polymerization (see the conversion of NVK in Figure 10B), is in agreement with the mechanism presented in Scheme 8. These results show the interest of developing new PICs with improved or extended light absorption properties.

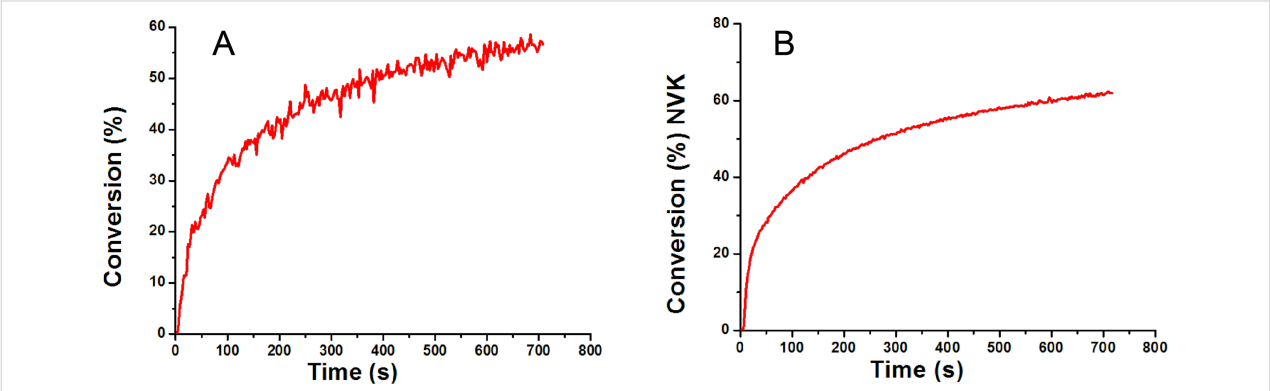

Figure 10: (A) Photopolymerization profile of EPOX; photoinitiating system: $Ir(piq)_2(tmd)/Ph_2I^+$/NVK (1%/2%/3%); laser diode at 532 nm exposure (~100 mW/cm²); under air. (B) Conversion profile for the NVK double bond in the course of the polymerization.

The PIC/MDEA/alkyl halide

The performance of the new proposed PIC for a reductive cycle in combination with an amine (MDEA) and an alkyl halide (phenacyl bromide; R–Br) to initiate a radical polymerization has been also checked. In full agreement with Scheme 11, the presence of three components is required. Indeed, Ir(piq)$_2$(tmd)/MDEA/R–Br is very efficient (Figure 11, curve 2) compared to Ir(piq)$_2$(tmd)/MDEA (Figure 11, curve 1).

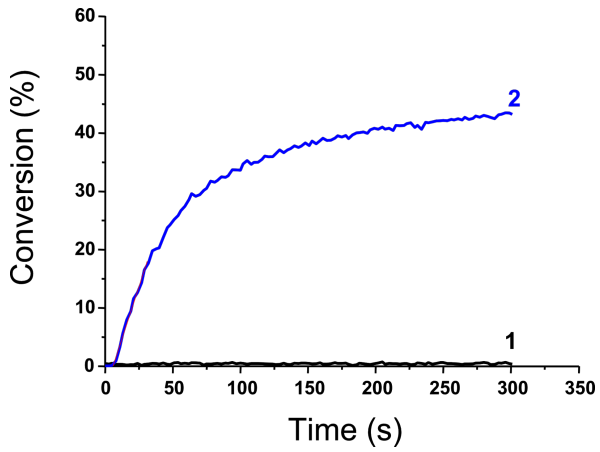

Figure 11: (A) Photopolymerization profile of TMPTA; initiating systems: (1) Ir(piq)$_2$(tmd)/MDEA (1%/2%) and (2) Ir(piq)$_2$(tmd)/MDEA/R-Br (1%/2%/3%); laser diode at 532 nm; in laminate.

Conclusion

Photoinitiator catalysts PICs appear as a new class of initiating systems usable in different photopolymerization reactions: FRP, CP and FRPCP. The associated systems are characterized by an outstanding photosensitivity; the catalytic pathways ensure a regeneration of the PIC and avoid any lost of reactivity upon irradiation. A bleaching of the sensitizer can be observed in excess of oxidation or reduction agent. In this case the polymerization of thick samples can be carried out. With this bleaching, colorless coatings can also be obtained. The search for new PICs and/or new redox agents might be of high interest as depicted by the present proposal of a new PIC (Ir(piq)$_2$(tmd)). This allows the design of multicomponent photoinitiating systems based on an excellent Ir complex working at $\lambda > 500$ nm, a goal that was never achieved before using other available Ir derivatives (e.g., the well known Ir(ppy)$_3$). The development of new catalytic methodologies still remains a huge challenge.

References

1. Nicewicz, D. A.; MacMillan, D. W. C. *Science* **2008,** *322,* 77–80. doi:10.1126/science.1161976
2. Nagib, D. A.; Scott, M. E.; MacMillan, D. W. C. *J. Am. Chem. Soc.* **2009,** *131,* 10875–10877. doi:10.1021/ja9053338
3. Shih, H.-W.; Vander Wal, M. N.; Grange, R. L.; MacMillan, D. W. C. *J. Am. Chem. Soc.* **2010,** *132,* 13600–13603. doi:10.1021/ja106593m
4. Narayanam, J. M. R.; Stephenson, C. R. J. *Chem. Soc. Rev.* **2011,** *40,* 102–113. doi:10.1039/b913880n
5. Dai, C.; Narayanam, J. M. R.; Stephenson, C. R. J. *Nat. Chem.* **2011,** *3,* 140–145. doi:10.1038/nchem.949
6. Nguyen, J. D.; Tucker, J. W.; Konieczynska, M. D.; Stephenson, C. R. J. *J. Am. Chem. Soc.* **2011,** *133,* 4160–4163. doi:10.1021/ja108560e
7. Ischay, M. A.; Lu, Z.; Yoon, T. P. *J. Am. Chem. Soc.* **2010,** *132,* 8572–8574. doi:10.1021/ja103934y
8. Du, J.; Yoon, T. P. *J. Am. Chem. Soc.* **2009,** *131,* 14604–14605. doi:10.1021/ja903732v
9. Yoon, T. P.; Ischay, M. A.; Du, J. *Nat. Chem.* **2010,** *2,* 527–532. doi:10.1038/nchem.687
10. Larraufie, M. H.; Pellet, R.; Fensterbank, L.; Goddard, J.-P.; Lacôte, E.; Malacria, M.; Ollivier, C. *Angew. Chem., Int. Ed.* **2011,** *50,* 4463–4466. doi:10.1002/anie.201007571
11. Courant, T.; Masson, G. *Chem.–Eur. J.* **2012,** *18,* 423–427. doi:10.1002/chem.201103062
12. Baralle, A.; Fensterbank, L.; Goddard, J.-P.; Ollivier, C. *Chem.–Eur. J.* **2013,** *19,* 10809–10813. doi:10.1002/chem.201301449
13. Neumann, M.; Fuldner, S.; König, B.; Zeitler, K. *Angew. Chem., Int. Ed.* **2011,** *50,* 951–954. doi:10.1002/anie.201002992
14. Zeitler, K. *Angew. Chem., Int. Ed.* **2009,** *48,* 9785–9789. doi:10.1002/anie.200904056
15. Fouassier, J. P.; Lavelée, J. *Photoinitiators for Polymer Synthesis: Scope, Reactivity and Efficiency;* Wiley-VCH: Weinheim, Germany, 2012. doi:10.1002/9783527648245
16. Lalevée, J.; Fouassier, J. P. Overview of Radical Initiation. In *Encyclopedia of Radicals in Chemistry, Biology and Materials;* Studer, A.; Chatgililoglu, C., Eds.; Wiley-VCH: Hoboken, NJ, USA, 2012. doi:10.1002/9781119953678
17. Crivello, J. V.; Aldersley, M. F. *J. Polym. Sci., Part A: Polym. Chem.* **2013,** *51,* 801–814. doi:10.1002/pola.26452
18. Kitano, H.; Ramachandran, K.; Bowden, N. B.; Scranton, A. B. *J. Appl. Polym. Sci.* **2013,** *128,* 611–618. doi:10.1002/app.38259
19. Gong, T.; Adzima, B. J.; Baker, N. H.; Bowman, C. N. *Adv. Mater.* **2013,** *25,* 2024–2028. doi:10.1002/adma.201203815
20. Bai, J.; Shi, Z. *J. Appl. Polym. Sci.* **2013,** *128,* 1785–1791. doi:10.1002/app.38286
21. Esen, D. S.; Arsu, N.; Da Silva, J. P.; Jockusch, S.; Turro, N. J. *J. Polym. Sci., Part A: Polym. Chem.* **2013,** *51,* 1865–1871. doi:10.1002/pola.26569
22. Balta, D. K.; Arsu, N. *J. Photochem. Photobiol., A: Chem.* **2013,** *257,* 54–59. doi:10.1016/j.jphotochem.2013.02.014
23. Korkut, S. E.; Temel, G.; Balta, D. K.; Arsu, N.; Kasım Şener, M. *J. Lumin.* **2013,** *136,* 389–394. doi:10.1016/j.jlumin.2012.12.025
24. Schneider, L. F. J.; Cavalcante, L. M.; Prahl, S. A.; Pfeifer, C. S.; Ferracane, J. L. *Dent. Mater.* **2012,** *28,* 392–397. doi:10.1016/j.dental.2011.11.014
25. Fabbri, P.; Valentini, L.; Bittolo Bon, S.; Foix, D.; Pasquali, L.; Montecchi, M.; Sangermano, M. *Polymer* **2012,** *53,* 6039–6044. doi:10.1016/j.polymer.2012.10.045
26. Fouassier, J. P. *Photoinitiation, Photopolymerization, Photocuring;* Hanser: Munich, 1995.
27. Davidson, S. *Exploring the Science, Technology and Application of UV and EB Curing;* Sita Technology Ltd.: London, 1999.

28. Neckers, D. C. *UV and EB at the Millenium;* Sita Technology Ltd.: London, 1999.
29. Dietliker, K. *A Compilation of Photoinitiators Commercially Available for UV Today;* Sita Technology Ltd.: London, 2002.
30. Belfied, K. D.; Crivello, J. V., Eds. *ACS Symposium series 847;* American Chemical Society: Washington, DC, USA, 2003.
31. Doğruyol, S. K.; Doğruyol, Z.; Arsu, N. *J. Lumin.* **2013,** *138,* 98–104. doi:10.1016/j.jlumin.2013.01.037
32. Santos, W. G.; Schmitt, C. C.; Neumann, M. G. *J. Photochem. Photobiol., A: Chem.* **2013,** *252,* 124–130. doi:10.1016/j.jphotochem.2012.12.007
33. Corakci, B.; Hacioglu, S. O.; Toppare, L.; Bulut, U. *Polymer* **2013,** *54,* 3182–3187. doi:10.1016/j.polymer.2013.04.008
34. Sangermano, M.; Sordo, F.; Chiolerio, A.; Yagci, Y. *Polymer* **2013,** *54,* 2077–2080. doi:10.1016/j.polymer.2013.02.026
35. Podsiadły, R.; Strzelczyk, R. *Dyes Pigm.* **2013,** *97,* 462–468. doi:10.1016/j.dyepig.2013.01.021
36. Shen, K.; Li, Y.; Liu, G.; Li, Y.; Zhang, X. *Prog. Org. Coat.* **2013,** *76,* 125–130. doi:10.1016/j.porgcoat.2012.08.020
37. Yang, J.; Tang, R.; Shi, S.; Nie, J. *Photochem. Photobiol. Sci.* **2013,** *12,* 923–929. doi:10.1039/c3pp00003f
38. Tasdelen, M. A.; Yagci, Y. In *Fundamentals of Controlled/Living Radical Polymerization;* Tang, B. Z.; Tsarevsky, N. V.; Sumerlin, B. S., Eds.; RSC Polymer Chemistry Series; RSC Publishing: London, 2013.
39. Balta, D. K.; Arsu, N.; Yagci, Y.; Jockusch, S.; Turro, N. J. *Macromolecules* **2007,** *40,* 4138–4141. doi:10.1021/ma0628735
40. Balta, D. K.; Arsu, N.; Yagci, Y.; Sundaresan, A. K.; Jockusch, S.; Turro, N. J. *Macromolecules* **2011,** *44,* 2531–2535. doi:10.1021/ma200147f
41. Cunningham, A. F., Jr.; Desobry, V. In *Radiation Curing in Polymer Science and Technology;* Fouassier, J. P.; Rabek, J. F., Eds.; Elsevier: London, 1993; Vol. 2, pp 323–374.
42. Kündig, E. P.; Xu, L.-H.; Kondratenko, M.; Cunningham, A. F., Jr.; Kunz, M. *Eur. J. Inorg. Chem.* **2007,** 2934–2943. doi:10.1002/ejic.200700115
43. Versace, D.-L.; Dalmas, F.; Fouassier, J.-P.; Lalevee, J. *ACS Macro Lett.* **2013,** *2,* 341–345. doi:10.1021/mz400081p
44. Tehfe, M. A.; Lalevée, J.; Gigmes, D.; Fouassier, J. P. *J. Polym. Sci., Part A: Polym. Chem.* **2010,** *48,* 1830–1837. doi:10.1002/pola.23956
45. Lalevée, J.; Blanchard, N.; Tehfe, M.-A.; Morlet-Savary, F.; Fouassier, J. P. *Macromolecules* **2010,** *43,* 10191–10195. doi:10.1021/ma1023318
46. Lalevée, J.; Blanchard, N.; Tehfe, M.-A.; Peter, M.; Morlet-Savary, F.; Fouassier, J. P. *Macromol. Rapid Commun.* **2011,** *32,* 917–920. doi:10.1002/marc.201100098
47. Lalevée, J.; Blanchard, N.; Tehfe, M.-A.; Peter, M.; Morlet-Savary, F.; Gigmes, D.; Fouassier, J. P. *Polym. Chem.* **2011,** *2,* 1986–1991. doi:10.1039/c1py00140j
48. Lalevée, J.; Blanchard, N.; Tehfe, M.-A.; Peter, M.; Morlet-Savary, F.; Fouassier, J. P. *Polym. Bull.* **2012,** *68,* 341–347. doi:10.1007/s00289-011-0541-9
49. Lalevée, J.; Peter, M.; Dumur, F.; Gigmes, D.; Blanchard, N.; Tehfe, M.-A.; Morlet-Savary, F.; Fouassier, J. P. *Chem.–Eur. J.* **2011,** *17,* 15027–15031. doi:10.1002/chem.201101445
50. Lalevée, J.; Tehfe, M. A.; Morlet-Savary, F.; Graff, B.; Dumur, F.; Gigmes, D.; Blanchard, N.; Fouassier, J. P. *Chimia* **2012,** *66,* 439–441.
51. Lalevée, J.; Dumur, F.; Mayer, C. R.; Gigmes, D.; Nasr, G.; Tehfe, M.-A.; Telitel, S.; Morlet-Savary, F.; Graff, B.; Fouassier, J. P. *Macromolecules* **2012,** *45,* 4134–4141. doi:10.1021/ma3005229
52. Lalevée, J.; Tehfe, M.-A.; Dumur, F.; Gigmes, D.; Blanchard, N.; Morlet-Savary, F.; Fouassier, J. P. *ACS Macro Lett.* **2012,** *1,* 286–290. doi:10.1021/mz2001753
53. Zhang, G.; Song, I. Y.; Ahn, K. H.; Park, T.; Choi, W. *Macromolecules* **2011,** *44,* 7594–7599. doi:10.1021/ma201546c
54. Tehfe, M.-A.; Lalevée, J.; Morlet-Savary, F.; Graff, B.; Blanchard, N.; Fouassier, J.-P. *Macromolecules* **2012,** *45,* 1746–1752. doi:10.1021/ma300050n
55. Tehfe, M.-A.; Lalevée, J.; Morlet-Savary, F.; Graff, B.; Blanchard, N.; Fouassier, J.-P. *ACS Macro Lett.* **2012,** *1,* 198–203. doi:10.1021/mz200140y
56. Lalevée, J.; Dumur, F.; Nechab, M.; Gigmes, D.; Fouassier, J. P. *Trends Photochem. Photobiol.* **2012,** *14,* 27–38.
57. Lalevée, J.; Tehfe, M. A.; Morlet-Savary, F.; Graff, B.; Fouassier, J. P. *Prog. Org. Coat.* **2011,** *70,* 83–90. doi:10.1016/j.porgcoat.2010.10.008
58. Tehfe, M.-A.; Dumur, F.; Telitel, S.; Gigmes, D.; Contal, E.; Bertin, D.; Morlet-Savary, F.; Graff, B.; Fouassier, J.-P.; Lalevée, J. *Eur. Polym. J.* **2013,** *49,* 1040–1049. doi:10.1016/j.eurpolymj.2013.01.023
59. Tehfe, M.-A.; Ma, L.; Graff, B.; Morlet-Savary, F.; Fouassier, J.-P.; Zhao, J.; Lalevée, J. *Macromol. Chem. Phys.* **2012,** *213,* 2282–2286. doi:10.1002/macp.201200489
60. Tehfe, M.-A.; Lalevée, J.; Telitel, S.; Sun, J.; Zhao, J.; Graff, B.; Morlet-Savary, F.; Fouassier, J.-P. *Polymer* **2012,** *53,* 2803–2808. doi:10.1016/j.polymer.2012.05.009
61. Tehfe, M.-A.; Gigmes, D.; Dumur, F.; Bertin, D.; Morlet-Savary, F.; Graff, B.; Lalevée, J.; Fouassier, J.-P. *Polym. Chem.* **2012,** *3,* 1899–1902. doi:10.1039/c1py00460c
62. Tehfe, M.-A.; Lalevée, J.; Morlet-Savary, F.; Graff, B.; Fouassier, J.-P. *Macromolecules* **2011,** *44,* 8374–8379. doi:10.1021/ma2017265
63. Tehfe, M.-A.; Dumur, F.; Contal, E.; Graff, B.; Gigmes, D.; Fouassier, J.-P.; Lalevée, J. *Macromol. Chem. Phys.* **2013,** *214,* 2189–2201. doi:10.1002/macp.201300362
64. Fors, B. P.; Hawker, C. J. *Angew. Chem., Int. Ed.* **2012,** *51,* 8850–8853. doi:10.1002/anie.201203639
65. Lalevée, J.; El-Roz, M.; Morlet-Savary, F.; Graff, B.; Allonas, X.; Fouassier, J. P. *Macromolecules* **2007,** *40,* 8527–8530. doi:10.1021/ma071489k
66. Telitel, S.; Dumur, F.; Faury, T.; Graff, B.; Tehfe, M.-A.; Gigmes, D.; Fouassier, J.-P.; Lalevée, J. *Beilstein J. Org. Chem.* **2013,** *9,* 877–890. doi:10.3762/bjoc.9.101
67. Tian, N.; Lenkeit, D.; Pelz, S.; Fischer, L. H.; Escudero, D.; Schiewek, R.; Klink, D.; Schmitz, O. J.; González, L.; Schäferling, M.; Holder, E. *Eur. J. Inorg. Chem.* **2010,** 4875–4885. doi:10.1002/ejic.201000610
68. Tehfe, M.-A.; Lalevée, J.; Gigmes, D.; Fouassier, J. P. *Macromolecules* **2010,** *43,* 1364–1370. doi:10.1021/ma9025702
69. Rehm, D.; Weller, A. *Isr. J. Chem.* **1970,** *8,* 259–271. doi:10.1002/ijch.197000029

Beilstein Journal of Organic Chemistry

Visible-light-induced, Ir-catalyzed reactions of *N*-methyl-*N*-((trimethylsilyl)methyl)aniline with cyclic α,β-unsaturated carbonyl compounds

Dominik Lenhart and Thorsten Bach*

Full Research Paper

Open Access

Address:
Department Chemie and Catalysis Research Center (CRC), Technische Universität München, Lichtenbergstr. 4, D-85747 Garching, Germany, Fax: +49-89-28913315

Email:
Thorsten Bach* - thorsten.bach@ch.tum.de

* Corresponding author

Keywords:
cyclization; electron transfer; iridium; photochemistry; photoredox catalysis; radical reactions

Beilstein J. Org. Chem. **2014,** *10,* 890–896.
doi:10.3762/bjoc.10.86

Received: 23 January 2014
Accepted: 24 March 2014
Published: 17 April 2014

This article is part of the Thematic Series "Organic synthesis using photoredox catalysis".

Guest Editor: A. G. Griesbeck

Abstract

N-Methyl-*N*-((trimethylsilyl)methyl)aniline was employed as reagent in visible-light-induced, iridium-catalyzed addition reactions to cyclic α,β-unsaturated carbonyl compounds. Typical reaction conditions included the use of one equivalent of the reaction substrate, 1.5 equivalents of the aniline and 2.5 mol % (in MeOH) or 1.0 mol % (in CH_2Cl_2) $[Ir(ppy)_2(dtbbpy)]BF_4$ as the catalyst. Two major reaction products were obtained in combined yields of 30–67%. One product resulted from aminomethyl radical addition, the other product was a tricyclic compound, which is likely formed by attack of the intermediately formed α-carbonyl radical at the phenyl ring. For five-membered α,β-unsaturated lactone and lactam substrates, the latter products were the only products isolated. For the six-membered lactones and lactams and for cyclopentenone the simple addition products prevailed.

Introduction

The photoinduced electron transfer (PET) of an amine to an excited oxidant followed by the loss of a cationic leaving group allows accessing a broad variety of α-aminoalkyl radicals [1-4]. As first shown by Mariano et al. [5,6] and by Pandey et al. [7] a trimethylsilyl (TMS) group is a suitable electrophilic leaving group for this purpose and addition reactions of α-aminoalkyl radicals to double bonds can be induced by irradiation of α-silylated amines in the presence of sensitizers such as 1,4-dicyanonaphthalene or 1,9-dicyanoanthracene. Addition reactions of this type have been broadly used for the formation of carbon–carbon bonds [8-22]. In non-silylated tertiary amines, a proton can act as a leaving group and photoinduced addition reactions of tertiary amines to enones are long known [23-28]. Mechanistically, addition reactions of this type can occur as a radical chain reaction because the addition product of the α-aminoalkyl radical is a carbon-centered radical, which can abstract a hydrogen atom from the tertiary amine [29,30]. Notable contributions to the field of direct tertiary amine addi-

tion reactions to enones were made by Hoffmann et al., who established the use of aromatic ketones as suitable PET catalysts for these reactions [31-37]. In Scheme 1, the addition reaction of *N*,*N*-dimethylaniline (**1**) to (5*R*)-menthyloxyfuran-2(5*H*)-one (**2**) is shown, which proceeds to the intriguing tricyclic product **4** employing 4,4'-bis(dimethylamino)benzophenone (**3**) as the catalyst [38]. In this case, the amine was used in large excess (15 equiv) and the chiral menthyl group was derived from (−)-menthol. It was later found that the reaction proceeds with a higher yield (73%) if acetone was employed as a co-solvent [39] and that the diastereoselectivity depends both on the stereogenic center at C5 and on the chirality of the menthyl (Men) backbone [40].

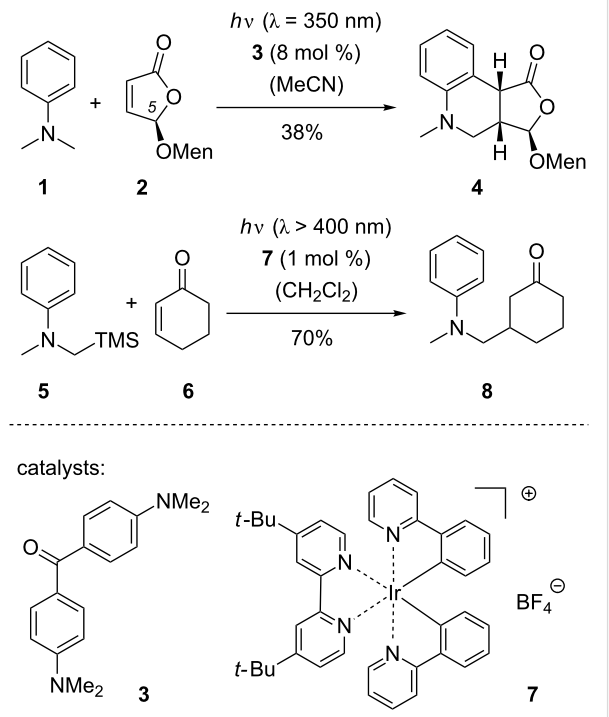

Scheme 1: PET-catalyzed addition of *N*,*N*-dimethylaniline (**1**) to furan-2(5*H*)-one **2** [38] and of *N*-methyl-*N*-((trimethylsilyl)methyl)aniline (**5**) to 2-cyclohexenone (**6**) [41].

In more recent work [41,42], Nishibayashi et al. showed that iridium complexes can serve as efficient PET catalysts for the addition of α-aminomethyl radicals [43-45] to enones. *N*-Methyl-*N*-((trimethylsilyl)methyl)aniline (**5**) for example served as substrate for the alkylation of 2-cyclohexenone (**6**) employing iridium catalyst **7**. When using the amine as the limiting reagent and an excess of enone (1.5 equiv) product **8** was obtained in 70% yield.

Based on our interest in photochemically induced addition reactions of α-aminoalkyl radicals [46,47], the potential of iridium catalysis attracted our interest and we wondered whether it would be possible to apply the title compound, *N*-methyl-*N*-((trimethylsilyl)methyl)aniline (**5**), in addition reactions to other cyclic α,β-unsaturated carbonyl compounds. In particular, we were interested to see whether cyclization reactions as for product **4** would be observed when using α,β-unsaturated lactones and lactams in combination with a silylated amine and an iridium catalyst. In this article, we provide full details of our studies in this field. Seven different substrates were tested as limiting reagents in the addition reactions and the structure of the respective products was elucidated.

Results and Dicussion

Addition to cyclic α,β-unsaturated lactones

Our work commenced with attempted addition reactions to the parent furan-2(5*H*)-one (**9**) and was conducted with a set of eight visible light lamps (Osram L 8W/640 cool white) [48]. A screen of potential catalysts (see Supporting Information File 2 for further details) in CH_2Cl_2 as the solvent (c = 0.1 M) revealed that $[Ir(ppy)_2(bpy)]BF_4$ (ppy = phenylpyridyl; bpy = 2,2'-bipyridine) and $[Ir(ppy)_2(dtbbpy)]BF_4$ (**7**) (dtbbpy = 4,4'-di-*tert*-butyl-2,2'-bipyridine) gave the best results while other iridium catalysts turned out to be inferior. Remarkably, the desired tricyclic product **10** was isolated as the only product while the direct addition product **11** was not observed. Contrary to that, the ruthenium catalyst $Ru(bpy)_3Cl_2$ delivered a mixture of both products in a ratio of 77/23. Apart from CH_2Cl_2, other solvents were tested (see Supporting Information File 2), none of which led to a significant yield improvement. It was observed, however, that the desired reaction was faster in polar solvents such as DMF, DMSO and MeOH. The reaction went to completion in four to five hours while 24 hours were required to reach full conversion in CH_2Cl_2. The direct addition product was detected as a side product both in DMF (**10**/**11** = 71/29) and in DMSO (82/18). In MeOH, however, only the tricyclic product **10** was formed. A slight yield improvement was observed when raising the catalyst loading in the latter case from 1 mol % to 2.5 mol % while a decrease of the catalyst concentration led to lower yields. The results of the reactions under optimized conditions are provided for CH_2Cl_2 and MeOH as the solvent in Scheme 2. Product **10**, which is a known compound and had been previously prepared by reduction of product **4**, was obtained as a single diastereoisomer [40].

In subsequent sets of experiments the reaction conditions of Scheme 2 were applied to other substrates. With 5,6-dihydro-2*H*-pyran-2-one (**12**) two major products **13** and **14** could be isolated (Scheme 3). If performed in CH_2Cl_2 the reaction remained incomplete after 24 hours. The substrate was recovered in 20% and products **13** and **14** were obtained in a ratio of 55/45 with the tricyclic product prevailing. A complete sep-

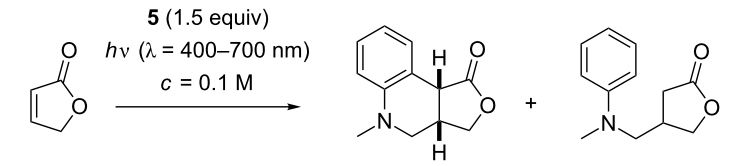

9		10	11
7 (1.0 mol %)	t = 24 h (CH_2Cl_2)	46%	–
7 (2.5 mol %)	t = 5 h (MeOH)	49%	–

Scheme 2: Ir-catalyzed formation of tricyclic product **10** by a domino radical addition reaction to α,β-unsaturated lactone **9**.

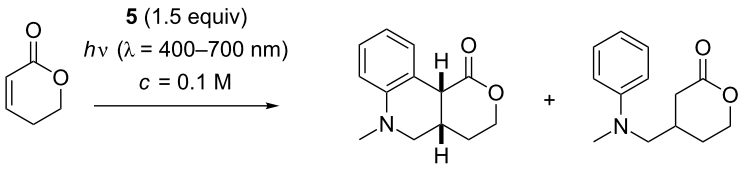

12		13	14
7 (1.0 mol %)	t = 24 h (CH_2Cl_2)	22%	18%
7 (2.5 mol %)	t = 5 h (MeOH)	10%	41%

Scheme 3: Ir-catalyzed addition reactions of *N*-methyl-*N*-((trimethylsilyl)methyl)aniline (**5**) to 5,6-dihydro-2*H*-pyran-2-one (**12**).

aration of the two compounds was not possible but it could be unambiguously shown that compound **13** was diastereomerically pure. Based on the ^{1}H NMR coupling constant ($^3J_{HH}$ = 7.3 Hz) between the two indicated (Scheme 3) protons it was assigned to be the *cis*-diastereoisomer. For the *trans*-diastereoisomer a distinctly larger coupling constant ($^3J_{HH} \geq$ 10 Hz) would be expected [49]. Primary addition product **14** could be isolated in pure form as it was the predominant reaction product when the reaction was performed in MeOH as the solvent. In this case the reaction went to completion after five hours and delivered product **14** in 41% yield.

Addition to cyclic α,β-unsaturated ketones

Based on the results obtained with five-membered lactone **9**, it was suprising to note that the related five-membered enone, 2-cyclopentenone (**15**), delivered mainly the direct addition product **17** instead of the tricyclic product **16**. The reactions (Scheme 4) went to completion within 24 hours (in CH_2Cl_2) and 4.5 hours (in MeOH). As for compounds **13** and **14**, a complete separation of the two products was not feasible by column chromatography. A mixture of **16** and **17** was obtained, which was free of impurities and in which the relative ratio of products could be established by ^{1}H NMR spectroscopy. From a preparative point of view, the result of the reaction in MeOH was more satisfactory because it delivered a combined yield of 67% for both addition products. The relative configuration of compound **16** is tentatively assigned as *cis* due to the coupling constant between the depicted (Scheme 4) protons ($^3J_{HH}$ = 7.0 Hz). The coupling constant is similar to the coupling constant for the known annulated *cis*-product **10** and is

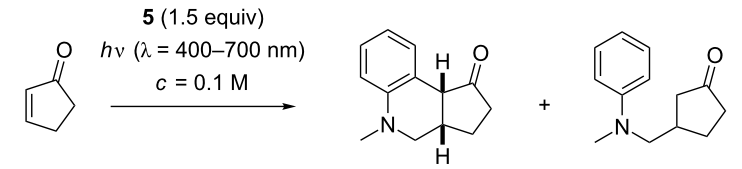

15		16	17
7 (1.0 mol %)	t = 24 h (CH_2Cl_2)	18%	28%
7 (2.5 mol %)	t = 4.5 h (MeOH)	13%	54%

Scheme 4: Ir-catalyzed addition reactions of *N*-methyl-*N*-((trimethylsilyl)methyl)aniline (**5**) to 2-cyclopentenone (**15**).

in agreement with coupling constants recorded for protons in related tricyclic compounds [50,51].

Replacing 2-cyclopentenone (**15**) by 2-cyclohexenone (**6**) led to the above-mentioned direct addition product **8** (Scheme 1), as previously reported by Nishibayashi et al. [41]. The yield we obtained when using the ketone as the limiting reagent and 1.5 equiv of the amine was 65%. There was no indication for the formation of a tricyclic product.

Addition to cyclic α,β-unsaturated lactams

Lactams offer the possibility of reactivity tuning by choosing an appropriate protecting group at the nitrogen atom. Since initial experiments with unprotected pyrrolin-2-one were not promising the respective *tert*-butyloxycarbonyl (Boc) and 4-toluenesulfonyl (Ts) derivatives **18a** and **18b** were prepared [52]. In CH_2Cl_2 as the solvent, the attempted addition reaction of *N*-methyl-*N*-((trimethylsilyl)methyl)aniline (**5**) turned out to be sluggish. With substrate **18a**, product **19a** was isolated in 23% yield after an irradiation time of 24 hours employing 1 mol % of catalyst **7**. With substrate **18b** the conversion was 64% after 24 hours at an increased catalyst loading of 2.5 mol %. Compound **19b** was isolated in 36% yield (56% based on conversion). Somewhat better results were recorded in MeOH as the solvent (Scheme 5). Irrespective of the protective group, the reaction was complete within six hours and delivered exclusively the tricyclic products **19**. The Boc-protected product **19a** was obtained in only 30% yield, however; the result indicates that the Boc protecting group is not ideal for reactions in MeOH as the solvent (vide infra). A higher yield (49%) was recorded for the Ts-protected product **19b**. The two protons at the ring junction show a similar coupling constant (^3J = 8.1 Hz for **19a**, ^3J = 7.9 Hz for **19b**) as the protons in the related lactone **10** suggesting a *cis*-annulation of the two heterocyclic rings.

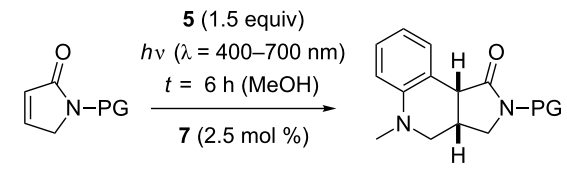

Scheme 5: Ir-catalyzed formation of tricyclic products **19** by a domino radical addition reaction to α,β-unsaturated lactams **18**.

The instability of Boc-substituted lactams upon irradiation in MeOH solution was also notable in attempted reactions of substrate **20** [53]. With a catalyst loading of 2.5 mol %, the combined yield (10%) of addition products **21** and **22** was disappointingly low at a conversion of 62% after seven hours. The reaction in CH_2Cl_2 proceeded more smoothly and delivered after an irradiation time of 24 hours the two products **21** and **22** in a combined yield of 44% (Scheme 6). There was no yield improvement if the catalyst loading was increased to 2.5 mol %.

With an excess of α,β-unsaturated lactam **20**, the reaction turned out to proceed with higher type selectivity. The domino process was suppressed and the plain addition product **22** was obtained in 75% yield (Scheme 7).

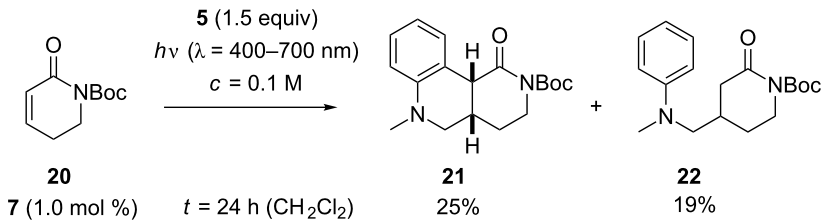

Scheme 6: Ir-catalyzed addition reactions of *N*-methyl-*N*-((trimethylsilyl)methyl)aniline (**5**) to α,β-unsaturated lactam **20**.

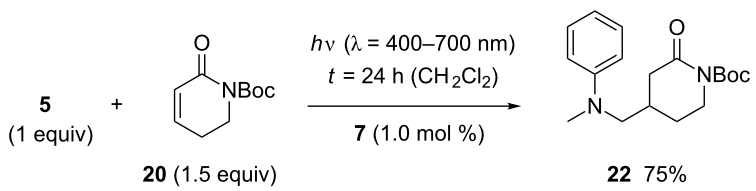

Scheme 7: Ir-catalyzed addition reactions of *N*-methyl-*N*-((trimethylsilyl)methyl)aniline (**5**) to α,β-unsaturated lactam **20** with the aniline being the limiting substrate.

The latter result suggested that the previously discussed (Scheme 3) addition reaction to 5,6-dihydro-2*H*-pyran-2-one (**12**) might also lead to a single product if performed with the aniline as the limiting agent. To our surprise, however, the relative product ratio remained unchanged when the substrate ratio **5**/**12** = 1.5/1 was decreased to 1/1.5.

Mechanistically, it is likely that the well-established photoredox cascade between aniline **5** and the photoexcited iridium complex **7** operates [54-58]. Oxidation of the aniline and loss of the trimethylsilyl group leads to an α-aminomethyl radical, which adds to the cyclic α,β-unsaturated carbonyl compound (Scheme 8). The intermediate radical **A** can undergo immediate reduction presumably by concomitant oxidation of the previously reduced iridium complex (path a), which provides the simple addition products (e.g., **14**, **17**, **22**) [41,42], or it attacks (path b) the adjacent phenyl group to form radical **B**. The further fate of radical **B** is likely an oxidation to the tricyclic products (e.g., **10**, **19**). The oxidation could occur by hydrogen transfer to the starting material, i.e., the α,β-unsaturated carbonyl compound [39], which would explain why the yields never exceeded 50%. Upon hydrogen transfer the α,β-unsaturated carbonyl compound would give a cyclic α-acyl radical, which would be capable to re-oxidize the reduced iridium complex thus completing the catalytic cycle. However, we have not been able to substantiate the latter hypothesis, e.g., by isolation of a saturated carbonyl compound.

Interestingly, we did not find a hint for a radical chain pathway, which would include hydrogen abstraction from the starting aniline **5** by intermediate **A**. The resulting radical would carry a trimethylsilyl group, which would be eventually found in the product. The absence of a trimethylsilyl group in the products indicates that reduction (path a) and cyclization (path b) are more efficient than hydrogen abstraction while hydrogen abstraction has been established as a radical chain propagating step in reactions performed with UV light [5,6,8,11,32,34,38-40].

Conclusion

In summary, it was shown that a photochemical generated aminomethyl radical – produced from *N*-methyl-*N*-((trimethylsilyl)methyl)aniline – adds readily not only to the previously reported cyclohexenone but to several cyclic α,β-unsaturated carbonyl compounds. Further reaction of the intermediate α-carbonyl radical was observed with five-membered substrates leading to synthetically interesting tricyclic products. The latter reaction suffers from the fact that oxidation of the putative intermediate **B** is required, which seems to occur at the expense of the substrate. If a suitable compound was found to adapt the role of an ancillary oxidant, yields could possibly be improved.

Supporting Information

Supporting Information File 1

Experimental section.
[http://www.beilstein-journals.org/bjoc/content/supplementary/1860-5397-10-86-S1.pdf]

Supporting Information File 2

Tables of all optimization experiments and copies of $^{1}H/^{13}C$ spectra of PET catalysis products.
[http://www.beilstein-journals.org/bjoc/content/supplementary/1860-5397-10-86-S2.pdf]

Acknowledgements

This research was supported by the Deutsche Forschungsgemeinschaft (GRK 1626) and by the Fonds der Chemischen Industrie.

References

1. Pandey, G. In *Molecular and Supramolecular Photochemistry: Organic Photochemistry;* Ramamurthy, V.; Schanze, K. S., Eds.; Marcel Dekker: New York, 1997; Vol. 1, pp 245–294.
2. Pandey, G. *Synlett* **1992,** 546–552. doi:10.1055/s-1992-21410
3. Yoon, U. C.; Mariano, P. S. *Acc. Chem. Res.* **1992,** *25,* 233–240. doi:10.1021/ar00017a005
4. Cohen, S. G.; Parola, A.; Parsons, G. H., Jr. *Chem. Rev.* **1973,** *73,* 141–161. doi:10.1021/cr60282a004
5. Yoon, U. C.; Kim, J. U.; Hasegawa, E.; Mariano, P. S. *J. Am. Chem. Soc.* **1987,** *109,* 4421–4423. doi:10.1021/ja00248a063
6. Hasegawa, E.; Xu, W.; Mariano, P. S.; Yoon, U. C.; Kim, J. U. *J. Am. Chem. Soc.* **1988,** *110,* 8099–8111. doi:10.1021/ja00232a023

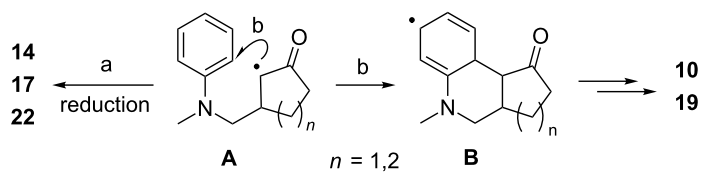

Scheme 8: Cyclization of putative radical **A** to intermediate **B** competes with reduction of **A** to form addition products, such as **14**, **17**, **22**.

7. Pandey, G.; Kumaraswamy, G.; Bhalerao, U. T. *Tetrahedron Lett.* **1989,** *30,* 6059–6062. doi:10.1016/S0040-4039(01)93854-7
8. Xu, W.; Jeon, Y. T.; Hasegawa, E.; Yoon, U. C.; Mariano, P. S. *J. Am. Chem. Soc.* **1989,** *111,* 406–408. doi:10.1021/ja00183a081
9. Jeon, J. T.; Lee, C.-P.; Mariano, P. S. *J. Am. Chem. Soc.* **1991,** *113,* 8847–8863. doi:10.1021/ja00023a038
10. Xu, W.; Zhang, X.-M.; Mariano, P. S. *J. Am. Chem. Soc.* **1991,** *113,* 8863–8878. doi:10.1021/ja00023a039
11. Zhang, X.-M.; Mariano, P. S. *J. Org. Chem.* **1991,** *56,* 1655–1660. doi:10.1021/jo00004a055
12. Pandey, G.; Reddy, G. D. *Tetrahedron Lett.* **1992,** *33,* 6533–6536. doi:10.1016/S0040-4039(00)79035-6
13. Jung, Y. S.; Swartz, W. H.; Xu, W.; Mariano, P. S.; Green, N. J.; Schultz, A. G. *J. Org. Chem.* **1992,** *57,* 6037–6047. doi:10.1021/jo00048a046
14. Pandey, G.; Reddy, G. D.; Kumaraswamy, G. *Tetrahedron* **1994,** *50,* 8185–8194. doi:10.1016/S0040-4020(01)85300-X
15. Meggers, E.; Steckhan, E.; Blechert, S. *Angew. Chem., Int. Ed. Engl.* **1995,** *34,* 2137–2139. doi:10.1002/anie.199521371
16. Das, S.; Kumar, J. S. D.; Shivaramayya, K.; George, M. V. *Tetrahedron* **1996,** *52,* 3424–3434. doi:10.1016/0040-4020(96)00022-1
17. Khim, S.-K.; Cederstrom, E.; Ferri, D. C.; Mariano, P. S. *Tetrahedron* **1996,** *52,* 3195–3222. doi:10.1016/0040-4020(95)01105-6
18. Jonas, M.; Blechert, S.; Steckhan, E. *J. Org. Chem.* **2001,** *66,* 6896–6904. doi:10.1021/jo010144b
19. Pandey, G.; Kapur, M. *Org. Lett.* **2002,** *4,* 3883–3886. doi:10.1021/ol026711e
20. Pandey, G.; Kapur, M.; Khan, M. I.; Gaikwad, S. M. *Org. Biomol. Chem.* **2003,** *1,* 3321–3326. doi:10.1039/b307455b
21. Pandey, G.; Bharadwaj, K. C.; Khan, M. I.; Shashidhara, K. S.; Puranik, V. G. *Org. Biomol. Chem.* **2008,** *6,* 2587–2595. doi:10.1039/b804278k
22. Kamijo, S.; Hoshikawa, T.; Inoue, M. *Org. Lett.* **2011,** *13,* 5928–5931. doi:10.1021/ol202659e
23. Cookson, R. C.; Hudec, J.; Mirza, N. A. *Chem. Commun.* **1968,** 180a. doi:10.1039/c1968000180a
24. Pienta, N. J.; McKimmey, J. E. *J. Am. Chem. Soc.* **1982,** *104,* 5501–5502. doi:10.1021/ja00384a048
25. Smith, D. W.; Pienta, N. J. *Tetrahedron Lett.* **1984,** *25,* 915–918. doi:10.1016/S0040-4039(01)80061-7
26. Pienta, N. J. *J. Am. Chem. Soc.* **1984,** *106,* 2704–2705. doi:10.1021/ja00321a041
27. Schuster, D. I.; Bonneau, R.; Dunn, D. A.; Rao, J. M.; Joussot-Dubien, J. *J. Am. Chem. Soc.* **1984,** *106,* 2706–2707. doi:10.1021/ja00321a042
28. Dunn, D. A.; Schuster, D. I.; Bonneau, R. *J. Am. Chem. Soc.* **1985,** *107,* 2802–2804. doi:10.1021/ja00295a040
29. Urry, W. H.; Juveland, O. O. *J. Am. Chem. Soc.* **1958,** *80,* 3322–3328. doi:10.1021/ja01546a033
30. Roy, R. B.; Swan, G. A. *J. Chem. Soc. C* **1969,** 1886–1891. doi:10.1039/J39690001886
31. Bertrand, S.; Hoffmann, N.; Pete, J.-P. *Tetrahedron Lett.* **1999,** *40,* 3173–3174. doi:10.1016/S0040-4039(99)00452-9
32. Bertrand, S.; Hoffmann, N.; Pete, J.-P. *Eur. J. Org. Chem.* **2000,** 2227–2238. doi:10.1002/1099-0690(200006)2000:12<2227::AID-EJOC2227>3.0.CO;2-8
33. Marinković, S.; Hoffmann, N. *Chem. Commun.* **2001,** 1576–1578. doi:10.1039/b104387k
34. Marinković, S.; Hoffmann, N. *Eur. J. Org. Chem.* **2004,** 3102–3107. doi:10.1002/ejoc.200400102
35. Harakat, D.; Pesch, J.; Marinković, S.; Hoffmann, J. *Org. Biomol. Chem.* **2006,** *4,* 1202–1205. doi:10.1039/b600220j
36. Gassama, A.; Ernenwein, C.; Hoffmann, N. *ChemSusChem* **2009,** *2,* 1130–1137. doi:10.1002/cssc.200900150
37. Jahjah, R.; Gassama, A.; Bulach, V.; Suzuki, C.; Abe, M.; Hoffmann, N.; Martinez, A.; Nuzillard, J.-C. *Chem.–Eur. J.* **2010,** *16,* 3341–3354. doi:10.1002/chem.200903045
38. Bertrand, S.; Hoffmann, N.; Pete, J.-P.; Bulach, V. *Chem. Commun.* **1999,** 2291–2292. doi:10.1039/a906051k
39. Bertrand, S.; Hoffmann, N.; Humbel, S.; Pete, J.-P. *J. Org. Chem.* **2000,** *65,* 8690–8703. doi:10.1021/jo001166l
40. Marinković, S.; Brulé, C.; Hoffmann, N.; Prost, E.; Nuzillard, J.-M.; Bulach, V. *J. Org. Chem.* **2004,** *69,* 1646–1651. doi:10.1021/jo030292x
41. Miyake, Y.; Ashida, Y.; Nakajima, K.; Nishibayashi, Y. *Chem. Commun.* **2012,** *48,* 6966–6968. doi:10.1039/c2cc32745g
42. Miyake, Y.; Nakajima, K.; Nishibayashi, Y. *J. Am. Chem. Soc.* **2012,** *134,* 3338–3341. doi:10.1021/ja211770y
43. McNally, A.; Prier, C. K.; McMillan, D. W. C. *Science* **2011,** *334,* 1114–1117. doi:10.1126/science.1213920
44. Kohls, P.; Jadhav, D.; Pandey, G.; Reiser, O. *Org. Lett.* **2012,** *14,* 672–675. doi:10.1021/ol202857t
45. Ju, X.; Li, D.; Li, W.; Yu, W.; Bian, F. *Adv. Synth. Catal.* **2012,** *354,* 3561–3567. doi:10.1002/adsc.201200608
46. Bauer, A.; Westkämper, F.; Grimme, S.; Bach, T. *Nature* **2005,** *436,* 1139–1140. doi:10.1038/nature03955
47. Selig, P.; Bach, T. *J. Org. Chem.* **2006,** *71,* 5662–5673. doi:10.1021/jo0606608
48. Alonso, R.; Bach, T. *Angew. Chem., Int. Ed.* **2014,** *53,* in press. doi:10.1002/anie.201310997
49. Thompson, H. W.; Long, D. J. *J. Org. Chem.* **1988,** *53,* 4201–4209. doi:10.1021/jo00253a009
50. Singh, R.; Parai, M. K.; Panda, G. *Org. Biomol. Chem.* **2009,** *7,* 1858–1867. doi:10.1039/b901632e
51. Xiong, X.-F.; Jia, Z.-J.; Du, W.; Jiang, K.; Liu, T.-Y.; Chen, Y.-C. *Chem. Commun.* **2009,** 6994–6996. doi:10.1039/b917408g
52. Curti, C.; Ranieri, B.; Battistini, L.; Rassu, G.; Zambrano, V.; Pelosi, G.; Casiraghi, G.; Zanardi, F. *Adv. Synth. Catal.* **2010,** *352,* 2011–2022. doi:10.1002/adsc.201000189
53. Garnier, E. C.; Liebeskind, L. S. *J. Am. Chem. Soc.* **2008,** *130,* 7449–7458. doi:10.1021/ja800664v
54. Yoon, T. P.; Ischay, M. A.; Du, J. *Nat. Chem.* **2010,** *2,* 527–532. doi:10.1038/nchem.687
55. Narayanam, J. M. R.; Stephenson, C. R. J. *Chem. Soc. Rev.* **2011,** *40,* 102–113. doi:10.1039/b913880n
56. Reckenthäler, M.; Griesbeck, A. G. *Adv. Synth. Catal.* **2013,** *355,* 2727–2744. doi:10.1002/adsc.201300751
57. Prier, C. K.; Rankic, D. A.; MacMillan, D. W. C. *Chem. Rev.* **2013,** *113,* 5322–5363. doi:10.1021/cr300503r
58. Xuan, J.; Lu, L.-Q.; Chen, J.-R.; Xiao, W.-J. *Eur. J. Org. Chem.* **2013,** 6755–6770. doi:10.1002/ejoc.201300596

Beilstein Journal of Organic Chemistry

Tailoring of organic dyes with oxidoreductive compounds to obtain photocyclic radical generator systems exhibiting photocatalytic behavior

Christian Ley*, Julien Christmann, Ahmad Ibrahim, Luciano H. Di Stefano and Xavier Allonas

Full Research Paper

Open Access

Address:
Laboratory of Macromolecular Photochemistry and Engineering, University of Haute Alsace, 3b rue Alfred Werner, 68093 Mulhouse, France

Email:
Christian Ley* - christian.ley@uha.fr

* Corresponding author

Keywords:
computation; electron transfer; kinetic; photocatalysis; photochemistry; photocyclic initiating system; photopolymerization; photoredox catalysis; radical generator

Beilstein J. Org. Chem. **2014,** *10,* 936–947.
doi:10.3762/bjoc.10.92

Received: 22 January 2014
Accepted: 02 April 2014
Published: 25 April 2014

This article is part of the Thematic Series "Organic synthesis using photoredox catalysis".

Guest Editor: A. G. Griesbeck

Abstract

The combination of a dye which absorbs the photon, an electron acceptor and an electron donor leading to energy conversion through electron transfer, was the basis of the so called three-component systems. In this paper, an experimental work combining Rose bengal dye with a triazine derivative as electron acceptor and ethyl 4-(dimethylamino)benzoate as electron donor, will underline the benefit of the photocyclic behavior of three-component systems leading to the dye regeneration. A thermodynamic approach of the photocycle is presented, followed by a mechanistic and computational study of ideal photocycles, in order to outline the specific kinetics occuring in so called photocatalytic systems. The simple kinetic model used is enough to outline the benefit of the cyclic system and to give the basic requirements in term of chemical combination needed to be fulfilled in order to obtain a photocatalytic behavior.

Introduction

Among the possible usage of light, the conversion of photons into chemical energy, as stored into radicals or ions, is of great interest. As a part of this research area, the development of photoradical generators (PRG) is still a lively topic that finds applications in triggering bioactivity [1], drug or fragrance release [2-4], microelectronics [5], water catalysis reduction [6-8], and laser imaging [9]. In organic chemistry, the development of new methods for organic synthesis was achieved by use of photolabile protective groups, which could be released under irradiation by light [10,11]. Since many decades in industry, PRG are used in photopolymerization, a field in which the PRG prompt the initiation of the polymerization through a chain

reaction [12]. Photopolymerization was first used over 4000 years ago in the mummification process [13]. During the last decades the number of commercial applications is still continuously increasing. By example, photopolymer applications are found in electronic materials [14], printing materials [15], optical and electro-optical materials [16,17], fabrication of devices and materials [18], adhesives and sealants [19], coatings [20] and surface modifications [21,22].

The great interest in PRG application to free radical polymerization (FRP) has led to the development of two major classes of photoinitiating systems (PIS): Type I and Type II. In Type I PIS, the excited states reached after light absorption undergo a cleavage leading to the production of two initiating radicals [5,23,24]. However, most Type I PIS are only active under UV–blue irradiation [25,26]. To overcome this spectral limitation, Type II PIS were developed. They contain the photosensitizer (PS) which absorbs the light and a coinitiator (Co) which reacts with PS excited states through hydrogen abstraction or electron transfer reaction (see Scheme 1). Numerous dyes were reported as PS [9,27-32]. Hydrogen donor coinitiators could be amines [33-38], ethers [39,40], sulfides [41-43] or thiols [43-45]. Electron transfer coinitiators could be borate salts [46,47], iodonium [48,49] or triazine [32] derivatives. However, if Type II PIS gain sensitivity in the visible part of the electromagnetic spectrum, their efficiency is lower than Type I PIS. To gain more reactivity the so-called three component systems (3-cpt) were developed by adding a redox additive to Type II systems [32,50-52]. A higher yield of initiating radicals is generally claimed in such cases. Moreover, the dye is recovered during the process and is newly available to absorb light, running into a new cycle [9,32]. These photocyclic initiating systems (PCIS), should then present a somehow constant absorbance, leading to constant and efficient absorption of the incident photons. Both features are responsible for the higher efficiency of PCIS [9,31,53-55] in photopolymerization reactions. Therefore, as the dye is regenerated during the photochemical reaction, a catalytic behavior appears, leading to the so-called photocatalytic system.

In this paper an experimental and mechanistic study of Type II PIS will be given and compared with a PCIS. Then, in order to improve the knowledge of PCIS, a thermodynamic and mechanistic approach of PCIS exhibiting an ideal photocatalytic behavior will be presented. The proposed scheme will be used as model to run some computation. This will permit to compare and discuss the advantages, the specificity of this kind of photocyclic systems and outline the important features and conditions which have to be fulfilled in order to obtain high performances for this kind of photocatalytic systems. This ideal approach will permit a better general understanding of the complex kinetics underlying PCIS chemical reactions, allowing a better and simplest selection of chemicals combination.

Results and Discussion

In order to outline this behavior, the photochemical consumption of the dye (i.e., photolysis) was studied in a typical Type II and a 3-cpt PCIS based on the Rose Bengal as dye, and a triazine derivative (TA) as an acceptor (coinitiator). In addition, an amine (ethyl 4-(dimethylamino)benzoate, EDB) was chosen as redox (electron donor) additive for the PCIS (see Scheme 1).

Type II photoinitiating system

In Scheme 2, the typical reaction mechanism of a dye (PS) with an electron acceptor (A) is depicted. After absorption of actinic light ($h\nu$), the PS reaches its singlet excited state ($^1PS^*$) and after intersystem crossing (k_{ISC}), its triplet excited state ($^3PS^*$). From both these excited states, an electron transfer can occur from the PS to A (with quenching rate constants $^1k_{q/A}$ and $^3k_{q/A}$, respectively). The oxidized form of the dye ($PS^{\bullet+}$) is formed together with the reduced acceptor ($A^{\bullet-}$) which lead to initiating radicals [33,48,49].

As a consequence, the PS is consumed (i.e., photolysed or bleached) during the photoinduced electron transfer reaction. Thus, according to Beer–Lambert's law, the absorbance of the system decreases during the reaction: this bleaching could be followed by UV–visible absorption spectroscopy.

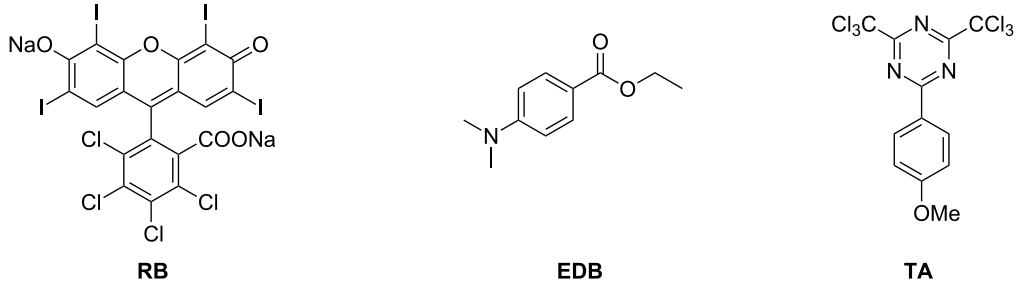

Scheme 1: Chemical structures of RB, EDB and TA.

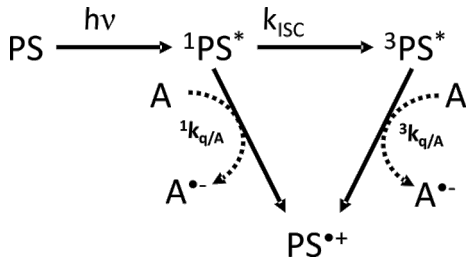

Scheme 2: Type II PIS mechanisms. PS: photosensitizer; ^{1,3}PS*: singlet and triplet PS excited states; PS$^{\bullet+}$: oxidized PS; A: electron acceptor coinitiator; A$^{\bullet-}$: reduced electron acceptor.

The photolysis of an acetonitrile solution of RB/TA was done within a 1 cm width cell with a monochromatic 532 nm laser diode tuned to 9 mW/cm^2 intensity. This will correspond to the 9 mW/cm^3 computation condition (vide infra). The initial concentration was $[RB]_0$ = 6.5 10^{-5} mol·L^{-1} (with ε = 31900 M^{-1}·cm^{-1} and a length of l = 1 cm, this corresponds to an initial absorbance of around 0.2 at 532 nm) and $[TA]_0$ = 10^{-3} mol·L^{-1}. The transmitted laser diode light was real-time recorded. It is thus possible to calculate the optical density $A(t)$ of the sample, which is then converted into [RB](t). It can be seen from Figure 1 that a fast decrease of [RB](t) occurs, so fast that the very beginning is not resolved by the detector. This indicates that the dye is consumed during irradiation, due to the electron transfer to TA. In about 100 s, the absorbance is almost zero indicating a complete consumption of the dye. As a consequence, the absorption spectrum completely vanishes after 5 min of irradiation, confirming the disappearance of the dye (see insert Figure 1). It should be noted that in the same conditions, no photolysis occurs for an acetonitrile solution of neat RB.

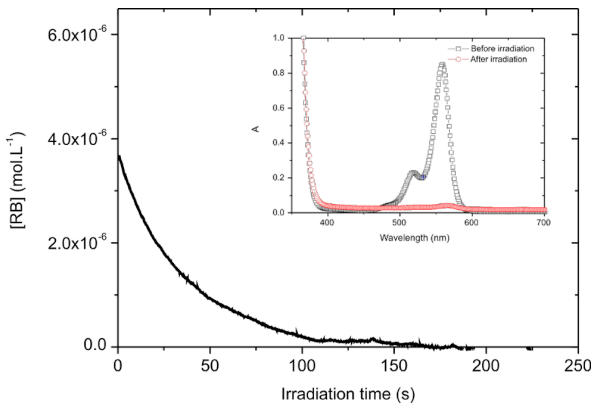

Figure 1: Evolution of RB concentration as a function of irradiation time (λ = 532 nm, 9 mW·cm^{-3}); insert: absorption spectra obtained before and after irradiation.

To quantify the consumption of the PS, the photolysis quantum yield ($\Phi_{photolysis}$) was determined. $\Phi_{photolysis}$ is defined by the ratio of the initial number of photosensitizer (PS) molecules present (N_{PS}) to the total number of absorbed photons (N_{abs}). It could be expressed by the following equation:

$$\Phi_{photolysis} = \frac{N_{PS}}{N_{abs}} = \frac{V \cdot [PS]_0}{V \cdot \int I_{abs}.dt} = \frac{[PS]_0}{\int I_{abs} \cdot dt} \quad (1)$$

where V is the volume of the irradiated solution. The absorbed photon concentration is given by:

$$\int I_{abs} dt = \int I_0 \left(1 - 10^{-A(t)}\right) dt \quad (2)$$

where I_0 is the incident light intensity on the cell (9 mW·cm^{-3}, i.e., 4·10^{-5} einstein·s^{-1}·cm^{-3}). The experimental measure of the absorbance $A(t)$ allows the calculation of $I_{abs}(t)$ and a numerical integration. Accordingly, the total concentration of absorbed photon is calculated as 3.43·10^{-4} mol·L^{-1} for RB/TA. It should be noted here that the missing first 1 second of the fast decay of $A(t)$ will represent, at maximum, 1.47·10^{-5} mol·L^{-1} of absorbed photons (by assuming a constant $A(t)$ = 0.2 during this 1 s). This overestimation represents less than 5% of the total absorbed photons and could be neglected. Then, dividing the initial RB concentration by these values, a photolysis quantum yield of 0.19 for RB/TA is obtained.

Photocyclic initiating system

A typical photocyclic initiating system (PCIS) consists of a light absorbing dye (PS), an electron acceptor (A) and an electron donor (D) (Scheme 3). In such systems, upon irradiation photoinduced electron transfer reaction between the dye and one of the components, for example A in Scheme 3, gives rise to a radical anion (A$^{\bullet-}$) and the oxidized PS (PS$^{\bullet+}$). Then, PS$^{\bullet+}$ can react with the electron donor D (k_{red}) to regenerate the PS ground state (photocyclic reaction), leading to the formation of one radical cation D$^{\bullet+}$. Generally, A$^{\bullet-}$ and D$^{\bullet+}$ will give rise to initiating radicals for free radical polymerization, to hydrogen by water reduction or oxygen by water oxidation [6-8], etc. In an ideal case, a photocatalytic behavior is ensured when there is enough redox donor to make the dye surviving during a long period of time. It will be shown below that this behavior has great advantages; the most immediate is the fact that the absorbance of the PCIS is kept constant.

In order to exemplify the behavior of the photocycle involving the dye, the acceptor and the donor, the absorbance of a RB/TA/EDB solution was monitored during irradiation as for the Type II PIS. EDB was chosen as electron donor for the PCIS,

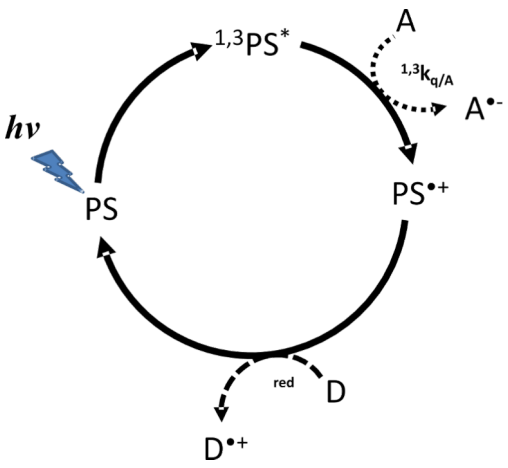

Scheme 3: Photocatalytic behavior occurring in three component PIS. PS: photosensitizer; $^{1,3}PS^{*}$: singlet and triplet PS excited states; A: electron acceptor; $A^{\bullet-}$: reduced form of acceptor; D: electron donor and $D^{\bullet+}$: oxidized donor.

because its reactivity toward ^{3}PS is low compared to that of TA (vide infra). This ensures that ^{3}PS will react mainly with TA in an oxidative cycle as proposed in Scheme 3. The solution was irradiated with the same laser diode and same output power. The same initial concentration of RB and TA was realized, and $[EDB]_0$ was fixed to 10^{-3} mol·L^{-1}. The experimental evolution of the [RB(t)] could be seen on Figure 2.

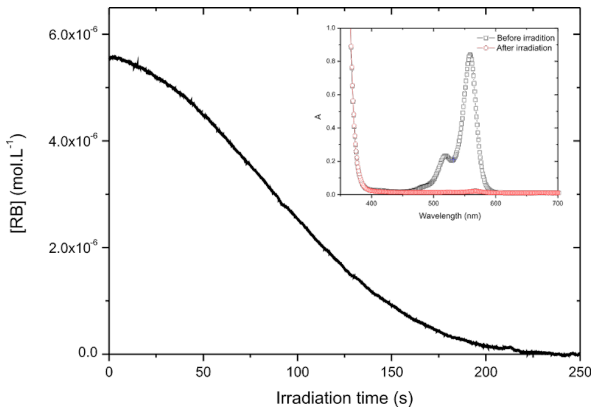

Figure 2: Evolution of [RB](t) in the photocyclic system RB/TA/EDB as a function of irradiation time (λ = 532 nm, 9 mW·cm^{-3}). Insert: absorption spectra obtained before and after irradiation.

Compared to the Type II PIS, the behavior is quite different: the absorbance decreases very slowly at the beginning of the process, being almost constant for a couple of seconds. Then, the absorbance slowly decreases due to an increase of the photolysis rate with irradiation time. After 250 seconds, the residual absorbance is zero: in the photocyclic system, the time required for complete consumption of the dye is two times longer than in Type II PIS. This confirms the dye regeneration within a photocycle exhibiting a photocatalytic behavior.

The longer experimental surviving time of RB in the PCIS is in qualitative agreement with the proposed schemes. To quantify the cyclic behavior and to compare clearly Type II and PCIS, the quantum yield of dye photolysis ($\Phi_{photolysis}$) was also determined for RB/TA/EDB. The total concentration of absorbed photons for the PCIS is 0.0139 mol·L^{-1}. Dividing the initial RB concentration by this value leads to a photolysis quantum yield of $4.7\cdot10^{-3}$. This extremely low photolysis quantum yield obtained for the PCIS means that more than 210 photons are needed to bleach one dye molecule. The turnover number becomes very high for the PCIS while for the Type II system, only 5 photons are needed to bleach RB. This clearly demonstrates the cyclic regeneration of the dye in the selected three-component combination presented here. As a conclusion, these experimental results clearly confirm the photocyclic behavior of the selected 3-cpt system RB/TA/EDB. However, to get more insight and to understand the benefits of this process, a better understanding of the thermodynamics and the kinetics is necessary.

Thermodynamics of the PCIS

Obviously, every mixture of an acceptor, a donor and a dye, would not give rise to a photocatalytic behavior. The components should be selected with care in order to get a cyclic behavior instead of competitive parallel reactions [54] where A and D compete to react with the PS excited states. Thus, a thermodynamic approach of the PCIS should help the selection of the candidates. Scheme 4 represents the different electron transfer reaction occurring in the oxidative PCIS according to the mechanism given in Scheme 3.

The first reaction is the electron transfer reaction between the dye ground state and the coinitiator. Its reactivity is governed by the corresponding Gibbs free energy change $\Delta G_{ET}^{GS} = E_{ox}^{PS} - E_{red}^{A}$ where E_{ox} and E_{red} are the half-wave oxidation and reduction potentials for the donor and the acceptor, respectively. ΔG_{ET}^{GS} must be as high as possible to prevent any dark reaction.

After absorption of light the PS goes into singlet or triplet excited states, in which it becomes both more oxidant and more reducer. As a consequence, electron transfer reaction can occur with the acceptor A (Scheme 3). The reaction must be as much exergonic as possible. The values of the Gibbs free energy

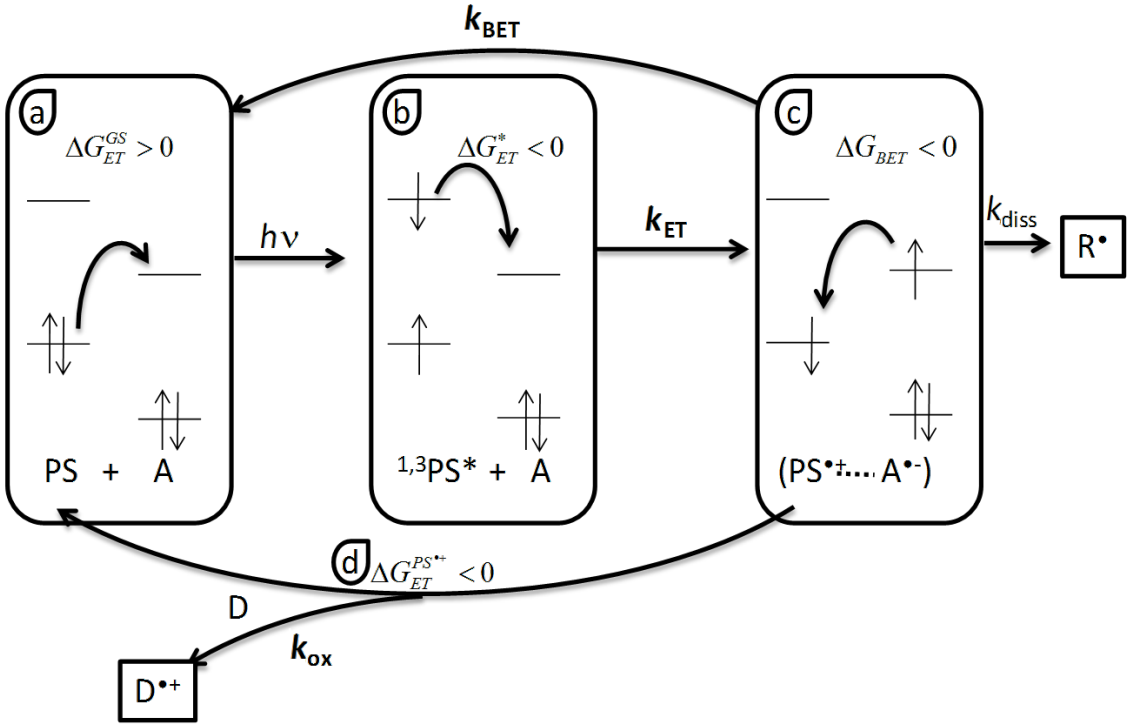

Scheme 4: Thermodynamics of an oxidative three components PCIS, a) ground state reaction (ΔG_{ET}^{GS}), b) excited state reaction (ΔG_{ET}^{*}), c) back electron transfer (BET, ΔG_{BET}), d) PS regeneration ($\Delta G_{ET}^{PS^{\bullet+}}$).

change ΔG_{ET}^{*} for photoinduced electron transfer is given by the Rehm–Weller equation [56]: $\Delta G_{ET}^{*} = E_{ox}^{PS} - E_{red}^{A} - E^{*} + C$, where E^{*} stands for the energy of the excited state. The Coulombic term C is usually neglected in polar solvent. ΔG_{ET}^{*} will determine the rate of electron transfer and the dye and the electron acceptor must be chosen such that ΔG_{ET}^{*} is negative enough to obtain a high electron transfer rate constant.

The third electron transfer step is the unwanted back electron transfer BET within the contact ion pair ($PS^{\bullet+}\cdots A^{\bullet-}$) which leads to initial reactants. This one is the more tricky to handle. ΔG_{BET} is given by $-\Delta G_{ET}^{GS} = E_{red}^{A} - E_{ox}^{PS}$. This reaction is generally quite exergonic and the rate compete with the dissociation rate k_{diss} of the contact ion pair into free solvated species. In practice BET reduce the overall radical generation quantum yields. Some new approaches allow to trigger this reaction [57,58].

The last important step is the dye regeneration. In order for the cycle and for the catalytic behavior to occur, the corresponding Gibbs free energy change $\Delta G_{ET}^{PS^{\bullet+}}$ should be negative. If one assumes that the reduction potential of $PS^{\bullet+}$ is given by the oxidation potential of PS, then $\Delta G_{ET}^{PS^{\bullet+}} = E_{ox}^{D} - E_{ox}^{PS}$. Thus, in order to achieve an efficient dye regeneration, the choice of the donor D should be carefully done to obtain an exergonic reduction of the oxidized PS.

This approach is also valid to a reductive catalytic cycle where the PS first reacts with the donor D, and then its reduced form is oxidized by the acceptor A. Table 1 summarizes the Gibbs free energy formula for estimation and the potential effect on the photocyclic behavior. The "Wanted values" row gives the values which must be obtained in order to get a possible photocyclic behavior of the selected components. The "Control" row summarizes the effect of the corresponding electron transfer on the PCIS final properties like shelf life, radical quantum yield and dye regeneration. One should also note that as $\Delta G_{BET} = -\Delta G_{ET}^{GS}$ it is always negative even if a positive value is wanted.

Computational studies of PCIS

As seen before, there are four-electron transfer reactions to manage in order to get a working PCIS. Moreover the full mechanistic description becomes more complicate by taking into account that both the oxidative and reductive pathways can be in competition (see Scheme 5). In order to get more insights into the description and comprehension of PCIS, a complete simulation of the photocyclic behavior of RB/TA/EDB was

Table 1: Gibbs free energy of the different electron transfer reactions occurring in a three component PCIS.

Gibbs free energy	Wanted values	Control
$\Delta G_{ET}^{GS} = E_{ox}^{PS} - E_{red}^{A}$	>0	Shelf life
$\Delta G_{ET}^{*} = E_{ox}^{PS} - E_{red}^{A} - E^{*} + C$	<0	Rate of electron transfer: radical quantum yields
$\Delta G_{BET} = E_{red}^{A} - E_{ox}^{PS} = -\Delta G_{ET}^{GS}$	>0	Control of back electron transfer: radical quantum yields
$\Delta G_{ET}^{PS^{\bullet+}} = E_{ox}^{D} - E_{ox}^{PS}$	<0	Regeneration of the PS: photolysis quantum yield

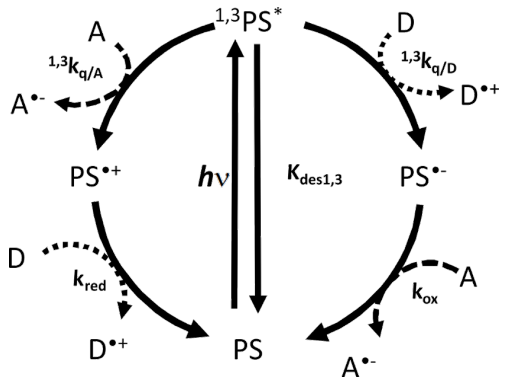

Scheme 5: General photocatalytic cycle occurring in three components photocyclic systems. Two cycles are in competition: on the right side the first reaction occurs with the donor D defining the reductive pathway, while on the left side the primary reaction occurs with the acceptor A leading to the oxidative pathway.

performed, comprising both a reductive and oxidative pathway (Scheme 5).

The full kinetic description of the reactions occurring in the complete cycle is displayed in Figure 3, where I_{abs} is the number of absorbed photons per second; k_{des1}, k_{des3} are the rate constants of singlet and triplet state deactivation to the ground state, respectively; k_{ISC} the rate constant of the intersystem crossing from ^{1}PS to ^{3}PS; $^1k_{q/A}$, $^3k_{q/A}$, ($^1k_{q/D}$, $^3k_{q/D}$) the bimolecular electron transfer rate constant of the singlet and triplet excited state of the PS by the acceptor A (donor D), respectively; k_{red} and k_{ox} are the rate constants of reduction and oxidation of PS$^{\bullet+}$ and PS$^{\bullet-}$, respectively.

The time evolution of ground state PS ^{0}PS, ^{1}PS ^{3}PS excited state, PS$^{\bullet+}$, PS$^{\bullet-}$, D, A, D$^{\bullet+}$ and A$^{\bullet-}$ are given by the following equations:

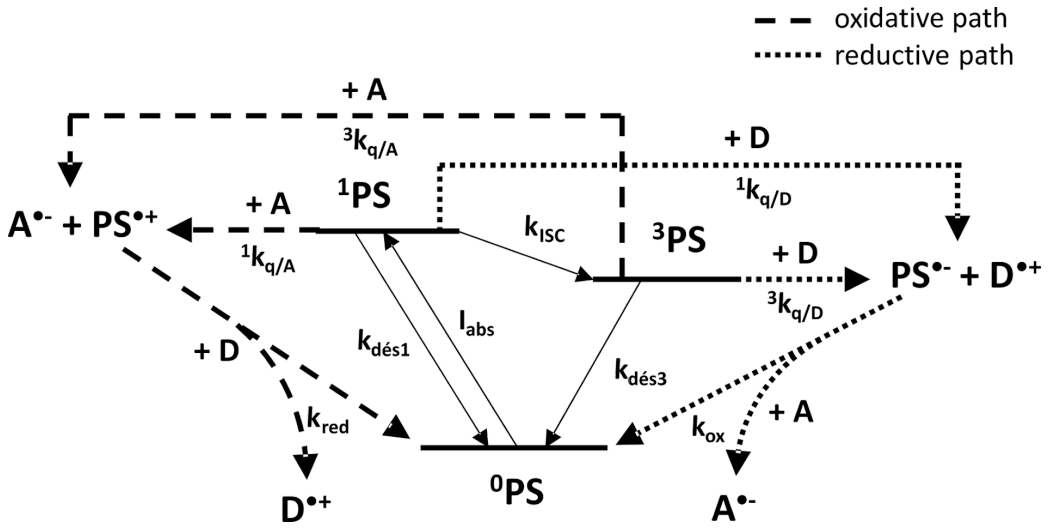

Figure 3: Mechanistic description of photocyclic system involved in the RB/TA/EDB system. The rate constants are defined in the text.

$$
\begin{aligned}
\frac{d\left[{}^{0}PS\right]}{dt} &= -I_{abs} + k_{des1}\left[{}^{1}PS\right] + k_{des3}\left[{}^{3}PS\right] + k_{redox/A}\left[PS^{\bullet-}\right][A] + k_{redox/D}\left[PS^{\bullet+}\right][D] \\
\frac{d\left[{}^{1}PS\right]}{dt} &= I_{abs} - k_{des1}\left[{}^{1}PS\right] - k_{CIS}\left[{}^{1}PS\right] - {}^{1}k_{q/D}\left[{}^{1}PS\right][D] - {}^{1}k_{q/A}\left[{}^{1}PS\right][A] \\
\frac{d\left[{}^{3}PS\right]}{dt} &= k_C IS[{}^{3}PS] - k_d es3[{}^{3}PS] - 3k_{(q/D)}[{}^{3}PS][D] - {}^{3}k_{(q/A)}[{}^{3}PS][A] \\
\frac{d\left[PS^{\bullet-}\right]}{dt} &= {}^{1}k_{q/D}\left[{}^{1}PS\right][D] + {}^{3}k_{q/D}\left[{}^{3}PS\right][D] - k_{redox/A}\left[PS^{\bullet-}\right][A] \\
\frac{d\left[PS^{\bullet+}\right]}{dt} &= {}^{1}k_{q/A}\left[{}^{1}PS\right][A] + {}^{3}k_{q/A}\left[{}^{3}PS\right][A] - k_{redox/D}\left[PS^{\bullet+}\right][D] \\
\frac{d[D]}{dt} &= -{}^{1}k_{q/D}\left[{}^{1}PS\right][D] - {}^{3}k_{q/D}\left[{}^{3}PS\right][D] - k_{redox/D}\left[PS^{\bullet+}\right][D] \\
\frac{d[A]}{dt} &= -{}^{1}k_{q/A}\left[{}^{1}PS\right][A] - {}^{3}k_{q/A}\left[{}^{3}PS\right][A] - k_{redox/A}\left[PS^{\bullet+}\right][A] \\
\frac{d\left[D^{\bullet-}\right]}{dt} &= -\frac{d[D]}{dt} = {}^{1}k_{q/D}\left[{}^{1}PS\right][D] + {}^{3}k_{q/D}\left[{}^{3}PS\right][D] + k_{redox/D}\left[PS^{\bullet+}\right][D] \\
\frac{d\left[A^{\bullet+}\right]}{dt} &= -\frac{d[A]}{dt} = {}^{1}k_{q/A}\left[{}^{1}PS\right][A] + {}^{3}k_{q/A}\left[{}^{3}PS\right][A] + k_{qredox/A}\left[PS^{\bullet-}\right][A]
\end{aligned}
\tag{3}
$$

The absorption of the light is given by:

$$I_{abs} = I_0 - I_T = I_0 - I_0 \cdot 10^{-A} = I_0\left(1 - 10^{-\varepsilon \cdot l \cdot [PS]}\right)$$

where I_0 and I_T are the incident and transmitted light intensity on/through the sample respectively (einstein·L^{-1}·s^{-1}), ε is the molar extinction coefficient of the PS at the irradiation wavelength and l is the cell thickness.

Simulation parameters

In order to simulate the photocyclic behavior, the different rate constants involved in the proposed mechanism were measured by time resolved spectroscopies (laser flash photolysis for triplet excited states and time correlated single photon counting for excited singlet states). The experimental quenching rate constants and their corresponding ΔG_{ET} are given in Table 2. As k_{red} and k_{ox} were not measurable, a value of $2 \cdot 10^3$ $M^{-1} \cdot s^{-1}$ was taken to perform the computations. This is justified by the fact that the radical recombination in the type II systems observed by laser flash photolysis occurs in the ms timescale. The last row of Table 2 contains the calculated Gibbs free energy of the dye regeneration redox reaction. These slightly endergonic values (0.42 and 0.12 eV) support the low k_{red} and k_{ox} rate constants used for computation.

The measured electron transfer rate constants are in line with the ΔG, confirming the low reactivity of ^{3}PS toward EDB. Intersystem crossing rate constant k_{ISC} was obtained from the triplet state quantum yield and singlet state lifetime according to [59]:

$$\varphi_0^T = \frac{k_{ISC}}{k_{des1} + k_{ISC}} = \frac{k_{ISC}}{1/\tau_0^S}$$

Table 2: Thermodynamic and kinetic parameters of the PCIS simulation, k_q: quenching rate constant of excited states.

Quencher	ΔG_{ET} (eV)/k_q ($M^{-1} \cdot s^{-1}$)				
	^{0}RB	^{1}RB	^{3}RB	RB$^{\bullet+}$	RB$^{\bullet-}$
EDB	2.07	−0.10/9.0 10^8	0.27/4.50 10^4	0.42/–	
TA	1.77	−0.40/6.0 10^9	−0.03/1.7 10^7		0.12/–

which leads to:

$$k_{ISC} = \frac{\varphi_0^T}{\tau_0^S} = \frac{0.81}{2.410^{-9}} \approx 3.410^8 M^{-1} \cdot s^{-1}$$

and to

$$k_{des1} = \frac{1}{\tau_0^S} - k_{ISC} = \frac{1}{2.410^{-9}} - 3.3810^8 \approx 7.910^7 M^{-1} \cdot s^{-1}$$

At this RB concentration, and in the absence of quencher, the triplet state lifetime was measured around 80 µs, leading to k_{des3}= 1.25·10^4 M^{-1}s^{-1}. The following parameters were used to perform the computation: the continuous incident light intensity I_0 was fixed to 9 mW·cm^{-2} at 532 nm (i.e., 4·10^{-5} einstein·L^{-1}·s^{-1}). The initial PS (i.e., RB) concentration was fixed to [RB]$_0$ = 6.50·10^{-6} M, with ε = 31900 M^{-1}·cm^{-1} and a cell length of 1 cm this corresponds to an absorbance of 0.2 at 532 nm, in line with the experiments. The initial concentration of the quenchers were fixed at [TA]$_0$ = 10^{-2} M and [EDB]$_0$ = 10^{-3} M for TA (acceptor A) and EDB (donor D).

Photophysical cycle

One must keep in mind that in PCIS, two cycles can occur: the photochemical one which involves the reaction of the dye excited states with chemical reactants, and an internal photophysical. This later is an energy waste, comprising the absorption of light, the deactivation by internal conversion and fluorescence of ^{1}PS to the ground state ^{0}PS, the intersystem crossing to ^{3}PS, and the deactivation of the ^{3}PS to ^{0}PS. In order to achieve high quantum yield for the conversion of the light energy, this photophysical cycle should be avoided as much as possible. This means that the excited states must live as long as possible, the quenching rate constants should be as high as possible (exergonic reaction with high $^{1,3}k_{q/A}$ and $^{1,3}k_{q/D}$), and a high concentration of D and A should be used (high pseudo first order rate constants $^{1,3}k_{q/A}$[A] and $^{1,3}k_{q/D}$[D]). This will prevent the probability of natural excited state deactivation to be high.

Simulation of Type II photoinitiating system

The Type II system studied here contains only RB as photosensitizer and an electron acceptor TA (or donor EDB). Both RB/TA and RB/EDB systems were calculated. Figure 4 shows the changes in RB, RB$^{\bullet+}$, TA, and TA$^{\bullet-}$ concentrations for the former system.

Two important conclusions are to be outlined. First, the ground state of the dye is quickly bleached: in about 4 seconds it has completely disappeared. Second: the final TA$^{\bullet-}$ concentration, i.e., the maximum number of initiating radicals produced is equal to the initial ground state RB concentration, i.e., 6.50·10^{-6} M. The final triazine concentration remains high because only 6.50·10^{-6} M of TA have reacted with the dye RB. The same conclusion can be drawn for the RB/EDB computation but with slower rates due to lower reactivity (i.e., $k_{q/D}$). As a conclusion, in Type II PIS the limiting component for radical generation is the concentration of the dye.

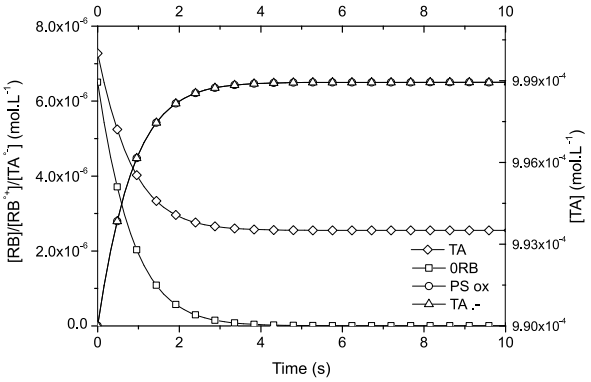

Figure 4: Evolution of RB, RB$^{\bullet+}$, TA, and TA$^{\bullet-}$ concentration with time for RB/TA system.

Simulation of photocyclic initiating system

In the photocyclic system, the initial pseudo first-order reaction rates are equal to $^3k_{q/A}$[TA]$_0$ = 1.7·10^5 s^{-1} for TA (acceptor A) and $^3k_{q/D}$[EDB]$_0$ = 4.5·10^1 s^{-1} for EDB (donor D). This means that the oxidative photocycle preferentially occurs, at least until $^3k_{q/A}$[TA] > $^3k_{q/D}$[EDB]. The plot of Log($^3k_{q/A}$[TA]) and Log($^3k_{q/D}$[EDB]) on Figure 5 show that it is the case for the first 310 sec of the reaction: during this period one can assume that the oxidative pathway is the main reaction.

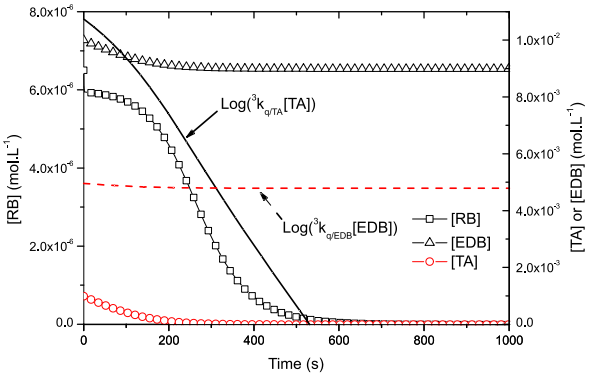

Figure 5: Evolution of RB, TA and EDB concentrations in the photocyclic system. The logarithm of oxidative and reductive pseudo first order reaction rates are given in plain and dashed lines, respectively.

The evolution of [RB], [TA] and [EDB] displayed on Figure 5 is also very interesting. Two major differences with Type II PIS should be outlined: first, the acceptor TA is totally consumed as its concentration falls to zero. Second, the ground state RB concentration, presents only a slight decrease during 200 s, i.e., as long as enough acceptor TA is present in the solution. This first part of the cycle should be explained by the reduction of the oxidized dye $RB^{\bullet+}$, by EDB leading to a recovery of the dye. As soon as no more TA is available (around 250 s) [RB] lowers faster to zero. In this second part the photocatalytic system is reduced to a conventional Type II system, where the dye is consumed during its reaction with the excess of amine EDB. If the TA acceptor is completely consumed this is not the case for the amine present in excess, only one TA equivalent is lost during the first part of the cycle, and [EDB] reduces to $0.9{\cdot}10^{-2}$ M. During the second part of the reaction, a more tiny $6.5{\cdot}10^{-6}$ M is consumed (i.e. the initial RB concentration, cf. type II PIS) leading to a final EDB concentration of $8.9935{\cdot}10^{-3}$ M.

On Figure 6, the evolution of $EDB^{\bullet+}$ and $TA^{\bullet-}$ concentrations are displayed together with RB. In the first part of the cycle (before 300 s) both radical curves are similar. Then, as soon as TA is consumed, no more $TA^{\bullet-}$ is produced and a final concentration of $1{\cdot}10^{-3}$ M is reached, i.e. the initial TA concentration. At this stage the $EDB^{\bullet+}$ also reaches $1{\cdot}10^{-3}$ M. During this second part, the reaction of excess EBD with RB leads to a tiny more $6.5{\cdot}10^{-6}$ M for $EDB^{\bullet+}$ and to the bleaching of the dye. Thus, the computed final total radical concentration is formally equal to $2.0065{\cdot}10^{-3}$ M.

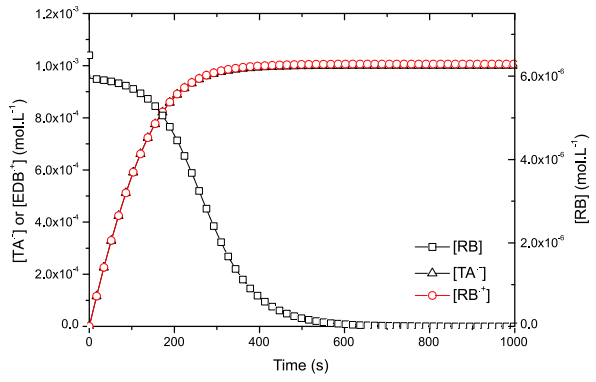

Figure 6: Evolution of radical concentrations $TA^{\bullet-}$ and $EDB^{\bullet+}$ together with [RB] in photocatalytic system.

It is worth emphasizing the important points and advantages of photocyclic systems:

1. the dye concentration is kept high for 250 s, this means that the absorbance of the solution is high, leading to a very high photon absorption of the solution during the first part of the cycle;

2. the final radical concentration is very high: $2.0065{\cdot}10^{-3}$ M i.e. 150 times the concentration obtained in Type II PIS;

3. the limiting component is no more the dye, but the co-initiator of lowest concentration, in the present case the acceptor TA.

All this phenomena explain the synergistic effect observed in some free radical polymerization.

Radical and photolysis quantum yields

As for the Type II systems, in order to quantify the catalytic behavior of the dye, the quantum yield of dye photolysis ($\Phi_{photolysis}$) in PCIS was determined. The radical quantum yield is defined by the ratio of the number of produced radical to the total number of absorbed photons (N_{abs}). It could be expressed by the following equation:

$$\Phi_{rad} = \frac{N_{rad}}{N_{abs}} = \frac{V \cdot \left(\left[A^{\bullet-}\right] + \left[R^{\bullet+}\right]\right)}{V \cdot \int I_{abs}.dt} = \frac{\left[A^{\bullet-}\right] + \left[R^{\bullet+}\right]}{\int I_{abs} \cdot dt} \quad (4)$$

The calculated quantum yield for Type II RB/TA and photocyclic RB/TA/EDB are given in Table 3.

Table 3: Calculated photolysis and radical quantum yields of the Type II and the PCIS.

	Type II RB/TA	PCIS RB/TA/EDB
Φphotolysis	0.475	$1.55{\cdot}10^{-3}$
Φrad	0.475	0.478

In Type II PIS both quantum yields are equal because the amount of radicals formed is equal to the amount of dye photolysed: as a consequence, only about two photons are needed to bleach one dye molecule, corresponding to a very low turnover number. Moreover we can see that the system has an average efficiency: according to Φ_{rad} one photon on two is lost for radical generation. For photocyclic system, the picture is somehow different: the photolysis quantum yield falls to $1.55{\cdot}10^{-3}$, meaning that more than 600 photons are needed to bleach one dye molecule: the turnover number becomes very high for the PCIS selected for the computation. However, if the photocatalytic behavior is very good, the radical quantum yield present an average value around 0.478, especially if one keep in

mind that it could rise up to two, theoretically. But this is in line with the low rate constant of electron transfer of RB excited singlet and triplet states: the wasting photophysical cycle is comparatively too fast, preventing any efficient chemical energy escape from the photophysical cycle

However one can see from the experimental results that the consumption of the dye is longer than awaited for the Type II PIS, while it is shorter for the photocatalytic system. This is confirmed by comparing the experimental photolysis quantum yields to the computed values: the experimental photolysis quantum yield is higher and the turn over number of the real photocatalytic system RB/TA/EDB is lower than expected, while the opposite stands for RB/TA. This should be due to the fact that the bleaching of the dye is not only a direct consequence of the electron transfer reaction but could be due also to secondary reactions between the radicals and the dye related intermediates. As a consequence, the experimental efficiency of the photocycle is lower than the simulated one. This is clear from the shape of the two experimental curves where the consumption of RB in RB/TA is initially fast and then decreases slower while the opposite stands for the RB/TA/EDB: the consumption increases due to an increase of radical in the solution.

Conclusion

In this paper experimental and full mechanistic studies of Type II PIS and 3-cpt photocatalytic systems were presented and compared. Some advantages that PCIS bear over classical Type II systems are: dye regeneration with high possible turnover (600), high radical production ($>10^{-3}$ M). But these studies also reveal the importance of component choice: great care must be taken in order to build photocatalytic radical generator by combination of three compounds. Especially a simple thermodynamic approach should help to select the candidates as a starting point. If the present paper was focused on PCIS application for free radical photopolymerization, it should be noted that the same type of system bearing the same underlying kinetics and mechanisms are used in the field of photocatalytic water reduction.

Experimental

Redox potentials were measured by cyclic voltammetry using a potentiostat (Princeton Applied Research 263A) at a scan rate of 1 V/s in acetonitrile, with platinum as both working and auxiliary electrodes, and a saturated calomel reference electrode (KCl in methanol). Measurements were performed in acetonitrile using 0.1 M of tetrabutylammonium hexafluorophosphate (Aldrich) as supporting electrolyte. The samples were bubbled with argon for 20 minutes prior to the analysis. Ferrocene was used as standard [60].

Steady sate UV–vis spectra were obtained on a Varian Cary 4000 UV–vis double beam spectrophotometer in 1 cm path quartz UV grade cell.

Laser flash photolysis experiments (LFP) were carried out exciting at 532 nm with a nanosecond Nd-YAG laser (Powerlite 9010, Continuum), operating at 10 Hz. The transient absorption analysis system (LP900, Edinburgh Instruments) uses a 450 W pulsed Xe arc lamp, a Czerny–Turner monochromator, a fast photomultiplier, and a transient digitizer (TDS 340, Tektronix) [61]. The instrumental response was about 7 ns. The observation wavelength is indicated in each case. Experiments were performed in acetonitrile under Ar bubbling.

A FluoroMax-4 (Horiba, Jobin-Yvon) spectrofluorometer coupled with a Time-Correlated Single-Photon Counting (TCSPC) accessory was used to measure the steady-state fluorescence spectra and singlet excited state lifetimes. NanoLEDs were used as pulsed excitation source leading to a time resolution of around 200 ps. The measurements were performed in acetonitrile solutions under argon bubbling at room temperature. The quenching rate constants k_q of the excited states were obtained according to the Stern–Volmer analysis where the reciprocal lifetime is plotted as a function of quencher concentration: [57].

Chemicals: Rose Bengal extra (RB) and ethyl 4-(dimethylamino)benzoate (EDB) were obtained from Aldrich, 2-(4-methoxyphenyl)-4,6-bis(trichloromethyl)-1,3,5-triazine (TA) was gifts from PCAS (France). Their chemical structures are given in Scheme 1.

References

1. Wang, X.; Werner, S.; Weiß, T.; Liefeith, K.; Hoffmann, V. *RSC Adv.* **2012,** *2,* 156–160. doi:10.1039/c1ra00599e
2. Muraoka, T.; Koh, C.-Y.; Cui, H.; Stupp, S. I. *Angew. Chem.* **2009,** *121,* 6060–6063. doi:10.1002/ange.200901524
3. Muraoka, T.; Koh, C.-Y.; Cui, H.; Stupp, S. I. *Angew. Chem., Int. Ed.* **2009,** *48,* 5946–5949. doi:10.1002/anie.200901524
4. Herrmann, A. *Photochem. Photobiol. Sci.* **2012,** *11,* 446–459. doi:10.1039/c1pp05231d
5. Dietliker, K. *A Compilation of Photoinitiators Commercially Available for UV Today;* SITA Technology Limited: Edinburgh/London, U.K., 2002.
6. Gärtner, F.; Denurra, S.; Losse, S.; Neubauer, A.; Boddien, A.; Gopinathan, A.; Spannenberg, A.; Junge, H.; Lochbrunner, S.; Blug, M.; Hoch, S.; Busse, J.; Gladiali, S.; Beller, M. *Chem.–Eur. J.* **2012,** *18,* 3220–3225. doi:10.1002/chem.201103670
7. Fukuzumi, S.; Hong, D.; Yamada, Y. *J. Phys. Chem. Lett.* **2013,** *4,* 3458–3467. doi:10.1021/jz401560x
8. Luo, S.-P.; Mejía, E.; Friedrich, A.; Pazidis, A.; Junge, H.; Surkus, A.-E.; Jackstell, R.; Denurra, S.; Gladialli, S.; Lochbrunner, S.; Beller, M. *Angew. Chem., Int. Ed.* **2013,** *52,* 419–423. doi:10.1002/anie.201205915

9. Ibrahim, A.; Ley, C.; Allonas, X.; Tarzi, O. I.; Chan Yong, A.; Carré, C.; Chevallier, R. *Photochem. Photobiol. Sci.* **2012,** *11,* 1682–1690. doi:10.1039/c2pp25099c
10. Bochet, C. G. *J. Chem. Soc., Perkin Trans. 1* **2002,** 125–142. doi:10.1039/B009522M
11. Klán, P.; Šolomek, T.; Bochet, C. G.; Blanc, A.; Givens, R.; Rubina, M.; Popik, V.; Kostikov, A.; Wirz, J. *Chem. Rev.* **2013,** *113,* 119–191. doi:10.1021/cr300177k
12. Fouassier, J. P.; Allonas, X.; Lalevee, J.; Dietlin, C. In *Photochemistry and Photophysics of Polymer Materials;* Allen, N. S., Ed.; Wiley: Hoboken, 2010; pp 351–419. doi:10.1002/9780470594179.ch10
13. Decker, C. J. *Coat. Technol.* **1987,** *59,* 97–106.
14. Peiffer, R. W. Applications of photopolymer technology. In *Photopolymerization: Fundamentals and Applications;* Scranton, A. B.; Bowman, C. N.; Peiffer, R. W., Eds.; American Chemical Society: Washington, DC, USA, 1997; pp 1–14. doi:10.1021/bk-1997-0673.ch001
15. Holman, R. *Eur. Coat. J.* **1995,** *9,* 610–612.
16. Sponsler, M. B. *J. Phys. Chem.* **1995,** *99,* 9430–9436. doi:10.1021/j100023a020
17. Löchel, B.; Maciossek, A.; Quenzer, H. J.; Wanger, B. *J. Electrochem. Soc.* **1996,** *143,* 237–244. doi:10.1149/1.1836415
18. Wakasa, K.; Chowdhury, N. A.; Priyawan, R.; Yoshida, Y.; Ikeda, A.; Hirose, T.; Yamaki, M. *J. Mater. Sci. Lett.* **1996,** *15,* 134–136. doi:10.1007/BF00291447
19. Shi, W.; Rånby, B. *J. Appl. Polym. Sci.* **1996,** *59,* 1951–1956. doi:10.1002/(SICI)1097-4628(19960321)59:12<1951::AID-APP18>3.0.CO;2-U
20. Decker, C. Photostabilization of macromolecular materials by UV-cured protective coatings. In *Polymer Durability;* Clough, R. L.; Billingham, N. C.; Grillen, K. T., Eds.; American Chemical Society: Washington, DC, USA, 1996; Vol. 249, pp 319–334. doi:10.1021/ba-1996-0249.ch021
21. Akiyama, H.; Momose, M.; Ichimura, K.; Yamamura, S. *Macromolecules* **1995,** *28,* 288–293. doi:10.1021/ma00105a040
22. Chan, C.-M.; Ko, T.-M.; Hiraoka, H. *Surf. Sci. Rep.* **1996,** *24,* 1–54. doi:10.1016/0167-5729(96)80003-3
23. Allonas, X.; Morlet-Savary, F.; Lallevée, J.; Fouassier, J.-P. *Photochem. Photobiol.* **2006,** *82,* 88–94. doi:10.1562/2005-05-20-RA-535
24. Jockusch, S.; Turro, N. J. *J. Am. Chem. Soc.* **1998,** *120,* 11773–11777. doi:10.1021/ja982463z
25. Crivello, J. V.; Dietliker, K. *Photoinitiators for Free Radical Cationic & Anionic Photopolymerisation;* John Wiley & Sons: New York, USA, 1999.
26. Green, W. A. *Industrial Photoinitiators: A Technical Guide;* CRC Press: Boca Raton FL, 2010. doi:10.1201/9781439827468
27. Allonas, X.; Fouassier, J. P.; Kaji, M.; Miyasaka, M.; Hidaka, T. *Polymer* **2001,** *42,* 7627–7634. doi:10.1016/S0032-3861(01)00275-0
28. Mallavia, R.; Fimia, A.; García, C.; Sastre, R. *J. Mod. Opt.* **2001,** *48,* 941–945. doi:10.1080/09500340108230965
29. Mauguière-Guyonnet, F.; Burget, D.; Fouassier, J. P. *Prog. Org. Coat.* **2007,** *59,* 37–45. doi:10.1016/j.porgcoat.2007.01.007
30. Mallavia, R.; Amat-Guerri, F.; Fimia, A.; Sastre, R. *Macromolecules* **1994,** *27,* 2643–2646. doi:10.1021/ma00087a041
31. Ibrahim, A.; Ley, C.; Tarzi, O. I.; Fouassier, J. P.; Allonas, X. *J. Photopolym. Sci. Technol.* **2010,** *23,* 101–108. doi:10.2494/photopolymer.23.101
32. Tarzi, O. I.; Allonas, X.; Ley, C.; Fouassier, J. P. *J. Polym. Sci., Part A: Polym. Chem.* **2010,** *48,* 2594–2603. doi:10.1002/pola.24039
33. Kucybaa, Z.; Pietrzak, M.; Paczkowski, J.; Linden, L.-A.; Rabek, J. F. *Polymer* **1996,** *37,* 4585–4591. doi:10.1016/0032-3861(96)00302-3
34. Hageman, H. J. *Prog. Org. Coat.* **1985,** *13,* 123–150. doi:10.1016/0033-0655(85)80021-2
35. Cook, W. D. *Polymer* **1992,** *33,* 600–609. doi:10.1016/0032-3861(92)90738-I
36. Mateo, J. L.; Bosch, P.; Lozano, A. E. *Macromolecules* **1994,** *27,* 7794–7799. doi:10.1021/ma00104a038
37. Hoyle, C. E.; Kim, K.-J. *J. Appl. Polym. Sci.* **1987,** *33,* 2985–2996. doi:10.1002/app.1987.070330831
38. Hoyle, C. E.; Keel, M.; Kim, K.-J. *Polymer* **1988,** *29,* 18–23. doi:10.1016/0032-3861(88)90194-2
39. Buback, M.; Gilbert, R. G.; Russell, G. T.; Hill, D. J. T.; Moad, G.; O'Driscoll, K. F.; Shen, J.; Winnik, M. A. *J. Polym. Sci., Part A: Polym. Chem.* **1992,** *30,* 851–863. doi:10.1002/pola.1992.080300516
40. Soh, S. K.; Sundberg, D. C. *J. Polym. Sci., Polym. Chem. Ed.* **1982,** *20,* 1299–1313. doi:10.1002/pol.1982.170200513
41. Andrzejewska, E. *Polymer* **1996,** *37,* 1039–1045. doi:10.1016/0032-3861(96)87288-0
42. Guttenplan, J. B.; Cohen, S. G. *J. Org. Chem.* **1973,** *38,* 2001–2007. doi:10.1021/jo00951a007
43. Lalevée, J.; Morlet-Savary, F.; El Roz, M.; Allonas, X.; Fouassier, J. P. *Macromol. Chem. Phys.* **2009,** *210,* 311–319. doi:10.1002/macp.200800566
44. Hoyle, C. E.; Bowman, C. N. *Angew. Chem., Int. Ed.* **2010,** *49,* 1540–1573. doi:10.1002/anie.200903924
45. Morgan, C. R.; Kyle, D. R. *UV Generated Oxygen Scavengers and Method for Determining their Effectiveness in Photopolymerizable Systems;* Technology Marketing Corporation: Norwalk, CT, USA, 1983.
46. Kabatc, J.; Celmer, A. *Polymer* **2009,** *50,* 57–67. doi:10.1016/j.polymer.2008.10.036
47. Kabatc, J.; Kucybała, Z.; Pietrzak, M.; Ścigalski, F.; Paczkowski, J. *Polymer* **1999,** *40,* 735–745. doi:10.1016/S0032-3861(98)00282-1
48. Padon, S. K.; Scranton, A. B. *J. Polym. Sci., Part A: Polym. Chem.* **2000,** *38,* 3336–3346. doi:10.1002/1099-0518(20000915)38:18<3336::AID-POLA110>3.0.CO;2-3
49. Padon, K. S.; Scranton, A. B. *J. Polym. Sci., Part A: Polym. Chem.* **2000,** *38,* 2057–2066. doi:10.1002/(SICI)1099-0518(20000601)38:11<2057::AID-POLA140>3.3.CO;2-X
50. Costela, A.; Costela, A.; Garcia-Moreno, I.; Sastre, R. *Macromol. Chem. Phys.* **2003,** *204,* 2233–2239. doi:10.1002/macp.200300010
51. Fouassier, J. P.; Allonas, X.; Burget, D. *Prog. Org. Coat.* **2003,** *47,* 16–36. doi:10.1016/S0300-9440(03)00011-0
52. Allonas, X.; Fouassier, J. P.; Kaji, M.; Murakami, Y. *Photochem. Photobiol. Sci.* **2003,** *2,* 224–229. doi:10.1039/b209203d
53. Grotzinger, C.; Burget, D.; Jacques, P.; Fouassier, J. P. *Macromol. Chem. Phys.* **2001,** *202,* 3513–3522. doi:10.1002/1521-3935(20011201)202:18<3513::AID-MACP3513>3.0.CO;2-Z
54. Kabatc, J.; Jurek, K. *Polymer* **2012,** *53,* 1973–1980. doi:10.1016/j.polymer.2012.03.027
55. Kabatc, J. *Polymer* **2010,** *51,* 5028–5036. doi:10.1016/j.polymer.2010.09.020

56. Rehm, D.; Weller, A. *Isr. J. Chem.* **1970,** *8,* 259–271. doi:10.1002/ijch.197000029
57. Kawamura, K.; Schmitt, J.; Barnet, M.; Salmi, H.; Ley, C.; Allonas, X. *Chem.–Eur. J.* **2013,** *19,* 12853–12858. doi:10.1002/chem.201300622
58. Kawamura, K.; Ley, C.; Schmitt, J.; Barnet, M.; Allonas, X. *J. Polym. Sci., Part A: Polym. Chem.* **2013,** *51,* 4325–4330. doi:10.1002/pola.26844
59. Turro, N. J.; Ramamurthy, V.; Scaiano, J. C. *Modern molecular photochemistry of organic molecules;* University science book: Sausalito, California, 2010.
60. Jacques, P.; Burget, D.; Allonas, X. *New J. Chem.* **1996,** *30,* 933.
61. Allonas, X.; Fouassier, J.-P.; Angiolini, L.; Caretti, D. *Helv. Chim. Acta* **2001,** *84,* 2577–2588. doi:10.1002/1522-2675(20010919)84:9<2577::AID-HLCA2577>3.0.CO;2-Q

License and Terms

Beilstein Journal of Organic Chemistry

Visible light mediated intermolecular [3 + 2] annulation of cyclopropylanilines with alkynes

Theresa H. Nguyen, Soumitra Maity and Nan Zheng*

Full Research Paper

Open Access

Address:
Department of Chemistry and Biochemistry, University of Arkansas, Fayetteville, Arkansas, 72701, USA

Email:
Nan Zheng* - nzheng@uark.edu

* Corresponding author

Keywords:
[3 + 2]; alkyne; annulation; cyclopropylaniline; photoredox catalysis; visible light

Beilstein J. Org. Chem. **2014,** *10,* 975–980.
doi:10.3762/bjoc.10.96

Received: 04 February 2014
Accepted: 04 April 2014
Published: 29 April 2014

This article is part of the Thematic Series "Organic synthesis using photoredox catalysis".

Guest Editor: A. G. Griesbeck

Abstract

Intermolecular [3 + 2] annulation of cyclopropylanilines with alkynes is realized using visible light photoredox catalysis, yielding a variety of cyclic allylic amines in fair to good yields. This method exhibits significant group tolerance particularly with heterocycles. It can also be used to prepare complex heterocycles such as fused indolines.

Introduction

Cyclopropanes have been used as a three-carbon synthon to prepare a diverse array of organic compounds [1-4]. The unusual reactivity, exhibited by cyclopropanes, is largely due to their inherent ring strain that makes cleavage of the C–C bonds facile [5]. A number of methods have been developed to regioselectively cleave cyclopropanes, generating synthetically useful intermediates that can be further manipulated [1-5]. For one subclass of cyclopropanes, cyclopropylamines, the requisite ring opening is often accomplished by one-electron oxidation of the parent amine. This oxidation step can be realized enzymatically [6-8], chemically [9-14], electrochemically [15,16], and photochemically [17-20]. Recently, visible light photoredox catalysis has emerged as a powerful method to manipulate the redox chemistry of organic compounds [21-26]. Amines have been used as an electron donor to reduce the excited state of photocatalysts, while they are oxidized to amine radical cations. Our group and others have taken advantage of this facile redox process and developed a number of synthetic methods that harness the synthetic potential of amine radical cations [21,27,28]. One of the reported methods from our group involves [3 + 2] annulation of cyclopropylanilines with alkenes [29]. We were intrigued by the possibility of extending this annulation method to include alkynes. The immediate benefits of using alkynes include eliminating the diastereoselectivity issue observed in the annulation of monocyclic cyclopropylanilines with alkenes and introducing an alkene functional

group into the annulation product. Furthermore, the synthesis of cyclic allylic amines is non-trivial in general [30]. Herein, we report intermolecular [3 + 2] annulation of monocyclic cyclopropylanilines with alkynes under visible light photoredox conditions.

Results and Discussion

Biphenylcyclopropylamine **1** and phenylacetylene (**2**) were chosen as the standard substrates to optimize the catalyst system for the [3 + 2] annulation with alkynes (Table 1). Similar to the annulation with alkenes [29], several reactivity patterns were observed. CH_3NO_2 was far superior to DMF and CH_3CN as the solvent (Table 1; entries 1–3). $Ru(bpz)_3(PF_6)_2$ was a more effective photocatalyst than $Ru(bpy)_3(PF_6)_2$ (Table 1, entry 4). Air was detrimental to the annulation reaction (Table 1, entry 5). However, we noticed the annulation with alkynes was slower than with alkenes, previously reported by our group [29]. To compensate for lower reactivity of alkynes, we investigated commercially available light resources that were stronger than 13 W compact fluorescent lamps (CFLs). 13 W CFLs were used as the light source to mediate the annulation with alkenes [29]. White 18 W LEDs were found to be more effective for the annulation with alkynes, resulting in a higher yield (Table 1, entry 6). Control studies showed that both the photocatalyst and light were required, though some background reaction was observed (Table 1, entries 7 and 8).

To determine the scope of this annulation process, a range of cyclopropylanilines with various electronic and steric characteristics were prepared and then subjected to the optimized catalyst system. The results of the scope studies are summarized in Figure 1. Both electron-donating (OMe, **7**, and OTBS, **8**) and electron-withdrawing (CF_3, **9**, **14**, **18**, and CN, **10**, **13**) substituents were well tolerated, and the annulation products were generally obtained in modest to good yields. The annulation process also tolerated steric hindrance. Hindered cyclopropylanilines, such as those possessing an *ortho*-isopropyl group, were satisfactorily converted to the annulation products (**6** and **12**). With respect to the other annulation partner, terminal alkynes substituted with an electron-withdrawing group were typically required for the annulation process. Alkyl-substituted terminal alkynes and internal alkynes were not reac-

Table 1: Catalyst screening.

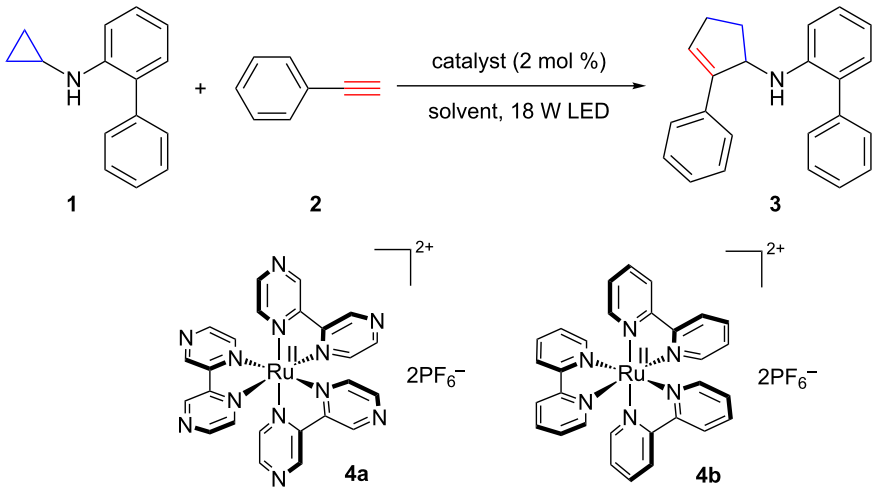

Entry[a]	Catalyst	Light	Solvent	GC yield of **3** [%][b]
1	**4a**	18 W LED	CH_3NO_2	82 (80)[c]
2	**4a**	18 W LED	DMF	20
3	**4a**	18 W LED	CH_3CN	36
4	**4b**	18 W LED	CH_3NO_2	55
5[d]	**4a**	18 W LED	CH_3NO_2	41
6	**4a**	13 W CFL	CH_3NO_2	68
7	none	18 W LED	CH_3NO_2	6
8	**4a**	none	CH_3NO_2	3

[a]Conditions: **1** (0.2 mmol), **2** (1 mmol), solvent (2 mL), degassed, irradiation at rt for 8 h. [b]Dodecane was used as an internal standard. [c]Isolated yield by silica gel chromatography. [d]The reaction was conducted in the presence of air.

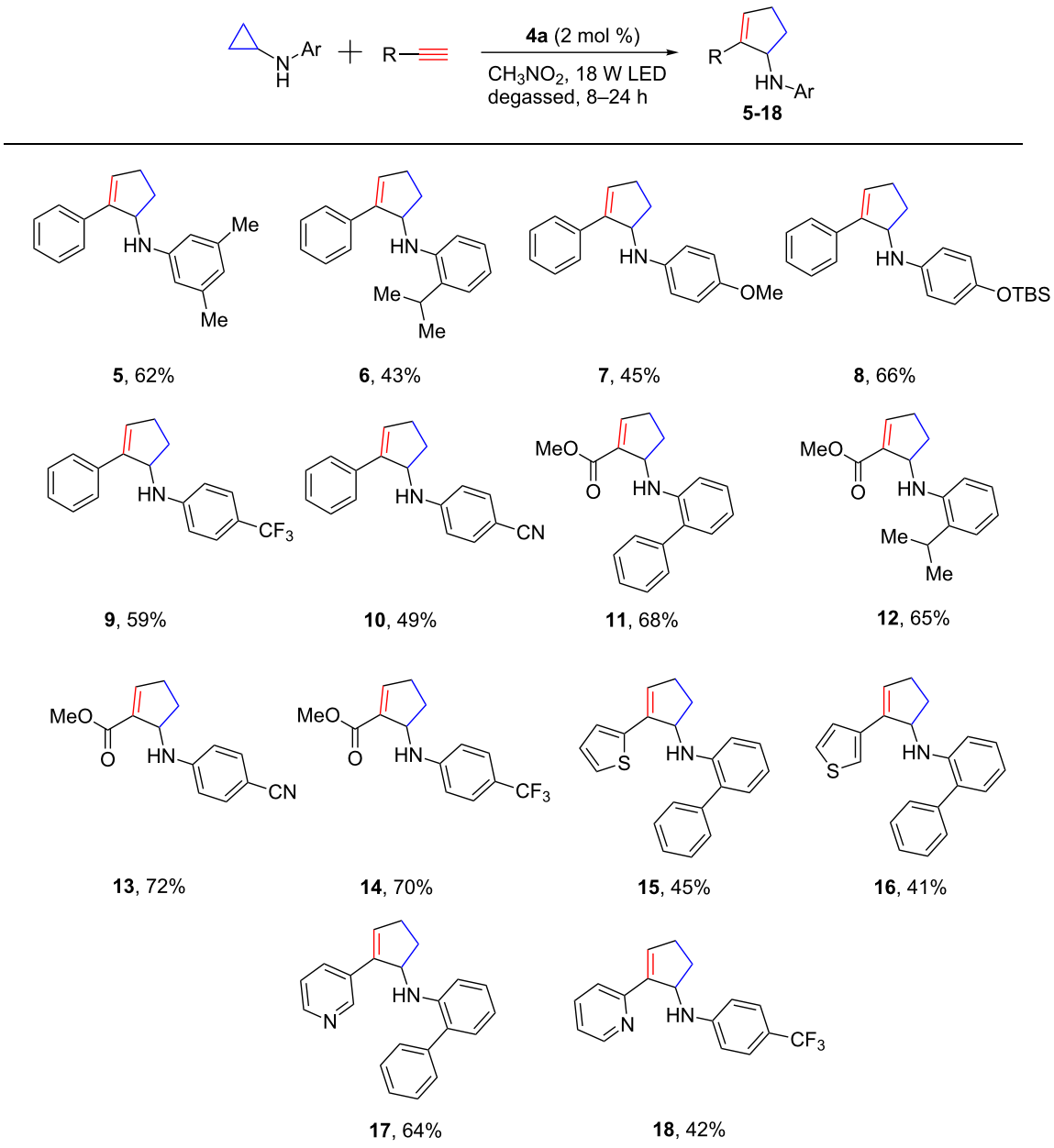

Figure 1: Substrate scope.

tive under the optimized conditions. This reactivity trend towards alkynes is consistent with that exhibited in intermolecular addition of nucleophilic carbon-based radicals to alkynes [31-33]. In addition to phenylacetylene, acetylenic methyl ester is a viable annulation partner, leading to annulation products **11**–**14** in good yields. Heterocycles are frequently used in organic electronic materials [34] and pharmaceuticals [35,36]. Therefore, the ability to incorporate them is usually considered a benchmark for developing new synthetic methods. This method has certainly passed this test as two pairs of heterocycle-containing alkynes underwent the [3 + 2] annulation with cyclopropylanilines uneventfully (**15**–**18**). The alkyne moiety at the C2 or C3 position of thiophene or pyridine showed similar reactivity towards the annulation.

Fused indolines are common structural motifs that appear in a number of biologically active alkaloids and pharmaceuticals [37,38]. The [3 + 2] annulation of monocyclic cyclopropylanilines with alkynes provides a fast entry to this motif (Scheme 1). Starting from commercially available 1-bromo-2-iodobenzene (**19**) and cycloproylamine, 2-bromo-*N*-cyclopropylaniline (**20**) was prepared in 75% yield via the Buch-

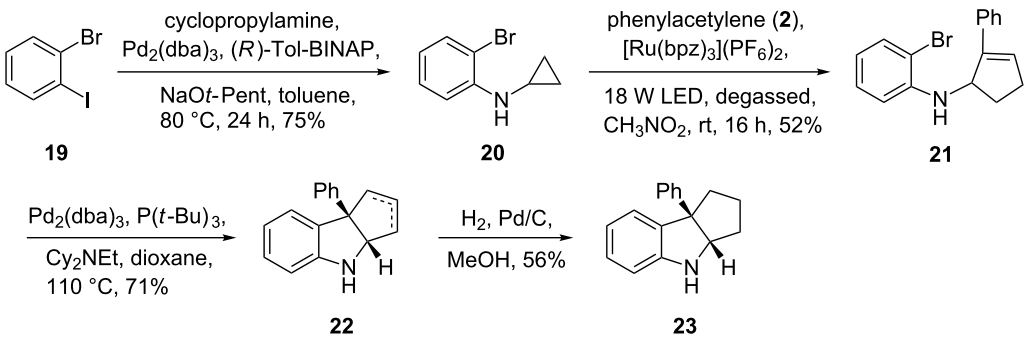

Scheme 1: Synthesis of a fused indoline.

wald–Hartwig amination [39,40]. The [3 + 2] annulation of 2-bromo-*N*-cyclopropylaniline (**20**) and phenylacetylene (**2**) was performed using the optimized catalyst system to provide cyclic allylic amine **21** in 52% yield. The fused indoline motif was formed via an intramolecular Heck reaction under Fu's conditions [41] to provide a mixture of two olefinic regioisomers **22**, which were converted to saturated fused indoline **23** under standard catalytic hydrogenation conditions in a combined yield of 40% from **21**.

Mechanistically, the annulation with alkynes probably proceeds through a pathway similar to the one we proposed for the annulation with alkenes (Scheme 2) [29]. The photoexcited $Ru(bpz)_3^{2+}$ oxidizes cyclopropylaniline **24** to the corresponding amine radical cation **25**, which triggers the cyclopropyl ring opening to generate distonic radical cation **26**. The primary carbon radical of **26** adds to the terminal carbon of alkyne **27** to afford vinyl radical **28**. Intramolecular addition of the vinyl radical to the iminium ion of distonic radical cation **28** closes the five membered ring and furnishes amine radical cation **29**. Finally, $Ru(bpz)_3^{1+}$ reduces amine radical cation **29** to the annulation product **30** while regenerating $Ru(bpz)_3^{2+}$. The proposed mechanism accounts for lower reactivity of alkynes towards intermolecular addition of nucleophilic carbon-centered radicals as well as their regiochemistry in the annulation [31-33]. Addition of radicals to alkynes generally occurs at the less hindered carbon, i.e., the terminal carbon.

Conclusion

In summary, we have successfully expanded the [3 + 2] annulation of cyclopropylanilines to include alkynes. This annulation process with alkynes has addressed some limitations existing in the annulation with alkenes. Moreover, the annulation products from alkynes are highly useful synthetic intermediates. Their utility is demonstrated by a four-step synthesis of fused indolines in which the [3 + 2] annulation with alkynes is used to set

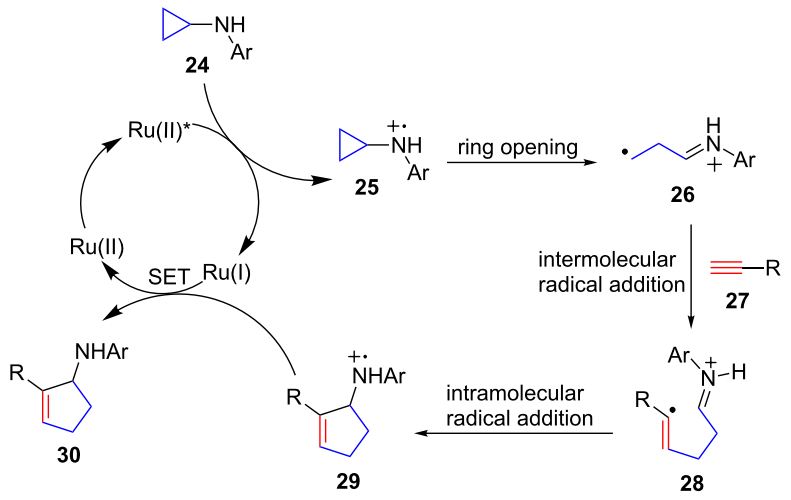

Scheme 2: Proposed catalytic cycle.

up the backbone of indolines. Continued studies in our group will focus on further expanding the scope of the [3 + 2] annulation to include substituted anilines and other types of π-bonds.

Experimental

General procedure for the [3 + 2] annulation of cyclopropylanilines with alkynes: an oven-dried test tube (16 × 125 mm) equipped with a stir bar was charged with $[Ru(bpz)_3](PF_6)_2 \cdot 2H_2O$ (2 mol %), cyclopropylaniline (0.2 mmol), alkyne (1.0 mmol), and dry CH_3NO_2 (2 mL). The test tube was sealed with a Teflon screw cap. The reaction mixture was degassed by Freeze–Pump–Thaw cycles and then irradiated at room temperature with one white LED (18 watts) positioned 8 cm from the test tube. After the reaction was complete as monitored by TLC, the mixture was diluted with diethyl ether and filtered through a short pad of silica gel. The filtrate was concentrated in vacuum and purified by silica gel flash chromatography to afford the desired allylic amine.

Supporting Information

Supporting Information File 1

Experimental procedures, compound characterization, and NMR spectra.
[http://www.beilstein-journals.org/bjoc/content/supplementary/1860-5397-10-96-S1.pdf]

Acknowledgements

This publication was supported by the University of Arkansas, Arkansas Bioscience Institute, Grant Number P30 GM103450 from the National Institute of General Medical Sciences of the National Institutes of Health (NIH), NSF Career Award under Award Number CHE-1255539. We thank Jiang Wang and Mack D. Clements for early experimental assistance.

References

1. Reissig, H.-U.; Zimmer, R. *Chem. Rev.* **2003,** *103,* 1151–1196. doi:10.1021/cr010016n
2. Yu, M.; Pagenkopf, B. L. *Tetrahedron* **2005,** *61,* 321–347. doi:10.1016/j.tet.2004.10.077
3. Carson, C. A.; Kerr, M. A. *Chem. Soc. Rev.* **2009,** *38,* 3051–3060. doi:10.1039/b901245c
4. Tang, P.; Qin, Y. *Synthesis* **2012,** 2969–2984. doi:10.1055/s-0032-1317011
5. Wong, H. N. C.; Hon, M.-Y.; Tse, C.-W.; Yip, Y.-C.; Tanko, J.; Hudlicky, T. *Chem. Rev.* **1989,** *89,* 165–198. doi:10.1021/cr00091a005
6. Zhong, B.; Silverman, R. B. *J. Am. Chem. Soc.* **1997,** *119,* 6690–6691. doi:10.1021/ja9711369
7. Shaffer, C. L.; Morton, M. D.; Hanzlik, R. P. *J. Am. Chem. Soc.* **2001,** *123,* 349–350. doi:10.1021/ja003048l
8. Wessjohann, L. A.; Brandt, W.; Thiemann, T. *Chem. Rev.* **2003,** *103,* 1625–1648. doi:10.1021/cr0100188
9. Hiyama, T.; Koide, H.; Nozaki, H. *Tetrahedron Lett.* **1973,** *14,* 2143–2144. doi:10.1016/S0040-4039(01)87579-1
10. Itoh, T.; Kaneda, K.; Teranishi, S. *Tetrahedron Lett.* **1975,** *16,* 2801–2804. doi:10.1016/S0040-4039(00)75244-0
11. Takemoto, Y.; Yamagata, S.; Furuse, S.; Hayase, H.; Echigo, T.; Iwata, C. *Chem. Commun.* **1998,** 651–652. doi:10.1039/A800125A
12. Loeppky, R. N.; Elomari, S. *J. Org. Chem.* **2000,** *65,* 96–103. doi:10.1021/jo991104z
13. Wimalasena, K.; Wickman, H. B.; Mahindaratne, M. P. D. *Eur. J. Org. Chem.* **2001,** 3811–3817. doi:10.1002/1099-0690(200110)2001:20<3811::AID-EJOC3811>3.0.CO;2-6
14. Lee, H. B.; Sung, M. J.; Blackstock, S. C.; Cha, J. K. *J. Am. Chem. Soc.* **2001,** *123,* 11322–11324. doi:10.1021/ja017043f
15. Li, X.; Grimm, M. L.; Igarashi, K.; Castagnoli, N., Jr.; Tanko, J. M. *Chem. Commun.* **2007,** 2648–2650. doi:10.1039/B702157G
16. Madelaine, C.; Six, Y.; Buriez, O. *Angew. Chem., Int. Ed.* **2007,** *46,* 8046–8049. doi:10.1002/anie.200702903
17. Rynbrandt, R. H.; Dutton, F. E. *J. Org. Chem.* **1975,** *40,* 3079–3081. doi:10.1021/jo00909a014
18. Lee, J.; Sun, U. J.; Blackstock, S. C.; Cha, J. K. *J. Am. Chem. Soc.* **1997,** *119,* 10241–10242. doi:10.1021/ja972115h
19. Ha, J. D.; Lee, J.; Blackstock, S. C.; Cha, J. K. *J. Org. Chem.* **1998,** *63,* 8510–8514. doi:10.1021/jo9817671
20. Blackburn, A.; Bowles, D. M.; Curran, T. T.; Kim, H. *Synth. Commun.* **2012,** *42,* 1855–1863. doi:10.1080/00397911.2010.545166
21. Prier, C. K.; Rankic, D. A.; MacMillan, D. W. C. *Chem. Rev.* **2013,** *113,* 5322–5363. doi:10.1021/cr300503r
22. Xi, Y.; Yi, H.; Lei, A. *Org. Biomol. Chem.* **2013,** *11,* 2387–2403. doi:10.1039/C3OB40137E
23. Xuan, J.; Xiao, W.-J. *Angew. Chem., Int. Ed.* **2012,** *51,* 6828–6838. doi:10.1002/anie.201200223
24. Tucker, J. W.; Stephenson, C. R. J. *J. Org. Chem.* **2012,** *77,* 1617–1622. doi:10.1021/jo202538x
25. Telpý, F. *Collect. Czech. Chem. Commun.* **2011,** *76,* 859–917. doi:10.1135/cccc2011078
26. Yoon, T. P.; Ischay, M. A.; Du, J. *Nat. Chem.* **2010,** *2,* 527–532. doi:10.1038/nchem.687
27. Shi, L.; Xia, W. *Chem. Soc. Rev.* **2012,** *41,* 7687–7697. doi:10.1039/C2CS35203F
28. Hu, J.; Wang, J.; Nguyen, T. H.; Zheng, N. *Beilstein J. Org. Chem.* **2013,** *9,* 1977–2001. doi:10.3762/bjoc.9.234
29. Maity, S.; Zhu, M.; Shinabery, R. S.; Zheng, N. *Angew. Chem., Int. Ed.* **2012,** *51,* 222–226. doi:10.1002/anie.201106162
30. Johannsen, M.; Jørgensen, K. A. *Chem. Rev.* **1998,** *98,* 1689–1708. doi:10.1021/cr970343o
31. Fischer, H.; Radom, L. *Angew. Chem., Int. Ed.* **2001,** *40,* 1340–1371. doi:10.1002/1521-3773(20010417)40:8<1340::AID-ANIE1340>3.0.CO;2-#
32. Giese, B.; Lachhein, S. *Angew. Chem., Int. Ed. Engl.* **1982,** *21,* 768–775. doi:10.1002/anie.198207681
33. Wille, U. *Chem. Rev.* **2013,** *113,* 813–853. doi:10.1021/cr100359d
34. Jiang, W.; Li, Y.; Wang, Z. *Chem. Soc. Rev.* **2013,** *42,* 6113–6127. doi:10.1039/C3CS60108K
35. Baumann, M.; Baxendale, I. R.; Ley, S. V.; Nikbin, N. *Beilstein J. Org. Chem.* **2011,** *7,* 442–495. doi:10.3762/bjoc.7.57
36. Baumann, M.; Baxendale, I. R. *Beilstein J. Org. Chem.* **2013,** *9,* 2265–2319. doi:10.3762/bjoc.9.265
37. Liu, D.; Zhao, G.; Xiang, L. *Eur. J. Org. Chem.* **2010,** 3975–3984. doi:10.1002/ejoc.201000323

38. Xuan, J.; Lu, L.-Q.; Chen, J.-R.; Xiao, W.-J. *Eur. J. Org. Chem.* **2013,** 6755–6770. doi:10.1002/ejoc.201300596
39. Surry, D. S.; Buchwald, S. L. *Chem. Sci.* **2011,** *2,* 27–50. doi:10.1039/C0SC00331J
40. Hartwig, J. F. *Acc. Chem. Res.* **2008,** *41,* 1534–1544. doi:10.1021/ar800098p
41. Littke, A. F.; Fu, G. C. *J. Am. Chem. Soc.* **2001,** *123,* 6989–7000. doi:10.1021/ja010988c

License and Terms

Beilstein Journal of Organic Chemistry

On the mechanism of photocatalytic reactions with eosin Y

Michal Majek*[1], Fabiana Filace[2] and Axel Jacobi von Wangelin*[1]

Full Research Paper

Open Access

Address:
[1]Institute of Organic Chemistry, University of Regensburg, Universitaetsstr. 31, 93040 Regensburg, Germany and [2]Institute of Organic Chemistry, University of Alcalá, Alcalá de Henares, Madrid, Spain

Email:
Michal Majek* - michal.majek@ur.de; Axel Jacobi von Wangelin* - axel.jacobi@ur.de

* Corresponding author

Keywords:
mechanism; organocatalysis; photocatalysis; photoredox catalysis; quantum yields; visible light

Beilstein J. Org. Chem. **2014,** *10,* 981–989.
doi:10.3762/bjoc.10.97

Received: 30 January 2014
Accepted: 10 April 2014
Published: 30 April 2014

This article is part of the Thematic Series "Organic synthesis using photoredox catalysis".

Guest Editor: A. G. Griesbeck

Abstract

A combined spectroscopic, synthetic, and apparative study has allowed a more detailed mechanistic rationalization of several recently reported eosin Y-catalyzed aromatic substitutions at arenediazonium salts. The operation of rapid acid–base equilibria, direct photolysis pathways, and radical chain reactions has been discussed on the basis of pH, solvent polarity, lamp type, absorption properties, and quantum yields. Determination of the latter proved to be an especially valuable tool for the distinction between radical chain and photocatalytic reactions.

Introduction

The ability of natural systems to harness solar energy for the genesis of matter has been fascinating mankind since time immemorial and has stimulated numerous reproduction attempts in the context of chemical synthesis over the last two centuries. The vast majority of photochemical reactions known until the 1980s exploited stoichiometric amounts of a photoactive molecular entity to drive a chemical transformation [1]. Only recently, a steadily growing number of homogeneous transition metal complexes which are redox-active and show absorption in the visible range of the solar spectrum have been demonstrated to catalyze light-driven organic reactions. The use of the pyridyl-based complexes $[Ru(bpy)_3]^{2+}$, $[Ir(ppy)_3]$ and $[Ir(ppy_2)(dtbbpy)]^{+}$ for the mediation of redox processes has certainly attracted the most interest, incipiently in photocatalytic reactions of activated organic electrophiles [2-8].

Despite the numerous examples of efficient catalytic photoredox transformations with organometallic dyes known to date, their high price, toxicity profile, and problematic recyclability might limit their more general use especially on

larger scales. However, the recent pursuit of environmentally more benign photoactive catalysts has focused on much cheaper metal-free dyes. Several commercially available fluorescein and xanthene dyes have been successfully applied to photoredox reactions, including radical substitutions at α-amino, β-carbonyl, and aryl moieties [9,10]. Among them, eosin Y, the 2',4',5',7'-tetrabromo derivative of fluorescein, has been most widely employed. The redox potential of the EY^+/EY^* pair of 1.1 V (vs. SCE) is experimentally not available as both of the compounds are short-lived intermediates. However, the redox potential can be obtained indirectly via analysis of the thermodynamic cycle involving the energy of the triplet state eosin Y* (T_1) (derived from fluorescence measurements) and the energy of the radical cation eosin $Y^{+\bullet}$ (derived from cyclovoltammetric experiments, for more details see Supporting Information File 1). Much effort has been directed at the oxidative quenching of eosin Y* (T_1) with suitable electrophiles in order to generate aryl radicals by a light-driven single-electron transfer (SET) process (i.e., one-electron reduction of Ar–X, see Scheme 1). Due to their easy reducibility, arenediazonium salts are especially attractive precursors which constitute versatile alternatives to haloarene-based strategies. They are readily available by diazotization of anilines, no toxic metals are required; the bond cleavage generates gaseous N_2 which escapes the reaction mixture. Photoredox reactions with arenediazonium salts are often more selective than traditional methods such as copper(II)-mediated Meerwein arylations [11] or protocols employing stoichiometric iron(II) or titanium(III) reductants in aqueous media [12-14]. This renaissance of arene diazonium chemistry has recently led to various applications of eosin Y to visible light-driven syntheses of biaryls [15], stilbenes [16], benzothiophenes [17], α-phenylketones [18], phenanthrenes [19], arylsulfides [20] and arylboron pinacolates [21] (Scheme 1).

Numerous mechanistic studies have been performed at reactions with organometallic photocatalysts [3-8], whereas much less attention has been directed at eosin Y-catalyzed reactions. The reductive quenching pathway of eosin Y, which operates in the photooxidation of isoquinolines [9], has been studied in a single report [22]. To the best of our knowledge, related data have not been collected for the much more widely used oxidative quenching. Most literature protocols were interpreted in analogy to the related $[Ru(bpy)_3Cl_2]$-catalyzed reactions and similar mechanisms were proposed (Scheme 2) [15-21]. These generally commence with the SET between excited eosin Y and the arenediazonium salt **I** to give aryl radical **II**. Nucleophilic attack onto reactive **II** generates the more stable complex **III** which is prone to back-electron transfer upon oxidative formation of the cationic species **IV**. Terminal elimination of X^+ (mostly a proton) gives the substitution product **V**. Two general pathways of back-electron transfer can be followed: Path A involves one-electron reduction of the radical cation state of the catalyst. Radical chain propagation (B) can occur when the SET occurs with another molecule of the starting material **I**. Some attempts have been made to differentiate between radical chain and

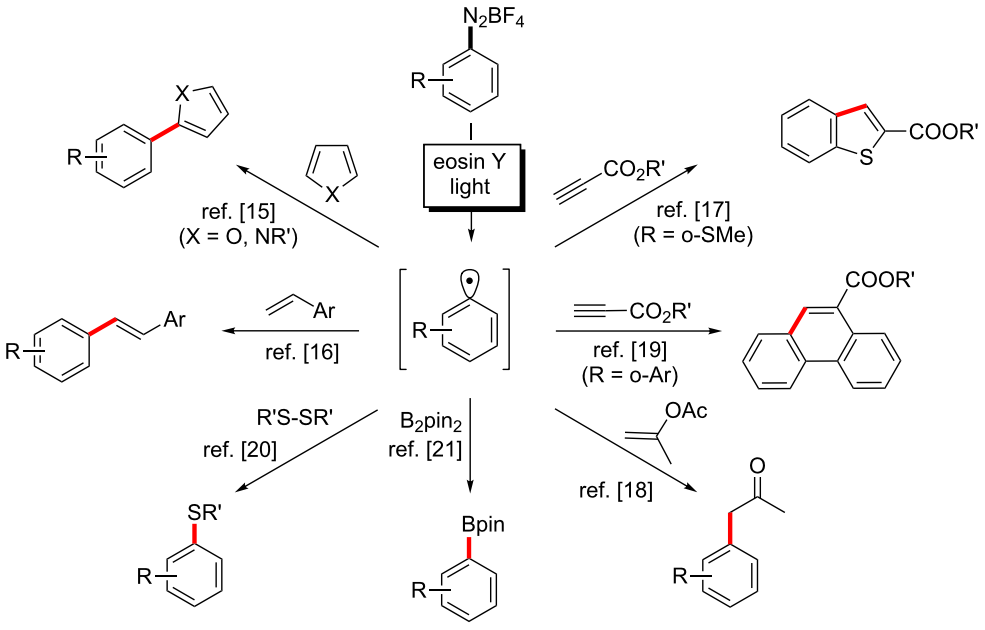

Scheme 1: Oxidative quenching of eosin Y with arenediazonium salts and reactions of the resultant aryl radicals.

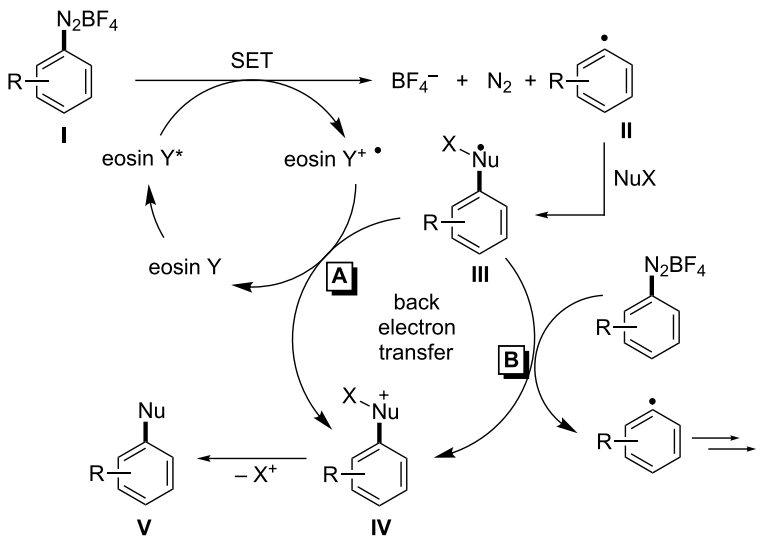

Scheme 2: Proposed general reaction mechanism of eosin Y-catalyzed substitutions with arene diazonium salts.

photocatalysis mechanisms by monitoring the reaction progress after the light sources have been switched off [20]. Clearly, such experiments neglect the existence of short radical chains and thus provide no conclusive evidence of the mechanism.

In general, the thermodynamic feasibility of a redox process is determined by the difference of redox potentials of the two half reactions. The redox potential of most arenediazonium salts (redox pair **I**/**II**, Scheme 2) is close to 0 V vs. SCE [23,24]. The redox potentials of the short-lived adducts **III**/**IV** are unknown and experimentally not (easily) available. However, it is likely that their potential is greater than 0 V in many cases which makes the radical species **III** a sufficiently strong reductant for arenediazonium salts of type **I**. After all, the unambiguous determination of the underlying reaction mechanisms is not possible without further spectroscopic, kinetic, and theoretical experiments. The studied systems are mostly too complex for transient absorption spectroscopy. We have so far failed to obtain any insight from photo-CIDNP NMR experiments. Therefore, we have decided to evaluate the efficiency of the radiation events of several recent literature protocols by recording the quantum yields Φ [15-17,19-21]. Furthermore, we have learned along the way that the reactions appear to be strongly dependent on the pH of the solution and the type of lamp used for irradiation. Here, we present a detailed study on the direct consequences of these three major factors for the outcome and mechanism of several recently reported eosin Y-catalyzed aromatic substitution protocols starting from arenediazonium salts [15-21].

Results and Discussion

Effect of pH on the efficiency of eosin Y-mediated photocatalysis

For better comparison, we have employed identical reagent concentrations and reaction conditions (solvents) as reported in the original papers [15-21]. Dry DMSO was mostly used as solvent, with the exception of the phenanthrene [19] and arylboron pinacolate [21] syntheses which were run in acetonitrile. Much to our surprise, the solutions of eosin Y and arenediazonium salts in acetonitrile were yellow (instead of the usual red colour; see Figure 1, conditions as in [21]) and did not exhibit intense fluorescence (Figure 2, conditions as in [21]). We have suspected this to be a consequence of facile acid–base reactions of the catalyst eosin Y. Indeed, immediate colour change was effected by addition of base (tetra-*n*-butylammonium hydroxide, TBAOH), and strong fluorescence occurred in the green spectrum. This dramatic pH effect on the spectroscopic properties of eosin Y solutions prompted us to further investigate this behaviour.

The organic dye eosin Y can exist in four different structures in solution: the spirocyclic form EY1, the neutral EY2, the monoanionic EY3, and the dianionic form EY4 (Scheme 3). Eosin Y contains two relatively acidic protons (pK_a 2.0, 3.8 in water) [25] which can be easily abstracted to give dianionic EY4. Lack of clarity exists in many publications on photoredox catalysis with regard to the nature of the employed dye. The authors either report the use of "eosin Y, spirit soluble" – which can be EY1 or EY2 according to the Sigma–Aldrich catalogue [26], or claim the use of the free acid EY2. The presence of

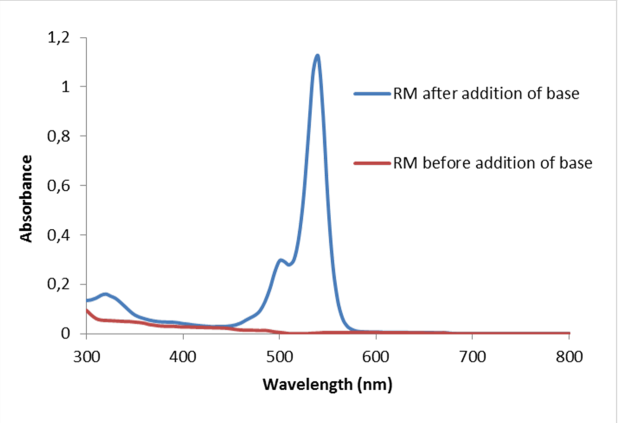

Figure 1: UV–vis spectra of the photoborylation reaction mixture (RM).

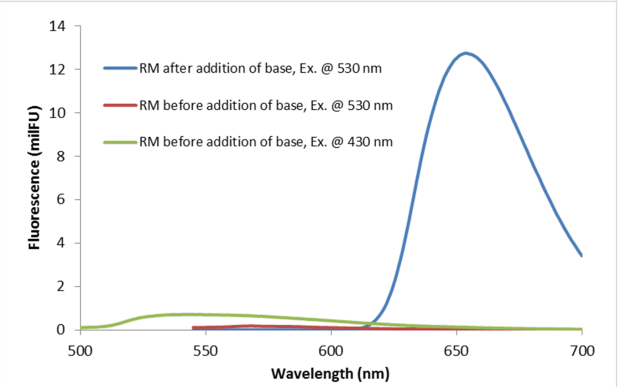

Figure 2: Fluorescence spectra of the photoborylation reaction mixture (RM). Ex. = excitation wavelength.

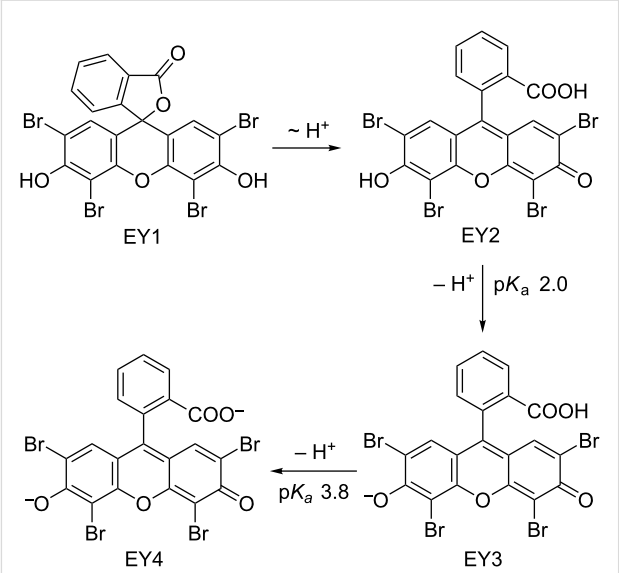

Scheme 3: Acid–base behaviour of eosin Y.

stoichiometric amounts of bases, e.g., in eosin Y-catalyzed photo-oxidative transformations with amines [9], results in the quantitative generation of the dianionic form EY4 under the reaction conditions. On the other hand, the SET-generation of aryl radicals from arenediazonium salts by photocatalysis proceeds in the absence of base. The non-aqueous conditions should not provide a significant buffering capacity. Here, the presence of only minute amount of impurities in the solvents or starting materials is sufficient to push the acid–base equilibria of the catalytic amounts of eosin Y in either direction.

The spirocyclic form EY1 contains an interrupted conjugation of the fluorone ring system and thus would be photocatalytically inactive under visible light irradiation. The neutral form EY2 exhibits only weak fluorescence when irradiated with visible light (Figure 2). Studies on related alkylated eosin derivatives suggest that this fluorescent state is very short lived and is therefore also not appropriate for photoredox catalysis [27]. The charged forms EY3 and EY4 are catalytically active, which in turn also means that solutions containing commercial "eosin Y, spirit soluble" would per se not trigger efficient photoredox catalysis. In such cases, catalytic activity as observed in recent publications by König et al. is dependent on the operation of acid–base equilibration (e.g., in DMSO solution) so that the employed eosin Y is converted in situ to the active species EY3 or EY4 [15-18]. Efforts to reproduce the photoredox synthesis of arylboron pinacolates in acetonitrile have so far failed in our hands when irradiating at 535 nm [21]. No product formation was observed, and the UV–vis spectra showed no appreciable absorption at this wavelength. However, the addition of minor quantities of base (TBAOH) to the reaction mixture resulted in strong absorption at 535 nm and good photocatalytic activity under irradiation. The substitution of acetonitrile with DMSO in the same reaction gave strong absorption at 535 nm and allowed the photocatalytic synthesis of the desired arylborinic ester in good yields in the absence of extra base. This discrepancy is most likely associated with the different properties of DMSO and acetonitrile as bases. DMSO is a stronger base than acetonitrile which enhances the acidity of most Brønsted acids in DMSO [28]. These observations lead to the conclusion that photoredox reactions catalyzed by eosin Y (or similar organic dyes) cannot be discussed without strict specification of the employed form of the dye and the reaction conditions. Conclusive mechanistic proposals of visible-light-driven reactions with these dyes also need to address the operation of acid–base equilibria and the pH dependence of absorption properties.

Effect of the light source on the eosin Y-mediated photocatalysis

Another reaction parameter which lacks clarity and consistency among the literature reports is the source of irradiation. Several

groups including ourselves have used commercial narrow-band LEDs with a maximum intensity at 535 nm (green light) [15-18,20]. Other reactions were irradiated with white light from broad-band compact fluorescent lamps (CFL) [19,21]. The determination of quantum yields requires the use of narrow-band light sources due to the variation of the optical density of the samples with the wavelength. Therefore, we have studied the impact of different irradiation types on the course of the photocatalytic reaction. Although the type of CFLs was not specified in the literature [19,21], the majority of commercial CFLs cover similar spectral ranges with the individual UV edge being significantly below 400 nm and with substantial radiation power in the region of 400–500 nm. A similar wavelength distribution is seen in the spectrum of commercial white-colored LEDs (see Supporting Information File 1 for spectrum). The activation energy of thermal heterolysis of arenediazonium ions is approx. 115 kJ/mol (1.19 eV) [29]. The energy of a photon at the edge of the visible spectrum (400 nm) is 3.1 eV so that such photons carry sufficient energy to heterolyze diazonium ions to give highly electrophilic aryl cations. Moreover, arenediazonium salts are known to form weak charge-transfer complexes with solvent molecules whose absorption tails into the visible range [30].

These observations support the notion that the use of broad-band visible irradiation indeed can have a profound effect on the outcome of a photocatalytic reaction. We have therefore examined if direct absorption of the arenediazonium ions can trigger a productive pathway under irradiation with broad-band light sources even in the absence of the photocatalyst. As representative examples we chose the recently reported syntheses of arylborinic esters [21] and phenanthrenes [19]. The absorption spectrum of a mixture of *para*-bromobenzenediazonium tetrafluoroborate (*p*-$BrC_6H_4N_2BF_4$) and bispinacolato diboron (B_2pin_2) in acetonitrile shows a significant shoulder of a UV-absorption band tailing into the visible part of the spectrum (Figure 3) [30]. At the UV–vis edge (400 nm), the absorbance of the system is still more than 0.1 which translates into 21% of all light being absorbed at this wavelength. When we performed the borylation reaction according to the literature report [21] but without the addition of the photocatalyst eosin Y, 54% yield of the borylation product were obtained by direct photolysis (Scheme 4). These observations are in full accord with a report of direct reaction of thermally generated aryl cations (from arenediazonium salts) with bispinacolato diboron to give the corresponding arylborinic esters [31]. It is thus very likely that direct light-triggered heterolysis of the starting material accounts for substantial amounts of product formation under conditions which were believed to proceed through photocatalytic SET.

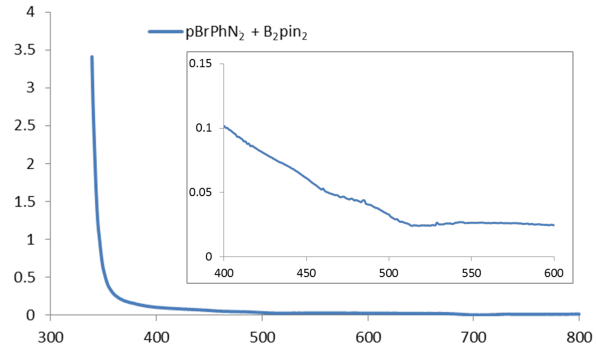

Figure 3: UV–vis spectrum of *p*-bromobenzenediazonium tetrafluoroborate ($pBrPhN_2$) and bispinacolato diboron (B_2pin_2) in acetonitrile.

A similar behaviour was found in our study of the phenanthrene synthesis [19]. A solution of *o*-biphenyldiazonium tetrafluoroborate in acetonitrile showed strong absorption between 400–500 nm with all light at the UV–vis edge at 400 nm being completely absorbed. This again indicates that direct photocleavage of the C–N bond might be operating. The cyclization reaction with ethyl propiolate according to the literature protocol [19] but in the absence of eosin Y did not afford any phenanthrene product (Scheme 5). Instead, a Ritter-type reaction proceeded to give the corresponding acetanilide after aqueous work-up which is consistent with the original report by Deronzier from 1984 [32]. The significant overlap of the absorption spectra of the arenediazonium salt recorded before and after the addition of eosin Y (Figure 4) suggests that direct photolysis of the C–N bond could account for the erosion of product yield in the catalytic process due to competitive hetero-

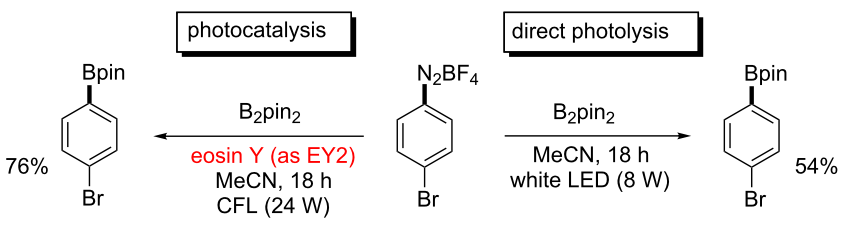

Scheme 4: Eosin Y-catalyzed and dye-free photolytic borylation.

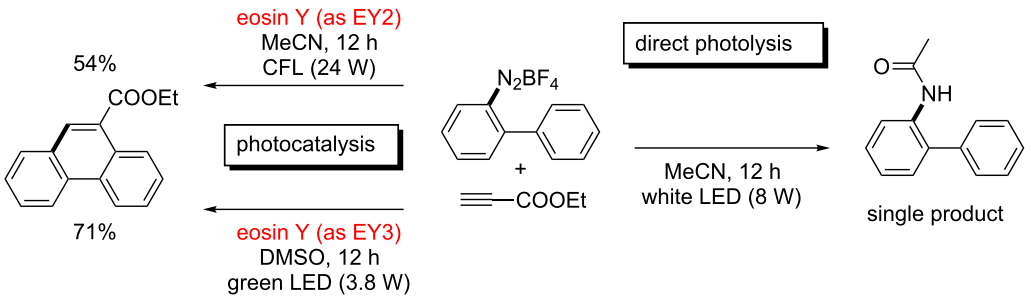

Scheme 5: Eosin Y-catalyzed and dye-free reactions with ethyl propiolate.

lysis of the substrate and subsequent ionic Ritter reaction. This notion was supported by our experiments performed in DMSO where a higher portion of the photocatalyst resides in the active EY3 and EY4 states. Following an otherwise identical protocol, irradiation at 535 nm resulted in the formation of the phenanthrene in 71% yield (cf. literature yield of 53%)[19].

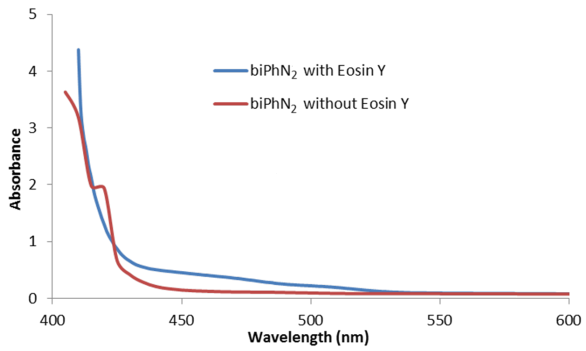

Figure 4: UV–vis spectra of *ortho*-biphenyldiazonium tetrafluoroborate ($biPhN_2$) in acetonitrile.

Quantum yields of eosin Y-catalyzed reactions

The determination of quantum yields of light-driven reactions provides valuable insight into the efficiency of the radiative processes and thus can be used for the mechanistic understanding of such processes. The magnitude of quantum yields Φ also describes how much energy is wasted into thermal dissipation in such systems, which is an especially critical parameter for the evaluation of sustainability of a photocatalytic process. The quantum yield is defined as the efficiency of a photochemical reaction in the studied system:

$$\Phi = (\text{rate of substrate conversion})/(\text{absorbed photon flux})$$

Theoretically, if a simple photocatalytic process is considered, the quantum yield would be in the range $0 < \Phi \leq 1$. It approaches unity as the efficiency of the photocatalytic step increases. In reality, quantum yields can exceed unity in cases where the products of the photocatalytic reaction induce (radical) chain reactions. Therefore, the determination of quantum yields Φ provides a meaningful answer to mechanistic ambiguities. For the eosin Y-catalyzed reactions with arenediazonium salts, conclusive answers to the distinction between photocatalytic and radical chain mechanisms can be derived directly from Φ.

A quantification of the photon flux is rather problematic. Recently, devices became available which use solar cells for the direct measurement of photon fluxes [33]. However, chemical actinometry constitutes a prevalent indirect method of photon flux measurement [34]. Several effective chemical actinometers are known for UV spectral studies whereas similar experiments in the visible range are much more limited by the availability of chemical actinometers. Even more challenging are photon flux determinations above 500 nm which marks the spectral cut-off of the commonly used Hatchard–Parker ferrioxalate. None of the chemical actinometers that operate in this region are commercially available. We therefore decided to prepare potassium Reineckate, a robust actinometer for the >500 nm region, according to a literature method [34,35].

Quantum yields Φ were measured for all aforementioned visible-light-driven reactions in the same solvent, DMSO. Irradiation was performed with a green LED (3.8 W) at 535 nm. All other reaction conditions were adopted from the individual literature reports [15-21]. For more details on the actinometry experiments and quantum yield determinations, see Supporting Information File 1. The observed quantum yields Φ of the studied reactions varied by almost two orders of magnitude, between 4.7 and 0.075. This already indicates the operation of different mechanisms in these aromatic substitution reactions with arene diazonium salts. The redox potentials of most substituted arene diazonium salts cluster with very little deviation around 0.0 V vs. SCE (±0.2 V) [23,24] so that the observed

differences in Φ can be largely attributed to different mechanistic pathways. Our experiments (Scheme 6) afforded quantum yields of Φ > 1 for the heterobiaryl coupling [15] and the Heck-type olefination with styrene [16], respectively. This indicates that in addition to a photocatalytic path (Scheme 2, A) radical-chain propagation is operating under the reaction conditions (Scheme 2, B). This contrasts with the other reactions where the quantum yields range between 0.6 and 0.075. In the original paper from Deronzier [32], where similar reactions under catalysis of $Ru(bpy)_3^{2+}$ were studied, Φ values of 0.46–0.78 were reported. Our actinometric experiments of the eosin Y-catalyzed phenanthrene synthesis [19] and photoborylation [21] gave similar quantum yields of 0.35 and 0.60, respectively. This suggests that the photocatalytic pathway is indeed populated (Scheme 2, A). Finally, the benzothiophene synthesis [17] and photothiolation [19] exhibited relatively low quantum yields which could be a consequence of non-productive processes that are responsible for the significant loss of energy. The presence of electron-rich alkylthiolate moieties in both systems could in principle effect reversible redox processes with the catalyst eosin Y which might account for the erosion of Φ.

Conclusion

In summary, we have investigated the impact of several reaction parameters on the outcome and mechanism of photocatalytic aromatic substitution reactions of arenediazonium salts in the presence of eosin Y. However, the significance of these data certainly extends to other light-driven reactions that lie beyond

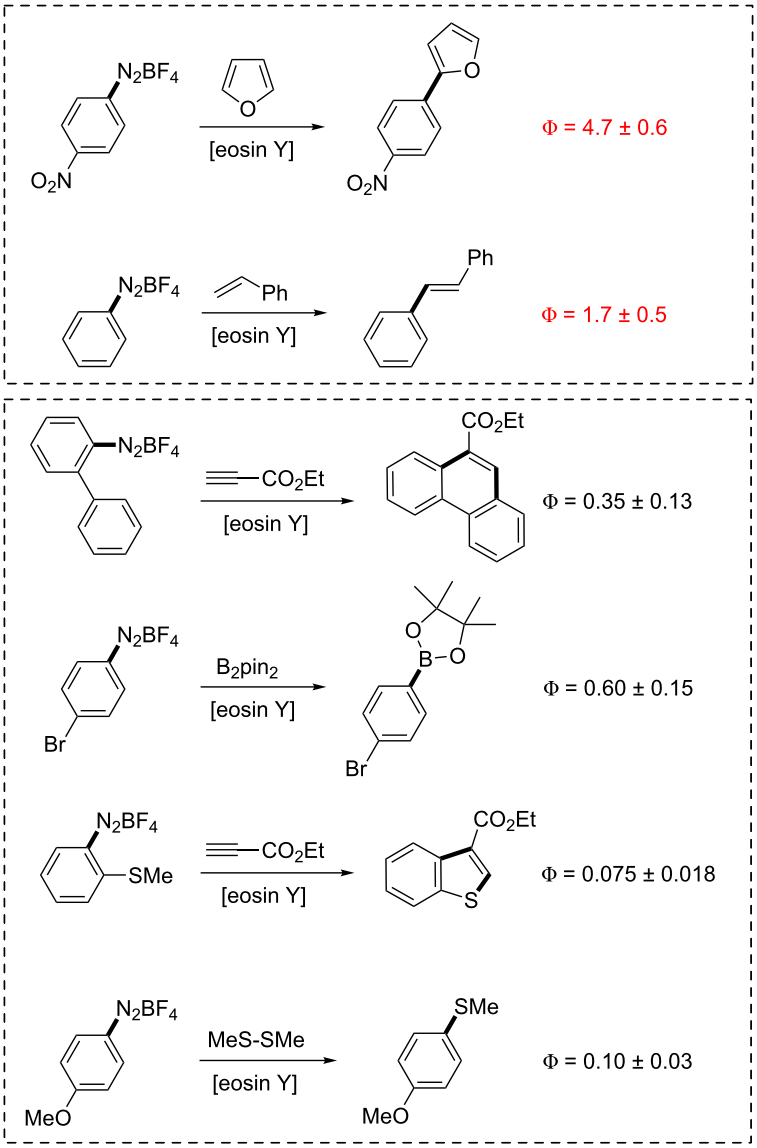

Scheme 6: Quantum yield determinations of selected visible-light-driven aromatic substitutions.

the focus of this study. Eosin Y (and many other organic photocatalysts) undergo rapid acid–base equilibria which significantly alter the photophysical properties. It is therefore of pivotal importance to ascertain the actual nature of the employed dye under the reaction conditions. Experimental details should always be given that specify the employed dye, the presence of acids and bases as well as the purity of the reagents, solvents, and additives. The use of broad-spectrum lamps in photocatalytic reactions with arenediazonium salts is strongly discouraged as they promote heterolytic C–N bond cleavage toward highly reactive aryl cation species. The standard reaction conditions of many literature reports involve concentrations which are orders of magnitude higher than those suitable for absorption spectroscopy studies. This means that even very inefficient transitions (at tailings of absorption maxima) can indeed trigger productive processes and therefore need to be addressed in mechanistic rationalizations. Quantum yield determinations with potassium Reineckate have now allowed the distinction between photocatalytic and radical-chain mechanisms. However, the operation of the prevalent pathway is likely dictated by the stability of the relevant catalytic intermediates.

Supporting Information

Supporting Information File 1

Experimental and analytical data.
[http://www.beilstein-journals.org/bjoc/content/supplementary/1860-5397-10-97-S1.pdf]

Acknowledgements

We gratefully acknowledge generous intellectual and financial support from the Graduate College on “Chemical Photocatalysis” of the Deutsche Forschungsgemeinschaft (DFG, fellowship to M.M.). We thank Prof. Burkhard König and Dr. Ilya Shenderovich (both UR) for technical support.

References

1. Griesbeck, A. G.; Oelgemöller, M.; Ghetti, F., Eds. *CRC Handbook of Organic Photochemistry and Photobiology,* 3rd ed.; CRC Press: Boca Raton, 2012.
2. Nguyen, J. D.; D’Amato, E. M.; Narayanam, J. M. R.; Stephenson, C. R. J. *Nat. Chem.* **2012,** *4,* 854–859. doi:10.1038/nchem.1452
3. Teplý, F. *Collect. Czech. Chem. Commun.* **2011,** *76,* 859–917. doi:10.1135/cccc2011078
4. Narayanam, J. M. R.; Stephenson, C. R. J. *Chem. Soc. Rev.* **2011,** *40,* 102–113. doi:10.1039/b913880n
5. Zeitler, K. *Angew. Chem., Int. Ed.* **2009,** *48,* 9785–9789. doi:10.1002/anie.200904056
6. Xuan, J.; Xiao, W.-J. *Angew. Chem., Int. Ed.* **2012,** *51,* 6828–6838. doi:10.1002/anie.201200223
7. Majek, M.; Jacobi von Wangelin, A. *Angew. Chem., Int. Ed.* **2013,** *52,* 5919–5921. doi:10.1002/anie.201301843
8. Reckenthäler, M.; Griesbeck, A. G. *Adv. Synth. Catal.* **2013,** *355,* 2727–2744. doi:10.1002/adsc.201300751
9. Hari, D. P.; König, B. *Org. Lett.* **2011,** *13,* 3852–3855. doi:10.1021/ol201376v
10. Condie, A. G.; González-Gómez, J. C.; Stephenson, C. R. J. *J. Am. Chem. Soc.* **2010,** *132,* 1464–1465. doi:10.1021/ja909145y
11. Rondestvedt, C. S. In *Organic Reactions;* Baldwin, J. E.; Bittman, R.; Boswell, G. A.; Heck, R. F.; Hirschmann, R. F.; Kende, A. S.; Leimgruber, W.; Marshall, J. A.; McKusick, B. C.; Meinwald, J.; Trost, B. M.; Weinstein, B., Eds.; Wiley: New York, 1976; pp 225–259.
12. Wetzel, A.; Ehrhardt, V.; Heinrich, M. R. *Angew. Chem., Int. Ed.* **2008,** *47,* 9130–9133. doi:10.1002/anie.200803785
13. Heinrich, M. R.; Wetzel, A.; Kirschstein, M. *Org. Lett.* **2007,** *9,* 3833–3835. doi:10.1021/ol701622d
14. Heinrich, M. R. *Chem.–Eur. J.* **2009,** *15,* 820–833. doi:10.1002/chem.200801306
15. Hari, D. P.; Schroll, P.; König, B. *J. Am. Chem. Soc.* **2012,** *134,* 2958–2961. doi:10.1021/ja212099r
16. Schroll, P.; Hari, D. P.; König, B. *ChemistryOpen* **2012,** *1,* 130–133. doi:10.1002/open.201200011
17. Hari, D. P.; Hering, T.; König, B. *Org. Lett.* **2012,** *14,* 5334–5337. doi:10.1021/ol302517n
18. Hering, T.; Hari, D. P.; König, B. *J. Org. Chem.* **2012,** *77,* 10347–10352. doi:10.1021/jo301984p
19. Xiao, T.; Dong, X.; Tang, Y.; Zhou, L. *Adv. Synth. Catal.* **2012,** *354,* 3195–3199. doi:10.1002/adsc.201200569
20. Majek, M.; Jacobi von Wangelin, A. *Chem. Commun.* **2013,** *49,* 5507–5509. doi:10.1039/c3cc41867g
21. Yu, J.; Zhang, L.; Yan, G. *Adv. Synth. Catal.* **2012,** *354,* 2625–2628. doi:10.1002/adsc.201200416
22. Liu, Q.; Li, Y.-N.; Zhang, H.-H.; Chen, B.; Tung, C.-H.; Wu, L.-Z. *Chem.–Eur. J.* **2012,** *18,* 620–627. doi:10.1002/chem.201102299
23. Allongue, P.; Delamar, M.; Desbat, B.; Fagebaume, O.; Hitmi, R.; Pinson, J.; Savéant, J.-M. *J. Am. Chem. Soc.* **1997,** *119,* 201–207. doi:10.1021/ja963354s
24. Combellas, C.; Jiang, D.-e.; Kanoufi, F.; Pinson, J.; Podvorica, F. I. *Langmuir* **2009,** *25,* 286–293. doi:10.1021/la8025792
25. Baristela, V. R.; Pellosi, D. S.; de Souza, F. D.; da Costa, W. F.; de Oliveira Santin, S. M.; de Souza, V. R.; Caetano, W.; Moisés de Oliveira, H. P.; Scarminio, I. S.; Hioka, N. *Spectrochim. Acta, Part A* **2011,** *79,* 889–897. doi:10.1016/j.saa.2011.03.027
26. *Aldrich Catalog. Handbook of Fine Chemicals;* Aldrich Chemicals: Milwaukee, WI, 2012.
27. del Valle, J. C.; Catalán, J.; Amant-Guerri, F. *J. Photochem. Photobiol., A* **1993,** *72,* 49–53. doi:10.1016/1010-6030(93)85084-L
28. Himmel, D.; Goll, S. K.; Leito, I.; Krossing, I. *Angew. Chem., Int. Ed.* **2010,** *49,* 6885–6888. doi:10.1002/anie.201000252
29. Crossley, M. L.; Kienle, R. H.; Benbrook, C. H. *J. Am. Chem. Soc.* **1940,** *62,* 1400–1404. doi:10.1021/ja01863a019
30. Hirose, Y.; Wahl, G. H.; Zollinger, H. *Helv. Chim. Acta* **1976,** *59,* 1427–1437. doi:10.1002/hlca.19760590504
31. Zhu, C.; Yamane, M. *Org. Lett.* **2012,** *14,* 4560–4563. doi:10.1021/ol302024m
32. Cano-Yelo, H.; Deronzier, A. *J. Chem. Soc., Perkin Trans. 2* **1984,** 1093–1098. doi:10.1039/p29840001093

33. Megerle, U.; Lechner, R.; König, B.; Riedle, E. *Photochem. Photobiol. Sci.* **2010,** *9,* 1400–1406. doi:10.1039/c0pp00195c
34. Kuhn, H. J.; Braslavsky, S. E.; Schmidt, R. *Pure Appl. Chem.* **2004,** *76,* 2105–2146. doi:10.1351/pac200476122105
35. Wegner, E. E.; Adamson, A. W. *J. Am. Chem. Soc.* **1966,** *88,* 394–404. doi:10.1021/ja00955a003

License and Terms

Beilstein Journal of Organic Chemistry

Direct C–H trifluoromethylation of di- and trisubstituted alkenes by photoredox catalysis

Ren Tomita, Yusuke Yasu, Takashi Koike* and Munetaka Akita*

Full Research Paper

Open Access

Address:
Chemical Resources Laboratory, Tokyo Institute of Technology, R1-27, 4259 Nagatsuta, Midori-ku, Yokohama 226-8503, Japan

Email:
Takashi Koike* - koike.t.ad@m.titech.ac.jp; Munetaka Akita* - makita@res.titech.ac.jp

* Corresponding author

Keywords:
electrophilic trifluoromethylating reagent; multi-substituted alkene; photoredox catalysis; radical reaction; trifluoromethylation

Beilstein J. Org. Chem. **2014,** *10,* 1099–1106.
doi:10.3762/bjoc.10.108

Received: 23 January 2014
Accepted: 14 April 2014
Published: 12 May 2014

This article is part of the Thematic Series "Organic synthesis using photoredox catalysis".

Guest Editor: A. G. Griesbeck

Abstract

Background: Trifluoromethylated alkene scaffolds are known as useful structural motifs in pharmaceuticals and agrochemicals as well as functional organic materials. But reported synthetic methods usually require multiple synthetic steps and/or exhibit limitation with respect to access to tri- and tetrasubstituted CF_3-alkenes. Thus development of new methodologies for facile construction of $C_{alkenyl}$–CF_3 bonds is highly demanded.

Results: The photoredox reaction of alkenes with 5-(trifluoromethyl)dibenzo[*b*,*d*]thiophenium tetrafluoroborate, Umemoto's reagent, as a CF_3 source in the presence of $[Ru(bpy)_3]^{2+}$ catalyst (bpy = 2,2'-bipyridine) under visible light irradiation without any additive afforded CF_3-substituted alkenes via direct $C_{alkenyl}$–H trifluoromethylation. 1,1-Di- and trisubstituted alkenes were applicable to this photocatalytic system, providing the corresponding multisubstituted CF_3-alkenes. In addition, use of an excess amount of the CF_3 source induced double C–H trifluoromethylation to afford geminal bis(trifluoromethyl)alkenes.

Conclusion: A range of multisubstituted CF_3-alkenes are easily accessible by photoredox-catalyzed direct C–H trifluoromethylation of alkenes under mild reaction conditions. In particular, trifluoromethylation of triphenylethene derivatives, from which synthetically valuable tetrasubstituted CF_3-alkenes are obtained, have never been reported so far. Remarkably, the present facile and straightforward protocol is extended to double trifluoromethylation of alkenes.

Introduction

The trifluoromethyl (CF_3) group is a useful structural motif in many bioactive molecules as well as functional organic materials [1-6]. Thus, the development of new methodologies for highly efficient and selective incorporation of a CF_3 group into diverse skeletons has become a hot research topic in the field of organic synthetic chemistry [7-12]. Recently, radical trifluoro-

methylation by photoredox catalysis [13-23] with ruthenium(II) polypyridine complexes (e.g., $[Ru(bpy)_3]^{2+}$ (bpy: 2,2'-bipyridine)), the relevant Ir cyclometalated complexes (e.g., *fac*-$Ir(ppy)_3$ (ppy: 2-phenylpyridine)) and organic dyes has been developed; the trifluoromethyl radical ($\cdot CF_3$) can be easily generated from conventional CF_3 radical precursors such as CF_3I, CF_3SO_2Cl and CF_3SO_2Na through visible-light-induced single-electron transfer (SET) processes [24-32]. On the other hand, we have intensively developed trifluoromethylations of olefins by the Ru and Ir photoredox catalysis using easy-handling and shelf-stable electrophilic trifluoromethylating reagents [33-36] ($^{+}\boldsymbol{CF_3}$) such as Umemoto's reagent (**1a**, 5-(trifluoromethyl)dibenzo[*b*,*d*]thiophenium tetrafluoroborate) and Togni's reagents **1b** (1-(trifluoromethyl)-1λ^3,2-benziodoxol-3(1*H*)-one) and **1c** (3,3-dimethyl-1,3-dihydro-1λ^3,2-benziodoxole) [37-41]. It was found that electrophilic trifluoromethylating reagents ($^{+}\boldsymbol{CF_3}$) can serve as more efficient CF_3 radical sources under mild photocatalytic reaction conditions. In addition, the putative β-CF_3 carbocation intermediate formed through SET photoredox processes is playing a key role in our reaction systems (vide infra).

Trifluoromethylated alkenes, especially multi-substituted CF_3-alkenes (3,3,3-trifluoropropene derivatives), have attracted our attention as fascinating scaffolds for agrochemicals, pharmaceuticals, and fluorescent molecules (Scheme 1) [3,42-45].

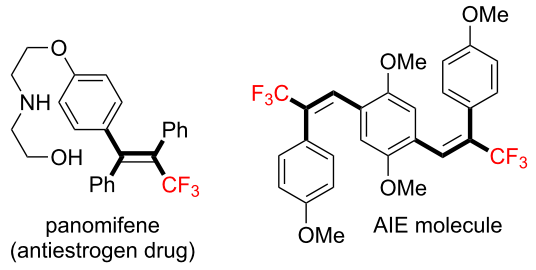

Scheme 1: Representative examples of multisubstituted CF_3-alkenes.

straightforward approach is direct C–H trifluoromethylation of alkenes (Scheme 2c). The groups of Loh, Besset, Cahard, Sodeoka and Xiao showed that copper catalysts can induce a C–H trifluoromethylation of alkenes by electrophilic CF_3 reagents ($^{+}\boldsymbol{CF_3}$) [65-69]. In addition, Cho et al. reported that the reaction of unactivated alkenes with gaseous CF_3I in the presence of a Ru photocatalyst, $[Ru(bpy)_3]^{2+}$, and a base, DBU (diazabicyclo[5,4,0]undec-7-ene) produced CF_3-alkenes through iodotrifluoromethylation of alkenes followed by base-induced E2 elimination [70]. To the best of our knowledge, however, the development of synthetic methods for tri- and tetrasubstituted CF_3 alkenes through $C_{alkenyl}$–H trifluoromethylation of simple alkenes have been left much to be desired.

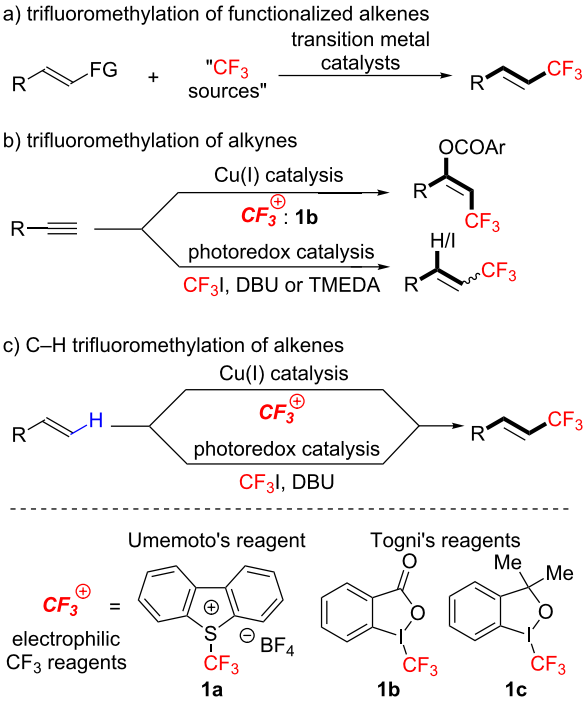

Scheme 2: Catalytic synthesis of CF_3-alkenes via trifluoromethylation.

Conventional approaches to CF_3-alkenes require multiple synthetic steps [46-54]. In contrast, "trifluoromethylation" is a promising protocol to obtain diverse CF_3-alkenes easily. Several catalytic synthetic methods via trifluoromethylation have been developed so far [38,55-62]. Most of these reactions require prefunctionalized alkenes as a substrate (Scheme 2a). Additionally, only a limited number of examples for synthesis of tri/tetra-substituted CF_3-alkenes have been reported so far. Recently, the groups of Szabó and Cho described trifluoromethylation of alkynes, leading to trifluoromethylated alkenes but the application to the synthesis of tetrasubstituted CF_3-alkenes is not well documented (Scheme 2b) [63,64]. Another

Previously, we reported on the synthesis of CF_3-alkenes via sequential photoredox-catalyzed hydroxytrifluoromethylation and dehydration (Scheme 3a) [37] and photoredox-catalyzed trifluoromethylation of alkenylborates (Scheme 3b) [38]. These results prompted us to explore photoredox-catalyzed C–H trifluoromethylation of di- and trisubstituted alkenes (Scheme 3c). Herein we disclose a highly efficient direct C–H trifluoromethylation of di- and trisubstituted alkenes with easy-handling and shelf-stable Umemoto's reagent **1a** by visible-light-driven photoredox catalysis under mild conditions. This photocatalytic protocol allows us easy access to a range of multi-substituted trifluoromethylated alkenes. In addition, our methodology can

be extended to a double trifluoromethylation of 1,1-disubstituted alkenes.

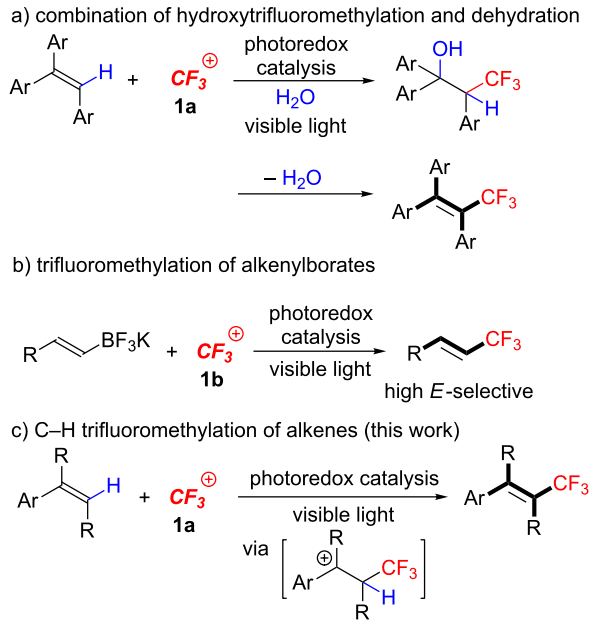

Scheme 3: Our strategies for synthesis of CF_3-alkenes.

Results and Discussion

The results of investigations on the reaction conditions are summarized in Table 1. We commenced examination of photocatalytic trifluoromethylation of 1,1-diphenylethene **2a** with 1 equivalent of Umemoto's reagent **1a** in the presence of 5 mol % *fac*-Ir(ppy)$_3$, a photoredox catalyst, and 2 equivalents of K_2HPO_4, a base, in [D_6]-DMSO under visible light irradiation (blue LEDs: λ_{max} = 425 nm) for 2 h. As a result, 3,3,3-trifluoro-1,1-diphenylpropene (**3a**) was obtained in an 82% NMR yield (Table 1, entry 1). The choice of $^+CF_3$ reagents turned out to be crucial for the yield of **3a**. Togni's reagents **1b** and **1c** gave **3a** in lower yields (Table 1, entries 2 and 3). We also found that DMSO is suitable for the present reaction (Table 1, entries 4–6). Other solvent systems gave substantial amounts of the hydroxytrifluoromethylated byproduct, which we reported previously [37]. In addition, the present C–H trifluoromethylation proceeds even in the absence of a base (Table 1, entry 7). Another photocatalyst, [Ru(bpy)$_3$](PF$_6$)$_2$, also promoted the present reaction, providing the product **3a** in an 85% NMR yield (Table 1, entry 8). The Ru catalyst is less expensive than the Ir catalyst; thus, we chose the Ru photocatalyst for the experiments onward. Notably, product **3a** was obtained neither in the dark nor in the absence of photocatalyst (Table 1, entries 9 and 10), strongly supporting that the photoexcited species of the photoredox catalyst play key roles in the reaction.

The scope and limitations of the present photocatalytic trifluoromethylation of alkenes are summarized in Table 2. 1,1-Diphenylethenes with electron-donating substituents, MeO (**2b**), and halogens, Cl (**2c**) and Br (**2d**), smoothly produced the corresponding trisubstituted CF_3-alkenes (**3b**–**d**) in good yields.

Table 1: Optimization of photocatalytic trifluoromethylation of 1,1-diphenylethene **2a**.[a]

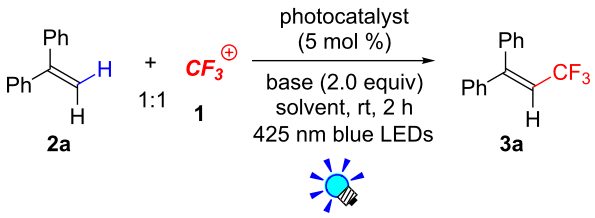

Entry	Photocatalyst	CF_3 reagent	Solvent	Base	NMR yield (%)
1	*fac*-Ir(ppy)$_3$	**1a**	[D_6]-DMSO	K_2HPO_4	82
2	*fac*-Ir(ppy)$_3$	**1b**	[D_6]-DMSO	K_2HPO_4	17
3	*fac*-Ir(ppy)$_3$	**1c**	[D_6]-DMSO	K_2HPO_4	47
4	*fac*-Ir(ppy)$_3$	**1a**	CD_3CN	K_2HPO_4	57
5	*fac*-Ir(ppy)$_3$	**1a**	CD_2Cl_2	K_2HPO_4	22
6	*fac*-Ir(ppy)$_3$	**1a**	[D_6]-acetone	K_2HPO_4	29
7	*fac*-Ir(ppy)$_3$	**1a**	[D_6]-DMSO	none	81
8	[Ru(bpy)$_3$](PF$_6$)$_2$	**1a**	[D_6]-DMSO	none	85
9	none	**1a**	[D_6]-DMSO	none	0
10[b]	[Ru(bpy)$_3$](PF$_6$)$_2$	**1a**	[D_6]-DMSO	none	0

[a]For reaction conditions, see the Experimental section. [b]In the dark.

Table 2: The scope of the present trifluoromethylation of alkenes.[a, b]

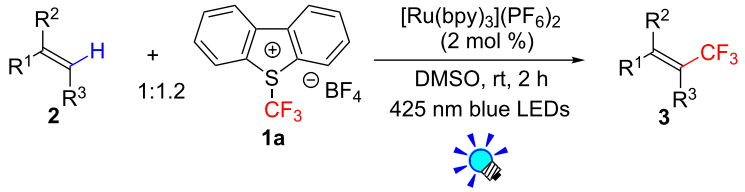

Trifluoromethylated products **3a–m**

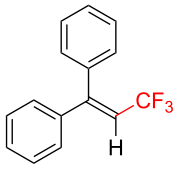

3a: 82%[c]

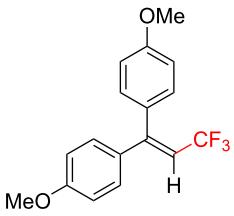

3b: 81%[c]

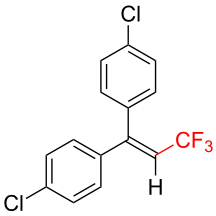

3c: 53%

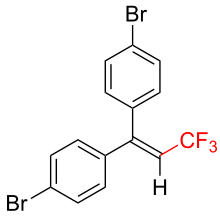

3d: 70%

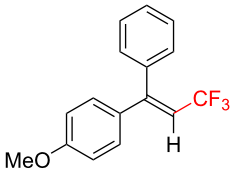

3e: 70%[c]
E/*Z* = 89/11[d]

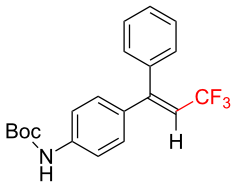

3f: 37%[e]
E/*Z* = 91/9[d]

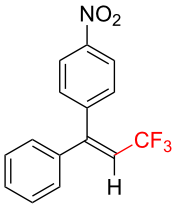

3g: 51%
E/*Z* = 17/83[d]

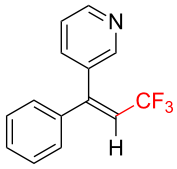

3h: 78%
E/*Z* = 33/67[d]

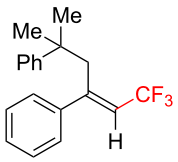

3i: 58%
E/*Z* = 88/12[d]

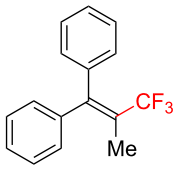

3j: 82%

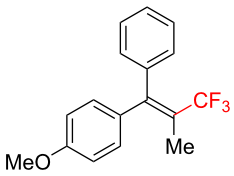

3k: 59%
E/*Z* = 74/26[d]

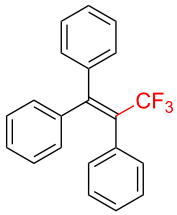

3l: 65%

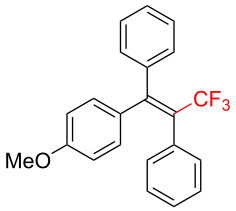

3m: 53%
E/*Z* = 88/12[d]

[a]For reaction conditions, see the Experimental section. [b]Isolated yields. [c]NMR yields. [d]*E*/*Z* ratios were determined by ^{19}F NMR spectroscopy of the crude product mixtures. [e]2,6-Lutidine (2 equiv) was added as a base.

In the reactions of unsymmetrically substituted substrates (**2e**–**h**), products were obtained in good to moderate yields but consisted of mixtures of *E* and *Z*-isomers. Based on the experimental results, the *E*/*Z* ratios are susceptible to the electronic structure of the aryl substituent. Reactions afforded the major isomers, in which the CF_3 group and the electron-rich aryl substituent are arranged in *E*-fashion. In addition, the present photocatalytic reaction can be tolerant of the Boc-protected amino group (**2f**) or pyridine (**2h**). Moreover, a substrate with an alkyl substituent, 2,4-diphenyl-4-methyl-1-pentene (**2i**), was also applicable to this transformation, whereas the reaction of 1,2-disubsituted alkenes such as *trans*-stilbene provided complicated mixtures of products.

Next, we extended the present C–H trifluoromethylation to trisubstituted alkenes. The reactions of 1,1-diphenylpropene derivatives **2j** and **2k** (*E*/*Z* = 1/1) afforded the corresponding tetrasubstituted CF_3-alkenes **3j** and **3k** in 82% and 59% (*E*/*Z* = 74/26) yields, respectively. Triphenylethenes **2l** and **2m** (only *E*-isomer) are also applicable to this photocatalytic C–H trifluoromethylation. Remarkably, the *E*-isomer of **3m** is a key intermediate for the synthesis of panomifene, which is known as

an antiestrogen drug [71,72]. These results show that the present protocol enables the efficient construction of a $C_{alkenyl}$–CF_3 bond through direct C–H trifluoromethylation of 1,1-disubstituted and trisubstituted aryl alkenes.

During the course of our study on the C–H trifluoromethylation of 1,1-diarylethenes **2**, we found that a detectable amount of bis(trifluoromethyl)alkenes **4** was formed through double C–H trifluoromethylation. In fact, the photocatalytic trifluoromethylation of **2a**,**b** and **d** with 4 equivalents of Umemoto's reagent **1a** in the presence of 5 mol % of $[Ru(bpy)_3](PF_6)_2$ with irradiation from blue LEDs for 3 h gave geminal bis(trifluoromethyl)ethene (**4a**,**b** and **d**) in 45, 80 and 24% NMR yields, respectively (Scheme 4). Substituents on the benzene ring significantly affect the present double trifluoromethylation. Reaction of the electron-rich alkene **2b** afforded 1,1-anisyl-2,2-bis(trifluoromethyl)ethene (**4b**) in a better yield than other alkenes **2a** and **2d**. Additionally, we found that photocatalytic trifluoromethylation of CF_3-alkene **3d** in the presence of an excess amount of Umemoto's reagent **1a** produced bis(trifluoromethyl)alkenes **4d** in a better yield (56% yield) compared to the above-mentioned one-pot double trifluoromethylation of **2d**.

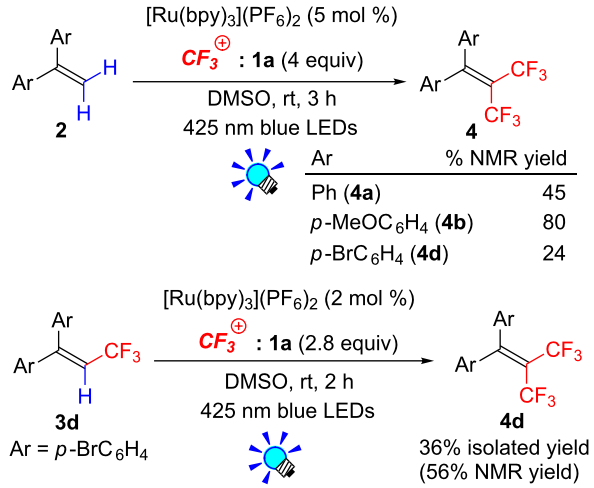

Scheme 4: Synthesis of geminal bis(trifluoromethyl)alkenes.

A possible reaction mechanism based on SET photoredox processes is illustrated in Scheme 5. According to our previous photocatalytic trifluoromethylation [37-41], the trifluoromethyl radical (·CF_3) is generated from an one-electron-reduction of electrophilic Umemoto's reagent **1a** by the photoactivated Ru catalyst, $*[Ru(bpy)_3]^{2+}$. ·CF_3 reacts with alkene **2** to give the benzyl radical-type intermediate **3'** in a regioselective manner. Subsequent one-electron-oxidation by highly oxidizing Ru species, $[Ru^{III}(bpy)_3]^{3+}$, produces β-CF_3 carbocation intermediate $\mathbf{3}^+$. Finally, smooth elimination of the olefinic proton, which is made acidic by the strongly electron-withdrawing CF_3 substituent, provides trifluoromethylated alkene **3**. Preferential formation of one isomer in the reaction of unsymmetrical substrates is attributed to the population of the rotational conformers of the β-CF_3 carbocation intermediate $\mathbf{3}^+$. Our experimental result is consistent with the previous report [71], which described *E*-selective formation of the tetrasubstituted CF_3-alkene **3m** via a β-CF_3 carbocation intermediate. In the presence of an excess amount of CF_3 reagent **1a**, further C–H trifluoromethylation of CF_3-alkene **3** proceeds to give bis(trifluoromethyl)alkene **4**.

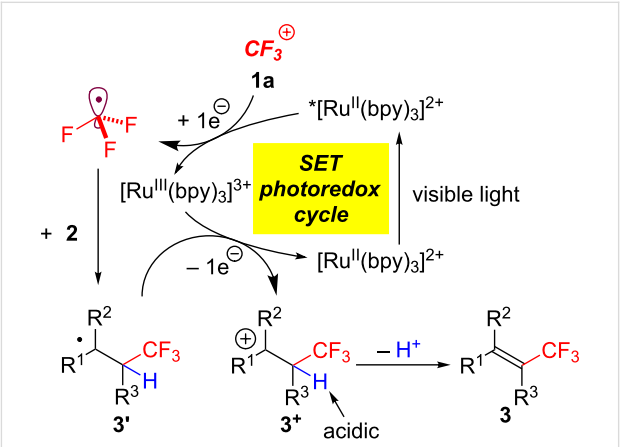

Scheme 5: A possible reaction mechanism.

We cannot rule out a radical chain propagation mechanism, but the present transformation requires continuous irradiation of visible light (Figure 1), thus suggesting that chain propagation is not a main mechanistic component.

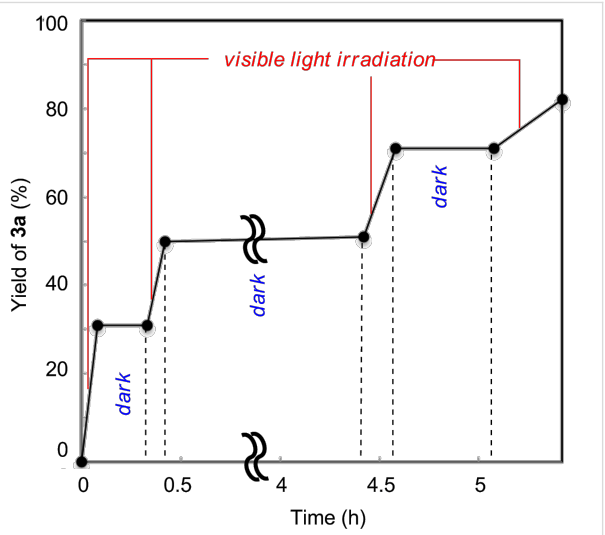

Figure 1: Time profile of the photocatalytic trifluoromethylation of **2a** with **1a** with intermittent irradiation by blue LEDs.

Conclusion

We have developed highly efficient C–H trifluoromethylation of alkenes using Umemoto's reagent as a CF_3 source by visible-light-driven photoredox catalysis. This reaction can be applied to multi-substituted alkenes, especially, 1,1-disubstituted and trisubstituted aryl alkenes, leading to tri- and tetrasubstituted CF_3-alkenes. The present straightforward method for the synthesis of multisubstituted CF_3-alkenes from simple aryl alkenes is the first report. In addition, we can extend the present photocatalytic system to double trifluoromethylation. Further development of this protocol in the synthesis of bioactive organofluorine molecules and fluorescent molecules is a continuing effort in our laboratory.

Experimental

Typical NMR experimental procedure (reaction conditions in Table 1)

Under N_2, $[Ru(bpy)_3](PF_6)_2$ (1.1 mg, 1.3 μmol), Umemoto's reagent **1a** (8.5 mg, 25 μmol), 1,1-diphenylethylene (**2a**, 4.3 μL, 25 μmol), $SiEt_4$ (~1 μL) as an internal standard, and $[D_6]$-DMSO (0.5 mL) were added to an NMR tube. The reaction was carried out at room temperature (water bath) under irradiation of visible light (placed at a distance of 2–3 cm from 3 W blue LED lamps: $h\nu$ = 425 ± 15 nm).

General procedure for the photocatalytic C−H trifluoromethylation of alkenes (reaction conditions in Table 2)

A 20 mL Schlenk tube was charged with Umemoto's reagent **1a** (102 mg, 0.3 mmol, 1.2 equiv), $[Ru(bpy)_3](PF_6)_2$ (4.3 mg, 2 mol %), alkene **2** (0.25 mmol), and DMSO (2.5 mL) under N_2. The tube was irradiated for 2 h at room temperature (water bath) with stirring by 3 W blue LED lamps ($h\nu$ = 425 ± 15 nm) placed at a distance of 2–3 cm. After the reaction, H_2O was added. The resulting mixture was extracted with Et_2O, washed with H_2O, dried (Na_2SO_4), and filtered. The filtrate was concentrated in vacuo. The product was purified by the two methods described below.

For products **3b**, **3e**, **3f**, **3g**, **3h**, **3k** and **3m**, the residue was purified by column chromatography on silica gel (eluent: hexane and diethyl ether) to afford the corresponding product **3**. Further purification of **3f** by GPC provided pure **3f**. For products **3a**, **3c**, **3d**, **3i**, **3j**, and **3l**, the residue was treated by mCPBA (74 mg, ca. 0.3 mmol) in CH_2Cl_2 to convert the dibenzothiophene to sulfoxide, which was more easily separated from the products. After the solution was stirred at room temperature for 2 h, an aqueous solution of $Na_2S_2O_3{\cdot}5H_2O$ was added to the solution, which was extracted with CH_2Cl_2. The organic layer was washed with H_2O, dried (Na_2SO_4), and filtered. The filtrate was concentrated in vacuo and the residue was purified by flash column chromatography on silica gel (eluent: hexane) to afford the corresponding product **3**. Further purification of **3c** and **3d** by GPC provided pure **3c** and **3d**.

Procedures for the photocatalytic double C−H trifluoromethylation of 1,1-bis(4-methoxyphenyl)ethylene (**2b**)

A 20 mL Schlenk tube was charged with Umemoto's reagent **1a** (340 mg, 1.0 mmol, 4 equiv), $[Ru(bpy)_3](PF_6)_2$ (10.7 mg, 5 mol %), **2b** (60 mg, 0.25 mmol), and DMSO (5 mL) under N_2. The tube was irradiated for 3 h at room temperature (water bath) with stirring by 3 W blue LED lamps ($h\nu$ = 425 ± 15 nm) placed at a distance of 2–3 cm. After reaction, H_2O was added. The resulting mixture was extracted with Et_2O, washed with H_2O, dried (Na_2SO_4), and filtered. The filtrate was concentrated in vacuo and the residue was purified by flash column chromatography on silica gel (hexane→hexane/Et_2O = 29:1) to afford **4b** as a product mixture with **3b**. Further purification by GPC provided pure **4b** in 44% isolated yield (42 mg, 0.11 mmol). Isolated yield was much lower than the NMR yield because of the difficulty of separation of **3b** and **4b**.

Supporting Information

Supporting information features experimental procedures and full spectroscopic data for all new compounds (**3c**, **3d**, **3f**, **3g**, **3h**, **3i**, **3k**, **4a**, and **4d**).

Supporting Information File 1

Experimental procedures and NMR spectra.
[http://www.beilstein-journals.org/bjoc/content/supplementary/1860-5397-10-108-S1.pdf]

Acknowledgements

This work was supported by a grant-in-aid from the Ministry of Education, Culture, Sports, Scienece of the Japanese Government (No 23750174), The Naito Foundation and the global COE program (the GCOE) "Education and Research Center for Emergence of New Molecular Chemistry".

References

1. Hiyama, T. In *Organofluorine Compounds: Chemistry and Applications;* Yamamoto, H., Ed.; Springer: Berlin, 2000. doi:10.1007/978-3-662-04164-2
2. Ojima, I. *Fluorine in Medicinal Chemistry and Chemical Biology;* Wiley-Blackwell: Chichester, 2009.
3. Shimizu, M.; Hiyama, T. *Angew. Chem., Int. Ed.* **2005,** *44,* 214–231. doi:10.1002/anie.200460441
4. Ma, J.-A.; Cahard, D. *J. Fluorine Chem.* **2007,** *128,* 975–996. doi:10.1016/j.jfluchem.2007.04.026

5. Shibata, N.; Mizuta, S.; Toru, T. *J. Synth. Org. Chem., Jpn.* **2008,** *66,* 215–228.
6. Ma, J.-A.; Cahard, D. *Chem. Rev.* **2008,** *108,* PR1–PR43. doi:10.1021/cr800221v
7. Tomashenko, O. A.; Grushin, V. V. *Chem. Rev.* **2011,** *111,* 4475–4521. doi:10.1021/cr1004293
8. Furuya, T.; Kamlet, A. S.; Ritter, T. *Nature* **2011,** *473,* 470–477. doi:10.1038/nature10108
9. Amii, H. *J. Synth. Org. Chem., Jpn.* **2011,** *69,* 752–762.
10. Studer, A. *Angew. Chem., Int. Ed.* **2012,** *51,* 8950–8958. doi:10.1002/anie.201202624
11. Macé, Y.; Magnier, E. *Eur. J. Org. Chem.* **2012,** 2479–2494. doi:10.1002/ejoc.201101535
12. Liang, T.; Neumann, C. N.; Ritter, T. *Angew. Chem., Int. Ed.* **2013,** *52,* 8214–8264. doi:10.1002/anie.201206566
13. Yoon, T. P.; Ischay, M. A.; Du, J. *Nat. Chem.* **2010,** *2,* 527–532. doi:10.1038/nchem.687
14. Narayanam, J. M. R.; Stephenson, C. R. J. *Chem. Soc. Rev.* **2011,** *40,* 102–113. doi:10.1039/b913880n
15. Teplý, F. *Collect. Czech. Chem. Commun.* **2011,** *76,* 859–917. doi:10.1135/cccc2011078
16. Tucker, J. W.; Stephenson, C. R. J. *J. Org. Chem.* **2012,** *77,* 1617–1622. doi:10.1021/jo202538x
17. Xuan, J.; Xiao, W.-J. *Angew. Chem., Int. Ed.* **2012,** *51,* 6828–6838. doi:10.1002/anie.201200223
18. Maity, S.; Zheng, N. *Synlett* **2012,** *23,* 1851–1856. doi:10.1055/s-0032-1316592
19. Shi, L.; Xia, W. *Chem. Soc. Rev.* **2012,** *41,* 7687–7697. doi:10.1039/c2cs35203f
20. Xi, Y.; Yi, H.; Lei, A. *Org. Biomol. Chem.* **2013,** *11,* 2387–2403. doi:10.1039/c3ob40137e
21. Hari, D. P.; König, B. *Angew. Chem., Int. Ed.* **2013,** *52,* 4734–4743. doi:10.1002/anie.201210276
22. Prier, C. K.; Rankic, D. A.; MacMillan, D. W. C. *Chem. Rev.* **2013,** *113,* 5322–5363. doi:10.1021/cr300503r
23. Reckenthäler, M.; Griesbeck, A. G. *Adv. Synth. Catal.* **2013,** *355,* 2727–2744. doi:10.1002/adsc.201300751
24. Nagib, D. A.; MacMillan, D. W. C. *Nature* **2011,** *480,* 224–228. doi:10.1038/nature10647
25. Nguyen, J. D.; Tucker, J. W.; Konieczynska, M. D.; Stephenson, C. R. J. *J. Am. Chem. Soc.* **2011,** *133,* 4160–4163. doi:10.1021/ja108560e
26. Ye, Y.; Sanford, M. S. *J. Am. Chem. Soc.* **2012,** *134,* 9034–9037. doi:10.1021/ja301553c
27. Mizuta, S.; Verhoog, S.; Engle, K. M.; Khotavivattana, T.; O'Duill, M.; Wheelhouse, K.; Rassias, G.; Médebielle, M.; Gourverneur, V. *J. Am. Chem. Soc.* **2013,** *135,* 2505–2508. doi:10.1021/ja401022x
28. Kim, E.; Choi, S.; Kim, H.; Cho, E. J. *Chem.–Eur. J.* **2013,** *19,* 6209–6212. doi:10.1002/chem.201300564
29. Wilger, D. J.; Gesmundo, N. J.; Nicewicz, D. A. *Chem. Sci.* **2013,** *4,* 3160–3165. doi:10.1039/c3sc51209f
30. Jiang, H.; Cheng, Y.; Zhang, Y.; Yu, S. *Eur. J. Org. Chem.* **2013,** 5485–5492. doi:10.1002/ejoc.201300693
31. Xu, P.; Xie, J.; Xue, Q.; Pan, C.; Cheng, Y.; Zhu, C. *Chem.–Eur. J.* **2013,** *19,* 14039–14042. doi:10.1002/chem.201302407
32. Koike, T.; Akita, M. *Top. Catal.* **2014**. doi:10.1007/s11244-014-0259-7
33. Umemoto, T. *Chem. Rev.* **1996,** *96,* 1757–1778. doi:10.1021/cr941149u
    And see references therein.
34. Eisenberger, P.; Gischig, S.; Togni, A. *Chem.–Eur. J.* **2006,** *12,* 2579–2586. doi:10.1002/chem.200501052
35. Kieltsch, I.; Eisenberger, P.; Togni, A. *Angew. Chem., Int. Ed.* **2007,** *46,* 754–757. doi:10.1002/anie.200603497
36. Shibata, N.; Matsnev, A.; Cahard, D. *Beilstein J. Org. Chem.* **2010,** *6,* No. 65. doi:10.3762/bjoc.6.65
37. Yasu, Y.; Koike, T.; Akita, M. *Angew. Chem., Int. Ed.* **2012,** *51,* 9567–9571. doi:10.1002/anie.201205071
38. Yasu, Y.; Koike, T.; Akita, M. *Chem. Commun.* **2013,** *49,* 2037–2039. doi:10.1039/c3cc39235j
39. Yasu, Y.; Koike, T.; Akita, M. *Org. Lett.* **2013,** *15,* 2136–2139. doi:10.1021/ol4006272
40. Koike, T.; Akita, M. *Synlett* **2013,** *24,* 2492–2505. doi:10.1055/s-0033-1339874
41. Yasu, Y.; Arai, Y.; Tomita, R.; Koike, T.; Akita, M. *Org. Lett.* **2014,** *16,* 780–783. doi:10.1021/ol403500y
42. Rivkin, A.; Chou, T.-C.; Danishefsky, S. J. *Angew. Chem., Int. Ed.* **2005,** *44,* 2838–2850. doi:10.1002/anie.200461751
43. Shimizu, M.; Takeda, Y.; Higashi, M.; Hiyama, T. *Angew. Chem., Int. Ed.* **2009,** *48,* 3653–3656. doi:10.1002/anie.200900963
44. Shimizu, M.; Takeda, Y.; Higashi, M.; Hiyama, T. *Chem.–Asian J.* **2011,** *6,* 2536–2544. doi:10.1002/asia.201100176
45. Shi, Z.; Davies, J.; Jang, S.-H.; Kaminsky, W.; Jen, A. K.-Y. *Chem. Commun.* **2012,** *48,* 7880–7882. doi:10.1039/c2cc32380j
46. Kimura, M.; Yamazaki, T.; Kitazume, T.; Kubota, T. *Org. Lett.* **2004,** *6,* 4651–4654. doi:10.1021/ol0481941
47. Konno, T.; Takehana, T.; Mishima, M.; Ishihara, T. *J. Org. Chem.* **2006,** *71,* 3545–3550. doi:10.1021/jo0602120
48. Takeda, Y.; Shimizu, M.; Hiyama, T. *Angew. Chem., Int. Ed.* **2007,** *46,* 8659–8661. doi:10.1002/anie.200703759
49. Shimizu, M.; Takeda, Y.; Hiyama, T. *Bull. Chem. Soc. Jpn.* **2011,** *84,* 1339–1341. doi:10.1246/bcsj.20110240
50. Prakash, G. K. S.; Krishnan, H. S.; Jog, P. V.; Iyer, A. P.; Olah, G. A. *Org. Lett.* **2012,** *14,* 1146–1149. doi:10.1021/ol300076y
51. Omote, M.; Tanaka, M.; Ikeda, A.; Nomura, S.; Tarui, A.; Sato, K.; Ando, A. *Org. Lett.* **2012,** *14,* 2286–2289. doi:10.1021/ol300670n
52. Debien, L.; Quiclet-Sire, B.; Zard, S. S. *Org. Lett.* **2012,** *14,* 5118–5121. doi:10.1021/ol3023903
53. Zine, K.; Petrignet, J.; Thibonnet, J.; Abarbri, M. *Synlett* **2012,** 755–759. doi:10.1055/s-0031-1290596
54. Aikawa, K.; Shimizu, N.; Honda, K.; Hioki, Y.; Mikami, K. *Chem. Sci.* **2014,** *5,* 410–415. doi:10.1039/c3sc52548a
55. Duan, J.; Dolbier, W. R., Jr.; Chen, Q.-Y. *J. Org. Chem.* **1998,** *63,* 9486–9489. doi:10.1021/jo9816663
56. Hafner, A.; Bräse, S. *Adv. Synth. Catal.* **2011,** *353,* 3044–3048. doi:10.1002/adsc.201100528
57. Cho, E. J.; Buchwald, S. L. *Org. Lett.* **2011,** *13,* 6552–6555. doi:10.1021/ol202885w
58. Parsons, A. T.; Senecal, T. D.; Buchwald, S. L. *Angew. Chem., Int. Ed.* **2012,** *51,* 2947–2950. doi:10.1002/anie.201108267
59. He, Z.; Luo, T.; Hu, M.; Cao, Y.; Hu, J. *Angew. Chem., Int. Ed.* **2012,** *51,* 3944–3947. doi:10.1002/anie.201200140
60. Li, Y.; Wu, L.; Neumann, H.; Beller, M. *Chem. Commun.* **2013,** *49,* 2628–2630. doi:10.1039/c2cc36554e
61. Li, Z.; Cui, Z.; Liu, Z.-Q. *Org. Lett.* **2013,** *15,* 406–409. doi:10.1021/ol3034059
62. Patra, T.; Deb, A.; Manna, S.; Sharma, U.; Maiti, D. *Eur. J. Org. Chem.* **2013,** 5247–5250. doi:10.1002/ejoc.201300473

63. Janson, P. G.; Ghoneim, I.; Ilchenko, N. O.; Szabó, K. J. *Org. Lett.* **2012,** *14,* 2882–2885. doi:10.1021/ol3011419
64. Iqbal, N.; Jung, J.; Park, S.; Cho, E. J. *Angew. Chem., Int. Ed.* **2014,** *53,* 539–542. doi:10.1002/anie.201308735
65. Feng, C.; Loh, T.-P. *Chem. Sci.* **2012,** *3,* 3458–3462. doi:10.1039/c2sc21164e
66. Egami, H.; Shimizu, R.; Sodeoka, M. *Tetrahedron Lett.* **2012,** *53,* 5503–5506. doi:10.1016/j.tetlet.2012.07.134
67. Feng, C.; Loh, T.-P. *Angew. Chem., Int. Ed.* **2013,** *52,* 12414–12417. doi:10.1002/anie.201307245
68. Wang, X.-P.; Lin, J.-H.; Zhang, C.-P.; Xiao, J.-C.; Zheng, X. *Beilstein J. Org. Chem.* **2013,** *9,* 2635–2640. doi:10.3762/bjoc.9.299
69. Besset, T.; Cahard, D.; Pannecoucke, X. *J. Org. Chem.* **2014,** *79,* 413–418. doi:10.1021/jo402385g
70. Iqbal, N.; Choi, S.; Kim, E.; Cho, E. J. *J. Org. Chem.* **2012,** *77,* 11383–11387. doi:10.1021/jo3022346
71. Németh, G.; Kapiller-Dezsofi, R.; Lax, G.; Simig, G. *Tetrahedron* **1996,** *52,* 12821–12830. doi:10.1016/0040-4020(96)00763-6
72. Liu, X.; Shimizu, M.; Hiyama, T. *Angew. Chem., Int. Ed.* **2004,** *43,* 879–882. doi:10.1002/anie.200353032
And see references for the bioactivity therein.

License and Terms

Beilstein Journal of Organic Chemistry

Homogeneous and heterogeneous photoredox-catalyzed hydroxymethylation of ketones and keto esters: catalyst screening, chemoselectivity and dilution effects

Axel G. Griesbeck* and Melissa Reckenthäler

Full Research Paper

Open Access

Address:
University of Cologne, Department of Chemistry, Organic Chemistry, Greinstr. 4, D-50939 Köln, Germany; Fax: +49(221)470 5057

Email:
Axel G. Griesbeck* - griesbeck@uni-koeln.de

* Corresponding author

Keywords:
alkylation; carbonyl; photocatalysis; photoredox catalysis; redox; semiconductor

Beilstein J. Org. Chem. **2014,** *10,* 1143–1150.
doi:10.3762/bjoc.10.114

Received: 03 February 2014
Accepted: 22 April 2014
Published: 19 May 2014

This article is part of the Thematic Series "Organic synthesis using photoredox catalysis".

Associate Editor: T. P. Yoon

Abstract

The homogeneous titanium- and dye-catalyzed as well as the heterogeneous semiconductor particle-catalyzed photohydroxymethylation of ketones by methanol were investigated in order to evaluate the most active photocatalyst system. Dialkoxytitanium dichlorides are the most efficient species for chemoselective hydroxymethylation of acetophenone as well as other aromatic and aliphatic ketones. Pinacol coupling is the dominant process for semiconductor catalysis and ketone reduction dominates the $Ti(OiPr)_4$/methanol or isopropanol systems. Application of dilution effects on the TiO_2 catalysis leads to an increase in hydroxymethylation at the expense of the pinacol coupling.

Introduction

Stimulated by the principles of sustainable chemical synthesis and the progress in our understanding of catalytic and photoinduced electron-transfer processes, in recent years photoredox catalysis emerged as a new and powerful area for advanced synthesis [1-10]. There are numerous features that characterize an effective photoredox catalytic cycle: light absorption, charge separation, charge transport and annihilation as well as the use of appropriate sacrificial compounds such as electron and hole donors, elements that also appear in the natural photosynthesis, the role model for all applications. Catalysts that can function as light-absorbing and as redox-activating species must combine several features: redox-inactivity in the electronic ground states, optimal absorption properties in the near UV or visible region and appropriate redox activity in the excited states. Many potent

photoredox catalysts with sufficient long-term stability are transition metal complexes with excited MLCT states that can be generated in the visible. Another important group of photocatalytic active compounds are semiconductor particles that absorb in the UV-A and near visible reagion. The widely used TiO_2 has found numerous applications in photochemical water detoxification or surface purification because of its favourable excited-state redox properties [11]. In synthetic applications of semiconductor photocatalysis two clearly distinguishable reaction protocols were designated as type A and B by Kisch and co-workers [12-15]. In the type A process, two different products are formed from the initially formed electron–hole pair, one from the substrate radical cation that is formed from electron transfer to the semiconductor valence band hole, the other from the substrate radical anion that is formed from reduction by the semiconductor conduction band electron. Mostly, one of these steps consumes a sacrificial electron/hole donor. In type B photocatalysis, combination of the radical ions leads to a new product without the need of sacrificial components. The latter process proceeds with a high degree of atom economy [16]. We have recently demonstrated this for the azido-hydroperoxidation of alkenes, a convenient method for the synthesis of 1,2-amino alcohols [17,18]. In the field of C–C coupling reactions, the direct hydroxyalkylation of carbonyl compounds and carbonyl analogs is a demanding task because the α-CH activation of alcohols must occur in the presence of the acidic and nucleophilic hydroxy group. Thus, protection and deactivation of this group is necessary for thermal processes. In contrast to that, photochemical redox activation is possible in the presence of titanium(IV) catalysts [19-22]. As shown in a series of papers by Sato and coworkers, carbonyl compounds **1** as well as imines couple with methanol to give the 1,2-diols or 1,2-amino alcohols, respectively, when irradiated in the presence of stoichiometric or sub-stoichiometric amounts of titanium tetrachloride (Scheme 1). In order to run these reactions to completion, not less than 0.5 equivalents of $TiCl_4$ were necessary which accounts for severe catalyst consumption. Furthermore, the addition of $TiCl_4$ to methanol solutions is cumbersome and it is unclear what species is catalytically active. These processes have thermal counterparts in reduced titanium-mediated chemistry, e.g., the Ti(III)/*t*-BuOOH-mediated hydroxymethylation of imines [23,24].

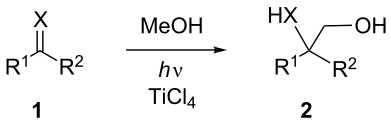

1 **2**

Scheme 1: Photohydroxymethylation of carbonyl compounds and imines.

In order to evaluate the nature of the active catalytic species in the photochemical homogenous titanium-catalyzed hydroxymethylation and to develop a truly catalytic process, we used a model reaction for catalyst screening (acetophenone/methanol) and applied the optimal homogenous reaction conditions involving titanium catalysis to other ketones and keto esters.

Results

Nature of the homogeneous catalytic titanium species

The original protocol for photocatalytic hydroxymethylation involves titanium tetrachloride in methanol as the reactive catalyst/donor mixture and carbonyl compounds as the acceptor components. During the exothermic dissolution process of $TiCl_4$ in methanol with formation of gaseous HCl, a slightly yellowish solution is formed that, after irradiation with UV-A light, turns into a bluish solution indicating the formation of reduced titanium species. Obviously, ligand exchange reactions lead to a series of chloro- and methoxy-titanium complexes that have different catalytic activities. In order to simulate the different complex stages, we applied different monomeric titanium complexes of the type $TiCl_n(OiPr)_{4-n}$ (n = 0, 1, 2, 3) [25-27] in the model process, the irradiation of a solution of acetophenone (**3**) in methanol (Scheme 2). In the absence of any titanium species, photolysis at 254 and 300 nm, respectively, led only to trace amounts of the hydroxymethylation product **4** via a (triplet carbonyl) excited-state hydrogen-transfer process, obviously a sluggish process under these conditions (Table 1). In the presence of titanium complexes $TiCl_n(OiPr)_{4-n}$, coupling and reduction products **4** and **6** were formed without pinacol **5** formation (Scheme 2).

In the presence of the tetraalkoxide $Ti(OiPr)_4$, only the reduction product **6** was detected which demonstrates that chlorotita-

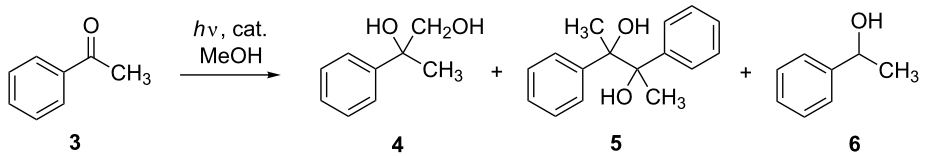

3 **4** **5** **6**

Scheme 2: Model process: photocatalyzed acetophenone/methanol reaction.

Table 1: Homogeneous sensitizer variation for the acetophenone model reaction.

catalyst[a]	irrad. wave-length (nm)	yield **4** (%)[b]	yield **5** (%)[b]	yield **6** (%)[b]
none	300	<5[c]	–	–
	254	<5[c]	–	–
$TiCl_4$	300	33	–	–
	254	34	–	–
$TiCl_3OiPr$	300	31	–	–
	254	47	–	–
$TiCl_2(OiPr)_2$	300	0	–	–
	254	60	–	–
$TiCl(OiPr)_3$	300	<5[d]	–	–
	254	<5[d]	–	–
$Ti(OiPr)_4$	300	–	–	–
	254	–	–	46
$Ti(OiPr)_4$/iPrOH[e]	254	–	–	43
$Ti(OiPr)_4/BF_3$[d]	254	45	–	–
$Ti(OiPr)_4/AlCl_3$[d]	254	49	–	–

[a]0.375 mmol catalyst in methanol (6 mL), 0.75 mmol acetophenone, irradiation time 72 h, rt; [b]isolated yields ; [c]trace amounts detected in ^{1}H NMR; [d]0.75 mmol added in methanol; [e]0.375 mmol cat. in isopropanol.

nium complexes are crucial for the desired reaction path. The results from $TiCl_4$ and $TiCl_3OiPr$ were nearly identical at both wavelengths whereas for $TiCl_2(OiPr)_2$ catalytic activity was preserved only for the 254 nm irradiation. These results show that different catalytically active species must exist that can be excited in different wavelength regions. $TiCl(OiPr)_3$ showed no activity at all, meaning that no further ligand exchange to a tetraalkoxide did occur from this complex. The optimal results concerning reaction time and yields were observed for the $TiCl_2(OiPr)_2$ species. The apparently different catalytic activity of titanium tetraalkoxide complexes could be switched back to hydroxymethylation in the presence of additional strong Lewis acids such as $AlCl_3$ or BF_3. These compounds alone did not show catalytic activity in methanol, only in combination with $Ti(OiPr)_4$. With the optimal homogenous reaction conditions in hand, we applied several other aromatic and aliphatic open chain and cyclic ketones as substrates (Scheme 3). Even benzophenone, a notorious pinacol forming substrate, gave moderate yields of the hydroxymethylation product **7**. Among the aromatic ketones, *para*-fluoroacetophenone was the most reactive ketone. Excellent yields were obtained for 2-pentanone where the product **18** was isolated without purification after extraction. For comparison, the results from the $Ti(OiPr)_4$ catalysis are included in Table 2. Additonally, the comparision with the heterogeneous TiO_2 photolyses demonstrates that under semiconductor conditions pinacolization becomes the major path, but only for aromatic ketones. Aliphatic ketones did not show conversion under TiO_2 photolyses.

These conditions were applied to keto ester substrates that feature an additional trapping site for the primary hydroxy group. We envisaged the formation of lactones from the corresponding hydroxymethylation products (Scheme 4). Methyl benzoylformate (**21**) gave a mixture of pinacol and the 1,2-diol without lactone formation. The higher homologs (Table 3, entries 2–4) resulted in the corresponding lactones with ring sizes of 5 and 6, respectively, with the δ-keto ester (Table 3, entry 4) leading to the δ-pentyrolactone and not the corresponding seven-membered lactone. The primary product from hydroxymethylation was also isolated from the reaction of the ε-keto ester **25** [40].

Heterogeneous and dye-sensitized photocatalysis

The results with the semiconductor particle TiO_2 P25 under low catalyst loading conditions appear in Table 2 for a series of ketone substrates. In order to explore the catalyst profile we tested other reaction conditions for the TiO_2 catalysis, other

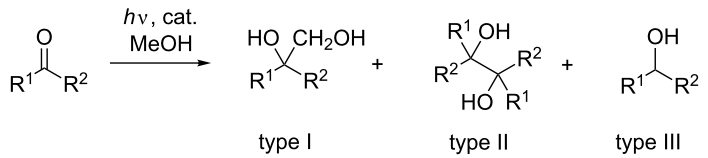

Scheme 3: Photocatalyzed acetophenone/methanol reaction: types I–III.

Table 2: Substrate variation under optimized conditions.

entry	Substrate	$TiCl_2(OiPr)_2$[a] yield (%)[c] type I	yield (%)[c] type I	TiO_2 P25[b] yield (%)[c] type II	$Ti(OiPr)_4$[a] yield (%)[c] type III
1	$Ph(CO)CH_3$	60 (**4** [28])	1 (**4**)	82 (**5** [29])	46 (**6** [30])
2	Ph(CO)Ph	28 (**7** [31])	20 (**7**)	71 (**8** [24])	50 (**9** [32])
3	2'-F-$Ph((CO)CH_3$	56 (**10**)	–	54 (**11**)	40 (**12** [33])
4	4'-MeO-$Ph(CO)CH_3$	–	–	23 (**13** [34])	–
5	4'-NO_2-$Ph(CO)CH_3$	19 (**14** [35])	–		–
6	4'-Me-$Ph(CO)CH_3$	27 (**15** [36])	6 (**15**)	54 (**16** [34])	16 (**17** [37])
7	$C_3H_7(CO)CH_3$	92 (**18** [38])	–		–
8	cyclohexanone	38 (**19** [39])[d]	–		–

[a]0.75 mmol ketone in methanol (6 mL), 0.5 equiv cat., irradiation time 72 h, λ = 254 nm ($TiCl_2(OiPr)_2$) and 300 nm ($Ti(OiPr)_4$), rt; [b]0.75 mmol ketone in methanol (6 mL), 1.4 wt % TiO_2 P25, irradiation time 48 h irradiation, λ = 350 nm, rt; [c]isolated yields; [d]mixture consisting of 9% 1,2-diol and 29% acetalization product with cyclohexanone (**20**).

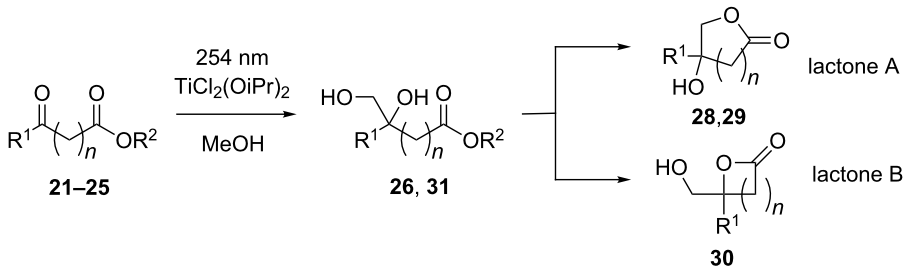

Scheme 4: Photohydroxymethylation and subsequent lactonization of keto esters.

Table 3: Photohydroxymethylation of keto esters: 1,2-diol and lactone formation.

entry	compound[a]	R^1	R^2	*n*	1,2-diol (%)[b]	lactone A (%)[b]	lactone B (%)[b]
1	**21**	Ph	Me	0	15 (**26** [41])[c]	–	–
2	**22**	Ph	Et	1	–	56 (**28** [42])	–
3	**23**	Me	Et	2	–	54 (**29**)	–
4	**24**	Me	Et	3	–	–	28 (**30** [43])
5	**25**	Me	Me	4	44 (**31**)	–	–

[a]0.75 mmol keto ester in methanol (6 mL), 0.5 equiv $TiCl_2(OiPr)_2$, irradiation time 72 h, λ = 254 nm, rt; [b]isolated yields; [c]additionally 11% of the corresponding pinacol **27** was formed.

metal-containing heterogeneous and homogeneous catalysts as well as the classical organic PET catalyst 9,10-dicyanoanthracene (DCA). The results are summarized in Table 4 for the model reaction of acetophenone in methanol (Scheme 5). Except for the $Ru(bpy)_3Cl_2$ system, all catalysts enabled a high degree of conversion and high yields of the pinacol **5** were detected. The hydroxymethylation product **4** was detected only in few experiments with a maximum yield of 6% from one TiO_2 experiment. The best results were obtained for TiO_2 P25 catalysis in the presence of molecular sieves (Table 4, entry 3). In all cases, the pinacol diastereoisomers were formed in nearly equal amounts. Also the change in irradiation wavelength did not lead to substantial changes in conversion and chemoselectivity. The formation of formaldehyde as the final oxidation product was proven qualitatively (colorless precipitation of polyformaldehyde was observed in most experiments) and by a GC–MS online detection of monomeric formaldehyde.

From these results, we reasoned that methanol oxidation is the primary event (e.g., from the DCA results) and acetophenone

Table 4: Heterogeneous sensitizer variation for model reaction in comparison with optimized homogeneous conditions for model process.

entry[a]	catalyst	loading	conversion (%)[b]	yield **4** (%)[b]	yield **5** (%)[b]
1	TiO_2 P25	2.8 wt %	77	–	66
2		2.8 wt %[c]	76	–	58
3		2.8 wt %[d]	96	3	83
4		2.8 wt %[e]	71	–	48
5		2.2 wt %	89	6	79
6		1.4 wt %	95	1	82
7		3.3 wt %	81	2	74
8	TiO_2-pigment	2.8 wt %	89	–	69
9	zinc white	2.8 wt %	79	–	69
10	WO_3, <100 nm	2.8 wt %	98	–	70
11		1.4 wt %	95	1	75
12	Fe_2O_3, <50 nm	2.8 wt %	92	–	75
13		1.4 wt %	95	–	80
14	ZnO, 6% Al doped, <50 nm	2.8 wt %	63	–	46
15	InSnO, <50 nm	2.8 wt %	65	–	45
16	$Ir(ppy)_3$	2.5 mol %	91	–	50
17		2.5 mol %[f]	65	–	55
18		0.5 mol %	89	–	82
19	$Ru(bpy)_3Cl_2$	2.5 mol %	27	–	1
20	DCA	2.5 mol %	95	1	94
21		0.5 mol %	96	1	92
22	none	–	<5%	–	–

[a]0.75 mmol acetophenone in methanol (6 mL), irradiation time 24 h, λ = 350 nm, rt; [b]determined by GC; [c]λ = 300 nm; [d]600 mg molecular sieves were added; [e]100 µL H_2O was added; [f]$Ir(ppy)_3$ regained from entry 16.

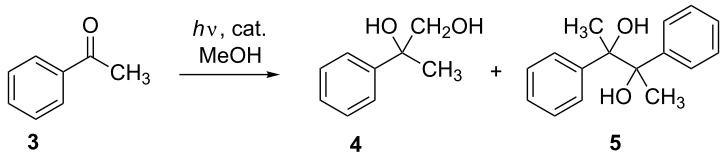

Scheme 5: Model reaction for heterogeneous and dye-sensitized catalysis.

reduction follows resulting in the corresponding hydroxybenzyl radicals that couple to give the pinacol **5**. Under this assumption, a decrease in ketone concentration should favour radical combination of the hydroxybenzyl and the (more reactive and easier oxidizable) hydroxymethyl radicals. As shown in Table 5, this is actually the case for the semiconductor particle TiO_2 P25 catalysis. If acetophenone is added to the photolysis solution constantly over a period of 24 h, the absolute amount of hydroxymethylation product **4** can be increased to 40%.

Discussion

Three product-forming routes can be assumed for the three classes of products observed in the study (Scheme 6): hydroxymethylation (route I), pinacolization (route II) and reduction/hydrogenation (route III). The crucial primary step for all processes is methanol oxidation [44]. By using appropriate reaction conditions, every route can be switched on exclusively. Hydroxymethylation is favoured if both hydroxyalkyl radicals are generated in close proximity by a coupled electron transfer/back transfer process. According to this expectation, the optimal conditions for route I are fulfilled for $TiCl_2(OR)_2$, a species that is capable of oxidizing methanol in the excited state and simultaneously acting as a ground-state Lewis acid that complexes the carbonyl compound. A much weaker Lewis acid such as $Ti(OR)_4$ is capable of methanol oxidation but prefers hydrogen transfer at the first or second oxidation event. The pinacolization route II is favoured for heterogeneous and dye-catalyzed conditions. Interestingly, the combination of TiO_2 P25 with an organic dye prefers largely the hydrogenation route III [45].

Table 5: Chemoselectivity modification by application of a dilution effect.

entry	drop rate	TiO_2 in methanol (30 mL)	reaction time	conversion (%)	yield **4** (%)	yield **5** (%)
1[a]	0.28 mmol/h	15 mg	18.7 h	92	36	52
2[a,b]	0.28 mmol/h	15 mg	18.2 h	82	25	38
3[a]	0.21 mmol/h	15 mg	24 h	95	33	55
4[a]	0.21 mmol/h	10 mg	24 h	89	13	60
5[c]	0.16 mmol/h	10 mg	24 h	96	40	50

[a]5 mmol acetophenone dissolved in methanol (10 mL) was slowly added to a TiO_2 P25 (15 mg/ 10 mg) suspension in methanol (30 mL) irradiated (300 nm) at 15 °C; [b]TiO_2 P25 suspension was cooled to −5 °C; [c]3.72 mmol acetophenone dissolved in methanol (10 mL) was slowly added to a TiO_2 P25 (10 mg) suspension in methanol (30 mL) irradiated (300 nm) at 15 °C.

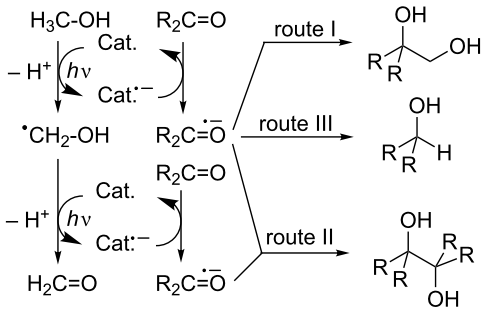

Scheme 6: Product forming routes I to III for photoredox catalysis of methanol/carbonyl compounds.

On the surface of the relatively large semiconductor particles, combination events are rare between the hydroxymethyl radical from methanol oxidation and the hydroxyalkyl radical from ketone reduction. Thus, further oxidation of the hydroxymethyl species to give methanol and another hydroxyalkyl radical is feasible. The combination of two hydroxyalkyl radicals is then dictated by diffusion kinetics (Scheme 7). The dilution experiments described in Table 5 indicate that the probability for pinacol formation is reduced by reducing the stationary concentration of the aromatic ketone. It was shown that hydroxymethyl radicals are formed from methanol during the photolysis of TiO_2 in the absence of additional acceptor compounds with formation of hydrogen and eventually formation of formaldehyde [46]. Both hydrogen and formaldehyde were also detected in our experiments by gas-phase analysis. Thus, higher amounts of hydroxymethyl radicals can be produced under lower concentration of the acceptor ketone and the probability of hydroxybenzyl radical dimerization (i.e., route II) is disfavoured under these conditions.

Supporting Information

Supporting Information File 1

Experimental part.
[http://www.beilstein-journals.org/bjoc/content/supplementary/1860-5397-10-114-S1.pdf]

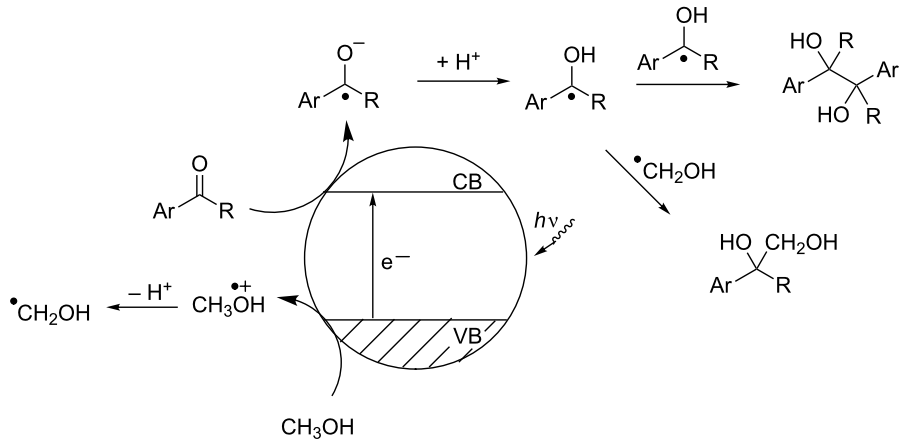

Scheme 7: Photoredox initiated steps on semiconductor particle surfaces, CB, VB = conduction and valence band.

References

1. Reckenthäler, M.; Griesbeck, A. G. *Adv. Synth. Catal.* **2013,** *355,* 2727–2744. doi:10.1002/adsc.201300751
2. Xi, Y.; Yi, H.; Lei, A. *Org. Biomol. Chem.* **2013,** *11,* 2387–2403. doi:10.1039/c3ob40137e
3. Prier, C. K.; Rankic, D. A.; MacMillan, D. W. C. *Chem. Rev.* **2013,** *113,* 5322–5363. doi:10.1021/cr300503r
4. Zou, Y.-Q.; Chen, J.-R.; Xiao, W.-J. *Angew. Chem., Int. Ed.* **2013,** *52,* 11701–11703. doi:10.1002/anie.201307206
5. König, B., Ed. *Photoredox Catalysis;* De Gruyter: Berlin/Boston, 2013.
6. Hu, J.; Wang, J.; Nguyen, T. H.; Zheng, N. *Beilstein J. Org. Chem.* **2013,** *9,* 1977–2001. doi:10.3762/bjoc.9.234
7. Tucker, J. W.; Stephenson, C. R. J. *J. Org. Chem.* **2012,** *77,* 1617–1622. doi:10.1021/jo202538x
8. Xuan, J.; Xiao, W.-J. *Angew. Chem., Int. Ed.* **2012,** *51,* 6828–6838. doi:10.1002/anie.201200223
9. Narayanam, J. M. R.; Jagan, M. R.; Stephenson, C. R. J. *Chem. Soc. Rev.* **2011,** *40,* 102–113. doi:10.1039/b913880n
10. Niwa, T. *J. Synth. Org. Chem., Jpn.* **2010,** *68,* 1307–1308.
11. Fujishima, A.; Rao, T. N.; Tryk, D. A. *J. Photochem. Photobiol., C* **2000,** *1,* 1–21. doi:10.1016/S1389-5567(00)00002-2
12. Keck, H.; Schindler, W.; Knoch, F.; Kisch, H. *Chem.–Eur. J.* **1997,** *3,* 1638–1645. doi:10.1002/chem.19970031013
13. Hörner, G.; Johne, P.; Künneth, R.; Twardzik, G.; Roth, H.; Clark, T.; Kisch, H. *Chem.–Eur. J.* **1999,** *5,* 208–217. doi:10.1002/(SICI)1521-3765(19990104)5:1<208::AID-CHEM208>3.0.CO;2-0
14. Hopfner, M.; Weiß, H.; Meissner, D.; Heinemann, F. W.; Kisch, H. *Photochem. Photobiol. Sci.* **2002,** *1,* 696–703. doi:10.1039/b204569a
15. Kisch, H. *Angew. Chem., Int. Ed.* **2013,** *52,* 812–847. doi:10.1002/anie.201201200
16. Trost, B. M. *Acc. Chem. Res.* **2002,** *35,* 695–705. doi:10.1021/ar010068z
17. Griesbeck, A. G.; Reckenthäler, M.; Uhlig, J. *Photochem. Photobiol. Sci.* **2010,** *9,* 775–778. doi:10.1039/c0pp00033g
18. Griesbeck, A. G.; Steinwascher, J.; Reckenthäler, M.; Uhlig, J. *Res. Chem. Intermed.* **2013,** *39,* 33–42. doi:10.1007/s11164-012-0629-3
19. Sato, T.; Izumi, G.; Imamura, T. *J. Chem. Soc., Perkin Trans. 1* **1976,** 788–791. doi:10.1039/p19760000788
20. Sato, T.; Yoshiie, S.; Imamura, T.; Hasegawa, K.; Miyahara, M.; Yamamura, S.; Ito, O. *Bull. Chem. Soc. Jpn.* **1977,** *50,* 2714–2730. doi:10.1246/bcsj.50.2714
21. Sato, T.; Yamaguchi, S.-i.; Kaneko, H. *Tetrahedron Lett.* **1979,** *20,* 1863–1864. doi:10.1016/S0040-4039(01)86861-1
22. Sato, T.; Kaneko, H.; Yamaguchi, S. *J. Org. Chem.* **1980,** *45,* 3778–3782. doi:10.1021/jo01307a011
23. Rossi, B.; Prosperini, S.; Pastori, N.; Clerici, A.; Punta, C. *Molecules* **2012,** *17,* 14700–14732. doi:10.3390/molecules171214700
24. Clerici, A.; Ghilardi, A.; Pastori, N.; Punta, C.; Porta, O. *Org. Lett.* **2012,** *10,* 5063–5066. doi:10.1021/ol802244n
25. Kamigaito, M.; Sawamoto, M.; Higashimura, T. *Macromolecules* **1995,** *28,* 5671–5675. doi:10.1021/ma00120a037
26. Birse, E. F.; McKenzie, A.; Murray, A. W. *J. Chem. Soc., Perkin Trans. 1* **1988,** 1039–1046. doi:10.1039/p19880001039
27. Reetz, M. T.; Westermann, J.; Steinbach, R.; Wenderoth, B.; Peter, R.; Ostarek, R.; Maus, S. *Chem. Ber.* **1985,** *118,* 1421–1440. doi:10.1002/cber.19851180412
28. Wang, A.; Jiang, H. *J. Org. Chem.* **2010,** *75,* 2321–2326. doi:10.1021/jo100125q
29. Stocker, J. H.; Kern, D. H. *J. Org. Chem.* **1968,** *33,* 291–294. doi:10.1021/jo01265a057
30. Lee, J. M.; Park, E. J.; Cho, S. H.; Chang, S. *J. Am. Chem. Soc.* **2008,** *130,* 7824–7825. doi:10.1021/ja8031218
31. Ortiz, J.; Guijarro, A.; Yus, M. *Eur. J. Org. Chem.* **1999,** 3005–3012. doi:10.1002/(SICI)1099-0690(199911)1999:11<3005::AID-EJOC3005>3.0.CO;2-7
32. Karthikeyan, J.; Jeganmohan, M.; Cheng, C.-H. *Chem.–Eur. J.* **2010,** *16,* 8989–8992. doi:10.1002/chem.201001160
33. Johnson, T. C.; Totty, W. G.; Wills, M. *Org. Lett.* **2012,** *14,* 5230–5233. doi:10.1021/ol302354z
34. Uchiyama, M.; Matsumoto, Y.; Nakamura, S.; Ohwada, T.; Kobayashi, N.; Yamashita, N.; Matsumiya, A.; Sakamoto, T. *J. Am. Chem. Soc.* **2004,** *126,* 8755–8759. doi:10.1021/ja039674a
35. Cleij, M.; Archelas, A.; Furstoss, R. *J. Org. Chem.* **1999,** *64,* 5029–5035. doi:10.1021/jo982101+
36. Chavan, S. P.; Khatod, H. S. *Tetrahedron: Asymmetry* **2012,** *23,* 1410–1415. doi:10.1016/j.tetasy.2012.09.008
37. Li, J.; Wang, C.; Xue, D.; Wei, Y.; Xiao, J. *Green Chem.* **2013,** *15,* 2685–2689. doi:10.1039/c3gc41133h
38. DeGoey, D. A.; Chen, H.-J.; Flosi, W. J.; Grampovnik, D. J.; Yeung, C. M.; Klein, L. L.; Kempf, D. J. *J. Org. Chem.* **2002,** *67,* 5445–5453. doi:10.1021/jo0162890
39. Itami, K.; Kamei, T.; Mitsudo, K.; Nokami, T.; Yoshida, J.-i. *J. Org. Chem.* **2001,** *66,* 3970–3976. doi:10.1021/jo015528g
40. Ito, S.; Matsumoto, M. *J. Org. Chem.* **1983,** *48,* 1133–1135. doi:10.1021/jo00155a051
41. Wang, Z.-M.; Sharpless, K. B. *Synlett* **1993,** 603–604. doi:10.1055/s-1993-22547
42. Eliel, E. L.; Bai, X.; Ohwa, M. *J. Chin. Chem. Soc.* **2000,** *47,* 63–70.
43. Sato, T.; Maeno, H.; Noro, T.; Fujisawa, T. *Chem. Lett.* **1988,** *17,* 1739–1742. doi:10.1246/cl.1988.1739
44. Bowker, M. *Green Chem.* **2011,** *13,* 2235–2246. doi:10.1039/c1gc00022e
45. Kohtani, S.; Nishioka, S.; Yoshioka, E.; Miyabe, H. *Catal. Commun.* **2014,** *43,* 61–65. doi:10.1016/j.catcom.2013.09.006
46. Micic, O. I.; Zhang, Y.; Cromack, K. R.; Trifunac, A. D.; Thurnauer, M. C. *J. Phys. Chem.* **1993,** *97,* 13284–13288. doi:10.1021/j100152a036

Beilstein Journal of Organic Chemistry

Visible-light photoredox catalyzed synthesis of pyrroloisoquinolines via organocatalytic oxidation/[3 + 2] cycloaddition/oxidative aromatization reaction cascade with Rose Bengal

Carlos Vila, Jonathan Lau and Magnus Rueping*

Letter

Open Access

Address:
Institute of Organic Chemistry, RWTH Aachen University, Landoltweg 1, D-52074 Aachen, Germany

Email:
Magnus Rueping* - magnus.rueping@rwth-aachen.de

* Corresponding author

Keywords:
alkaloids; [3 + 2] cycloaddition; organocatalysis; oxidation; photochemistry; photoredox catalysis; Rose Bengal; visible-light

Beilstein J. Org. Chem. **2014,** *10,* 1233–1238.
doi:10.3762/bjoc.10.122

Received: 20 February 2014
Accepted: 30 April 2014
Published: 27 May 2014

This article is part of the Thematic Series "Organic synthesis using photoredox catalysis".

Guest Editor: A. G. Griesbeck

Abstract

Pyrrolo[2,1-*a*]isoquinoline alkaloids have been prepared via a visible light photoredox catalyzed oxidation/[3 + 2] cycloaddition/oxidative aromatization cascade using Rose Bengal as an organo-photocatalyst. A variety of pyrroloisoquinolines have been obtained in good yields under mild and metal-free reaction conditions.

Introduction

Pyrrolo[2,1-*a*]isoquinolines constitute the core structure of the natural products family lamellarin alkaloids (Figure 1) [1-4]. These alkaloids display numerous biological activities such as inhibitor of human topoisomerase I by lamellarin D [5] or inhibition of HIV integrase by lamellarin α-20-sulfate [6,7]. Moreover lamellarin I and lamellarin K also showed potential antitumor activities [8,9]. Due to their potential biological activities, the synthesis of pyrrolo[2,1-*a*]isoquinolines has become a very interesting, important and attractive goal in organic synthesis [10-20]. For example, dipolar [3 + 2] cycloaddition using azomethine ylides [21] is a powerful class of reactions that permits the synthesis of structural complex molecules in a straightforward way and has been used for the efficient synthesis of this type of compounds [22-26]. Recently, several metal mediated syntheses using a [3 + 2] cycloaddition reaction have been described in the literature. Porco Jr. et al. [27] described a silver-catalyzed cycloisomerization/dipolar cycloaddition for the synthesis of the pyrrolo[2,1-*a*]isoquinolines. Wang and co-workers described a copper catalyzed oxidation/[3 + 2] cycloaddition/aromatization cascade [28]. Also, Xiao disclosed a very elegant oxidation/[3 + 2] cycloaddition/aromatization cascade catalyzed by $[Ru(bpy)_3]^{3+}$ under

irradiation with visible light [29]. In this context, very recently Zhao reported the same reaction using C_{60}-Bodipy hybrids [30] and porous material immobilized iodo-Bodipy [31] as photocatalysts, obtaining in both cases good yields for different pyrrolo[2,1-*a*]isoquinolines. Finally, Lu presented in 2013 a dirhodium complex for the synthesis of these compounds [32]. Despite these elegant and important syntheses of pyrrolo[2,1-*a*]isoquinolines through dipolar [3 + 2] cycloaddition, the development of metal-free syntheses using visible light photoredox catalysis with simple organic dyes remained unexplored. Visible-light photoredox catalysis has emerged as an important field and has attracted increasing attention in recent years [33-42]. Thus, in the last years spectacular advances in visible-light photoredox catalysis have been made and this kind of catalysis has become a powerful tool in organic synthesis. In this context, the use of organic dyes as photoredox catalysts [40-42] has been demonstrated by several groups [43-61] and became a useful alternative to the inorganic photoredox catalysts that are expensive and sometimes toxic. The organic dyes have very important qualities such as being inexpensive, environmentally friendly and easy to handle. As a part of our ongoing research on photoredox catalysis [62-72], we herein present a synthesis of pyrrolo[2,1-*a*]isoquinolines through an oxidation/[3+2] cycloaddition/aromatization cascade catalyzed by Rose Bengal under irradiation with green LEDs.

Results and Discussion

Initially, we focused on the reaction between methyl dihydroisoquinoline ester **1a** and *N*-methylmaleimide (**2a**) catalyzed by Rose Bengal. Although the [3 + 2] cycloaddition occurs smoothly in the presence of Rose Bengal (5 mol %) in acetonitrile under irradiation with visible light, the reaction was not selective affording the dihydropyrrolo[2,1-*a*]isoquinoline **3aa** in 35% yield and the hexahydropyrrolo[2,1-*a*]isoquinoline **4aa** in 26% yield, after column chromatography (Scheme 1).

In order to improve the selectivity of the reaction to the aromatized product **3aa**, *N*-bromosuccinimide was added to the reaction mixture when the starting materials were completely consumed [29-31,73]. In this case the desired product **3aa** was obtained in 72% yield (Table 1, entry 1). Other organic dyes such as Rhodamine B or Eosin Y were less efficient compared to Rose Bengal (Table 1, entries 2 and 3, respectively). Several solvents were tested without an improvement in the yield of the product (Table 1, entries 4–9). Finally, after tuning the relative amounts of the reagents, the product **3aa** was isolated in 76% yield (Table 1, entry 12).

With the optimal conditions in hand, we examined the substrate scope for the photoreaction catalyzed by Rose Bengal (Scheme 2). Various tetrahydroisoquinolines with different

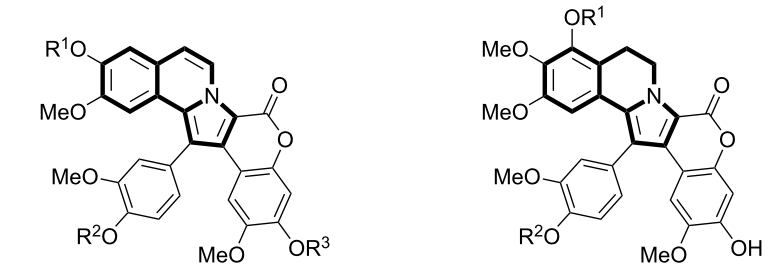

Figure 1: Representative examples of lamellarin alkaloids.

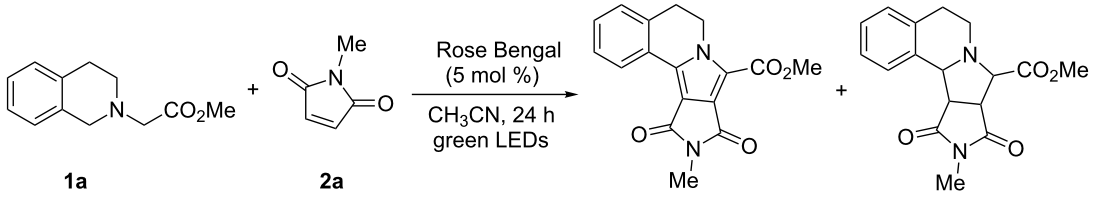

Scheme 1: Photocatalytic metal free construction of pyrrolo[2,1-*a*]isoquinolines.

Table 1: Optimization of the reaction conditions.[a]

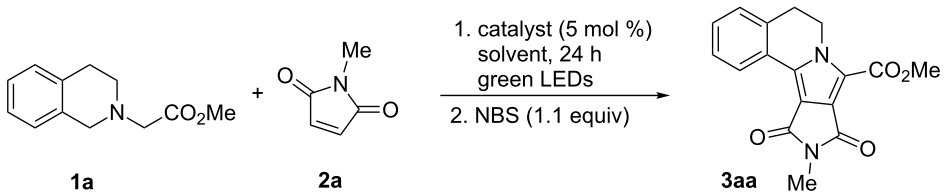

Entry	Catalyst	Solvent	Yield (%)[b]
1	Rose Bengal	CH_3CN	72
2	Rhodamine B	CH_3CN	11
3	Eosin Y	CH_3CN	40
4	Rose Bengal	THF	29
5	Rose Bengal	CH_2Cl_2	26
6	Rose Bengal	toluene	14
7	Rose Bengal	DMF	65
8	Rose Bengal	MeOH	52
9	Rose Bengal	EtOAc	16
10[c]	Rose Bengal	CH_3CN	64
11[d]	Rose Bengal	CH_3CN	60
12[e]	Rose Bengal	CH_3CN	76

[a]Reaction conditions: **1a** (0.2 mmol), **2a** (0.2 mmol), organic dye (5 mol %), solvent (1 mL), green LEDs irradiation for 24 hours. NBS (1.1 equiv) was added to the reaction mixture and stirring was continued for 1 hour. [b]Yields of the isolated products after column chromatography. [c]1.25 equiv of **1a** was used. [d]1.25 equiv of **2a** was used. [e]1.1 equiv of **1a** was used.

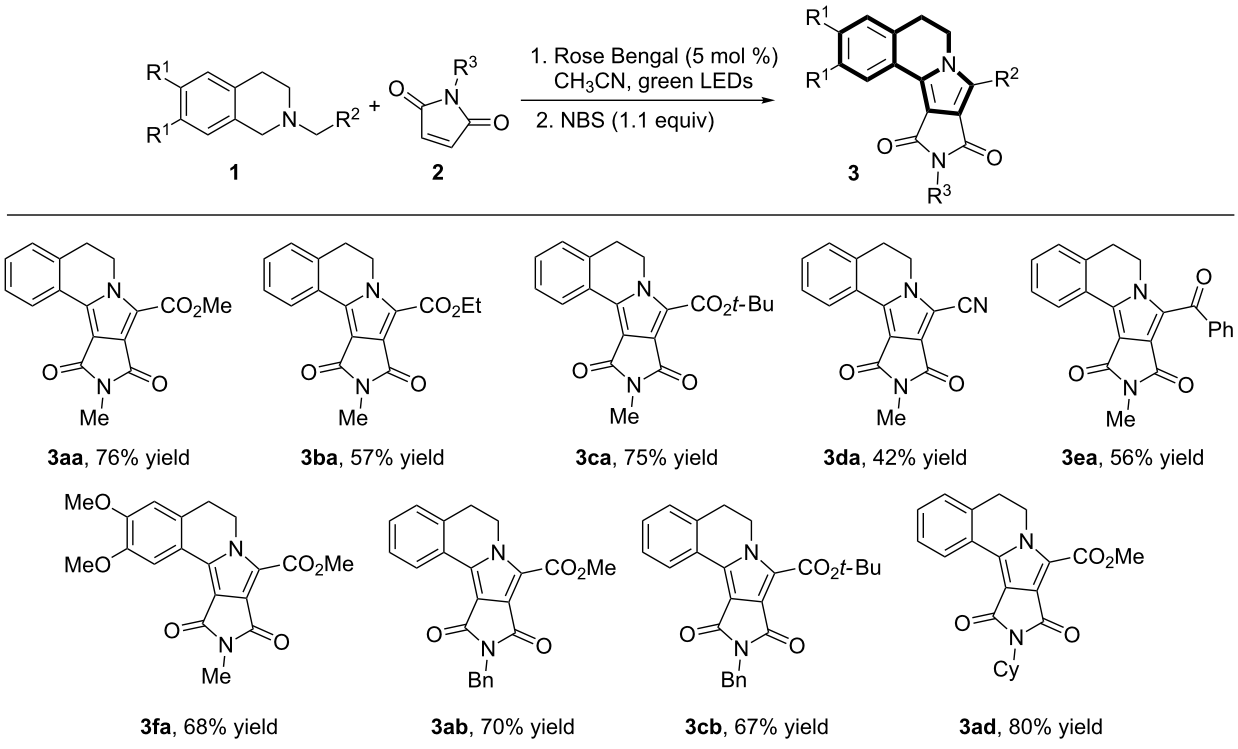

Scheme 2: Evaluation of the substrate scope.

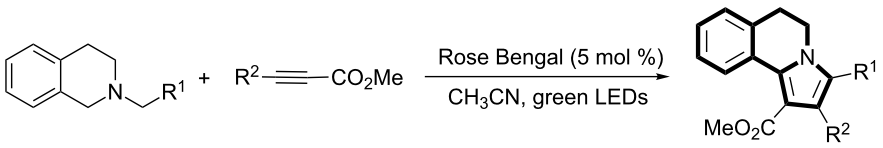

1a, $R^1 = CO_2Me$
1b, $R^1 = CO_2Et$
1d, $R^1 = CN$

5a, $R^2 = H$
5b, $R^2 = CO_2Me$

6aa, $R^1 = CO_2Me$, $R^2 = H$, 30% yield
6ab, $R^1 = R^2 = CO_2Me$, 52% yield
6bb, $R^1 = CO_2Et$, $R^2 = CO_2Me$, 44% yield
6db, $R^1 = CN$, $R^2 = CO_2Me$, 65% yield

Scheme 3: Evaluation of the substrate scope with activated alkynes.

electron-withdrawing groups (R^2) such as methyl ester (**1a**), ethyl ester (**1b**), *tert*-butyl ester (**1c**), cyano (**1d**) or aromatic ketone (**1e**) were reacted with *N*-methylmaleimide (**2a**) and gave the corresponding products **3** in moderate to good yields. In addition, different *N*-substituted maleimides were tested under the optimized reaction conditions to give the corresponding products with good yields. Incorporation of methoxy groups at C-6 and C-7 in the dihydroisoquinoline core was well tolerated, affording the corresponding product **3fa** in 68% yield.

To demonstrate the synthetic utility of the oxidation/[3 + 2] cycloaddition/aromatization cascade we examined other dipolarophiles such as activated alkynes **5**. In this case, the addition of NBS was not necessary, and the corresponding products **6** were isolated in moderate yields (Scheme 3).

Conclusion

In conclusion, we have developed a metal-free photoredox oxidation/[3 + 2] dipolar cycloaddition/oxidative aromatization cascade catalyzed by Rose Bengal using visible-light. This protocol offers a "green" and straightforward synthesis of pyrrolo[2,1-*a*]isoquinolines starting from readily available maleimides and tetrahydroisoquinolines. Further investigations to expand the scope and potential of this methodology are underway in our laboratory.

Supporting Information

Supporting Information File 1

Experimental details and characterization of the synthesized compounds.
[http://www.beilstein-journals.org/bjoc/content/supplementary/1860-5397-10-122-S1.pdf]

References

1. Bailly, C. *Curr. Med. Chem.: Anti-Cancer Agents* **2004,** *4,* 363–378. doi:10.2174/1568011043352939
2. Handy, S. T.; Zhang, Y. *Org. Prep. Proced. Int.* **2005,** *37,* 411–445. doi:10.1080/00304940509354977
3. Fan, H.; Peng, J.; Hamann, M. T.; Hu, J.-F. *Chem. Rev.* **2008,** *108,* 264–287. doi:10.1021/cr078199m
4. Pla, D.; Albericio, F.; Alvarez, M. *Anti-Cancer Agents Med. Chem.* **2008,** *8,* 746–760. doi:10.2174/187152008785914789
5. Marco, E.; Laine, W.; Tardy, C.; Lansiaux, A.; Iwao, M.; Ishibashi, F.; Bailly, C.; Gago, F. *J. Med. Chem.* **2005,** *48,* 3796–3807. doi:10.1021/jm049060w
6. Reddy, M. V. R.; Rao, M. R.; Rhodes, D.; Hansen, M. S. T.; Rubins, K.; Bushman, F. D.; Venkateswarlu, Y.; Faulkner, D. *J. Med. Chem.* **1999,** *42,* 1901–1907. doi:10.1021/jm9806650
7. Aubry, A.; Pan, X.-S.; Fisher, L. M.; Jarlier, V.; Cambau, E. *Antimicrob. Agents Chemother.* **2004,** *48,* 1281–1288. doi:10.1128/AAC.48.4.1281-1288.2004
8. Reddy, S. M.; Srinivasulu, M.; Satanarayana, N.; Kondapi, A. K.; Venkateswarlu, Y. *Tetrahedron* **2005,** *61,* 9242–9247. doi:10.1016/j.tet.2005.07.067
9. Quesada, A. R.; Garcia Grávalos, M. D.; Fernández Puentes, J. L. *Br. J. Cancer* **1996,** *74,* 677–682. doi:10.1038/bjc.1996.421
10. Heim, A.; Terpin, A.; Steglich, W. *Angew. Chem., Int. Ed. Engl.* **1997,** *36,* 155–156. doi:10.1002/anie.199701551
11. Ploypradith, P.; Mahidol, C.; Sahakitpichan, P.; Wongbundit, S.; Ruchirawat, S. *Angew. Chem., Int. Ed.* **2004,** *43,* 866–868. doi:10.1002/anie.200352043
12. Boger, D. L.; Boyce, C. W.; Labroli, M. A.; Sehon, C. A.; Jin, Q. *J. Am. Chem. Soc.* **1999,** *121,* 54–62. doi:10.1021/ja982078+
13. Banwell, M. G.; Flynn, B. L.; Stewart, S. G. *J. Org. Chem.* **1998,** *63,* 9139–9144. doi:10.1021/jo9808526
14. Handy, S. T.; Zhang, Y.; Bregman, H. *J. Org. Chem.* **2004,** *69,* 2362–2366. doi:10.1021/jo0352833
15. Ploypradith, P.; Kagan, R. K.; Ruchirawat, S. *J. Org. Chem.* **2005,** *70,* 5119–5125. doi:10.1021/jo050388m
16. Ohta, T.; Fukuda, T.; Ishibashi, F.; Iwao, M. *J. Org. Chem.* **2009,** *74,* 8143–8153. doi:10.1021/jo901589e
17. Gupton, J. T.; Clough, S. C.; Miller, R. B.; Lukens, J. R.; Henry, C. A.; Kanters, R. P. F.; Sikorski, J. A. *Tetrahedron* **2003,** *59,* 207–215. doi:10.1016/S0040-4020(02)01475-8
18. Fujikawa, N.; Ohta, T.; Yamaguchi, T.; Fukuda, T.; Ishibashi, F.; Iwao, M. *Tetrahedron* **2006,** *62,* 594–604. doi:10.1016/j.tet.2005.10.014
19. Chen, L.; Xu, M.-H. *Adv. Synth. Catal.* **2009,** *351,* 2005–2012. doi:10.1002/adsc.200900287
20. Yadav, J. S.; Gayathri, K. U.; Reddy, B. V. S.; Prasad, A. R. *Synlett* **2009,** 43–46. doi:10.1055/s-0028-1087387

21. Najera, C.; Sansano, J. M. *Curr. Org. Chem.* **1998,** *7,* 1105–1150. doi:10.2174/1385272033486594
22. Ishibashi, F.; Miyazaki, Y.; Iwao, M. *Tetrahedron* **1997,** *53,* 5951–5962. doi:10.1016/S0040-4020(97)00287-1
23. Banwell, M. G.; Flynn, B. L.; Hockless, D. C. R. *Chem. Commun.* **1997,** 2259–2260. doi:10.1039/a705874h
24. Cironi, P.; Manzanares, I.; Albericio, F.; Álvarez, M. *Org. Lett.* **2003,** *5,* 2959–2962. doi:10.1021/ol0351192
25. Ploypradith, P.; Petchmanee, T.; Sahakitpichan, P.; Litvinas, N. D.; Ruchirawat, S. *J. Org. Chem.* **2006,** *71,* 9440–9448. doi:10.1021/jo061810h
26. Grigg, R.; Heaney, F. *J. Chem. Soc., Perkin Trans. 1* **1989,** 198–200. doi:10.1039/p19890000198
27. Su, S.; Porco, J. A., Jr. *J. Am. Chem. Soc.* **2007,** *129,* 7744–7745. doi:10.1021/ja072737v
28. Yu, C.; Zhang, Y.; Zhang, S.; Li, H.; Wang, W. *Chem. Commun.* **2011,** *47,* 1036–1038. doi:10.1039/c0cc03186k
29. Zou, Y.-Q.; Lu, L.-Q.; Fu, L.; Chang, N.-J.; Rong, J.; Chen, J.-R.; Xiao, W.-J. *Angew. Chem., Int. Ed.* **2011,** *50,* 7171–7175. doi:10.1002/anie.201102306
30. Huang, L.; Zhao, J. *Chem. Commun.* **2013,** *49,* 3751–3753. doi:10.1039/c3cc41494a
31. Guo, S.; Zhang, H.; Huang, L.; Guo, Z.; Xiong, G.; Zhao, J. *Chem. Commun.* **2013,** *49,* 8689–8691. doi:10.1039/c3cc44486d
32. Wang, H.-T.; Lu, C.-D. *Tetrahedron Lett.* **2013,** *54,* 3015–3018. doi:10.1016/j.tetlet.2013.04.004
33. Zeitler, K. *Angew. Chem., Int. Ed.* **2009,** *48,* 9785–9789. doi:10.1002/anie.200904056
34. Yoon, T. P.; Ischay, M. A.; Du, J. *Nat. Chem.* **2010,** *2,* 527–532. doi:10.1038/nchem.687
35. Narayanam, J. M. R.; Stephenson, C. R. J. *Chem. Soc. Rev.* **2011,** *40,* 102–113. doi:10.1039/b913880n
36. Xuan, J.; Xiao, W.-J. *Angew. Chem., Int. Ed.* **2012,** *51,* 6828–6838. doi:10.1002/anie.201200223
37. Shi, L.; Xia, W. *Chem. Soc. Rev.* **2012,** *41,* 7687–7697. doi:10.1039/c2cs35203f
38. Prier, C. K.; Rankic, D. A.; MacMillan, D. W. C. *Chem. Rev.* **2013,** *113,* 5322–5363. doi:10.1021/cr300503r
39. Hu, J.; Wang, J.; Nguyen, T. H.; Zheng, N. *Beilstein J. Org. Chem.* **2013,** *9,* 1977–2001. doi:10.3762/bjoc.9.234
40. Ravelli, D.; Fagnoni, M. *ChemCatChem* **2012,** *4,* 169–171. doi:10.1002/cctc.201100363
41. Ravelli, D.; Fagnoni, M.; Albini, A. *Chem. Soc. Rev.* **2013,** *42,* 97–113. doi:10.1039/c2cs35250h
42. Nicewicz, D. C.; Nguyen, T. M. *ACS Catal.* **2014,** *4,* 355–360. doi:10.1021/cs400956a
43. Liu, H.; Feng, W.; Kee, C. W.; Zhao, Y.; Leow, D.; Pan, Y.; Tan, C.-H. *Green Chem.* **2010,** *12,* 953–956. doi:10.1039/b924609f
44. Pan, Y.; Kee, C. W.; Chen, L.; Tan, C.-H. *Green Chem.* **2011,** *13,* 2682–2685. doi:10.1039/c1gc15489c
45. Pan, Y.; Wang, S.; Kee, C. W.; Dubuisson, E.; Yang, Y.; Loh, K. P.; Tan, C.-H. *Green Chem.* **2011,** *13,* 3341–3344. doi:10.1039/c1gc15865a
46. Neumann, M.; Füldner, S.; König, B.; Zeitler, K. *Angew. Chem., Int. Ed.* **2011,** *50,* 951–954. doi:10.1002/anie.201002992
47. Hari, D. P.; König, B. *Org. Lett.* **2011,** *13,* 3852–3855. doi:10.1021/ol201376v
48. Liu, Q.; Li, Y.-N.; Zhang, H.-H.; Chen, B.; Tung, C.-H.; Wu, L.-Z. *Chem.–Eur. J.* **2012,** *18,* 620–627. doi:10.1002/chem.201102299
49. Fidaly, K.; Ceballos, C.; Falguières, A.; Veitia, M. S.-I.; Guy, A.; Ferroud, C. *Green Chem.* **2012,** *14,* 1293–1297. doi:10.1039/c2gc35118h
50. Fu, W.; Guo, W.; Zou, G.; Xu, C. *J. Fluorine Chem.* **2012,** *140,* 88–94. doi:10.1016/j.jfluchem.2012.05.009
51. Hari, D. P.; Schroll, P.; König, B. *J. Am. Chem. Soc.* **2012,** *134,* 2958–2961. doi:10.1021/ja212099r
52. Hari, D. P.; Hering, T.; König, B. *Org. Lett.* **2012,** *14,* 5334–5337. doi:10.1021/ol302517n
53. Neumann, M.; Zeitler, K. *Org. Lett.* **2012,** *14,* 2658–2661. doi:10.1021/ol3005529
54. Hamilton, D. S.; Nicewicz, D. A. *J. Am. Chem. Soc.* **2012,** *134,* 18577–18580. doi:10.1021/ja309635w
55. Rueping, M.; Vila, C.; Bootwicha, T. *ACS Catal.* **2013,** *3,* 1676–1680. doi:10.1021/cs400350j
56. Grandjean, J.; Nicewicz, D. A. *Angew. Chem., Int. Ed.* **2013,** *52,* 3967–3971. doi:10.1002/anie.201210111
57. Riener, M.; Nicewicz, D. A. *Chem. Sci.* **2013,** *4,* 2625–2629. doi:10.1039/c3sc50643f
58. Wilger, D. J.; Gesmundo, N. J.; Nicewicz, D. A. *Chem. Sci.* **2013,** *4,* 3160–3165. doi:10.1039/c3sc51209f
59. Nguyen, T. M.; Nicewicz, D. A. *J. Am. Chem. Soc.* **2013,** *135,* 9588–9591. doi:10.1021/ja4031616
60. Perkowski, A. J.; Nicewicz, D. A. *J. Am. Chem. Soc.* **2013,** *135,* 10334–10337. doi:10.1021/ja4057294
61. Pitre, S. P.; McTiernan, C. D.; Ismaili, H.; Scaiano, J. C. *J. Am. Chem. Soc.* **2013,** *135,* 13286–13289. doi:10.1021/ja406311g
62. Rueping, M.; Vila, C.; Koenings, R. M.; Poscharny, K.; Fabry, D. C. *Chem. Commun.* **2011,** *47,* 2360–2362. doi:10.1039/c0cc04539j
63. Rueping, M.; Zhu, S.; Koenings, R. M. *Chem. Commun.* **2011,** *47,* 8679–8681. doi:10.1039/c1cc12907d
64. Rueping, M.; Leonori, D.; Poisson, T. *Chem. Commun.* **2011,** *47,* 9615–9617. doi:10.1039/c1cc13660g
65. Rueping, M.; Zhu, S.; Koenings, R. M. *Chem. Commun.* **2011,** *47,* 12709–12711. doi:10.1039/c1cc15643h
66. Rueping, M.; Zoller, J.; Fabry, D. C.; Poscharny, K.; Koenings, R. M.; Weirich, T. E.; Mayer, J. *Chem.–Eur. J.* **2012,** *18,* 3478–3481. doi:10.1002/chem.201103242
67. Rueping, M.; Koenings, R. M.; Poscharny, K.; Fabry, D. C.; Leonori, D.; Vila, C. *Chem.–Eur. J.* **2012,** *18,* 5170–5174. doi:10.1002/chem.201200050
68. Rueping, M.; Vila, C.; Szadkowska, A.; Koenigs, R. M.; Fronert, J. *ACS Catal.* **2012,** *2,* 2810–2815. doi:10.1021/cs300604k
69. Zhu, S.; Rueping, M. *Chem. Commun.* **2012,** *48,* 11960–11962. doi:10.1039/c2cc36995h
70. Zhu, S.; Das, A.; Bui, L.; Zhou, H.; Curran, D. P.; Rueping, M. *J. Am. Chem. Soc.* **2013,** *135,* 1823–1829. doi:10.1021/ja309580a
71. Rueping, M.; Vila, C. *Org. Lett.* **2013,** *15,* 2092–2095. doi:10.1021/ol400317v
72. Vila, C.; Rueping, M. *Green Chem.* **2013,** *15,* 2056–2059. doi:10.1039/c3gc40587g
73. Tóth, J.; Váradi, L.; Dancsó, A.; Blaskó, G.; Töke, L.; Nyerges, M. *Synlett* **2007,** 1259–1263. doi:10.1055/s-2007-977461

Beilstein Journal of Organic Chemistry

Cyclization–endoperoxidation cascade reactions of dienes mediated by a pyrylium photoredox catalyst

Nathan J. Gesmundo and David A. Nicewicz*

Letter

Open Access

Address:
Department of Chemistry, University of North Carolina at Chapel Hill, Chapel Hill, NC 27599-3290, USA

Email:
David A. Nicewicz* - nicewicz@unc.edu

* Corresponding author

Keywords:
alkene; cascade; endoperoxide; oxidation; photoredox catalysis

Beilstein J. Org. Chem. **2014,** *10,* 1272–1281.
doi:10.3762/bjoc.10.128

Received: 19 February 2014
Accepted: 06 May 2014
Published: 03 June 2014

This article is part of the Thematic Series "Organic synthesis using photoredox catalysis".

Guest Editor: A. G. Griesbeck

Abstract

Triarylpyrylium salts were employed as single electron photooxidants to catalyze a cyclization–endoperoxidation cascade of dienes. The transformation is presumed to proceed via the intermediacy of diene cation radicals. The nature of the diene component was investigated in this context to determine the structural requirements necessary for successful reactivity. Several unique endoperoxide structures were synthesized in yields up to 79%.

Introduction

Endoperoxides are a structurally unique class of naturally-occurring compounds that feature a reactive cyclic peroxide moiety of varying ring sizes (Figure 1). The lability of the endocyclic peroxide O–O bond engenders these compounds with a range of important biological functions, most notably, antimalarial and antitumor activity (e.g., artemisinin, yingzhaosu A and merulin C) [1-4]. From a synthetic standpoint, the installation of the endoperoxide moiety presents a significant challenge due to its susceptibility to reduction and for this reason, is ideally introduced late-stage in target-oriented synthesis. Additionally, many endoperoxide natural products possess architecturally complex frameworks (e.g., artemisinin, yingzhaosu A, muurolan-4,7-peroxide) [5] that pose significant synthetic challenges.

Classical approaches to the introduction of cyclic peroxides typically rely on cycloadditions of alkenes and dienes with singlet oxygen. However, ene processes can often compete, leading to complex mixtures of hydroperoxide adducts [1,6-8]. More recently, cyclization reactions of hydroperoxides with pendant alkenes or alkynes have been developed. Selected examples include Pd(II)-catalyzed hydroalkoxylation reactions of unsaturated hydroperoxides [9], Au(I)-catalyzed endoperoxidation of alkynes [10] and Brønsted acid-catalyzed enantioselective acetalization/oxa-Michael addition cascade reactions of peroxyquinols [11].

While these extant methods are effective at installing the endoperoxide functional group, our interest lay in developing strate-

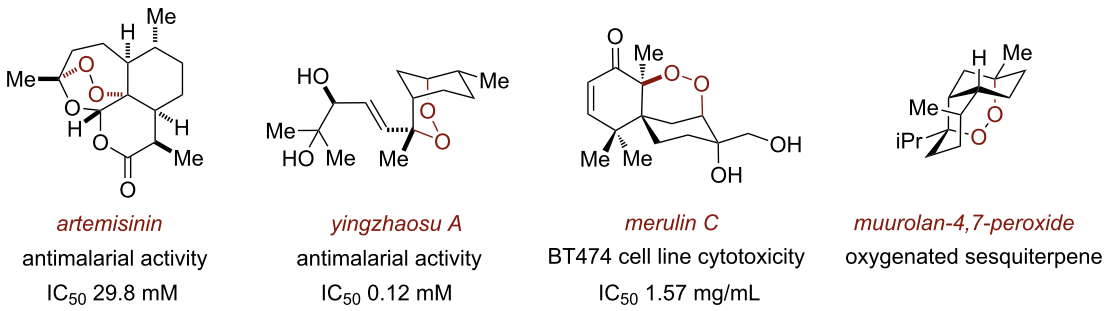

Figure 1: Selected examples of endoperoxide-containing natural products.

gies that simultaneously forged both the cyclic peroxide as well as the carbon framework to rapidly build molecular complexity. For this reason, we were inspired by the work of Miyashi, who, during the course of the investigation of the cation radical Cope rearrangement, discovered an intriguing endoperoxide-forming reaction (Scheme 1, reaction 1). Upon exposure of 1,5 and 1,6-dienes to catalytic quantities of 9,10-dicyanoanthracene (DCA) under UV irradiation in the presence of oxygen, bicyclic endoperoxides were obtained [12]. Formation of the 1,2-dioxanes was presumed to occur via single electron oxidation of the diene by the excited state DCA followed by either 6-*endo* or 7-*endo* cyclization modes to generate a fleeting distonic cation radical species. Interception of the distonic cation radical by triplet oxygen and back electron transfer completes the catalytic cycle. While later reports expanded the scope of this transformation modestly [13,14], we felt that this strategy had potential to be a more general method. Indeed, during the course of this work, the Yoon research group disclosed a similar strategy employing $Ru(bpz)_3^{2+}$ as the photooxidant to effect a 5-*exo* cyclization/endoperoxidation cascade of bis(styrene) substrates (Scheme 1, reaction 2) [15]. More recently, Kamata and Kim have employed this reaction manifold to forge endoperoxides from 1,2-divinylarene precursors [16].

We envisioned that the scope of this transformation could be extended to include non-styrenal dienes as well as alternative cyclization modes, provided that a potent single electron oxidant could be identified (E_{red} > +1.5 V vs SCE). Given the paucity of ground-state single electron oxidants capable of this task, we elected to employ photooxidation catalysts. Additionally, we sought to select visible light-activated organic single electron oxidants that do not readily sensitize singlet oxygen [17-19]. For these reasons, we were attracted to the use of triarylpyrylium salts, as they have excited state reduction potentials in excess of +1.7 V vs SCE (Scheme 2) [20]. In addition, prior work demonstrates that these catalysts are productive in cation radical mediated [4 + 2], [2 + 2], oxygenation, and rearrangement chemistry [21,22]. We also sought to delineate the reactivity of the diene with respect to its structure to better predict the mode of diene cation radical cyclization (5-*exo* vs

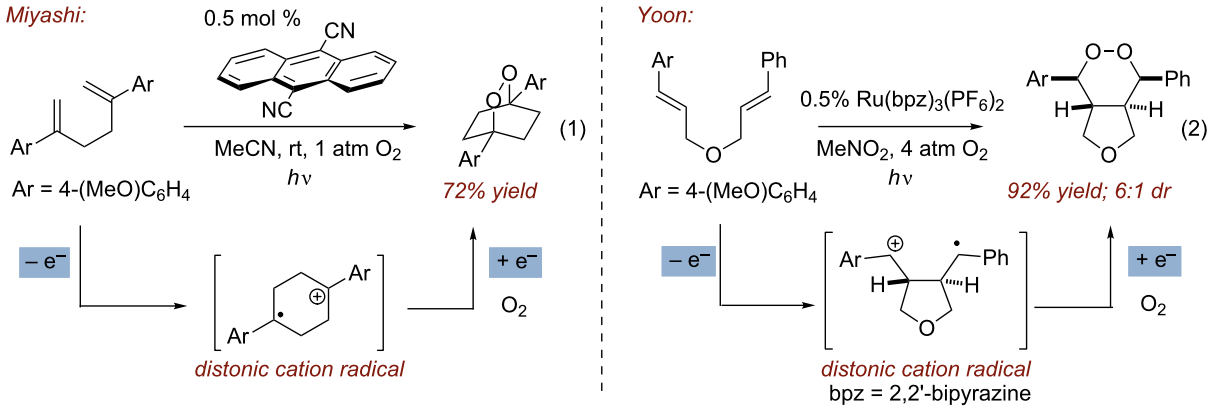

Scheme 1: Endoperoxide formation via cation radicals. In both examples, single electron oxidation is followed quickly by cyclization to form stabilized distonic cation radical intermediates. The distonic intermediates are trapped by O_2 and furnish the shown bicyclic products after reduction.

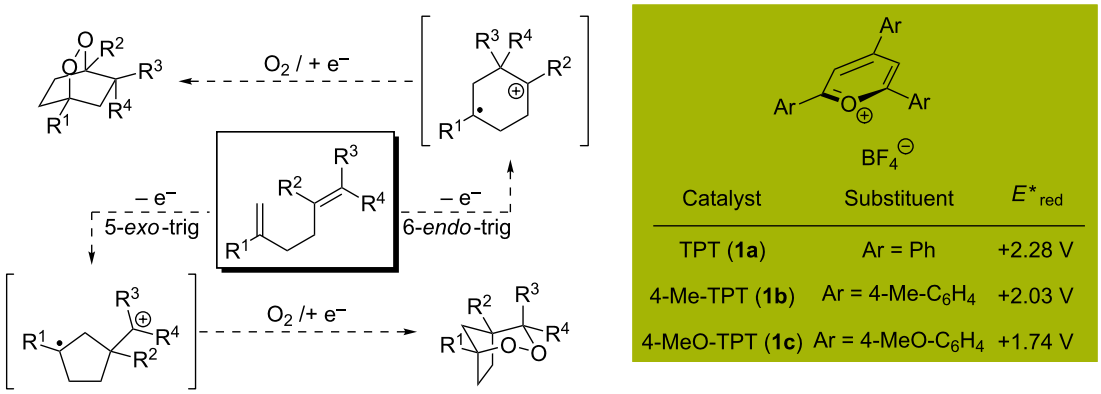

Scheme 2: Diversification strategy for endoperoxide synthesis by single electron transfer. E^*_{red} vs SCE [20].

6-*endo*). Herein is reported an organocatalytic photoredox-mediated strategy for the endoperoxidation of 1,5-dienes using $^3O_2$ to rapidly generate complex endoperoxide frameworks.

Results and Discussion

Reaction optimization

We began our investigation into endoperoxidation conditions with diene **2a** as the substrate as it contained both a styene and an aliphatic alkene. Using catalyst **1c** in DCM at −41 °C under irradiation with 470 nm LEDs afforded endoperoxide **3a** in 40% yield after 5 hours (Table 1, entry 1). The observed endoperoxide was attributed to a 5-*exo* cyclization mode of the diene cation radical followed by capture of molecular oxygen. The use of acetonitrile as solvent gave none of the desired adducts (Table 1, entry 2). Further improvement of the chemical yield of **3a** was realized by increasing the reaction concentration

Table 1: Reaction Optimization and Control Experiments.

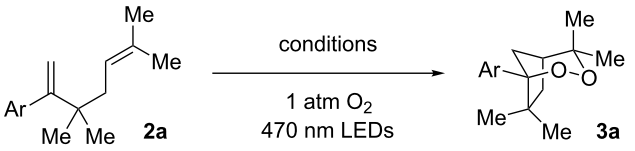

Ar = 4-MeO-C_6H_4 Ar = 4-MeO-C_6H_4

Entry	Conditions[a]	Conversion	Yield[b]
1	2 mol % **1c** 0.01 M DCM, −41 °C	100%	40%
2	2 mol % **1c** 0.01 M MeCN, −41 °C	100%	0%
3	2 mol % **1c** 0.02 M DCM, −41 °C	100%	63%
4	1 mol % **1c** 0.05 M DCM, −41 °C	100%	63%
5	0.7 mol % **1c** 0.07 M DCM, −41 °C	100%	70%
6[c]	Excluding O_2	11%	0%
7	Excluding *hv*	0%	0%
8	Excluding catalyst **1c**	0%	0%
9	9-Mes-10-Me-Acr-BF_4 in place of **1c**	100%	0%
10[d]	Rose Bengal in place of **1c**	100%	0%

All reactions carried out in oxygen-saturated solvents unless otherwise noted. [a]−41 °C found to be the optimum temperature during initial substrate/reaction optimization. [b]Yields with respect to $(Me_3Si)_2O$ ^1H NMR internal standard. [c]Reaction carried out under N_2 atmosphere in DCM. [d]Reaction carried out in oxygen saturated MeOH at room temperature using a white flood lamp.

(Table 1, entries 3–5), resulting in a 70% yield (^{1}H NMR) of the endoperoxide (Table 1, entry 5). In all reactions, substrate conversion was 100%, with the remainder of the mass balance in all cases representing oxidative decomposition pathways. When O_2 was excluded from the reaction (Table 1, entry 6), none of the endoperoxide was observed. Not surprisingly, exclusion of light or catalyst **1c** from the reaction (Table, 1 entries 7 and 8 respectively) resulted in no product formation. Interestingly, when 9-mesityl-10-methylacridinium tetrafluoroborate, which has been used with success in other photooxidation processes [23-26], was used in place of **1c**, complete consumption of **2a** was observed, but **3a** was not produced. Once again only oxidative decomposition pathways seemed active, this time possibly due to superoxide formation. Lastly, to exclude the intervention of a singlet oxygen mechanism, we conducted the reaction in the presence of Rose Bengal. Under these conditions, we observed only $^1O_2$ ene reactivity with the isoprenyl group (65% yield of hydroperoxide), underscoring the unique reactivity garnered by this catalyst system (see Supporting Information File 1 for hydroperoxide characterization). Suitable crystals of **3a** provided X-ray confirmation of the endoperoxide structure (Figure 2).

Figure 2: ORTEP of **3a**.

We invoke a mechanism similar to that proposed by Miyashi [12] and Yoon [15] in their respective transformations (Scheme 3). Following excitation of triarylpyrylium tetrafluoroborate catalyst **1**, one-electron oxidation of the 1,5-diene substrate produces localized cation radical intermediate **4** and pyranyl radical **1**$^\bullet$. Cyclization of diene cation radical **4** then forms stabilized distonic cation radical intermediate **5**, which is intercepted by O_2 to form **6**. Single electron reduction, either from **1**$^\bullet$ to regenerate active catalyst **1** or from another substrate equivalent in a chain process, forms the desired bicyclic endoperoxide.

DFT calculations suggest that the formation of the initial distonic cation radical **5** is exothermic by approximately 3 kcal/mol relative to cation radical **4** [27]. Superficially, this is rationalized by the increased substitution on **5** relative to **4**. In addition, the majority of the spin density on **5** is located on the isoprenyl group (DFT-**5**, Scheme 3). This may be fortuitous as

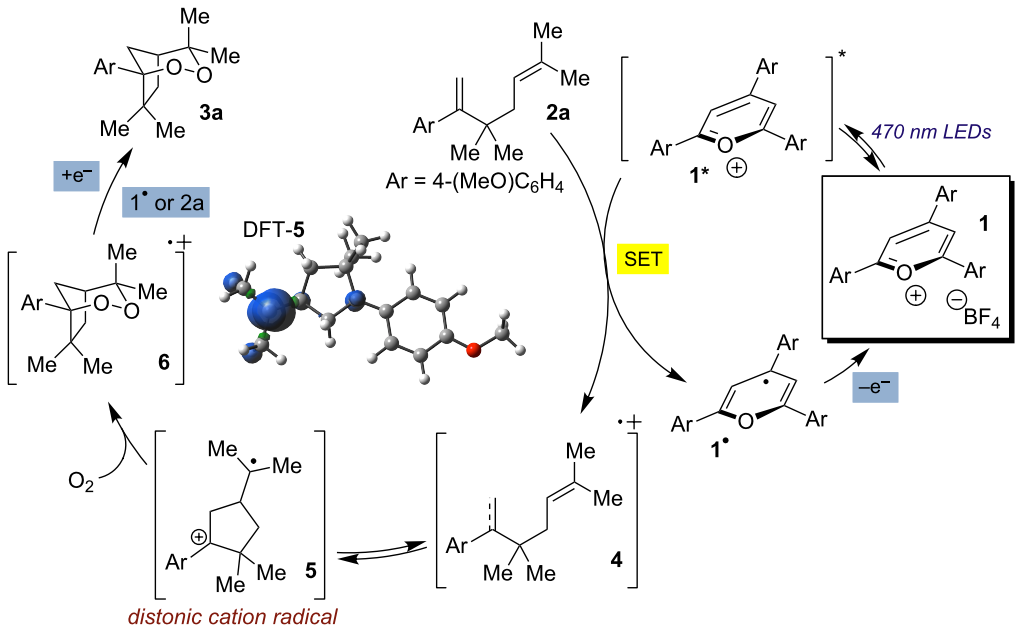

Scheme 3: Proposed mechanism for endoperoxide synthesis from tethered dienes.

stereoselectivity in the oxygen addition step is irrelevant, whereas the opposite scenario involving a benzylic radical intermediate would require a stereospecific addition of oxygen to the same face of the cyclopentane system as the isoprenyl cation in order for endoperoxide formation to occur.

With optimized conditions identified, we sought to examine the scope of the reaction with respect to the diene structure. Miyashi's 1,5-diene (**2b**; $E_{1/2}^{Ox}$ = 1.22 V vs SCE [12]) afforded a 50% yield of the expected endoperoxide along with ~5% of a 1,4-dione, presumably from double oxidative cleavage of the 1,5-diene (Table 2, entry 1). Unfortunately, attempts to move away from **2b** to less electron-rich dienes such as **2c**, **2d** and **2e** (Table 1, entries 2–4), failed to produce any of the desired endoperoxide products and mainly oxidative cleavage adducts were observed.

Given the lack of reactivity of this alkene substitution pattern, we turned our attention to the investigation of diene structures similar to successful endoperoxidation substrate **2a**. Removal of

Table 2: Diene structure investigation for endoperoxidation cascade.

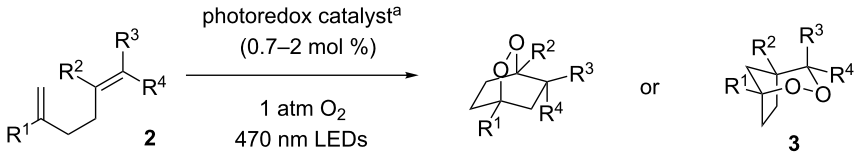

Entry	Substrate	Expected adduct	Yield[b]
1	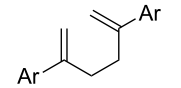 Ar = 4-MeO-C_6H_4 **2b**	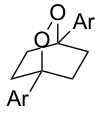 **3b**	50%
2	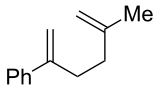 **2c**	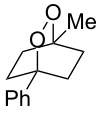 **3c**	0%
3	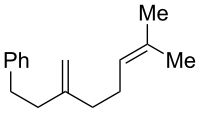 **2d**	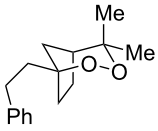 **3d**	0%
4	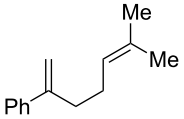 **2e**	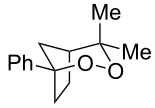 **3e**	0%
5	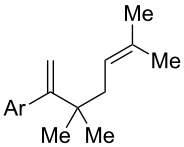 Ar = 4-MeO-C_6H_4 **2a**	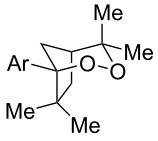 **3a**	66%
6	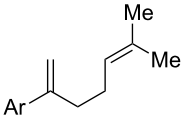 Ar = 4-MeO-C_6H_4 **2f**	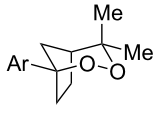 **3f**	32%

Table 2: Diene structure investigation for endoperoxidation cascade. (continued)

7	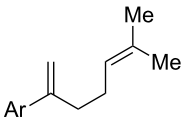 Ar = 2,4-$(MeO)_2$-C_6H_3 **2g**	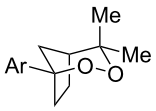 **3g**	9%
8	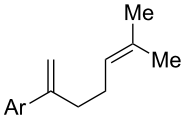 Ar = 3,4-$(MeO)_2$-C_6H_3 **2h**	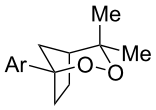 **3h**	0%
9	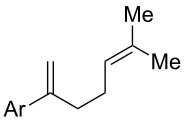 Ar = 2-MeO-C_6H_4 **2i**	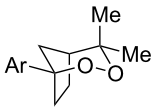 **3i**	16%
10	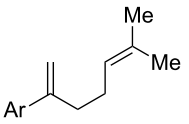 Ar = 4-Me-C_6H_4 **2j**	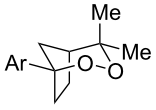 **3j**	0%
11	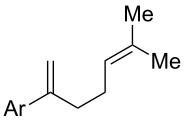 Ar = 4-Cl-C_6H_4 **2k**	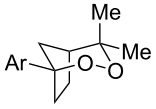 **3k**	0%
12	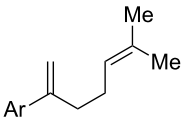 Ar = 2-furyl **2l**	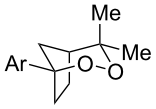 **3l**	0%

All reactions carried out in oxygen-saturated solvents. Solvents examined: DCM, $CHCl_3$, MeCN, PhMe, acetone. [a]Catalysts **1a**, **1b**, and **1c** screened for reactivity with all substrates. [b]Average of two isolated yields.

the geminal dimethyl group (**2f**) resulted in significantly diminished yields of the endoperoxide adduct, likely due to the lack of a Thorpe–Ingold effect present in **2a**. These experiments also demonstrated that the electron-rich arene was necessary for reactivity (cf. **2e** and **2f**; Table 2, entries 4 and 6). The importance of the electron-rich arene may lie in the necessary distonic cation radical intermediate: the electron-rich arene may provide greater stability to the distonic intermediate formed after 5-*exo*-trig cyclization, ultimately ensuring it remains to intercept oxygen. A further survey of the styrene component supported this hypothesis. While electron-rich styrenes gave modest amounts of product formation (**2f**, **2g** and **2i**; Table 2, entries 6, 7 and 9), styrenes with either weakly donating (4-Me; Table 2, entry 10) or even withdrawing (4-Cl; Table 2, entry 11) functionality furnished none of the expected endoperdoxides. In these cases, oxidative degradation was observed as was the case with the highly oxidizable 2-furyl group (Table 2, entry 12). Interestingly, 3,4-dimethoxystyrene-substituted diene **2h** also gave none of the desired adduct, which we attributed to lack of charge density on the alkene [28,29].

We next investigated the endoperoxidation cascade by replacing the isoprenyl substituent with a variety of other alkenes. A pendant styrene afforded the desired endoperoxide adduct in 68% yield, albeit with no diastereocontrol (**2m**, 1:1 dr; Table 3, entry 1). A diene bearing a tetrasubstituted alkene (**2n**) was reactive in this context, giving polycyclic endoperoxide **3n** in 64% yield (6.5:1 dr). The use of 1,2-, 1,1-dialkyl as well as monoalkyl-substituted alkenes appeared to completely disfavor

Table 3: Variation of the tethered alkene component.

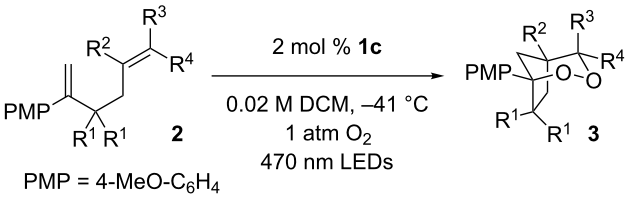

Entry	Substrate	Observed product	Yield[a]
1[b]	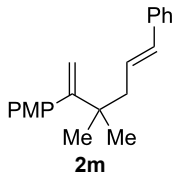 **2m**	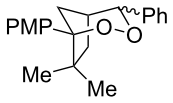 **3m**	68%, 1:1 d.r.
2[c]	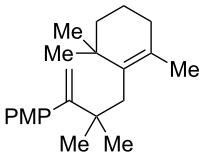 **2n**	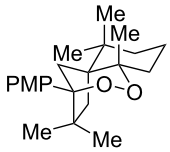 **3n**	64%, 6.5:1 d.r.
3[d]	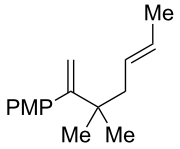 **2o**	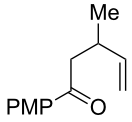 **3o**	36%
4[d]	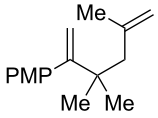 **2p**	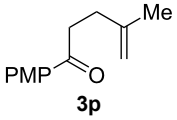 **3p**	37%
5[d]	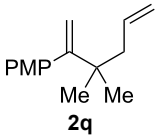 **2q**	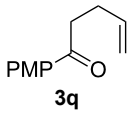 **3q**	27%
6[e]	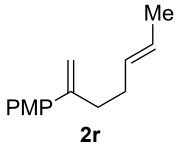 **2r**	–	0%
7[e]	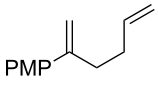 **2s**	–	0%

Reactions carried out in oxygen-saturated solvents. [a]Average of two isolated yields. [b]1:1 mixture of separable diastereomers. [c]6.5:1 mixture of inseparable diastereomers. Presumed major diastereomer shown. [d]Desired endoperoxide never observed. [e]Multiple conditions tested, no productive chemistry observed.

the endoperoxidation pathway and resulted in the unexpected isolation of α-allyl ketones (Table 3, entries 3–5) in modest yields. Based on the Miyashi precedent, the formation of these adducts can be rationalized by invoking a formal [3,3]-rearrangement of the initial cation radical intermediate. The competing 6-*endo* cyclization mode and formation of distonic cation radical **9** ultimately provides access to the more stabilized cation radical **10**, which undergoes oxidative cleavage to afford the corresponding α-allyl ketones (Scheme 4). In the absence of the geminal dimethyl group (**2r**, **2s**), neither the Cope-like reactivity or the endoperoxidation was observed (Table 3, entries 6 and 7).

Lastly, we elected to explore cyclization modes similar to the Yoon work under the developed conditions. Diene **2t** was anticipated to undergo 6-*exo*-trig cyclization to form the necessary distonic cation radical intermediate (Table 4, entry 1). The expected trioxabicyclo[3.3.1]nonane product was formed, albeit

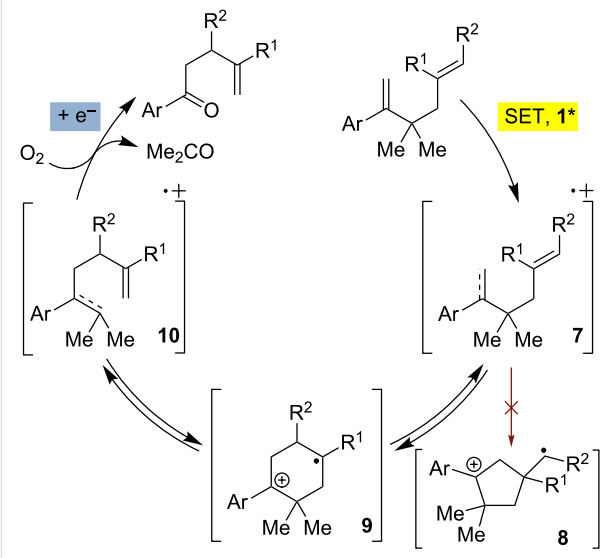

Scheme 4: Competing formal [3,3] pathway.

Table 4: Other cyclization modes and substrate designs.

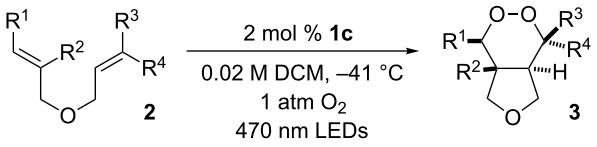

Entry	Substrate	Desired product	Yield[a]
1[b]	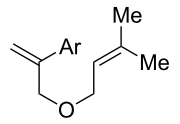 Ar = 4-MeO-C_6H_4 **2t**	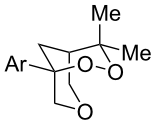 Ar = 4-MeO-C_6H_4 **3t**	16%
2	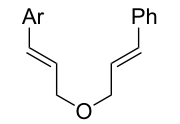 Ar = 4-MeO-C_6H_4 **2u**	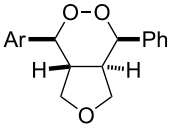 Ar = 4-MeO-C_6H_4 **3u**	79%, 5.7:1 d.r.
3	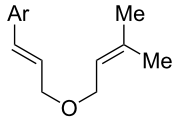 Ar = 4-MeO-C_6H_4 **2v**	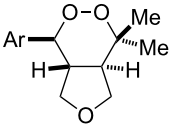 Ar = 4-MeO-C_6H_4 **3v**	<5%
4[c]	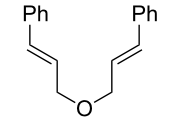 **2w**	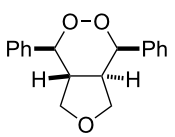	0%

Reactions carried out in oxygen-saturated dichloromethane. [a]Average of two isolated yields. [b]Carried out in 0.4 M DCE after solvent and concentration optimization. [c]Catalysts **1a** or **1b** were also tested but failed to furnish the endoperoxide.

in low yields (16%), where the remainder of the mass balance was attributed to oxidative degradation.

Bis(styrene) **2u** afforded the identical fused 1,2-dioxane observed in Yoon's report in 79% yield (5.7:1 dr). Tethered trisubstituted aliphatic alkene substrate **2v**, along with bis(styrene) substrate **2w** were unfortunately unsuccessful, producing neither of the desired fused 1,2-dioxane products in appreciable amounts. Degradation pathways were dominant for **2v** and mainly unreacted starting material was observed **2w**.

Conclusion

In the presence of an organic single electron photooxidant, a variety of dienes were demonstrated to undergo a cyclization/endoperoxidation cascade sequence to form 1,2-dioxanes. Requirements for successful diene reactivity are the presence of an oxidizable olefin and an alkene that can efficiently react with the putative alkene cation radical to form a more stable distonic cation radical. If available, a Cope-like pathway can compete and suppress endoperoxide formation. With these parameters in mind, this reaction could provide a platform for the discovery of novel biologically-active endoperoxides.

Supporting Information

Supporting Information File 1

Experimental procedures and characterization data.
[http://www.beilstein-journals.org/bjoc/content/supplementary/1860-5397-10-128-S1.pdf]

Supporting Information File 2

X-ray data.
[http://www.beilstein-journals.org/bjoc/content/supplementary/1860-5397-10-128-S2.pdf]

Acknowledgements

We gratefully acknowledge the David and Lucile Packard Foundation for financial support. Additionally, we thank Nathan Romero for DFT calculations and Dr. Peter White for X-ray analysis.

References

1. Ando, W., Ed. *Organic Peroxides;* John Wiley & Sons: New York, 1992.
2. Dembitsky, V. M. *Eur. J. Med. Chem.* **2008,** *43,* 223–251. doi:10.1016/j.ejmech.2007.04.019
3. Li, H.; Huang, H.; Shao, C.; Huang, H.; Jiang, J.; Zhu, X.; Liu, Y.; Liu, L.; Lu, Y.; Li, M.; Lin, Y.; She, Z. *J. Nat. Prod.* **2011,** *74,* 1230–1235. doi:10.1021/np200164k
4. Chokpaiboon, S.; Sommit, D.; Bunyapaiboonsri, T.; Matsubara, K.; Pudhom, K. *J. Nat. Prod.* **2011,** *74,* 2290–2294. doi:10.1021/np200491g
5. Adio, A. M.; König, W. A. *Phytochemistry* **2005,** *66,* 599–609. doi:10.1016/j.phytochem.2005.01.015
6. Adam, W.; Griesbeck, A. G. In *CRC Handbook of Organic Photochemistry and Photobiology;* Horspool, W. M.; Song, P., Eds.; CRC Press: Boca Raton, 1992.
7. Bloodworth, A. J.; Eggelte, H. J. In *Singlet Oxygen;* Frimer, A. A., Ed.; CRC Press: Boca Raton, 1985; Vol. II.
8. Iesce, M. R. In *Synthetic Organic Photochemistry;* Griesbeck, A. G.; Mattay, J., Eds.; Marcel Dekker: New York; pp 299–363.
9. Harris, J. R.; Waetzig, S. R.; Woerpel, K. A. *Org. Lett.* **2009,** *11,* 3290–3293. doi:10.1021/ol901046z
10. Krabbe, S. W.; Do, D. T.; Johnson, J. S. *Org. Lett.* **2012,** *14,* 5932–5935. doi:10.1021/ol302848m
11. Rubush, D. M.; Morges, M. A.; Rose, B. J.; Thamm, D. H.; Rovis, T. *J. Am. Chem. Soc.* **2012,** *134,* 13554–13557. doi:10.1021/ja3052427
12. Miyashi, T.; Konno, A.; Takahashi, Y. *J. Am. Chem. Soc.* **1988,** *110,* 3676–3677. doi:10.1021/ja00219a062
13. Takahashi, Y.; Okitsu, O.; Ando, M.; Miyashi, T. *Tetrahedron Lett.* **1994,** *35,* 3953–3956. doi:10.1016/S0040-4039(00)76711-6
14. Kamata, M.; Ohta, M.; Komatsu, K.-i.; Kim, H.-S.; Wataya, Y. *Tetrahedron Lett.* **2002,** *43,* 2063–2067. doi:10.1016/S0040-4039(02)00166-1
15. Parrish, J. D.; Ischay, M. A.; Lu, Z.; Guo, S.; Peters, N. R.; Yoon, T. P. *Org. Lett.* **2012,** *14,* 1640–1643. doi:10.1021/ol300428q
16. Kamata, M.; Hagiwara, J.-i.; Hokari, T.; Suzuki, C.; Fujino, R.; Kobayashi, S.; Kim, H.-S.; Wataya, Y. *Res. Chem. Intermed.* **2013,** *39,* 127–137. doi:10.1007/s11164-012-0637-3
17. Narayanam, J. M. R.; Stephenson, C. R. J. *Chem. Soc. Rev.* **2011,** *40,* 102–113. doi:10.1039/b913880n
18. Xuan, J.; Xiao, W.-J. *Angew. Chem., Int. Ed.* **2012,** *51,* 6828–6838. doi:10.1002/anie.201200223
19. Prier, C. K.; Rankic, D. A.; MacMillan, D. W. C. *Chem. Rev.* **2013,** *113,* 5322–5363. doi:10.1021/cr300503r
20. Martiny, M.; Steckhan, E.; Esch, T. *Chem. Ber.* **1993,** *126,* 1671–1682. doi:10.1002/cber.19931260726
See for excited state reduction potential converted from E vs NHE to E vs SCE.
21. Miranda, M. A.; Garcia, H. *Chem. Rev.* **1994,** *94,* 1063–1089. doi:10.1021/cr00028a009
22. Kamata, M.; Kaneko, J.-i.; Hagiwara, J.-i.; Akaba, R. *Tetrahedron Lett.* **2004,** *45,* 7423–7428. doi:10.1016/j.tetlet.2004.08.077
23. Hamilton, D. S.; Nicewicz, D. A. *J. Am. Chem. Soc.* **2012,** *134,* 18577–18580. doi:10.1021/ja309635w
24. Fukuzumi, S.; Ohkubo, K. *Chem. Sci.* **2013,** *4,* 561–574. doi:10.1039/c2sc21449k
25. Nguyen, T. M.; Nicewicz, D. A. *J. Am. Chem. Soc.* **2013,** *135,* 9588–9591. doi:10.1021/ja4031616
26. Perkowski, A. J.; Nicewicz, D. A. *J. Am. Chem. Soc.* **2013,** *135,* 10334–10337. doi:10.1021/ja4057294
27. *Gaussian 09,* Revision D.01; Gaussian, Inc.: Wallingford CT, 2013.
28. Riener, M.; Nicewicz, D. A. *Chem. Sci.* **2013,** *4,* 2625–2629. doi:10.1039/c3sc50643f
29. Yamashita, T.; Yasuda, M.; Isami, T.; Tanabe, K.; Shima, K. *Tetrahedron* **1994,** *50,* 9275–9286. doi:10.1016/S0040-4020(01)85505-8

BEILSTEIN JOURNAL OF ORGANIC CHEMISTRY

Visible light photoredox-catalyzed deoxygenation of alcohols

Daniel Rackl, Viktor Kais, Peter Kreitmeier and Oliver Reiser*

Full Research Paper

Open Access

Address:
Institute of Organic Chemistry, University of Regensburg, 93053 Regensburg, Germany

Email:
Oliver Reiser* - Oliver.Reiser@chemie.uni-regensburg.de

* Corresponding author

Keywords:
C–O bond activation; deoxygenation; photochemistry; photoredox catalysis; visible light

Beilstein J. Org. Chem. **2014,** *10,* 2157–2165.
doi:10.3762/bjoc.10.223

Received: 04 June 2014
Accepted: 27 August 2014
Published: 10 September 2014

This article is part of the Thematic Series "Organic synthesis using photoredox catalysis".

Guest Editor: A. G. Griesbeck

Abstract

Carbon–oxygen single bonds are ubiquitous in natural products whereas efficient methods for their reductive defunctionalization are rare. In this work an environmentally benign protocol for the activation of carbon–oxygen single bonds of alcohols towards a reductive bond cleavage under visible light photocatalysis was developed. Alcohols were activated as 3,5-bis(trifluoromethyl)-substituted benzoates and irradiation with blue light in the presence of $[Ir(ppy)_2(dtb\text{-}bpy)](PF_6)$ as visible light photocatalyst and Hünig's base as sacrificial electron donor in an acetonitrile/water mixture generally gave good to excellent yields of the desired defunctionalized compounds. Functional group tolerance is high but the protocol developed is limited to benzylic, α-carbonyl, and α-cyanoalcohols; with other alcohols a slow partial C–F bond reduction in the 3,5-bis(trifluoromethyl)benzoate moiety occurs.

Introduction

The dwindling supply of hydrocarbons from fossil resources calls for the usage of renewable resources for the synthesis of fine chemicals in the future [1]. This strategy suffers from the relative high degree of functionalization of feedstock materials, which is often not desired in fine chemicals and further leads to compatibility issues in chemical transformations. Carbon–oxygen single bonds are common elements in natural materials and their reduction to non-functionalized carbon–hydrogen bonds decreases complexity and increases compatibility of those materials in further chemical manipulations in accordance with established oil-based protocols developed in the chemical industry during the last century.

A classical radical deoxygenation reaction using over-stoichiometric amounts of highly noxious chemicals [2] is the Barton–McCombie reaction, although nowadays several improved protocols are available [3]. Radical deoxygenations can also be carried out electrochemically [4] or photochemically [5-9]. In all these cases an activation of the hydroxy group is necessary, either via conversion to the corresponding halide or formation of an ester derivative, which consequently generates over-stoichiometric amounts of byproducts. Related to this work, Stephenson et al. elegantly succeeded in the direct deoxygenation of alcohols by their in situ conversion to iodides using triphenylphospine and iodine followed by visible light-medi-

ated reduction with amines as stoichiometric sacrificial electron donor and *fac*-Ir(ppy)$_3$ (ppy = 2-phenylpyridine) as photoredox catalyst (Scheme 1) [10]. This protocol is applicable to a broad range of alcohols. It also greatly advanced the quest to develop sustainable methods for the deoxygenation of alcohols. Yet, several redox steps, i.e., the stoichiometric transformation of triphenylphosphine to triphenylphospine oxide and iodine to iodide, are required, which appears to be problematic for establishing a sustainable protocol that allows the recycling and reuse of the reagents involved. Herein we report a redox economic deoxygenation method of alcohols in which formation of radicals is achieved under visible light photocatalysis and the auxiliary activation group can be readily recovered and reused.

This method, ultimately requiring only energy and a tertiary amine as stoichiometric reductant, gives high yields after short illumination times under mild conditions for the deoxygenation of benzylic alcohols, α-hydroxycarbonyl, and α-cyanohydrin compounds. Moreover, the selective catalytic monoacylation of diols is possible, thus allowing efficient monodeoxygenations as exemplified in the conversion of (+)-diethyl tartrate to unnatural (+)-diethyl malate.

Results and Discussion

Following the lead of photochemical deoxygenations under UV light irradiation (vide supra) we envisioned carboxylic ester derivatives as substrates for initial test reactions. Benzoate esters were chosen due to the potentially very facile recovery of the benzoic acids used for activation. Through variation of the substitution pattern of benzoates we intended to shift the electrochemical reduction potentials of the substances into a region that could be accessed by common visible light photocatalysts. The substituents should be as inert as possible in order not to interfere with the photochemical reaction itself. Therefore different trifluoromethyl-substituted benzoates were prepared and subjected to cyclovoltametric measurements. 3,5-Bis(trifluoromethyl)-substituted benzoate **3** showed the most promising reduction potential of the compounds investigated (Scheme 2) and was therefore expected to be most susceptible for an initial photoredox electron transfer that we considered in analogy to the Barton–McCombie technology to be crucial to trigger deoxygenations.

Initial deoxygenation experiments were carried out with either $Ru(bpy)_3Cl_2·6H_2O$ [bpy = 2,2'-bipyridine] or $[Ir(ppy)_2(dtb\text{-}bpy)](PF_6)$ [ppy = 2-phenylpyridine; dtb-bpy = 4,4′-di-*tert*-

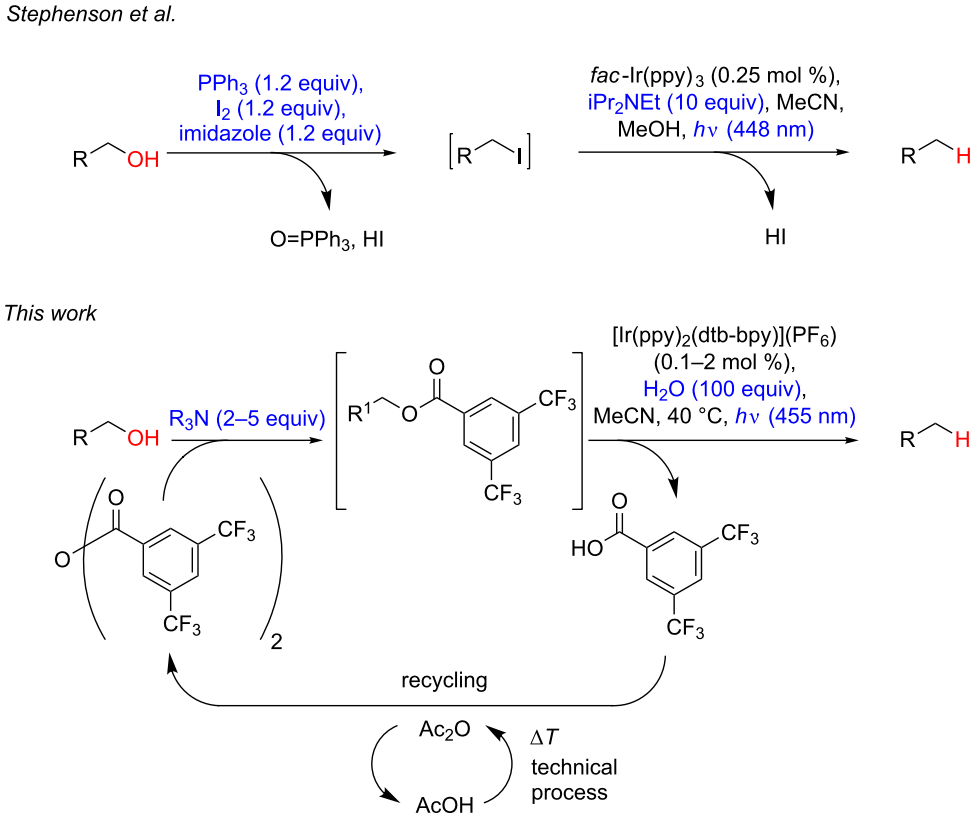

Scheme 1: Strategies for the visible light-catalysed deoxygenation of alcohols (reagents needed in (over-)stoichiometric quantities are depicted in blue).

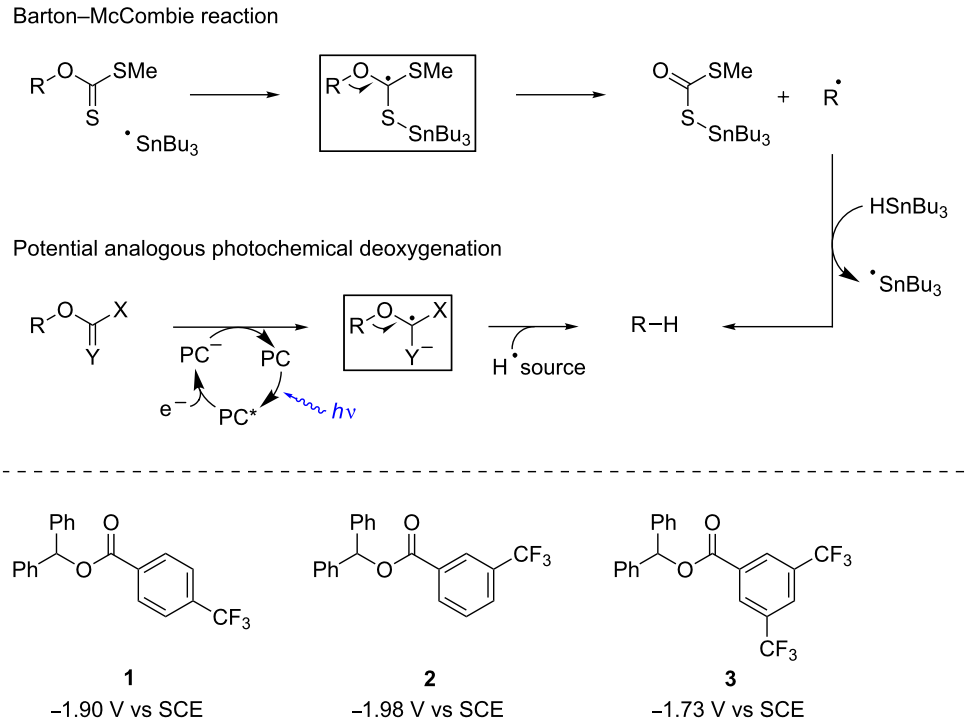

Scheme 2: Reduction potentials of investigated derivatives **1–3** in DMF.

butyl-2,2′-bipyridine] as photocatalysts, Hantzsch ester (diethyl 1,4-dihydro-2,6-dimethyl-3,5-pyridinedicarboxylate) as hydrogen donor, and iPr_2NEt as sacrificial electron donor in DMF (Scheme 3). Light generated from a high power LED was channeled into the reaction solution in a Schlenk tube through a glass rod from above while magnetic stirring and heating was applied from below. This reaction setup is superior compared to conventional ones that are carried out in a vessel with external irradiation: a high light intensity can be achieved for irradiation and reaction temperatures can be manipulated very conveniently by heating in a conventional oil bath while carrying out the photoreaction. Also light pollution is kept to a minimum, which renders the apparatus an optimal device for the fast setup of test reactions.

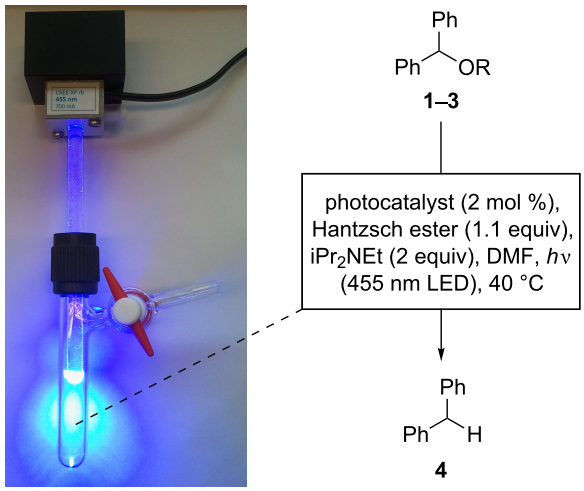

Scheme 3: Initial reaction conditions for deoxygenation candidates **1–3**.

In agreement with the reduction potentials, 3,5-bis(trifluoromethyl)-substituted benzoate **3** gave the best results in the deoxygenation reaction while esters **1** and **2** led to incomplete reactions after 16 h of irradiation (Table 1). The performance of $[Ir(ppy)_2(dtb\text{-}bpy)](PF_6)$ was in all cases superior as compared to $Ru(bpy)_3Cl_2{\cdot}6H_2O$, possibly due to its increased reduction potential ($E^0 = -1.51$ V vs $E^0 = -1.31$ V) [11].

Having identified a promising activation group for deoxygenation in combination with an iridium-based photocatalyst, different solvents and reaction temperatures were examined for the conversion of **3** (Table 2). Gratifyingly, toxic DMF could be replaced with more benign acetonitrile without appreciable decreasing the yield (Table 2, entry 2). The reaction also proceeded in less polar solvents (Table 2, entries 3 and 4), albeit yields were significantly lower. When the reaction was performed at ambient temperature **4** was only formed in 41% yield after 16 h of irradiation (Table 2, entry 5). Control experi-

Table 1: Comparison of different esters and photocatalysts in deoxygenation reaction.

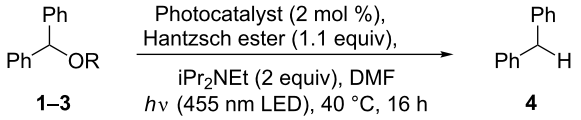

Photocatalyst	Compound yield [%][a]		
	1	**2**	**3**
$Ru(bpy)_3Cl_2·6H_2O$	5	8	10
$[Ir(ppy)_2(dtb\text{-}bpy)](PF_6)$	18	20	85

[a]All yields determined by GC–FID with dodecane as internal standard.

Table 2: Solvent/temperature dependence and control experiments of deoxygenation reaction with 3,5-bis(trifluoromethyl)benzoate **3**[a].

Entry	Solvent, modification	Yield (%)[b]
1	DMF	85
2	MeCN	80
3	DCM	20
4	THF	22
5	MeCN, rt	41
6	MeCN, w/o photocatalyst	7
7	MeCN, w/o light source	15
8	MeCN, w/o Hantzsch ester	91
9	MeCN, w/o iPr_2NEt	53

[a]Conditions see Table 1. [b]All yields determined by GC–FID with dodecane as internal standard.

ments suggest that the deoxygenation reaction of 3,5-bis(trifluoromethyl)benzoate **3** is indeed a photochemically mediated process (Table 2, entries 6 and 7): when either the photocatalyst (Table 2, entry 6) or the light source (Table 2, entry 7) was omitted significantly lower yields were obtained. Leaving out Hantzsch ester (Table 2, entry 8) apparently does not impede the deoxygenation while carrying out the reaction without Hünig's base lowers the yield (Table 2, entry 9), nevertheless, **4** was still formed to a significant extent. These results suggest that Hantzsch ester is not necessary as the hydrogen source but likewise that reductive quenching of the photocatalyst is not exclusively accomplished by Hünig's base.

We assumed that the mechanism of the deoxygenation reaction involves an electron uptake of the ester moiety from the reductively quenched photocatalyst followed by mesolysis and subsequent hydrogen abstraction (Scheme 4). Quantum mechanical calculations (B3LYP/6-31G*) for benzhydryl 3,5-bis(trifluoromethyl)benzoate (**3**) revealed that the electron density of the presumed transient radical anion is mainly located at the phenyl moiety of the benzoate – and not in the desired anti-bonding σ*(C–O) (Scheme 5). Protonation of the radical anion would lead to a neutral radical species, which in the calculations reflects in a shift of electron density towards the C–O bond to be cleaved.

Consequently, a mixture of acetonitrile/water (14:1) was explored as reaction medium, resulting to our delight in dramatically reduced reaction times to achieve full conversion. Starting from bis(trifluoromethyl)benzoates, quantitative formation of the deoxygenated products could be already observed after 20 minutes of irradiation.

A simple iridium-catalyzed hydrogenation mechanism as an alternative for a photochemical pathway of the reaction could be ruled out; in the presence of 5 atm H_2 without irradiation under otherwise unchanged reaction conditions no deoxygenation of the benzoates could be observed even after prolonged reaction times.

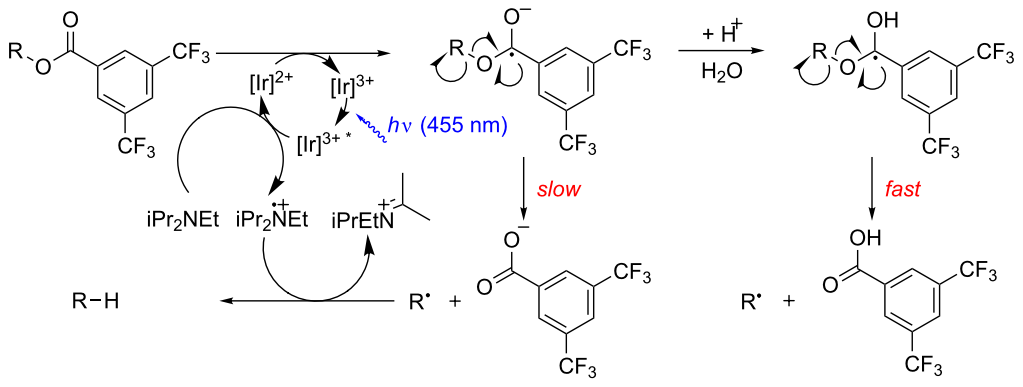

Scheme 4: Proposed reaction mechanism with and without additional water.

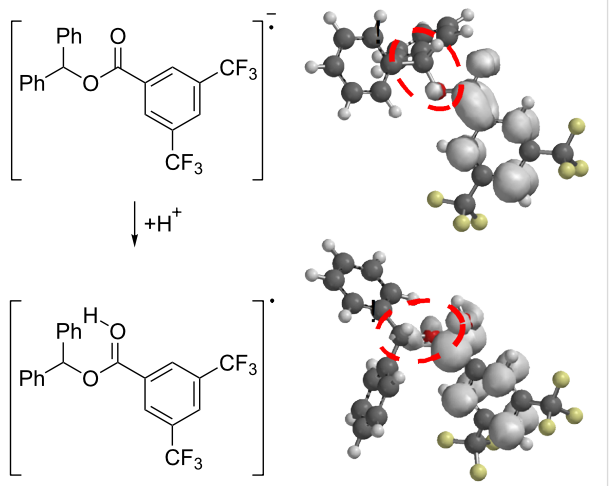

Scheme 5: Calculated spin densities of the radical anion and its protonated species.

With the newly optimized reaction conditions at hand different benzylic alcohol derivatives were investigated (Table 3). Uniformly very good isolated yields after short reaction times were achieved in case of dibenzylic alcohol derivatives. Steric bulk (Table 3, entry 2), as well as a broad range of functional groups with different electronic properties, i.e., an electron-donating *p*-methoxy substituent (Table 3, entry 3), electron-withdrawing *p*-nitro substituent (Table 3, entry 4), ester group containing systems (Table 3, entry 5), chlorinated derivatives (Table 3, entry 6) and electron-deficient heteroaromatic systems (Table 3, entry 7) were well tolerated, giving the corresponding deoxygenated products in analytical pure form in high yields after filtration through a short plug of silica gel. Noteworthy, no reduction of reducible groups such as nitro (Table 3, entry 4) or chloro (Table 3, entry 5) was observed. Moving to monobenzyl alcohols, e.g., replacement of one aromatic group with an alkyl chain resulted in prolonged reaction times but nevertheless acceptable yields of the deoxygenated products (Table 3, entries 8 and 9). With α-carbonyl-substituted benzylic alcohol derivatives irradiation times could be reduced again and defunctionalized materials were isolated in moderate to good yields (Table 3, entries 10 and 11). Bis(trifluoromethyl)benzoic acid **5** could easily be recovered (>90%) in an acid–base extraction step.

Also bis(trifluoromethyl)benzoates of non-benzylic α-cyanohydrin **6a** and α-hydroxycarbonyl compounds **6b–e** turned out to be amenable for the desoxygenation process (Table 4).

Table 3: Preparative deoxygenation reactions.

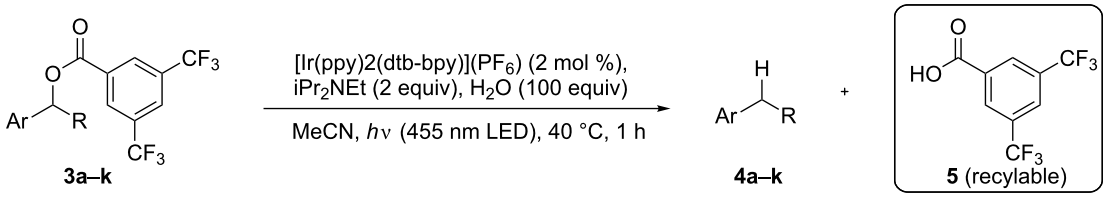

Entry	Substrate	Product	Yield (%)[a]
1	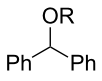 **3a**	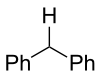 **4a**	95
2	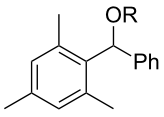 **3b**	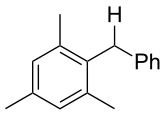 **4b**	86
3	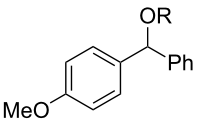 **3c**	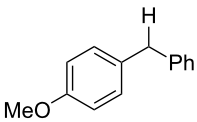 **4c**	87
4	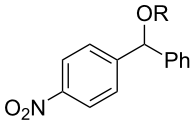 **3d**	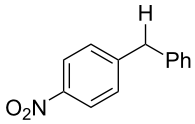 **4d**	91

Table 3: Preparative deoxygenation reactions. (continued)

5	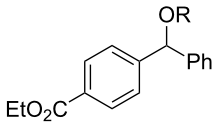 **3e**	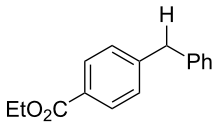 **4e**	93
6	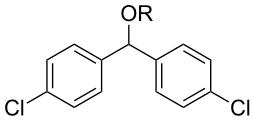 **3f**	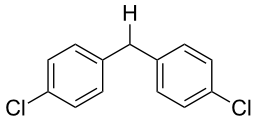 **4f**	92
7	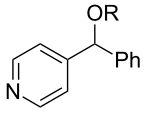 **3g**	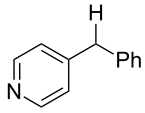 **4g**	86
8	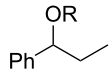 **3h**	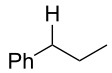 **4h**	66[b,c]
9	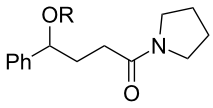 **3i**	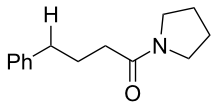 **4i**	79[c]
10	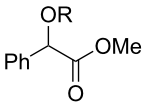 **3j**	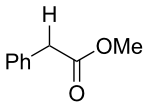 **4j**	83
11	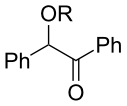 **3k**	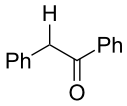 **4k**	67

[a]Isolated yields of reactions conducted at a 0.2–1.0 mmol scale. [b]Determined by GC with dodecane as internal standard. [c]16 h reaction time.

Table 4: Preparative deoxygenation reactions of non-benzylic benzoates. [a]

Entry	Substrate	Product	Yield (%)
1	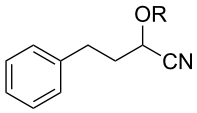 **6a**	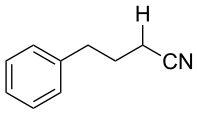 **7a**	86
2	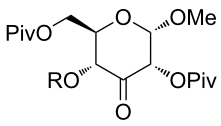 **6b**	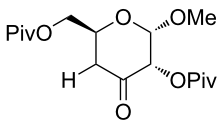 **7b**	79
3	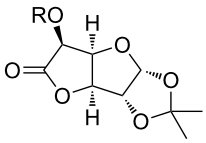 **6c**	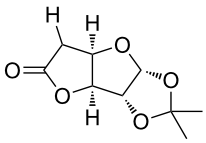 **7c**	14[b]

Table 4: Preparative deoxygenation reactions of non-benzylic benzoates. [a] (continued)

4	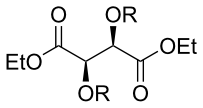 **6d**	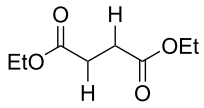 **7d**	69[c,d]
5	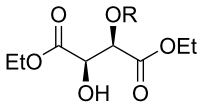 **6e**	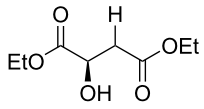 **7e**	99

[a]Conditions see Table 3. [b]Parent compound was prone to hydrolysis under reaction conditions. [c]16 h reaction time. [d]^{1}H NMR yield.

Especially interesting from a preparative point of view, the monodeoxygenation of diethyl tartrate to maleate could be achieved from **6e** in excellent yields (Table 4, entry 5). Notably, after screening various Lewis acids (Supporting Information File 1) it was found that **6e** could be selectively prepared by copper(II) chloride-catalyzed benzoylation of diol **8** with anhydride **9**, which in turn can be generated from its acid **5** by treatment with acetic anhydride (Scheme 6).

Since acetic anhydride is technically being produced by thermal dehydration of acetic acid [12], the overall sequence to the benzoylated starting material **6e** does not require any type of activation reagents such as thionyl chloride or DCC that are often used for ester formation, but ultimately only requires energy in form of heat. After the photochemical deoxygenation, 3,5-bis(trifluoromethyl)benzoic acid (**5**) is formed, which can be easily recovered in high yield and from which anhydride **9** can be regenerated as described above.

Attempts to deoxygenate simple alkyl-substituted alcohols (primary, secondary and tertiary) were not successful; for example under typical conditions 3,5-bis(trifluoromethyl)benzoates such as **10** gave **12** where one trifluoromethyl group was completely reduced to a methyl group in 52% yield (Scheme 7). Apparently, electron transfer to the benzoate group is still possible however, the subsequent C–O bond cleavage does not occur, presumably due to the energetically unfavorable primary radical intermediate that would result via the desired cleavage of the C–O bond. Instead, carbon–fluorine cleavage, leading to a benzylic radical, is the preferred pathway.

To unambiguously rule out that the methyl group in **12** originates from a substitution process with acetonitrile as the methyl source, the reaction was carried out in deuterated acetonitrile. No deuterium incorporation was observed which proved that acetonitrile is not responsible for the presence of the methyl group in **12**. Performing the reaction in the presence of TEMPO (2,2,6,6-tetramethylpiperidine-1-oxyl) gave, beside reduction product **12**, adduct **13** which suggests that the methyl group originates from a sequential reduction of the C–F bonds through a radical pathway. In addition a test for fluoride with $[Fe(SCN)(H_2O)_5]^{2+}$ in an evaporated aliquot of the irradiated reaction mixture was positive. Increasing the amount of Hünig's base acting as sacrificial electron donor in the initial reduction step of **10** led to full conversion of the starting material and gave **12** as the only reaction product in 77% isolated yield.

For larger scale applications it would be desirable to install the activating benzoate group in situ rather than in a foregoing reaction step. Also, considering its high price the employment of only small amounts of iridium-based catalyst and lower priced triethylamine instead of costly diisopropylethylamine would be

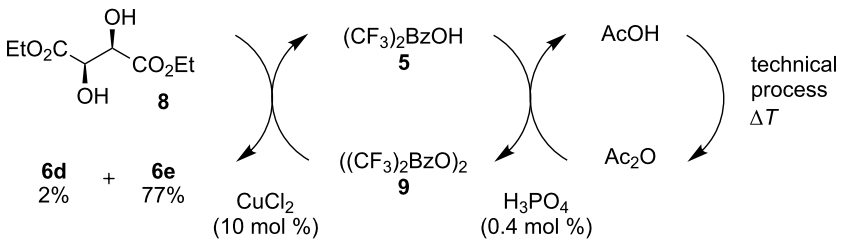

Scheme 6: Synthesis of monobenzoate **6e**.

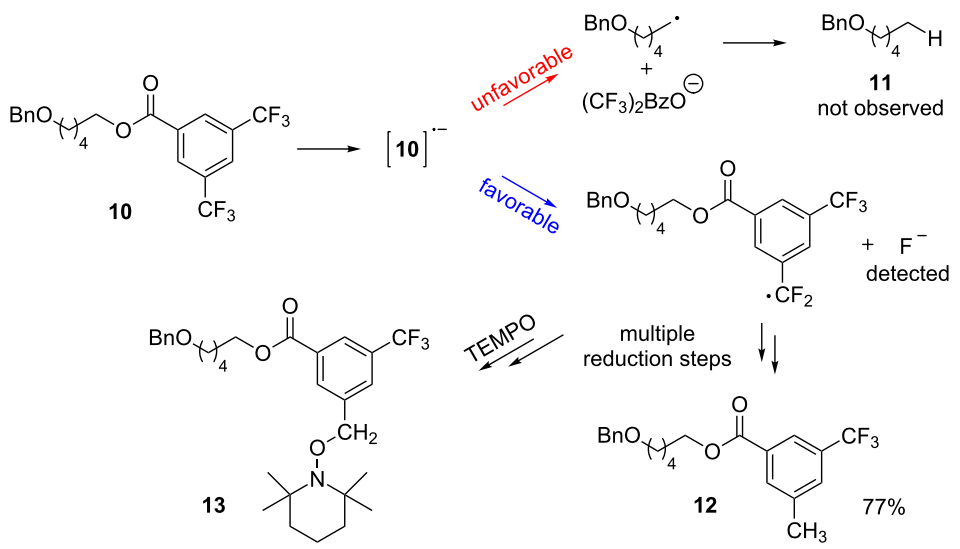

Scheme 7: Reduction of benzoate moiety in case of non-benzylic alcohols.

desirable. Taking **14** as model compound it could be shown that the overall deoxygenation process can be optimized and simplified in this regard by the in situ formation of the 3,5-bis(trifluoromethyl)benzoate **3a** which in turn could then be converted to deoxygenated compound **4a** in 91% yield (Scheme 8) in a flow process using a microreactor (see Supporting Information File 1).

Conclusion

In summary a protocol for the deoxygenation of benzylic alcohols, α-hydroxycarbonyl and α-cyanohydrin compounds under visible light photocatalysis was developed using 3,5-bis(trifluoromethyl)benzoic anhydride for alcohol activation. Since 3,5-bis(trifluoromethyl)benzoic acid can be recycled and reactivated under redox neutral conditions, and moreover, the in situ activation of alcohols with this auxiliary is possible we envision that an overall continuous process could be developed for the deoxygenation of alcohols by this protocol. That ultimately only requires heat, triethylamine as a sacrificial electron donor and visible light, forming water as the only byproduct. Therefore, we believe that despite the relatively expensive activation of alcohols as 3,5-bis(trifluoromethyl)benzoic acid esters, the deoxygenation protocol described here could become also attractive for large-scale applications.

Experimental

General procedure for photochemical deoxygenations: A Schlenk tube was charged with photocatalyst (20 µmol, 2.0 mol %), benzoate (1.00 mmol, 1.00 equiv), sealed with a screw cap and subsequently evacuated and backfilled with N_2 (3×). Solvent (20 mL), Hünig's base (0.35 mL, 2.0 mmol, 2.0 equiv), and degassed water (1.8 mL, 100 mmol, 100 equiv) were added and the reaction mixture was magnetically stirred until a homogeneous solution was obtained. The reaction mixture was degassed by freeze-pump-thaw (5×) and the screw cap was replaced with a Teflon-sealed inlet for a glass rod, through which irradiation with a 455 nm high power LED took place from above while the reaction was magnetically stirred and heated in an aluminum block from below. After the reaction the mixture was diluted with 100 mL Et_2O, washed with 50 mL 10% Na_2CO_3, 50 mL H_2O, 50 mL brine, and dried over Na_2SO_4. After evaporation the crude mixture was purified by filtration through a short plug of flash silica gel with a mixture of petrol ether and ethyl acetate.

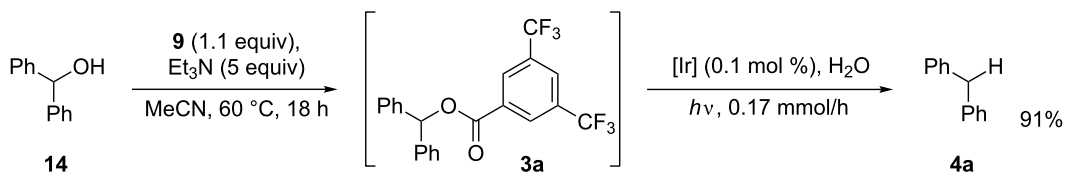

Scheme 8: Optimized conditions for larger scale applications.

Supporting Information

Supporting Information File 1

Experimental details, characterization data and spectra.
[http://www.beilstein-journals.org/bjoc/content/supplementary/1860-5397-10-223-S1.pdf]

Acknowledgements

This work was supported by the GRK 1626 (“Chemical Photocatalysis”) of the DFG.

References

1. Dodds, D. R.; Gross, R. A. *Science* **2007,** *318,* 1250–1251. doi:10.1126/science.1146356
2. Barton, D. H. R.; McCombie, S. W. *J. Chem. Soc., Perkin Trans. 1* **1975,** 1574–1585. doi:10.1039/p19750001574
3. Studer, A.; Amrein, S. *Angew. Chem., Int. Ed.* **2000,** *39,* 3080–3082. doi:10.1002/1521-3773(20000901)39:17<3080::AID-ANIE3080>3.0.CO;2-E
4. Lam, K.; Markó, I. E. *Org. Lett.* **2008,** *10,* 2773–2776. doi:10.1021/ol800944p
5. Saito, I.; Ikehira, H.; Kasatani, R.; Watanabe, M.; Matsuura, T. *J. Am. Chem. Soc.* **1986,** *108,* 3115–3117. doi:10.1021/ja00271a057
6. Prudhomme, D. R.; Wang, Z.; Rizzo, C. J. *J. Org. Chem.* **1997,** *62,* 8257–8260. doi:10.1021/jo971332y
7. Shen, B.; Jamison, T. F. *Aust. J. Chem.* **2013,** *66,* 157–164. doi:10.1071/CH12426
8. Bordoni, A.; de Lederkremer, R. M.; Marino, C. *Carbohydr. Res.* **2006,** *341,* 1788–1795. doi:10.1016/j.carres.2006.04.012
9. Bordoni, A.; de Lederkremer, R. M.; Marino, C. *Tetrahedron* **2008,** *64,* 1703–1710. doi:10.1016/j.tet.2007.12.005
10. Nguyen, J. D.; Reiß, B.; Dai, C.; Stephenson, C. R. J. *Chem. Commun.* **2013,** *49,* 4352–4354. doi:10.1039/c2cc37206a
11. Nguyen, J. D.; D’Amato, E. M.; Narayanam, J. M. R.; Stephenson, C. R. J. *Nat. Chem.* **2012,** *4,* 854–859. doi:10.1038/nchem.1452
12. Arpe, H.-J. *Industrielle Organische Chemie,* 6th ed.; Wiley-VCH: Weinheim, Germany, 2007; p 536.

License and Terms

BEILSTEIN JOURNAL OF ORGANIC CHEMISTRY

Visible-light-induced bromoetherification of alkenols for the synthesis of β-bromotetrahydrofurans and -tetrahydropyrans

Run Lin, Hongnan Sun, Chao Yang*, Youdong Yang, Xinxin Zhao and Wujiong Xia*

Full Research Paper

Open Access

Address:
State Key Lab of Urban Water Resource and Environment, the Academy of Fundamental and Interdisciplinary Sciences, Harbin Institute of Technology, Harbin 150080, P. R. China

Email:
Chao Yang* - xyyang@hit.edu.cn; Wujiong Xia* - xiawj@hit.edu.cn

* Corresponding author

Keywords:
alkenols; bromoetherification; photoredox catalysis; visible light

Beilstein J. Org. Chem. **2015,** *11,* 31–36.
doi:10.3762/bjoc.11.5

Received: 17 October 2014
Accepted: 23 December 2014
Published: 08 January 2015

Associate Editor: T. P. Yoon

Abstract

A visible-light-induced photoredox-catalyzed bromoetherification of alkenols is described. This approach, with CBr_4 as the bromine source through generation of bromine in situ, provides a mild and operationally simple access to the synthesis of β-bromotetrahydrofurans and -tetrahydropyrans with high efficiency and regioselectivity.

Introduction

The halocyclization of alkenes provides an excellent synthetic method for halogenated heterocycles [1-3]. In recent years, haloaminocyclization [4,5], halolactonization [6,7] and haloetherification [8,9] of alkenes have received considerable attention from chemists, and various approaches have been made in this area. Initially, the classical synthetic pathway for bromocyclization proceeds utilizing bromine [10]. However, molecular bromine is hazardous and difficult to handle. Further research show that *N*-bromosuccinimide (NBS) is an effective alternative for the bromocyclization [11-14]. Furthermore, Wei Sun and co-workers disclosed an intriguing strategy to access the haloetherfication of alkenols with *N*-chlorosuccinimide (NCS), leading to the synthesis of β-chlorotetrahydrofurans [15]. Recently we have reported that visible-light-induced photoredox catalysis could serve as a more environmental-friendly alternative reaction system to obtain Br_2 in situ from CBr_4, an oxidative quencher of photoredox catalyst [16-22]. Thus, as part of difunctionalization of alkenes, with our continuous investigations on the photoredox catalytic reactions [16,23-27], herein we report our preliminary studies on visible-light-induced photoredox-catalyzed bromoetherification of alkenols using CBr_4 as the bromine source.

Results and Discussion

Our initial studies were focused on the reaction of alkenol **1a** as a model reaction for optimizing the reaction conditions. We were encouraged by the discovery that when **1a**, CBr_4 and $Ru(bpy)_3Cl_2$ were irradiated by blue LEDs in MeCN for

4 hours, *trans*-β-bromotetrahydrofuran **2a** was obtained via 5-*endo* bromoetherification reaction, although the yield was only 31% (Table 1, entry 2). We have reported the bromoetherification of compound **1a** as an example in our previous article [16]. However, considering the value of this strategy for the synthesis of β-bromotetrahydrofurans and -tetrahydropyrans, further research were carried out to optimize the reaction conditions. Moreover, the stereochemistry of the bromotetrahydrofurans compound **2a** was misidentified before. Herein, the stereochemistry of the bromotetrahydrofurans compound **2a** was determined by NOE spectra, for details see Supporting Information File 1. After a screening of selected solvents, we found solvents had a significant effect on the reaction efficiency (Table 1, entries 1–5). The reaction in DMSO led to the highest yield up to 94% (Table 1, entry 1). In addition, 2 equivalents of CBr_4 were required for the efficient transformation (Table 1, entries 6 and 7). Furthermore, when the catalyst loading was reduced to even 1 mol %, the reaction also gave a comparable result (Table 1, entry 8). It should be pointed out that no reaction was observed in the absence of light or photocatalyst.

With the optimized reaction conditions in hand, various substituted butenols were subsequently investigated for the scope of the reaction. As shown in Table 2, electronically distinct styrenes ranging from electron-rich to electron-deficient

Table 1: Survey on the photocatalytic bromoetherification of alkenols.

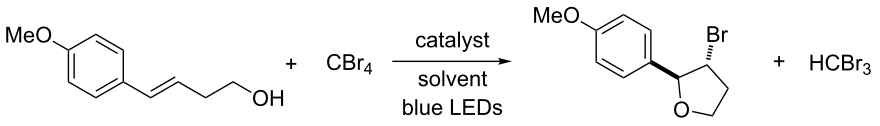

1a **2a**

Entry	Conditions	Time (h)	Yield (%)[b]
1	Standard conditions[a]	4	94
2	CH_3CN as solvent	4	31
3	DCM as solvent	12	28
4	THF as solvent	24	71
5	DMF as solvent	22	77
6	Only 1 equiv CBr_4 was used	6	76
7	Only 1.5 equiv CBr_4 was used	5	88
8	Only 1 mol % $Ru(bpy)_3Cl_2$ was used	7	90

[a]Standard conditions: alkenol **1a** (0.2 mmol, 1 equiv), CBr_4 (0.4 mmol, 2 equiv), $Ru(bpy)_3Cl_2$ (0.006 mmol, 3 mol %) in dry DMSO (0.1 M) irradiated by blue LEDs (1 W); [b]isolated yield.

Table 2: Photocatalytic bromoetherification of butenols.[a]

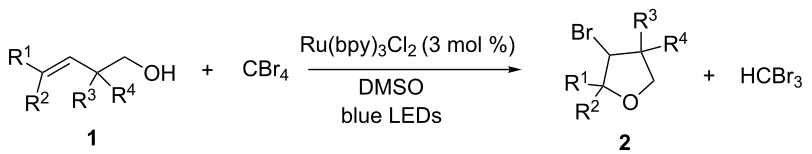

1 **2**

Entry	Substrate	Product	Yield (%)[b]
	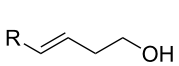		
1	R = 4-OMePh	**2a**	94
2	R = 3-OMePh	**2b**	93
3	R = 2-OMePh	**2c**	89
4	R = Ph	**2d**	88

Table 2: Photocatalytic bromoetherification of butenols.[a] (continued)

5	R = 4-MePh	**2e**	90
6	R = 3-MePh	**2f**	85
7	R = 2-MePh	**2g**	84
8	R = 4-BrPh	**2h**	90
9	R = 3-BrPh	**2i**	87
10	R = 2-BrPh	**2j**	86
11	R = 4-FPh	**2k**	89
12	R = 4-NO_2Ph	**2l**	74
13	R = 2,4-diOMePh	**2m**	93
14	R = 2,5-diOMePh	**2n**	84
15	R = 2-OMe-5-ClPh	**2o**	88
16	R = 2-OMe-naphthalen-1-yl	**2p**	86
	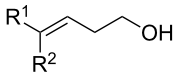	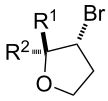	
17	R^1 = 4-OTBDPSPh, R^2 = Me	**2q**	87
18	R^1 = R^2 = 4-OMePh	**2r**	83
19	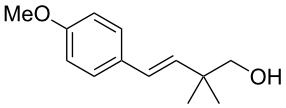	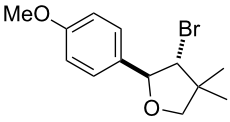 **2s**	90

[a]Standard conditions: butenol **1** (0.2 mmol, 1 equiv), CBr_4 (0.4 mmol, 2 equiv), $Ru(bpy)_3Cl_2$ (0.006 mmol, 3 mol %) in dry DMSO (0.1 M) irradiated by blue LEDs (1W) for 4 h; [b]isolated yield.

provided good yields of the desired 5-*endo* bromoetherification products (Table 2, entries 1–16). Additionally, trisubstituted alkenols were also examined and showed high reactivity (Table 2, entries 17 and 18). The alkenol with geminal dimethyl substituent produced the expected 5-*endo* bromoetherification product in 90% yield (Table 2, entry 19).

To further demonstrate the general value of this strategy, a number of longer-chain pentenols were prepared and submitted to the optimized reaction conditions. As can be seen in Table 3, various styrenes were reacted efficiently to form the substituted tetrahydropyrans in high yield via 6-*endo* bromoetherification (Table 3, entries 1 and 2). Furthermore, not only primary alco-

Table 3: Photocatalytic bromoetherification of pentenols[a].

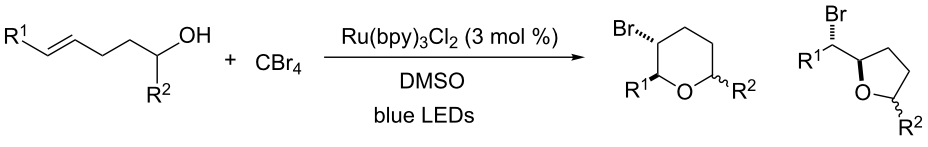

1 6-*endo*-**2** 5-*exo*-**3**

Entry	Substrate	Product	Yield (%)[b]
	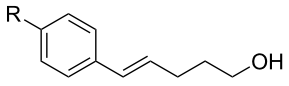	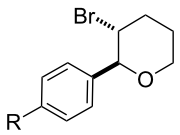	
1	R = 4-OMe	**2t**	91
2	R = 4-Me	**2u**	87

Table 3: Photocatalytic bromoetherification of pentenols[a]. (continued)

	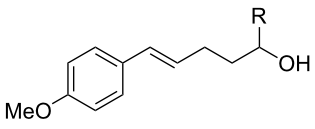	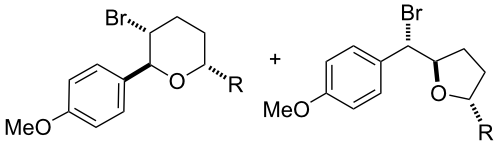	
3	R = Me	**2v**:**3v** = 1:1.1	74
4	R = Ph	**2w**:**3w** = 1:1.3	80
5	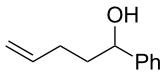	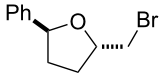 **3x**	84

[a]Standard conditions: pentenol **1** (0.2 mmol, 1 equiv), CBr_4 (0.4 mmol, 2 equiv), $Ru(bpy)_3Cl_2$ (0.006 mmol, 3 mol %) in dry DMSO (0.1 M) irradiated by blue LEDs (1 W) for 4 hours; [b]isolated yield.

hols but also secondary alcohols were tolerated using the reaction conditions albeit a mixture of 6-*endo* and 5-*exo* bromoetherification products obtained (Table 3, entries 3 and 4). Interestingly, for terminal alkene, the 5-*exo* bromoetherification product was achieved in 84% yield (Table 3, entry 5).

To add more credence to the involvement of bromine in this protocol, a control experiment was conducted by reaction of alkenol **1a** with liquid bromine in DMSO which led to *trans*-β-bromotetrahydrofuran **2a** in 95% yield (Scheme 1). Such a result is in accordance with the case of **1a** reacted under the standard reaction conditions of this protocol.

Based upon the above results, the mechanism is proposed as shown in Scheme 2. Firstly, oxidative quenching of the visible-light-induced excited state $Ru(bpy)_3^{2+}$* by CBr_4, generates Br^- along with the $Ru(bpy)_3^{3+}$ complex. Then bromine was generated in situ through the oxidation of Br^- by $Ru(bpy)_3^{3+}$ [16], sequential reaction with alkene **1a** forms the three-membered bromonium intermediate **4** [28]. Finally, intramolecular nucleophilic cyclization furnishes the desired product β-bromotetrahydrofuran **2a**.

Conclusion

In summary, we have developed a mild and operationally simple method for the bromoetherification of alkenols with CBr_4 as the bromine source, utilizing visible-light-induced phototedox catalysis. The reaction proceeds with high efficiency and regioselectivity for the synthesis of β-bromotetrahydrofurans and -tetrahydropyranes.

Experimental

General procedure for the photocatalytic bromoetherification of alkenols

To a 10 mL round bottom flask equipped with a magnetic stir bar were added alkenols **1** (0.2 mmol), CBr_4 (132 mg, 0.4 mmol), $Ru(bpy)_3Cl_2$ (4.6 mg, 0.006 mmol) and dry DMSO (2 mL). The mixture was irradiated with blue LEDs (1 W) at room temperature without being degassed for 4 hours. Then water was added and the aqueous layer was extracted with ethyl

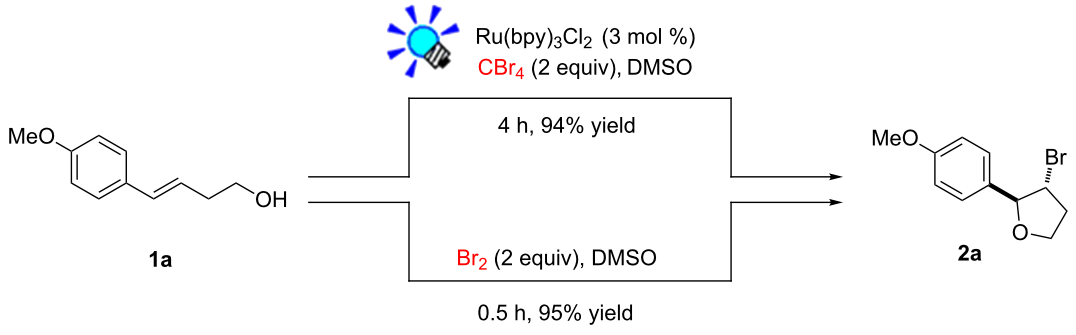

Scheme 1: Control experiment with liquid bromine for bromoethrification of alkenols.

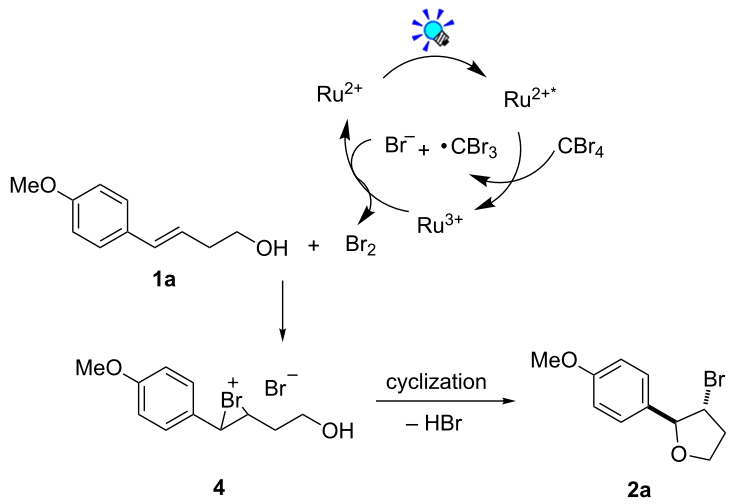

Scheme 2: Proposed mechanism for the photocatalytic bromoetherification of alkenols.

acetate. The combined organic layers were washed with brine, dried over anhydrous Na_2SO_4 and concentrated. The residue was purified by flash column chromatography to give the final products **2**.

Supporting Information

Supporting Information File 1

^1H and ^{13}C NMR spectra for products.
[http://www.beilstein-journals.org/bjoc/content/supplementary/1860-5397-11-5-S1.pdf]

Acknowledgements

We are grateful for the financial support from China NSFC (Nos. 21272047, 21372055 and 21472030), SKLUWRE (No. 2014DX01), the Fundamental Research Funds for the Central Universities (Grant No. HIT.BRETIV.201310) and HLJNSF (B201406).

References

1. French, A. N.; Bissmire, S.; Wirth, T. *Chem. Soc. Rev.* **2004,** *33,* 354–362. doi:10.1039/b310389g
2. Rodríguez, F.; Fañanás, F. J. In *Handbook of Cyclization Reactions;* Ma, S., Ed.; Wiley-VCH: New York, 2010; Vol. 4, pp 951–990.
3. Denmark, S. E.; Kuester, W. E.; Burk, M. T. *Angew. Chem., Int. Ed.* **2012,** *51,* 10938–10953. doi:10.1002/anie.201204347
4. Amjad, M.; Knight, D. W. *Tetrahedron Lett.* **2006,** *47,* 2825–2828. doi:10.1016/j.tetlet.2006.02.017
5. Cui, J.; Jia, Q.; Feng, R.-Z.; Liu, S.-S.; He, T.; Zhang, C. *Org. Lett.* **2014,** *16,* 1442–1445. doi:10.1021/ol500238k
6. Dowle, M. D.; Davies, D. I. *Chem. Soc. Rev.* **1979,** *8,* 171–197. doi:10.1039/cs9790800171
7. Ranganathan, S.; Muraleedharan, K. M.; Vaish, N. K.; Jayaraman, N. *Tetrahedron* **2004,** *60,* 5273–5308. doi:10.1016/j.tet.2004.04.014
8. Cardillo, G.; Orena, M. *Tetrahedron* **1990,** *46,* 3321–3408. doi:10.1016/S0040-4020(01)81510-6
9. Montaña, A. M.; Batalla, C.; Barcia, J. A. *Curr. Org. Chem.* **2009,** *13,* 919–938. doi:10.2174/138527209788452135
10. Staninets, V. I.; Shilov, E. A. *Russ. Chem. Rev.* **1971,** *40,* 272–283. doi:10.1070/RC1971v040n03ABEH001918
11. Cook, C.-h.; Cho, Y.-s.; Jew, S.-s.; Jung, Y.-H. *Arch. Pharmacal Res.* **1985,** *8,* 39–41. doi:10.1007/BF02897564
12. Feldman, K. S.; Crawford Mechem, C.; Nader, L. *J. Am. Chem. Soc.* **1982,** *104,* 4011–4012. doi:10.1021/ja00378a042
13. Crich, D.; Sartillo-Piscil, F.; Quintero-Cortes, L.; Wink, D. J. *J. Org. Chem.* **2001,** *67,* 3360–3364. doi:10.1021/jo016388d
14. Huang, D.; Wang, H.; Xue, F.; Guan, H.; Li, L.; Peng, X.; Shi, Y. *Org. Lett.* **2011,** *13,* 6350–6353. doi:10.1021/ol202527g
15. Zeng, X.; Miao, C.; Wang, S.; Xia, C.; Sun, W. *Chem. Commun.* **2013,** *49,* 2418–2420. doi:10.1039/c2cc38436a
16. Zhao, Y.; Li, Z.; Yang, C.; Lin, R.; Xia, W. *Beilstein J. Org. Chem.* **2014,** *10,* 622–627. doi:10.3762/bjoc.10.53
17. Zeitler, K. *Angew. Chem., Int. Ed.* **2009,** *48,* 9785–9789. doi:10.1002/anie.200904056
18. Yoon, T. P.; Ischay, M. A.; Du, J. *Nat. Chem.* **2010,** *2,* 527–532. doi:10.1038/nchem.687
19. Narayanam, J. M. R.; Stephenson, C. R. J. *Chem. Soc. Rev.* **2011,** *40,* 102–113. doi:10.1039/b913880n
20. Xuan, J.; Xiao, W.-J. *Angew. Chem., Int. Ed.* **2012,** *51,* 6828–6838. doi:10.1002/anie.201200223
21. Shi, L.; Xia, W. *Chem. Soc. Rev.* **2012,** *41,* 7687–7697. doi:10.1039/c2cs35203f
22. Prier, C. K.; Rankic, D. A.; MacMillan, D. W. C. *Chem. Rev.* **2013,** *113,* 5322–5363. doi:10.1021/cr300503r
23. Zhao, G.; Yang, C.; Guo, L.; Sun, H.; Chen, C.; Xia, W. *Chem. Commun.* **2012,** *48,* 2337–2339. doi:10.1039/c2cc17130a
24. Zhao, G.; Yang, C.; Guo, L.; Sun, H.; Lin, R.; Xia, W. *J. Org. Chem.* **2012,** *77,* 6302–6306. doi:10.1021/jo300796j
25. Sun, H.; Yang, C.; Gao, F.; Li, Z.; Xia, W. *Org. Lett.* **2013,** *15,* 624–627. doi:10.1021/ol303437m
26. Guo, L.; Yang, C.; Zheng, L.; Xia, W. *Org. Biomol. Chem.* **2013,** *11,* 5787–5792. doi:10.1039/c3ob41245h

27. Sun, H.; Yang, C.; Lin, R.; Xia, W. *Adv. Synth. Catal.* **2014,** *356,* 2775–2780. doi:10.1002/adsc.201400476
28. Roberts, I.; Kimball, G. E. *J. Am. Chem. Soc.* **1937,** *59,* 947–948. doi:10.1021/ja01284a507

License and Terms

BEILSTEIN JOURNAL OF ORGANIC CHEMISTRY

Eosin Y-catalyzed visible-light-mediated aerobic oxidative cyclization of *N*,*N*-dimethylanilines with maleimides

Zhongwei Liang[1,2], Song Xu[1,2,3], Wenyan Tian[1,2] and Ronghua Zhang[*1,2]

Full Research Paper

Open Access

Address:
[1]Department of Chemistry, Tongji University, Siping Road 1239, Shanghai 200092, China, [2]Key Laboratory of Yangtze River Water Environment, Ministry of Education, Siping Road 1239, Shanghai 200092, China and [3]College of Biological, Chemical Sciences and Engineering, Jiaxing University, Jiahang Road 118, Zhejiang 314001, China

Email:
Ronghua Zhang[*] - rhzhang@tongji.edu.cn

* Corresponding author

Keywords:
aerobic oxidative cyclization; C–H functionalization; Eosin Y; photoredox catalysis; visible light

Beilstein J. Org. Chem. **2015,** *11,* 425–430.
doi:10.3762/bjoc.11.48

Received: 04 December 2014
Accepted: 16 March 2015
Published: 01 April 2015

This article is part of the Thematic Series "Organic synthesis using photoredox catalysis".

Guest Editor: A. G. Griesbeck

Abstract

A novel and simple strategy for the efficient synthesis of the corresponding tetrahydroquinolines from *N*,*N*-dimethylanilines and maleimides using visible light in an air atmosphere in the presence of Eosin Y as a photocatalyst has been developed. The metal-free protocol involves aerobic oxidative cyclization via sp^3 C–H bond functionalization process to afford good yields in a one-pot procedure under mild conditions.

Introduction

Over the past several years, visible light photoredox catalysis has become a powerful and promising tool and has been productively used to drive chemical transformations in the field of organic synthesis [1-6]. The approach takes full advantage of visible light, which is clean, abundant, and renewable. The pioneering work in this research area, reported by the groups of MacMillan [7-9], Yoon [10,11], Stephenson [12,13] and others [14-18], has demonstrated that ruthenium and iridium complexes as visible light photoredox catalysts are capable of catalyzing a broad range of useful reactions. A variety of new methods have been developed to accomplish known and new chemical transformations by means of these transition metal-based photocatalysts so far.

However, the ruthenium and iridium catalysts usually are high-cost, potentially toxic and not sustainable. Similar to the redox properties of these organometallic complexes, some metal-free organic dyes such as Eosin Y, Rose Bengal, Fluorescein, and Methylene Blue, have shown superiority of their applications as photocatalysts, which are easy to handle, environmentally friendly, inexpensive, and have great potential for applications in visible-light-mediated photoredox reactions [19-27].

More recently, visible-light-induced sp^3 C–H bond functionalization adjacent to nitrogen atoms has been extensively studied and has become a fundamental organic transformation [28-38]. Tertiary amine **A** generally generates a nucleophilic α-amino-

alkyl radical **B** or an electrophilic iminium ion **C** via visible-light photoredox catalysis. Unfortunately the research of the α-aminoalkyl radical is limited in photochemical synthesis because it tends to form the iminium ion by one electron oxidation (Scheme 1) [39-41].

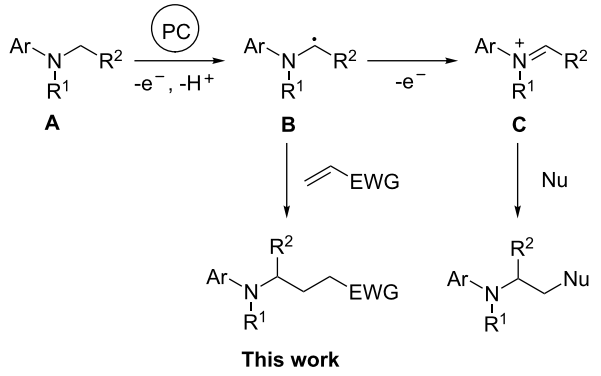

Scheme 1: Visible-light-induced sp^3 C–H bond functionalization of tertiary amines.

In the context of this research background, we investigated the α-aminoalkyl radical route to achieve the aerobic oxidative cyclization of *N*,*N*-dimethylanilines with maleimides to form the corresponding tetrahydroquinoline derivatives under organic dye Eosin Y catalysis. Swan and Roy reported the reaction using benzoyl peroxide as catalyst at low temperature as early as 1968 [42]. In 2011, Miura and co-workers achieved this transformation using a copper catalyst and air as the terminal oxidant [43]. Bian and co-workers presented the same reaction using $[Ru(bpy)_3]^{3+}$ as photoredox catalyst under irradiation with visible light next year [44]. Herein, we show an environmentally friendly aerobic oxidative cyclization methodology that avoids the use of metal catalysts and makes full use of air as oxidant.

Results and Discussion

Our investigations for the envisaged protocol commenced with the reaction of *N*,*N*-dimethylaniline (**1a**) (0.5 mmol) with *N*-phenylmaleimide (**2a**) (0.25 mmol) in MeCN (3 mL) in the presence of 3 mol % Eosin Y under an air atmosphere (with no air bubbling). The reaction mixture was irradiated with visible light (two 9 W blue LEDs) at room temperature. Gratifyingly, the desired product tetrahydroquinoline **3a** was obtained in 82% yield after 18 h (Table 1, entry 1). We screened a number of metal-free organic dyes for photocatalysts. Of the dyes screened, Eosin Y showed the highest efficiency (Table 1, entry 1), Rose Bengal gave a slightly lower yield (Table 1, entry 2), whereas Methylene Blue and Fluorescein gave poor yields (Table 1, entries 3 and 4). Under an O_2 atmosphere, the yield of

Table 1: Screening and control experiments[a].

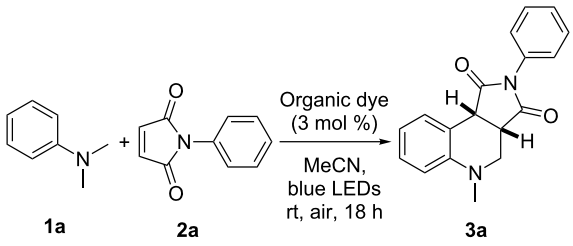

Entry	Organic dye	Oxidant	Yield (%)[b]
1	Eosin Y	air	82
2	Rose Bengal	air	67
3	Methylene Blue	air	trace
4	Fluorescein	air	trace
5	Eosin Y	O_2[c]	77
6	Eosin Y	air	69[d]
7	Eosin Y	air	73[e]
8	none	air	n.r.
9	Eosin Y	air	n.r.[f]
10	Eosin Y	none	trace[g]

[a]Reaction conditions: **1a** (0.5 mmol), **2a** (0.25 mmol), organic dye (3 mol %), MeCN (3 mL), two 9 W Blue LEDs irradiation under an air atmosphere at rt. [b]Isolated yield of the product **3a**; n.r. = no reaction. [c]Under O_2 (1 atm, balloon). [d]0.25 mmol of **1a** and 0.25 mmol of **2a** were used. [e]0.25 mmol of **1a** and 0.5 mmol of **2a** were used. [f]The reaction was carried out in the dark. [g]Under N_2.

tetrahydroquinoline product **3a** was decreased to 77% (Table 1, entry 5). When the molar proportion of **1a** and **2a** was adjusted to 1:1 and 1:2, the yield of **3a** decreased (Table 1, entries 6 and 7). Then, a series of control experiments were carried out, which indicated that Eosin Y, visible light and air are all essential for the reaction (Table 1, entries 8–10).

Next, we optimized the reaction conditions with respect to solvent and catalyst dosage. MeCN was found to be the best solvent (Table 2, entry 1) among DMF, DCE, DCM, DMSO, acetone, dioxane, and $MeNO_2$. When the amount of Eosin Y was decreased from 3 mol % to 2 mol % or increased from 3 mol % to 4 mol %, the yield of the tetrahydroquinoline product **3a** was slightly reduced (Table 2, entries 9 and 10). Thus, the optimum catalyst dosage of Eosin Y was found to be 3 mol %.

With the optimized conditions in hand, the substrate scope of this reaction was examined (Scheme 2). The reaction is mild and tolerates many functional groups. *N*,*N*-dimethylaniline and substituted *N*,*N*-dimethylanilines incorporating methyl and bromo on the phenyl ring reacted with **2** to afford the corresponding tetrahydroquinolines **3** in good yields. *N*-arylmaleimides with electron-donating groups such as methyl, methoxy

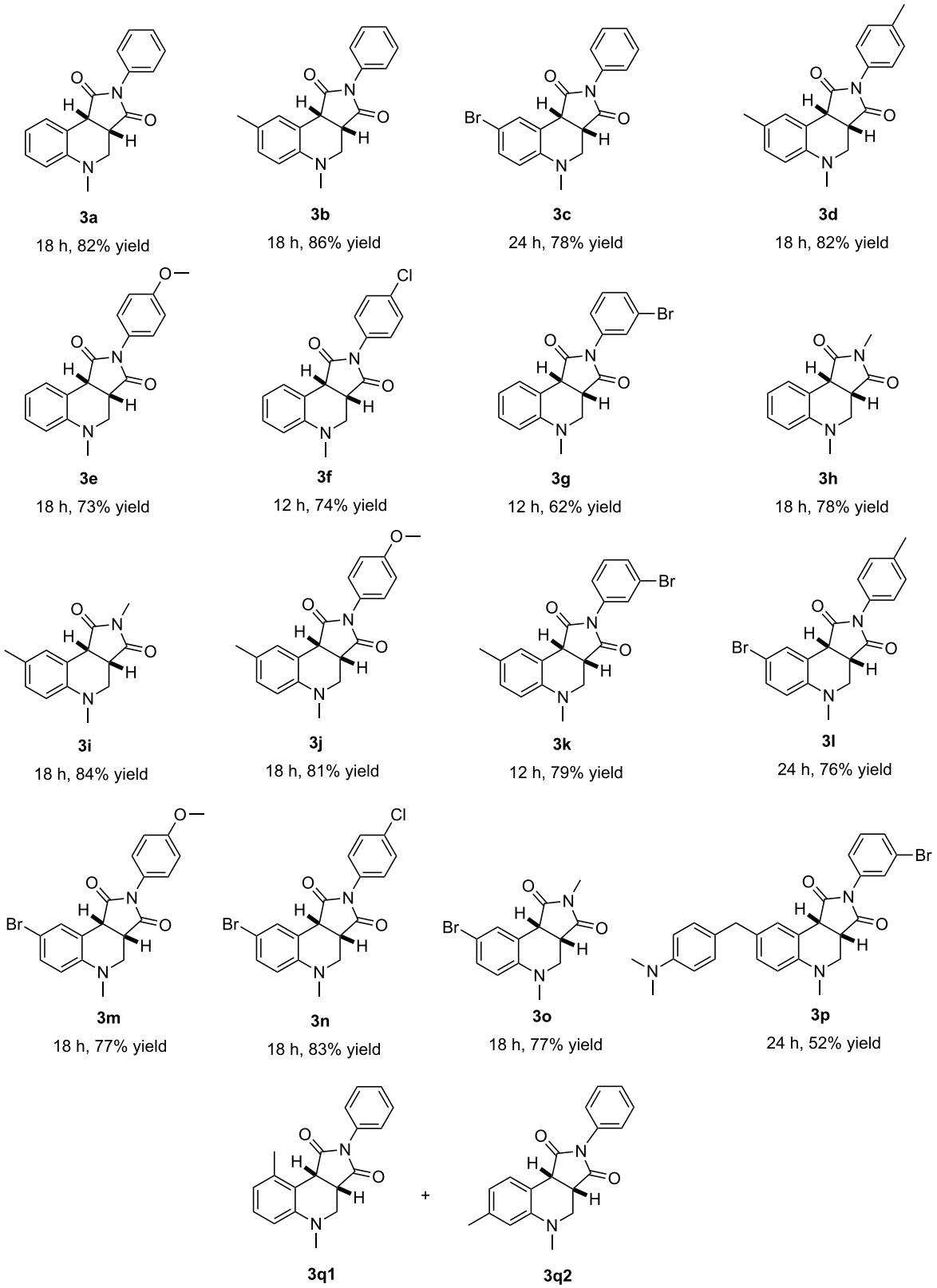

Scheme 2: Substrate scope for aerobic oxidative cyclization of *N*,*N*-dimethylanilines with maleimides.

Table 2: Optimization of reaction conditions[a].

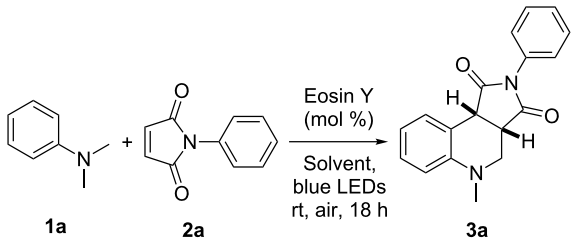

1a 2a 3a

Entry	Eosin Y (mol %)	Solvent	Yield (%)[b]
1	3	MeCN	82
2	3	DMF	47
3	3	DCE	71
4	3	DCM	37
5	3	DMSO	trace
6	3	acetone	64
7	3	dioxane	51
8	3	$MeNO_2$	58
9	2	MeCN	80
10	4	MeCN	77

[a]Reaction conditions: **1a** (0.5 mmol), **2a** (0.25 mmol), solvent (3 mL), two 9 W blue LEDs irradiation under an air atmosphere at rt. [b]Isolated yield of the product **3a**.

and electron-withdrawing groups such as chloro, bromo, and *N*-methylmaleimide all underwent the aerobic oxidative cyclization to give the corresponding products in good yields. When using 4,4'-methylenebis(*N*,*N*-dimethylaniline) as the substrate, the reaction occurred only on one side and the yield of the product **3p** is 52%. The reaction of *N*,*N*,3-trimethylaniline and *N*-phenylmaleimide resulted in the formation of a mixture of regioisomers **3q1** and **3q2** with 81% combined yield. The major product was the sterically more hindered **3q1** [43-45].

On the basis of our observations and literature reported [19,36,38,43,44], a proposed mechanism for the formation of the corresponding tetrahydroquinolines **3** form *N*,*N*-dimethylanilines **1** and maleimides **2** is depicted in Scheme 3. On absorption of visible light, the ground state of Eosin Y (EY) is induced to its single excited state ($^1EY^*$), which moves to its more stable triplet excited state ($^3EY^*$) through inter system crossing (ISC) [46,47]. $^3EY^*$ may undergo an oxidative or reductive quenching cycle [48-50]. In this mechanism, a single electron transfer (SET) from **1** to $^3EY^*$ generates the amine radical cation **4**, and at the same time, $^3EY^*$ is reduced to the $EY^{\bullet-}$. In the presence of oxygen, the photoredox catalytic cycle of EY is finished via a SET oxidation, with the production of a superoxide radical anion $O_2^{\bullet-}$. Deprotonation of **4** generates

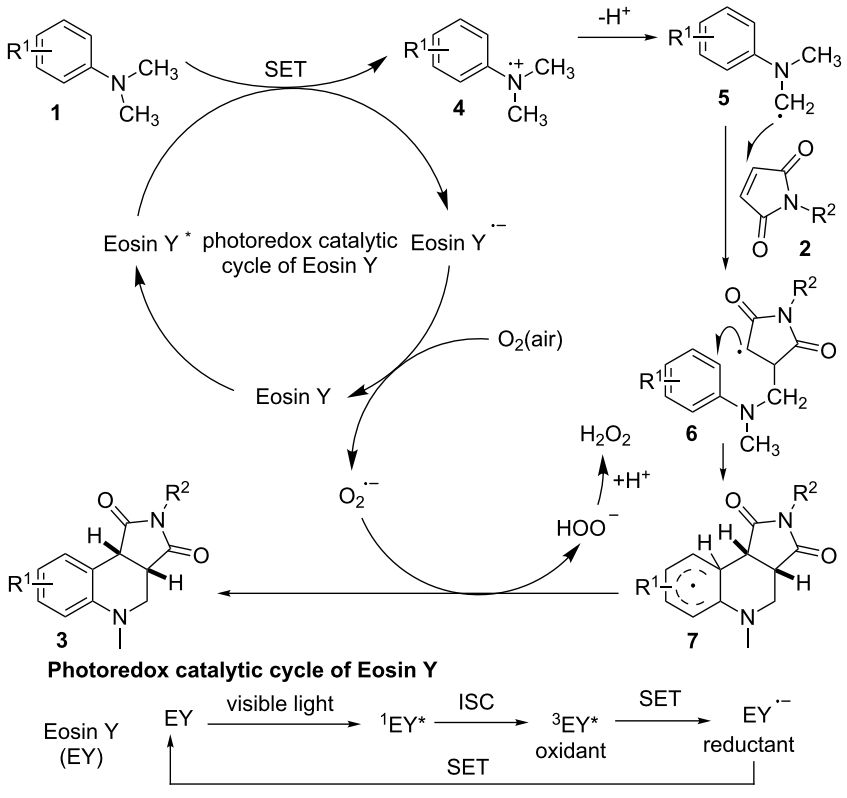

Scheme 3: A proposed reaction mechanism.

α-aminoalkyl radical **5**. Then **5** reacts with **2** to generate radical **6**, and the latter then undergoes cyclization to form intermediate **7**. Proton and electron transfer from **7** to $O_2^{\bullet-}$ yields the final product **3** and HOO^-. The HOO^- will be subsequently protonated to yield H_2O_2 as the by-product. H_2O_2 was detected after the reaction was completed by using KI/starch indicator (see the Supporting Information File 1). The involvement of radical pathway was supported by experimental result that the reaction was suppressed in the presence of TEMPO.

Conclusion

In conclusion, we report an efficient metal-free method for the synthesis of corresponding tetrahydroquinolines from *N*,*N*-dimethylanilines and maleimides using molecular oxygen as oxidant and Eosin Y as catalyst under the irradiation of visible light. The protocol is significantly green because it utilizes visible light and atmospheric oxygen as the greenest reagents, and metal-free, cheap Eosin Y with a relatively low loading as the photocatalyst to deliver the product at room temperature in a simple one-pot procedure. This methodology expands the range of substrates in the area of visible light photoredox reactions.

Supporting Information

Supporting Information File 1

Experimental section and characterization of the synthesized compounds.
[http://www.beilstein-journals.org/bjoc/content/supplementary/1860-5397-11-48-S1.pdf]

Acknowledgements

We gratefully acknowledge the financial support from the Natural Science Foundation of China (No. 20972113/B020502).

References

1. Prier, C. K.; Rankic, D. A.; MacMillan, D. W. C. *Chem. Rev.* **2013,** *113,* 5322–5363. doi:10.1021/cr300503r
2. Xuan, J.; Xiao, W.-J. *Angew. Chem., Int. Ed.* **2012,** *51,* 6828–6838. doi:10.1002/anie.201200223
3. Schultz, D. M.; Yoon, T. P. *Science* **2014,** *343,* 985–993. doi:10.1126/science.1239176
4. Yoon, T. P.; Ischay, M. A.; Du, J. *Nat. Chem.* **2010,** *2,* 527–532. doi:10.1038/nchem.687
5. Narayanam, J. M. R.; Stephenson, C. R. J. *Chem. Soc. Rev.* **2011,** *40,* 102–113. doi:10.1039/b913880n
6. Zeitler, K. *Angew. Chem., Int. Ed.* **2009,** *48,* 9785–9789. doi:10.1002/anie.200904056
7. Pirnot, M. T.; Rankic, D. A.; Martin, D. B. C.; MacMillan, D. W. C. *Science* **2013,** *339,* 1593–1596. doi:10.1126/science.1232993
8. Nicewicz, D. A.; MacMillan, D. W. C. *Science* **2008,** *322,* 77–80. doi:10.1126/science.1161976
9. Nagib, D. A.; MacMillan, D. W. C. *Nature* **2011,** *480,* 224–228. doi:10.1038/nature10647
10. Ischay, M. A.; Anzovino, M. E.; Du, J.; Yoon, T. P. *J. Am. Chem. Soc.* **2008,** *130,* 12886–12887. doi:10.1021/ja805387f
11. Du, J.; Yoon, T. P. *J. Am. Chem. Soc.* **2009,** *131,* 14604–14605. doi:10.1021/ja903732v
12. Dai, C.; Narayanam, J. M. R.; Stephenson, C. R. J. *Nat. Chem.* **2011,** *3,* 140–145. doi:10.1038/nchem.949
13. Narayanam, J. M. R.; Tucker, J. W.; Stephenson, C. R. J. *J. Am. Chem. Soc.* **2009,** *131,* 8756–8757. doi:10.1021/ja9033582
14. Zou, Y.-Q.; Lu, L.-Q.; Fu, L.; Chang, N.-J.; Rong, J.; Chen, J.-R.; Xiao, W.-J. *Angew. Chem., Int. Ed.* **2011,** *50,* 7171–7175. doi:10.1002/anie.201102306
15. Zou, Y.-Q.; Chen, J.-R.; Liu, X.-P.; Lu, L.-Q.; Davis, R.-L.; Jørgensen, K. A.; Xiao, W.-J. *Angew. Chem., Int. Ed.* **2012,** *51,* 784–788. doi:10.1002/anie.201107028
16. Fan, W.; Li, P. *Angew. Chem., Int. Ed.* **2014,** *53,* 12201–12204. doi:10.1002/anie.201407413
17. Zhu, S.; Das, A.; Bui, L.; Zhou, H.; Curran, D. P.; Rueping, M. *J. Am. Chem. Soc.* **2013,** *135,* 1823–1829. doi:10.1021/ja309580a
18. Sun, H.; Yang, C.; Gao, F.; Li, Z.; Xia, W. *Org. Lett.* **2013,** *15,* 624–627. doi:10.1021/ol303437m
19. Neumann, M.; Füldner, S.; König, B.; Zeitler, K. *Angew. Chem., Int. Ed.* **2011,** *50,* 951–954. doi:10.1002/anie.201002992
20. Liu, H.; Feng, W.; Kee, C. W.; Zhao, Y.; Leow, D.; Pan, Y.; Tan, C.-H. *Green Chem.* **2010,** *12,* 953–956. doi:10.1039/b924609f
21. Gu, X.; Li, X.; Chai, Y.; Yang, Q.; Li, P.; Yao, Y. *Green Chem.* **2013,** *15,* 357–361. doi:10.1039/C2GC36683E
22. Li, X.; Gu, X.; Li, Y.; Li, P. *ACS Catal.* **2014,** *4,* 1897–1900. doi:10.1021/cs5005129
23. Pitre, S. P.; McTiernan, C. D.; Ismaili, H.; Scaiano, J. C. *J. Am. Chem. Soc.* **2013,** *135,* 13286–13289. doi:10.1021/ja406311g
24. Vila, C.; Lau, J.; Rueping, M. *Beilstein J. Org. Chem.* **2014,** *10,* 1233–1238. doi:10.3762/bjoc.10.122
25. Hari, D. P.; König, B. *Org. Lett.* **2011,** *13,* 3852–3855. doi:10.1021/ol201376v
26. Chen, L.; Chao, C. S.; Pan, Y.; Dong, S.; Teo, Y. C.; Wang, J.; Tan, C.-H. *Org. Biomol. Chem.* **2013,** *11,* 5922–5925. doi:10.1039/c3ob41091a
27. Majek, M.; Filace, F.; Jacobi von Wangelin, A. *Beilstein J. Org. Chem.* **2014,** *10,* 981–989. doi:10.3762/bjoc.10.97
28. Dai, X.; Cheng, D.; Guan, B.; Mao, W.; Xu, X.; Li, X. *J. Org. Chem.* **2014,** *79,* 7212–7219. doi:10.1021/jo501097b
29. Rueping, M.; Vila, C.; Koenigs, R. M.; Poscharny, K.; Fabry, D. C. *Chem. Commun.* **2011,** *47,* 2360–2362. doi:10.1039/c0cc04539j
30. Rueping, M.; Leonori, D.; Poisson, T. *Chem. Commun.* **2011,** *47,* 9615–9617. doi:10.1039/c1cc13660g
31. Rueping, M.; Zhu, S.; Koenigs, R. M. *Chem. Commun.* **2011,** *47,* 12709–12711. doi:10.1039/c1cc15643h
32. McNally, A.; Prier, C. K.; MacMillan, D. W. C. *Science* **2011,** *334,* 1114–1117. doi:10.1126/science.1213920
33. Miyake, Y.; Nakajima, K.; Nishibayashi, Y. *Chem. – Eur. J.* **2012,** *18,* 16473–16477. doi:10.1002/chem.201203066
34. Rueping, M.; Koenigs, R. M.; Poscharny, K.; Fabry, D. C.; Leonori, D.; Vila, C. *Chem. – Eur. J.* **2012,** *18,* 5170–5174. doi:10.1002/chem.201200050
35. Zhu, S.; Rueping, M. *Chem. Commun.* **2012,** *48,* 11960–11962. doi:10.1039/c2cc36995h
36. Hu, J.; Wang, J.; Nguyen, T. H.; Zheng, N. *Beilstein J. Org. Chem.* **2013,** *9,* 1977–2001. doi:10.3762/bjoc.9.234

37. Ruiz Espelt, L.; Wiensch, E. M.; Yoon, T. P. *J. Org. Chem.* **2013,** *78,* 4107–4114. doi:10.1021/jo400428m
38. Xie, J.; Jin, H.; Xu, P.; Zhu, C. *Tetrahedron Lett.* **2014,** *55,* 36–48. doi:10.1016/j.tetlet.2013.10.090
39. Wayner, D. D. M.; Dannenberg, J. J.; Griller, D. *Chem. Phys. Lett.* **1986,** *131,* 189–191. doi:10.1016/0009-2614(86)80542-5
40. Miyake, Y.; Nakajima, K.; Nishibayashi, Y. *J. Am. Chem. Soc.* **2012,** *134,* 3338–3341. doi:10.1021/ja211770y
41. Kohls, P.; Jadhav, D.; Pandey, G.; Reiser, O. *Org. Lett.* **2012,** *14,* 672–675. doi:10.1021/ol202857t
42. Roy, R. B.; Swan, G. A. *Chem. Commun.* **1968,** 1446–1447. doi:10.1039/C19680001446
43. Nishino, M.; Hirano, K.; Satoh, T.; Miura, M. *J. Org. Chem.* **2011,** *76,* 6447–6451. doi:10.1021/jo2011329
44. Ju, X.; Li, D.; Li, W.; Yu, W.; Bian, F. *Adv. Synth. Catal.* **2012,** *354,* 3561–3567. doi:10.1002/adsc.201200608
45. Ju, X.; Liang, Y.; Jia, P.; Li, W.; Yu, W. *Org. Biomol. Chem.* **2012,** *10,* 498–501. doi:10.1039/c1ob06652h
46. Shimidzu, T.; Iyoda, T.; Koide, Y. *J. Am. Chem. Soc.* **1985,** *107,* 35–41. doi:10.1021/ja00287a007
47. Neckers, D. C.; Valdes-Aguilera, O. M. Photochemistry of the Xanthene Dyes. In *Adv. Photochem.;* Volman, D. H.; Hammond, G. S.; Neckers, D. C., Eds.; John Wiley & Sons: Hoboken, NJ, USA, 1993; Vol. 18, pp 315–394. doi:10.1002/9780470133491.ch4
48. Lazarides, T.; McCormick, T.; Du, P.; Luo, G.; Lindley, B.; Eisenberg, R. *J. Am. Chem. Soc.* **2009,** *131,* 9192–9194. doi:10.1021/ja903044n
49. Lee, S. H.; Nam, D. H.; Park, C. B. *Adv. Synth. Catal.* **2009,** *351,* 2589–2594. doi:10.1002/adsc.200900547
50. Encinas, M. V.; Rufs, A. M.; Bertolotti, S. G.; Previtali, C. M. *Polymer* **2009,** *50,* 2762–2767. doi:10.1016/j.polymer.2009.04.024

License and Terms

BEILSTEIN JOURNAL OF ORGANIC CHEMISTRY

Photocatalytic nucleophilic addition of alcohols to styrenes in Markovnikov and anti-Markovnikov orientation

Martin Weiser, Sergej Hermann, Alexander Penner and Hans-Achim Wagenknecht*

Full Research Paper

Open Access

Address:
Institute of Organic Chemistry, Karlsruhe Institute of Technology (KIT), Fritz-Haber-Weg 6, 76131 Karlsruhe, Germany

Email:
Hans-Achim Wagenknecht* - Wagenknecht@kit.edu

* Corresponding author

Keywords:
electron transfer; perylene bisimide; photocatalysis; photochemistry; pyrene

Beilstein J. Org. Chem. **2015,** *11,* 568–575.
doi:10.3762/bjoc.11.62

Received: 09 January 2015
Accepted: 08 April 2015
Published: 27 April 2015

This article is part of the Thematic Series "Organic synthesis using photoredox catalysis".

Guest Editor: A. G. Griesbeck

Abstract

The nucleophilic addition of methanol and other alcohols to 1,1-diphenylethylene (**1**) and styrene (**6**) into the Markovnikov- and anti-Markovnikov-type products was selectively achieved with 1-(*N*,*N*-dimethylamino)pyrene (Py) and 1,7-dicyanoperylene-3,4:9,10-tetracarboxylic acid bisimide (PDI) as photoredox catalysts. The regioselectivity was controlled by the photocatalyst. For the reductive mode towards the Markovnikov-type regioselectivity, Py was applied as photocatalyst and triethylamine as electron shuttle. This approach was also used for intramolecular additions. For the oxidative mode towards the anti-Markovnikov-type regioselectivety, PDI was applied together with Ph–SH as additive. Photocatalytic additions of a variety of alcohols gave the corresponding products in good to excellent yields. The proposed photocatalytic electron transfer mechanism was supported by detection of the PDI radical anion as key intermediate and by comparison of two intramolecular reactions with different electron density. Representative mesoflow reactor experiments allowed to significantly shorten the irradiation times and to use sunlight as “green” light source.

Introduction

Photocatalysts are organic or inorganic compounds that couple the physical process of light absorption with a chemical reaction by means of time, space and energetics, in order to catalyse it. With respect to the “green” character of sunlight as unlimited natural light source and the availability of LEDs as cheap and reliable artificial light sources, the research field of photoredox catalysis has tremendously grown over the past decade [1-7]. Transition metal complexes, mainly $[Ru(bpy)_3]^{2+}$ [7], were most often used as photocatalysts, whereas the potential of organic compounds and dyes has not yet been fully exploited [8]. The way towards a really complete organo-type photoredox catalysis has mainly been established for eosin Y as an important alternative for $[Ru(bpy)_3]^{2+}$ [9].

Photocatalytic nucleophilic additions of amines and alcohols to olefins, especially styrenes, became an increasingly important

task due to their potential and versatile applicability in chemical syntheses. Their non-photochemical counterparts require acids, bases or transition metal complexes as catalysts [10]. The first examples of photochemical olefin aminations were reported by Cookson et al. [11] and Kawanisi et al. [12] in the 1960s/70s, and Lewis identified exciplex states as key intermediates [13,14]. The corresponding photohydration worked only if the aromatic olefins as starting material were directly excited by UV light [15,16]. The first approach towards a photocatalytic version of this type of reaction came from Arnold, Maroulis et al. [17,18]. They demonstrated that electron-rich naphthalenes are able to photoinitiate methanol additions to olefins into the Markovnikov orientation and proposed an oxidative electron transfer mechanism for this process [17]. Complementarily, electron-poor naphthalenes yielded the anti-Markovnikov-type addition of cyanide to styrene [18]. Recently, we showed by a library of different chromophores that 1-(*N*,*N*-dimethyl-amino)pyrene (Py) can be applied as photocatalyst for the nucleophilic addition of methanol to styrene derivatives into the Markovnikov orientation [19]. Most recently, Nicewicz et al. published the hydrofunctionalization of alkenes to the anti-Markovnikov products by photoredox catalysis using 9-mesityl-10-methylacridinium [20,21]. Herein, we want to present our complementary approach to perform inter- and intramolecular nucleophilic additions of alcohols to styrene derivatives by photocatalysis. The regioselectivity – Markovnikov or anti-Markovnikov – can simply be controlled by the chosen photocatalyst, either Py or 1,7-dicyanoperylene-3,4:9,10-tetracarboxylic acid bisimide (PDI).

Results and Discussion

Photocatalytic complementarity

The photocatalytic complementarity of the two different routes (to the Markovnikov or anti-Markovnikov addition products of styrene derivatives) results from the two types of photoinduced charge transfer initiated by the photoexcited catalyst (Scheme 1). If an electron-poor chromophore is applied, the first step that follows irradiation is an electron transfer leading to one-electron oxidation of the substrate styrene and may involve intermediates such as exciplexes. Nucleophilic attack and loss of the proton of the alcohol yield a radical at the benzylic position that explains the anti-Markovnikov-type selectivity of this photocatalytic process. Back charge transfer to the photocatalyst closes the photocatalytic cycle and subsequent protonation yields the anti-Markovnikov-type addition product. In contrast, an electron-rich chromophore photoinduces an electron transfer onto the substrate. The corresponding radical anion is protonated rapidly to the neutral radical that is the key intermediate to explain the Markovnikov selectivity of this route. Both steps, electron transfer and protonation, could also occur in one proton-coupled electron transfer step. Back electron transfer to the photocatalyst finishes the photocatalytic cycle of this process, and subsequent nucleophilic attack accompanied by deprotonation gives the Markovnikov-type addition product.

Reductive route: Markovnikov regioselectivity

For the reductive mode of photocatalysis towards the Markovnikov-oriented addition products, we recently applied Py as photocatalyst and 1,1-diphenylethylene (**1**) as test substrate (Scheme 2). It was assumed that inefficient back electron transfer was responsible for low yields of the MeOH addition product **2** and rapid degradation of the photocatalyst Py. This problem could be solved by adding triethylamine which served as electron shuttle between back electron transfer that regenerates the photocatalyst and the final step of product formation. The substrate scope of this optimized photocatalytic conditions revealed that electron-poor α-phenylstyrenes and styrenes are

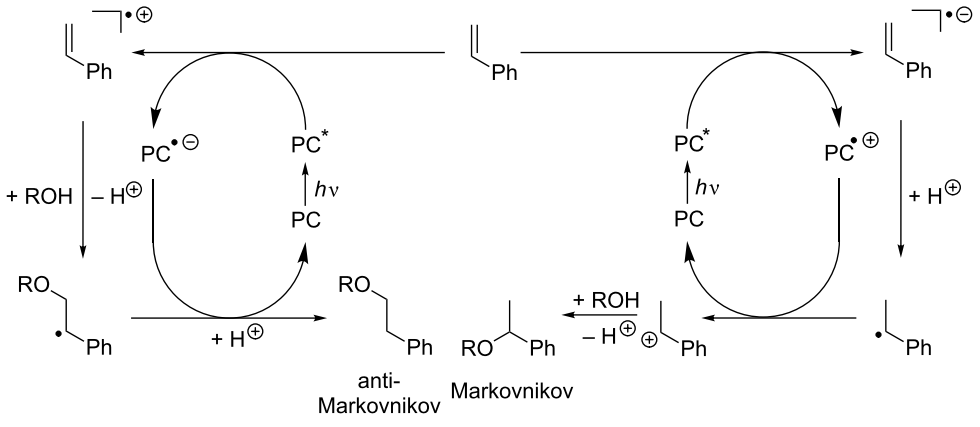

Scheme 1: Photooxidation of the substrate and reductive quenching of the photocatalyst (left) vs photoreduction of the substrate and oxidative quenching of the photocatalyst (right) give two complementary photocatalytic cycles yielding either anti-Markovnikov-type or Markovnikov-type selectivity for the nucleophilic addition of alcohols to styrene derivatives.

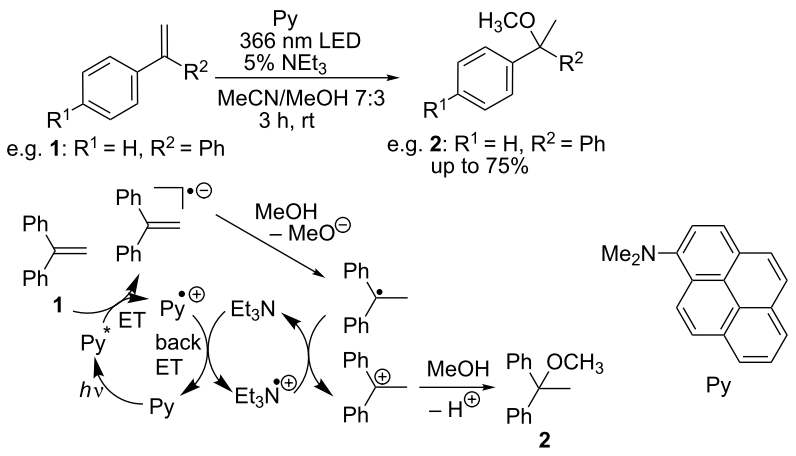

Scheme 2: Mechanism of the Markovnikov-type photocatalytic addition of methanol to 1,1-diphenylethylene (**1**) and other α-phenylstyrenes in the presence of 10 mol % of Py (ET = electron transfer).

preferred which further supported the reductive electron transfer mechanism [19].

This photocatalysis was applied also for intramolecular additions. In the particular case of substrate **3**, Et_3N as electron shuttle could not be used; it provided a competing nucleophile since the desired nucleophile could not be added in high excess. In order to shift the reaction more towards the intramolecular alternative, the photoredox catalysis was performed in high dilution (2 mM). The product **4** could be identified in 60% yield (Scheme 3).

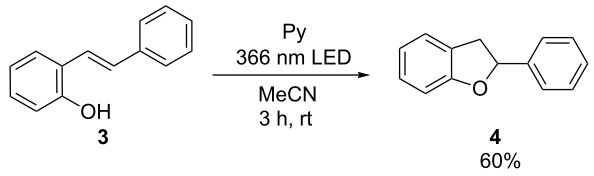

Scheme 3: Intramolecular photocatalytic addition with substrate **3**; reaction conditions: **3** (2 mM), Py (2 mM), in MeCN, argon atmosphere, 3 h, 25 °C, 366 nm high-power LED, **3** and **4** identified and quantified by GC–MS.

This example showed that the addition of Et_3N as electron shuttle was not required in all cases. A more detailed look on the problem of inefficient back electron transfer indicated that loss of polar attraction after rapid protonation of the substrate radical anion might lead to diffusion and separation of the photocatalyst from the intermediate product-forming radical cation. If it was assumed that back electron transfer was a strongly distance dependant process, the photocatalyst might not be regenerated and hence removed from the catalytic cycle. This scenario could potentially be improved by a substrate binding site on the photocatalyst that keeps the substrate in the vicinity of Py as long as it is required for forward and back electron transfer.

Oxidative route: anti-Markovnikov regioselectivity

For the oxidative mode of photocatalysis towards the anti-Markovnikov-oriented addition products, PDI (Scheme 4) was applied as photocatalyst. Its absorption maximum in CH_2Cl_2 is located at 525 nm that makes it an excellent candidate for photoirradiation by both sunlight and green light-emitting diodes. Furthermore, based on $E_{red}(PDI/PDI^{\bullet-})$ = −0.28 V (measured by cyclic voltammetry, vs SCE, see Supporting Information File 1) and E_{00} = 2.35 eV (see Supporting Information File 1), PDI is an electron deficient chromophore with an excited state oxidation potential of 2.07 V. In combination with the oxidation potential of 1.81 V (vs SCE) [22] for substrate **1** the driving force ΔG of initial oxidation was estimated by Rehm–Weller to be around 250 meV. In general, irradiations were carried out in quartz glass cuvettes at a constant temperature of 30 °C, using a 250 mW high-power LED (λ = 530 nm) as light source while stirring.

Preliminary experiments with substrate **1** revealed that formation of benzophenone was nearly completely prevented by carefully degassing the reaction mixture. A previous report of Neunteufel and Arnold considered the electron transfer from the catalyst onto the substrate as key step [23]. In agreement with that proposal, the Stern–Volmer plots (see Supporting Information File 1) showed that fluorescence of PDI is significantly quenched in the presence of **1**. The critical step, however, seemed to be the back electron transfer that recovers the photocatalyst from the PDI radical anion after nucleophilic addition,

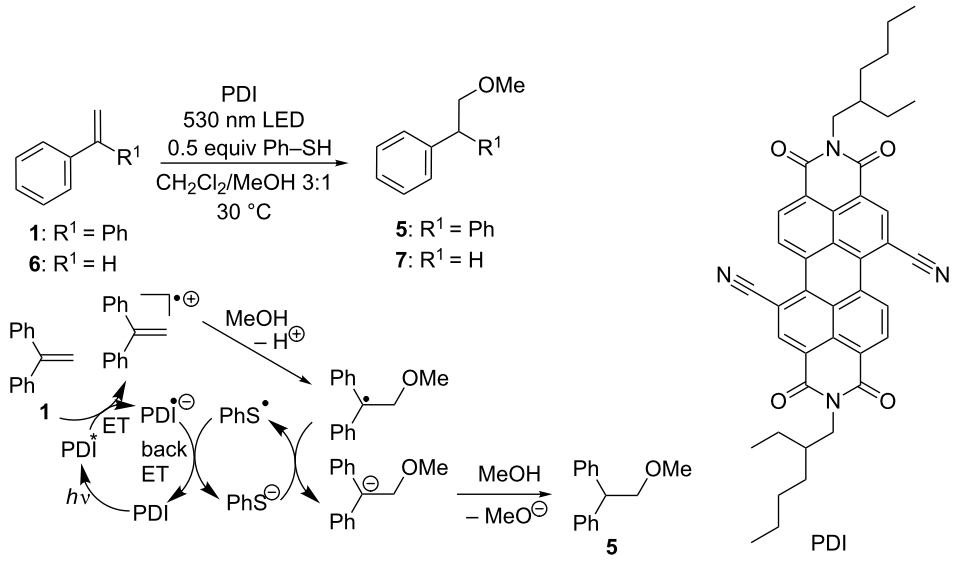

Scheme 4: Proposed mechanism of the anti-Markovnikov-type photocatalytic addition of methanol to 1,1-diphenylethylene (**1**) and styrene (**6**) yielding the corresponding products **5** and **7** (ET = electron transfer).

since addition of Ph–SH as electron and proton shuttle helped to significantly accelerated reactions [20,21]. In this respect, oxidative and reductive mode behaved similarly since both types of photocatalysis needed a suitable electron shuttle as additive. Comparison of MeOH addition reactions to substrate **1** in the presence of 0.4 and 1.0 equivalents of Ph–SH as additive showed differences in conversion rates, especially during the first six hours of irradiation (Figure 1). With stoichiometric amounts of Ph–SH full conversion was achieved within six hours, whereas 40 mol % only reached 70% of conversion at that time.

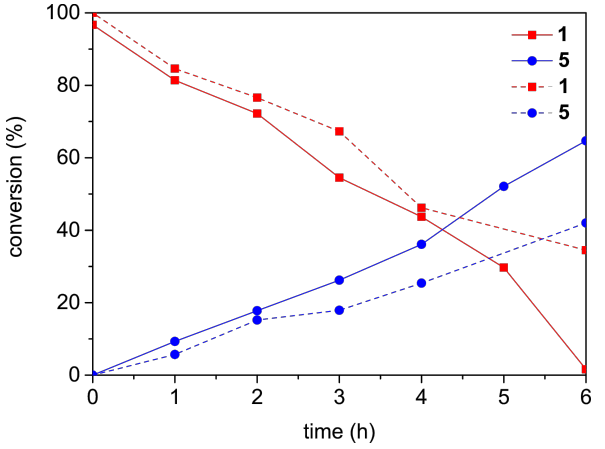

Figure 1: Conversion of substrate **1** and formation of product **5** observed during photocatalysis with PDI in the presence of 0.4 equiv (dashed lines) and 1.0 equiv (solid lines) of Ph–SH as additive; reaction conditions: **1** (20 mM), Ph–SH (20 mM), PDI (0.5 mM), in CH_2Cl_2/MeOH 3:1 (4 mL), argon atmosphere, 30 °C, 250 mW LED, λ = 530 nm, **1** and **5** identified and quantified by GC–MS.

Nucleophilic addition of a variety of alcohols to substrate **1** gave the corresponding products in excellent yields (Table 1). Especially the conversion of **1** with benzyl alcohol was significantly slower, since longer irradiations were needed. Only the addition of phenol failed completely. Since isopropanol and *tert*-butanol as sterically demanding nucleophiles gave the corresponding addition products in good yields, it was assumed that the acidity of benzyl alcohol, and more significantly of phenol, weakened the nucleophilicity for this type of reaction. Styrene (**6**) has an oxidation potential of 1.94 V (vs SCE) [22] and, hence, could also be oxidized by the chosen photocatalyst PDI. The corresponding photocatalytic nucleophilic additions to **6** (Table 1) yielded less of each product, which was in agreement with the higher oxidation potential (compared to **1**). Here again, the addition of phenol showed no significant amounts of product formation.

We representatively demonstrated the dependency of the performance of photocatalysis with substrate **1** on different PDI concentrations (Figure 2). After three hours, the yields of methanol addition product **5** differed only slightly, but on a longer timescale (12 h and longer) the yields diverged as expected. The reaction with 2 mol % of PDI was finished after 24 h, whereas the reaction with only 1 mol % reached full conversion only after 12 additional hours of irradiation time.

Table 1: Photocatalytic nucleophilic addition of alcohols to **1** and **6**[a].

nucleophile	substrate **1**		substrate **6**
	yields (%)[b] of **5** after 12 h irradiation	yields (%)[b] of **5** after 24 h irradiation	yields (%)[b] of **7** after 42 h irradiation
methanol	69	100	32
ethanol	75	100	21
propanol	64	100	24
butanol	66	100	21
isopropanol	63	100	19
tert-butanol	78	98	19
benzyl alcohol	52	84	8[c]
phenol	n.d.	0	0

[a]Reaction conditions: **1** or **6** (25 mM), Ph–SH (12.5 mM), PDI (0.5 mM), in CH_2Cl_2/alcohol 3:1 (4 mL), argon atmosphere, 30 °C, 250 mW LED, λ = 530 nm, **1**, **6** and products identified and quantified by GC–MS. [b]Averaged yield from at least two independent reactions. As no byproducts have been detected conversion matches yield. [c]Conversion = 24%.

The usage of just 0.2 and 0.5 mol % PDI increased the irradiation time at least to 36 h, and it was considered doubtful if prolonged irradiation would complete the reactions.

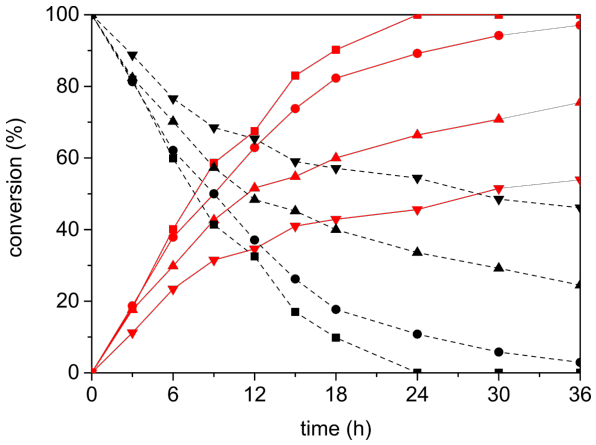

Figure 2: Conversion of substrate **1** (black dashed) and formation of product **5** (red solid) observed during photocatalysis with different amounts of PDI as photocatalyst; reaction conditions: **1** (25 mM), Ph–SH (12.5 mM), PDI (0.05 (▼), 0.125 (▲), 0.25 (●), 0.50 (■) mM), in CH_2Cl_2/alcohol 3:1 (4 mL), argon atmosphere, 30 °C, 250 mW LED, λ = 530 nm, **1** and **5** identified and quantified by GC–MS.

During these photocatalytic experiments, the colour of the solution changed from orange to blue after the first seconds of irradiation and turned back to orange just when the reaction was finished. If the irradiation of the photocatalytic sample was stopped it took about an hour until the blue color completely disappeared and obviously the chromophore relaxed back to the ground state. Spectroelectrochemistry measurements (see Supporting Information File 1) revealed that the blue colored intermediate could be assigned to the radical anion of PDI as photocatalyst whose half-lifetime was determined to be approximately 4 min (Figure 3). The appearance of this intermediate strongly supported the proposed electron transfer mechanism of this type of photocatalysis (Scheme 4).

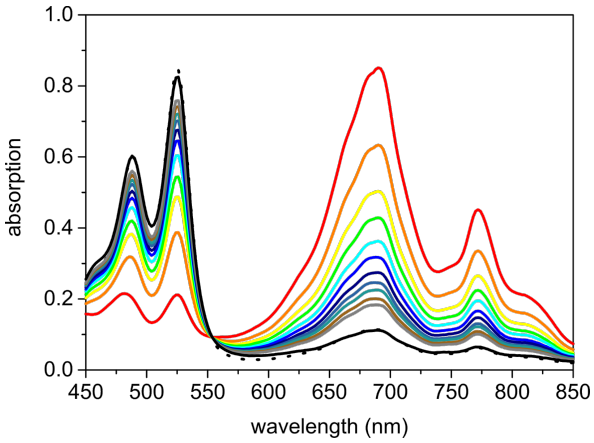

Figure 3: Spectra of PDI before (dotted black) and after excitation (red), then every 2 min until ground state is reached after 30 min (solid black). Reaction conditions: **1** (25 mM), Ph–SH (12.5 mM), PDI (0.02 mM), in CH_2Cl_2/MeOH 3:1 (4 mL), argon atmosphere, 25 °C, irradiation by 2 LEDs (250 mW), λ = 530 nm.

Although the intramolecular additions of substrates **8** and **10** in the presence of PDI as photocatalyst yielded the corresponding products **9** and **11** only in moderate yields (Scheme 5), they additionally support the proposed photocatalytic mechanism (Scheme 4). Comparison of product formation after 18 h showed that the methoxy substituted product **9** was obtained in approximately double yield compared to **11**. Obviously, the photooxidation of the electron-rich double bond in substrate **8** by electron transfer occured faster than the one in substrate **10**. These results indicate that the initial charge transfer was the rate-limiting step of this photocatalytic process.

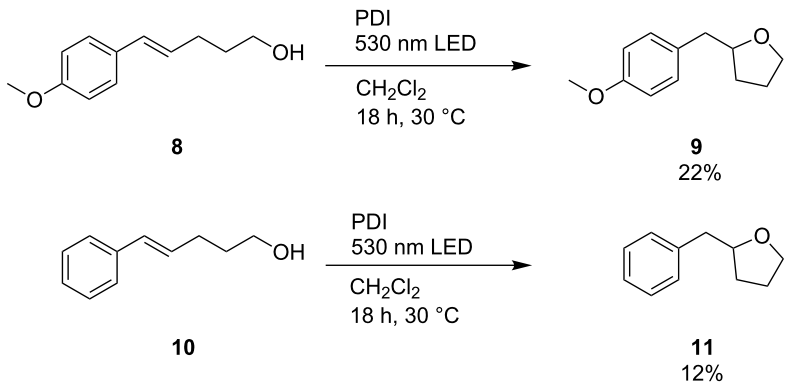

Scheme 5: Intramolecular additions of substrates **8** and **10** to demonstrate the effect of different electron densities of the double bond. Reaction conditions: **8** or **10** (25 mM), Ph–SH (12.5 mM), PDI (0.5 mM), in CH_2Cl_2 (4 mL), argon atmosphere, 30 °C, 250 mW LED, λ = 530 nm, **8**–**11** identified and quantified by GC–MS.

The photocatalytic capability of PDI was representatively compared to that of 9-mesityl-10-methylacridinium perchlorate (MesAcr) which was applied by Nicewicz et al. for similar additions [20,21]. After 3 h irradiation at 448 nm by two LEDs (250 mW) in the presence of MesAcr (otherwise identical experimental conditions as those described in Table 1) product **5** was formed in 30% yield, whereas the corresponding reaction with PDI as the photocatalyst yields 49% when PDI is irradiated at 530 nm and 59% when irradiated at 470 nm. These irradiations were performed with the corresponding LEDs and yields were identical with conversions.

Finally, the nucleophilic addition of methanol to **1** using PDI as photocatalyst was representatively executed in two mesoflow reactors, since flow chemistry has significant advantages over batch chemistry, such as easier temperature control, larger surface-to-volume ratio and more efficient photoirradiation. Two setups were used to transfer the reaction to continuous-flow systems. The first mesoflow reactor was equipped with four 250 mW high-power LEDs (λ = 530 nm), a syringe pump, and temperature control to 30 °C. The second one was constructuted for exposure to sunlight and consisted of a PTFE tubing to demonstrate applicability of this photocatalysis without need for electricity. Mesoflow experiments were executed using either sunlight, to give 72% yield over only 1 h, or four high-power LEDs, to give 76% yield over 3 h (Table 2). As control that **1** was not excited directly by sunlight, a sample without PDI was set into sunlight and, as expected, yielded no product.

Table 2: Photocatalytic experiments with **1** in flow reactors[a].

setup	yield of **5** (%)
mesoflow reactor 1[b]	76[c]
mesoflow reactor 2[d]	72[e]
sunlight w/o PDI[f]	0

[a]Reaction conditions: **1** (25 mM), Ph–SH (12.5 mM), PDI (0.5 mM), in CH_2Cl_2/MeOH 3:1, argon atmosphere, reactants identified and quantified by GC–MS. [b]Syringe pump with flow rate of 300 µL/h, 220 min, 30 °C, 4 × 250 mW LED, λ = 530 nm. [c]Conversion = 88%. [d]4 mL, rt, sunlight, 17/04/14, Karlsruhe, 11 a.m. until noon. [e]Conversion = 100%. [f]1 h, no conversion; 1 month, 51% conversion mainly to benzophenone.

Conclusion

The photocatalytic complementarity of the two different routes to either the Markovnikov- or anti-Markovnikov-type nucleophilic alcohol addition to styrene derivatives was accomplished by Py and PDI as photoredox catalysts. The regioselectivity was controlled by the type of photoinduced charge transfer that was initiated by the photoexcited catalyst. For the reductive mode towards the Markovnikov orientation, Py was applied as photocatalyst. It was previously elucidated that inefficient back electron transfer required the addition of Et_3N as electron shuttle that closed the photocatalytic cycle since back electron transfer occurred more efficiently. The photocatalytic process was used also for intramolecular additions. For the oxidative mode towards the anti-Markovnikov-type regioselectivety, PDI was a highly suitable photocatalyst based on its electrochemical and optical properties. Photocatalytic additions of a variety of alcohols to styrene derivatives gave the corresponding products in good to excellent yields. Similar to the reductive mode, the oxidative nucleophilic addition needed the additive Ph–SH as electron and proton shuttle. The proposed photocatalytic electron transfer mechanism was supported by the observation of the PDI radical anion as key intermediate and by comparison of two intramolecular reactions with different electron density. Representative mesoflow reactor experiments revealed that the irradiation times can be significantly shortened and sunlight can

be used as a "green" light source. The yields of methanol addition using PDI as photocatalyst were higher than those obtained with MesAcr as literature-known photocatalyst. These results provide a good basis to extend this photocatalytic approach to other nucleophilic additions as synthetically valuable olefin functionalizations, including C–C bond formations.

Experimental

Materials and methods. All chemicals were purchased from Aldrich, ABCR and TCI. GC–MS data were recorded on a Varian GC–MS System (gas-phase chromatograph 431-GC, mass spectrometer 210-MS). Absorption spectra were determined with a Perkin Elmer Lambda 750 UV–vis spectrometer. Fluorescence was measured with a Horiba Scientific FluoroMax 4 spectrofluorometer with step width of 1 nm and an integration time of 0.2 s.

Photocatalytic experiments with Py. Irradiations have been executed in a 4 mL cuvette equipped with a magnetic stir bar. The samples were prepared with stem solutions and final concentrations of the substrates (2 mM) and Py (2 mM) in MeCN. The solution was then degassed using the freeze pump thaw method and afterwards irradiated with a 366 nm LED while stirring. Samples have been taken under argon counterflow to prevent oxygen from getting into the reaction mixture.

Photocatalytic experiments with PDI. Irradiations have been executed in a 4 mL cuvette equipped with a magnetic stir bar. The samples were prepared with stem solutions and final concentrations of the substrates (25 mM), Ph–SH (12.5 mM) and PDI (0.5 mM) in either CH_2Cl_2 or CH_2Cl_2/alcohol 3:1 mixtures. The solution was then degassed using the freeze pump thaw method and afterwards irradiated with a 530 nm LED while stirring. Samples have been taken under argon counterflow to prevent oxygen from getting into the reaction mixture.

Supporting Information

Supporting Information File 1

Spectral data: Cyclic voltammogram of PDI, determination of E_{00} of PDI, Stern–Volmer plots of PDI in the presence of substrate **1**, spectroelectrochemistry of PDI, pictures of the mesoflow setups.
[http://www.beilstein-journals.org/bjoc/content/supplementary/1860-5397-11-62-S1.pdf]

Acknowledgements

Financial support by the DFG (grant Wa 1386/17-1 and GRK 1626) and KIT is gratefully acknowledged.

References

1. Xuan, J.; Xiao, W.-J. *Angew. Chem., Int. Ed.* **2012,** *51,* 6828–6838. doi:10.1002/anie.201200223
2. Xi, Y.; Yi, H.; Lei, A. *Org. Biomol. Chem.* **2013,** *11,* 2387–2403. doi:10.1039/c3ob40137e
3. Reckenthäler, M.; Griesbeck, A. G. *Adv. Synth. Catal.* **2013,** *355,* 2727–2744. doi:10.1002/adsc.201300751
4. Tucker, J. W.; Stephenson, C. R. J. *J. Org. Chem.* **2012,** *77,* 1617–1622. doi:10.1021/jo202538x
5. Ravelli, D.; Fagnoni, M.; Albini, A. *Chem. Soc. Rev.* **2013,** *42,* 97–113. doi:10.1039/C2CS35250H
6. Yoon, T. P.; Ischay, M. A.; Du, J. *Nat. Chem.* **2010,** *2,* 527–532. doi:10.1038/nchem.687
7. Prier, C. K.; Rankic, D. A.; MacMillan, D. W. C. *Chem. Rev.* **2013,** *113,* 5322–5363. doi:10.1021/cr300503r
8. Fukuzumi, S.; Ohkubo, K. *Org. Biomol. Chem.* **2014,** *12,* 6059–6071. doi:10.1039/C4OB00843J
9. Hari, D. P.; König, B. *Chem. Commun.* **2014,** *50,* 6688–6699. doi:10.1039/C4CC00751D
10. Müller, T. E.; Hultzsch, K. C.; Yus, M.; Foubelo, F.; Tada, M. *Chem. Rev.* **2008,** *108,* 3795–3892. doi:10.1021/cr0306788
11. Cookson, R. C.; de B. Costa, S. M.; Hudec, J. *J. Chem. Soc. D* **1969,** 753–754. doi:10.1039/c29690000753
12. Kawanisi, M.; Matsunaga, K. *J. Chem. Soc., Chem. Commun.* **1972,** 313–314. doi:10.1039/C39720000313
13. Lewis, F. D.; Ho, T.-I. *J. Am. Chem. Soc.* **1977,** *99,* 7991–7996. doi:10.1021/ja00466a035
14. Lewis, F. D.; Bassani, D. M.; Reddy, G. D. *Pure Appl. Chem.* **1992,** *64,* 1271–1277. doi:10.1351/pac199264091271
15. Wan, P.; Culshaw, S.; Yates, K. *J. Am. Chem. Soc.* **1982,** *104,* 2509–2515. doi:10.1021/ja00373a029
16. McEwen, J.; Yates, K. *J. Am. Chem. Soc.* **1987,** *109,* 5800–5808. doi:10.1021/ja00253a035
17. Arnold, D. R.; Maroulis, A. J. *J. Am. Chem. Soc.* **1977,** *99,* 7355–7356. doi:10.1021/ja00464a044
18. Maroulis, A. J.; Shigemitsu, Y.; Arnold, D. R. *J. Am. Chem. Soc.* **1978,** *100,* 535–541. doi:10.1021/ja00470a029
19. Penner, A.; Bätzner, E.; Wagenknecht, H.-A. *Synlett* **2012,** *23,* 2803–2807. doi:10.1055/s-0032-1317532
20. Nicewicz, D. A.; Hamilton, D. S. *Synlett* **2014,** *25,* 1191–1196. doi:10.1055/s-0033-1340738
21. Romero, N. A.; Nicewicz, D. A. *J. Am. Chem. Soc.* **2014,** *136,* 17024–17035. doi:10.1021/ja506228u
22. Shiraishi, Y.; Saito, N.; Hirai, T. *Chem. Commun.* **2006,** 773–775. doi:10.1039/b515137f
23. Neunteufel, R. A.; Arnold, D. R. *J. Am. Chem. Soc.* **1973,** *95,* 4080–4081. doi:10.1021/ja00793a060